

**NASA TECHNICAL
MEMORANDUM**

NASA TM X-74011

NASA TM X-74011

**WIND-TUNNEL RESULTS OF THE AERODYNAMIC
CHARACTERISTICS OF A 1/8-SCALE MODEL OF A
TWIN-ENGINE SHORT-HAUL TRANSPORT**

John W. Paulson, Jr.

**(NASA-TM-X-74011) WIND-TUNNEL RESULTS OF
THE AERODYNAMIC CHARACTERISTICS OF A
1/8-SCALE MODEL OF A TWIN ENGINE SHORT-HAUL
TRANSPORT (NASA) 228 p HC A11/MF A01**

N77-21047

Unclass

CSCI 01A G3/02 245+1

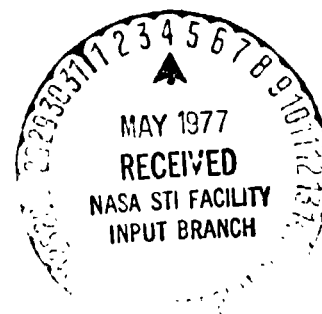
April 1977

**This informal documentation medium is used to provide accelerated or
special release of technical information to selected users. The contents
may not meet NASA formal editing and publication standards, may be re-
vised, or may be incorporated in another publication.**



**National Aeronautics and
Space Administration**

**Langley Research Center
Hampton, Virginia 23665**



1 Report No. NASA TM X-74011		2. Government Accession No.		3. Recipient's Catalog No.	
4 Title and Subtitle WIND-TUNNEL RESULTS OF THE AERODYNAMIC CHARACTERISTICS OF A 1/8-SCALE MODEL OF A TWIN-ENGINE SHORT-HAUL TRANSPORT				5. Report Date April 1977	
				6. Performing Organization Code	
7 Author(s) John W. Paulson, Jr.				8. Performing Organization Report No.	
9 Performing Organization Name and Address Langley Research Center Hampton, Virginia 23665				10 Work Unit No. 513-52-01-24	
				11 Contract or Grant No.	
12 Sponsoring Agency Name and Address National Aeronautics and Space Administration Washington, DC 20546				13 Type of Report and Period Covered Technical memorandum	
				14 Sponsoring Agency Code	
15. Supplementary Notes					
16 Abstract <p>A wind-tunnel test has been conducted in the Langley V/STOL tunnel to define the aerodynamic characteristics of a 1/8-scale twin-engine short-haul transport. The model was tested in both the cruise and approach configurations with various control surfaces deflected. Data were obtained out of ground effect for the cruise configuration and both in and out of ground effect for the approach configuration. These data are intended to be a reference point to begin the analysis of the flight characteristics of the NASA Terminal Configured Vehicle (TCV) and are presented without analysis.</p>					
17. Key Words (Suggested by Author(s)) Terminal Configured Vehicle Aerodynamic characteristics Ground effects Spoilers				18. Distribution Statement Unclassified - Unlimited Subject Category 02	
19 Security Classif. (of this report) Unclassified		20. Security Classif. (of this page) Unclassified		21. No. of Pages 228	
				22. Price* \$8.00	

WIND-TUNNEL RESULTS OF THE AERODYNAMIC CHARACTERISTICS
OF A 1/8-SCALE MODEL OF A TWIN-ENGINE
SHORT-HAUL TRANSPORT

John W. Paulson, Jr.
Langley Research Center

SUMMARY

A wind-tunnel test has been conducted in the Langley V/STOL tunnel to define the aerodynamic characteristics of a 1/8-scale twin-engine short-haul transport. The model was tested in both the cruise and approach configurations with various control surfaces deflected. Data were obtained out of ground effect for the cruise configuration and both in and out of ground effect for the approach configuration. These data are intended to be a reference point to begin the analysis of the flight characteristics of the NASA Terminal Configured Vehicle (TCV) and are presented without analysis.

INTRODUCTION

The NASA Terminal Configured Vehicle (TCV) Program Office has acquired a twin-engine short-haul transport (see figs. 1 and 2). This aircraft has been fitted with a second flight deck and extensive instrumentation for flight testing and evaluation of new terminal area flight operations, including automatic approach and landing (ref. 1). Many of the operational procedures will be flown and evaluated by pilots in a groundbased simulator before actual flight testing takes place. In order to have an accurate simulation, the aerodynamic characteristics of the airplane must be well defined. The first step in defining the characteristics of the TCV has been an extensive wind-tunnel

investigation of a 1/8-scale model of the airplane in and out of ground effect in the Langley V/STOL tunnel. The model was tested in both the cruise and approach configuration with control surfaces deflected. Angle of attack ranged from $\alpha = -4^\circ$ to stall and sideslip angle ranged from $\beta = 5^\circ$ to -15° .

SYMBOLS

The data are presented in the stability axis system shown in figure 3. The model moment center was 25 percent of the mean aerodynamic chord. All measurements and calculations were made in U.S. Customary Units; however, all values contained herein are given in both S.I. and U.S. Customary Units (see ref. 2).

b wing span, m (ft)

\bar{c} mean aerodynamic chord, m (ft)

C_D drag coefficient, $\frac{\text{Drag}}{qS}$

C_L lift coefficient, $\frac{\text{Lift}}{qS}$

C rolling-moment coefficient, $\frac{\text{Rolling moment}}{qSb}$

C_m pitching-moment coefficient, $\frac{\text{Pitching moment}}{qS\bar{c}}$

C_n yawing-moment coefficient, $\frac{\text{Yawing moment}}{qSb}$

C_Y side-force coefficient, $\frac{\text{Side force}}{qS}$


FRL fuselage reference line

G.H. ground height, m (ft)

q free-stream dynamic pressure, kPa (lbf/ft²)

S wing area, m² (ft²)

V_∞ free-stream velocity, m/sec (ft/sec)

WCP wing chord plane 

α angle of attack, deg

β sideslip angle, deg

δ control surface deflection angle, deg

Subscripts:

ail aileron

elev elevator

sp spoiler

stab stabilizer

rud rudder

1,2,3,4 spoiler segment numbers
5,6,7,8

Model component designations:

F fuselage

W wing with spoilers

F	trailing-edge flaps, Krueger flaps, and leading-edge slats undeflected
F ₃₀ , F ₄₀	trailing-edge flaps deflected 30° or 40° with Krueger flaps and leading-edge slats deployed in approach configuration
N	engine nacelles
G	landing gear down
H _T	horizontal stabilizer and elevator
V _T	vertical tail and rudder

MODEL DESCRIPTION

The model was a 1/8-scale twin-engine short-haul transport configuration shown in figure 4. A sketch with components labeled is given in figure 5, and overall dimensions are given in table 1. A closeup of the right wing showing the F₄₀ configuration with spoilers 6,7,8 deflected is given in figure 6.

Control surface deflections are given in table 2 and were, in general, defined such that a positive deflection would produce a negative aerodynamic moment on the configuration. Since the flaps and spoilers moved in only one direction, those deflections were all considered to be positive. The trailing-edge flaps, Krueger flaps, leading-edge slats, and spoilers were separate pieces for each deflection angle, while the ailerons, elevator, and rudder deflections were set with brackets or pins. The stabilizer was remotely controlled using an electric motor and drive screw system. The spoilers were made in sections and could be deflected separately. In general, the spoilers were defined to be flight spoilers when either sections 2,3 or sections 1,2,3

were deflected and defined to be direct-lift control (DLC) and spoilers when a symmetrical set of sections 2,3 and 6,7 or 1,2,3,6,7,8 were deflected.

Detailed measurements of the model were made after the investigation and some discrepancies between the full-scale airplane and the model were found. The major difference was the dimension of leading-edge slat gap. The full-scale slat gap to mean aerodynamic chord ratio varies from 0.0099 at the inboard edge of the center slat to 0.0028 at the outboard edge of the outboard slat. The model dimensions varied from 0.0081 to 0.0062. Also the vane gap for the right-hand outboard flap was slightly incorrect.

TEST PROCEDURES

The model was tested in both the cruise (F, W, F, N, H_t, V_t) and approach ($F, W, F_{30,40}, N, G, H_t, V_t$) configurations. In the cruise configuration, all control surfaces except the stabilizer and elevator were set equal to zero. In the approach configurations, the flaps were set at F_{30} or F_{40} with the gear down and various other control surfaces deflected. Data were obtained for the cruise configuration out of ground effect (OGE) over a range of $\alpha = -4^\circ$ to stall and $\beta = 5^\circ$ to -15° . Data were obtained for the approach configurations both in and out of ground effect. The OGE data were obtained at $\alpha = -4^\circ$ to stall and $\beta = 5^\circ$ to -15° . The in ground effect (GE) data were obtained at several angles of attack and ground heights as given in table 3 at $\beta = 5^\circ$ to -15° . The small number of data points and higher initial ground height at the higher angles of attack was due to hardware geometry preventing the model from being lowered to the tunnel floor. The ground heights in table 3 are full-scale distance from the surface to the bottom of the main gear wheel.

All data were obtained at a dynamic pressure of 1.44 kPa (30.0 lbf/ft²). Transition strips were placed on the wing and the horizontal and vertical tails according to the method of reference 3.

PRESENTATION OF RESULT

The OGE data were corrected to free air values by using the wall correction methods of references 4, 5, and 6. These methods all gave similar corrections to α , C_D , C_L , and C_m . The IGE data were corrected for the effects of the tunnel walls and ceiling with the effect of the floor not taken into account. This procedure is given in reference 5.

The data have been reduced to coefficient form and are presented in the following figures:

	<u>Figure</u>
Fuselage and empennage characteristics (OGE)	7,8
Horizontal tail-off characteristics for cruise and approach configurations (OGE and IGE)	9-11
Horizontal tail-off characteristics for approach configurations with DLC spoilers (OGE and IGE).	12-15
Stabilizer and elevator effects on cruise configurations (OGE) . . .	16-18
Alternate approach (F ₃₀) configuration with DLC spoiler (OGE and IGE).	19-21
Approach configuration (F ₄₀) (OGE and IGE)	22,23
Stabilizer and elevator effects on approach configurations with DLC spoilers (OGE and IGE).	24-28
DLC spoiler effects on the approach configurations (OGE and IGE) . .	29-33
Flight spoiler effects on the approach configurations (OGE and IGE).	34,35
Aileron effects on the approach configurations (OGE and IGE)	36,37

	<u>Figure</u>
Rudder effect on the approach configurations (OGE).	38,39
Landing gear effects on the approach configurations	40
Dynamic pressure effects on the approach configuration.	41
Flap deflection effects with horizontal tail off and on (OGE) . . .	42

CONCLUDING REMARKS

These data are presented without analysis and are not intended to be final definition of the aerodynamic characteristics of the twin-engine short-haul transport. Rather, these data are intended to be a reference point to begin the analysis of the TCV aircraft. These data will be combined with flight data and pilot evaluation data to define the flight characteristics of the TCV airplane for simulated terminal area operations, including automatic approach and landing.

It should be noted that, as mentioned in the model description, the leading-edge slat gap and one element of the right-hand trailing-edge flap were incorrectly set. Since this was not discovered until after the tunnel entry, no attempt to determine the effects of these discrepancies has been possible. It does, appear, however, that the model stalls at a lower angle of attack than the full-scale airplane and this may be due to the incorrect gap settings.

REFERENCES

1. Reeder, John P.; Taylor, Robert T.; and Walsh, Thomas M.: New Design and Operating Techniques and Requirements for Improved Aircraft Terminal Area Operations. NASA TM X-72006, 1974
2. Mechtly, E. A.: The International System of Units - Physical Constants and Conversion Factors (Second Revision). NASA SP-7012, 1973
3. Braslow, Albert L.; and Knox, Eugene C.: Simplified Method for Determination of Critical height of Distributed Roughness Particles for Boundary-Layer Transition at Mach Numbers From 0 to 5. NACA TN 4363, 1958
4. Pope, A.; and Harper, J. J.: Low-Speed Wind-Tunnel Testing. John Wiley & Sons, Inc., New York, N.Y., 1966
5. Recant, I. G.: Wind-Tunnel Investigation of Ground Effects on Wings with Flaps. NACA TN 705, 1939
6. Gillis, C. L.; Polhamus, E. C.; and Gray, J. L., Jr.: Charts for Determining Jet Boundary Corrections for Complete Models in 7 x 10 Foot Closed Rectangular Wind Tunnels. NACA ARR L5G31, 1945

Table 1

Model Dimensions

Fuselage length, m (ft)	3.45 (11.34)
Overall length, m (ft)	3.58 (11.75)
Wing	
Area, m ² (ft ²)	1.42 (15.31)
Span, m (ft)	3.54 (11.63)
Mean aerodynamic chord, m (ft)	0.43 (1.40)
Sweep of quarter chord, deg	25
Aspect ratio	8.83
Taper ratio	0.34
Horizontal tail span, m (ft)	1.37 (4.50)
Vertical tail height, m (ft)	0.75 (2.46)
Overall height, m (ft)	1.41 (4.63)

Table 2
Control Surface Deflections

<u>Control Surface</u>	<u>Range of Deflection</u>
Inboard and outboard flap	$0^{\circ}, 30^{\circ}, 40^{\circ}$ (nominal)
Leading-edge slats	
Cruise configuration	1,2,3,4,5,6 closed
Approach configuration	1,2,5,6 fully deployed (31.5° from WCP)
	4,5 partially deployed (20° from WCP)
Krueger flaps	
Cruise configuration	closed
Approach configuration	fully deployed (112° from WCP)
Ailerons	$0^{\circ}, \pm 10^{\circ}, \pm 15^{\circ}, \pm 21^{\circ}$ (from WCP)
Ground spoilers	$0^{\circ}, 60^{\circ}$ (from local wing upper surface)
DLC spoiler or flight spoilers	$0^{\circ}, 3^{\circ}, 6^{\circ}, 9^{\circ}, 12^{\circ}, 15^{\circ}, 20^{\circ}, 30^{\circ}, 40^{\circ}$ (from local wing upper surface)
Stabilizer	2.6° to -15° (from FRL)
Elevator	$0^{\circ}, \pm 10^{\circ}$ (from horizontal tail chord line)
Rudder	$0^{\circ}, \pm 10^{\circ}, \pm 16^{\circ}, \pm 21^{\circ}, \pm 25^{\circ}$ (from vertical tail chord line)

Table 3

Nominal Angle-Of-Attack and Gear Heights Tested in Ground Effect

α	Gear height, m (ft)		α	Gear height, m (ft)	
-1°	0.9	(3.0)	7°	1.5	(4.8)
	1.4	(4.6)		2.2	(7.2)
	2.6	(8.6)		4.6	(15.0)
	5.0	(16.4)		9.4	(31.0)
	9.8	(32.0)		16.6	(54.6)
	11.5	(37.6)			
1°	0.7	(2.3)	9°	2.4	(8.0)
	1.0	(3.3)		4.6	(15.0)
	2.2	(7.2)		9.4	(31.0)
	4.6	(15.9)		15.7	(51.5)
	9.4	(31.0)			
	12.8	(41.9)			
3°	0.7	(2.3)	11°	3.7	(12.2)
	1.0	(3.3)		4.6	(15.0)
	2.2	(7.2)		9.4	(31.0)
	4.6	(15.0)		17.4	(57.1)
	9.4	(31.0)			
	14.2	(46.5)			
5°	0.7	(2.3)	13°	5.0	(16.4)
	1.0	(3.3)		9.4	(31.0)
	2.2	(7.2)		17.4	(57.1)
	4.6	(15.0)			
	9.4	(31.0)			
	15.3	(50.2)			



Figure 1. - Side view of a twin-engine short-haul transport.

REPRODUCED
ORIGINAL



Figure 2. - Three-quarter front view of a twin-engine short-haul transport.

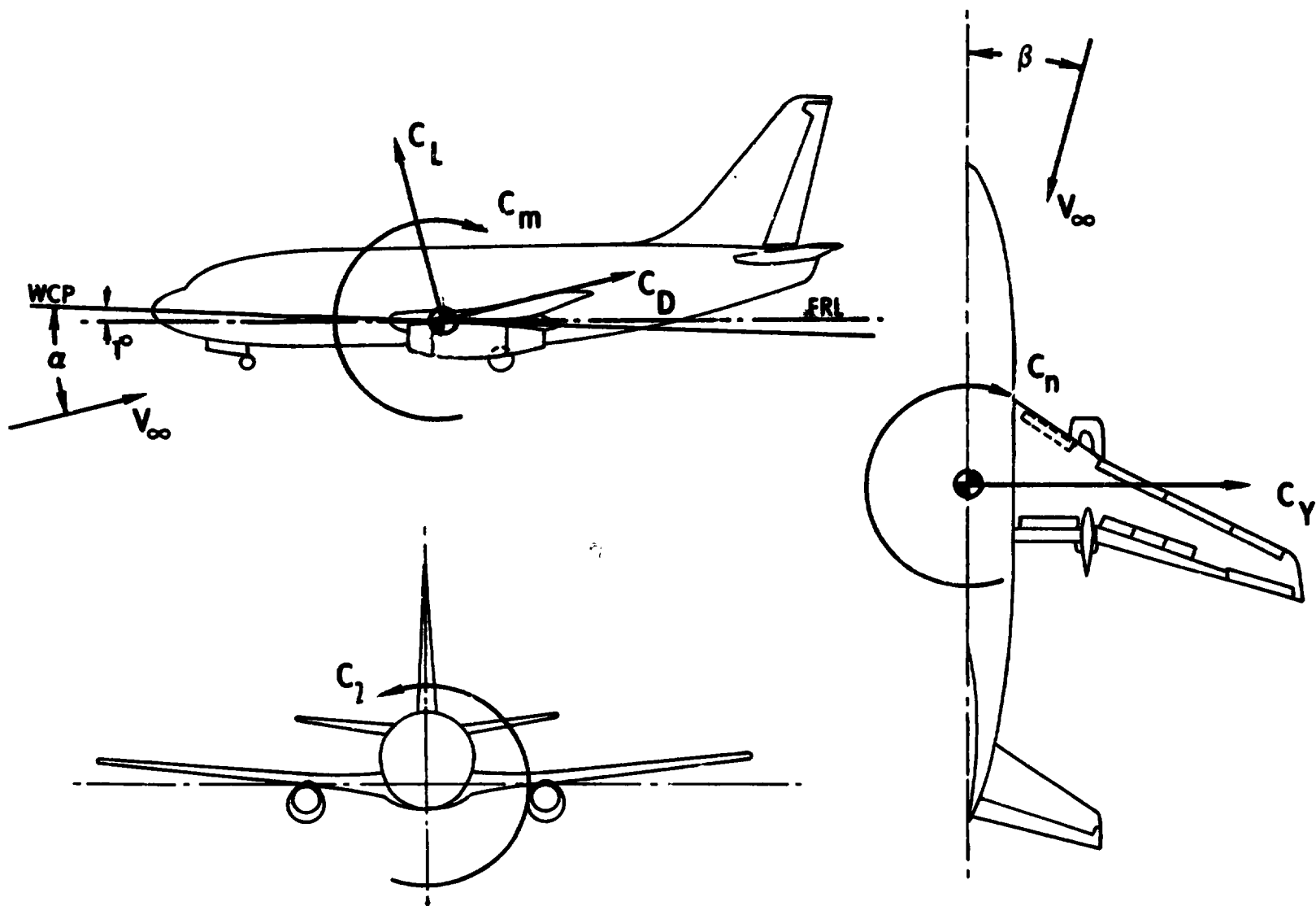


Figure 3. - Stability axis system used for data presentation.

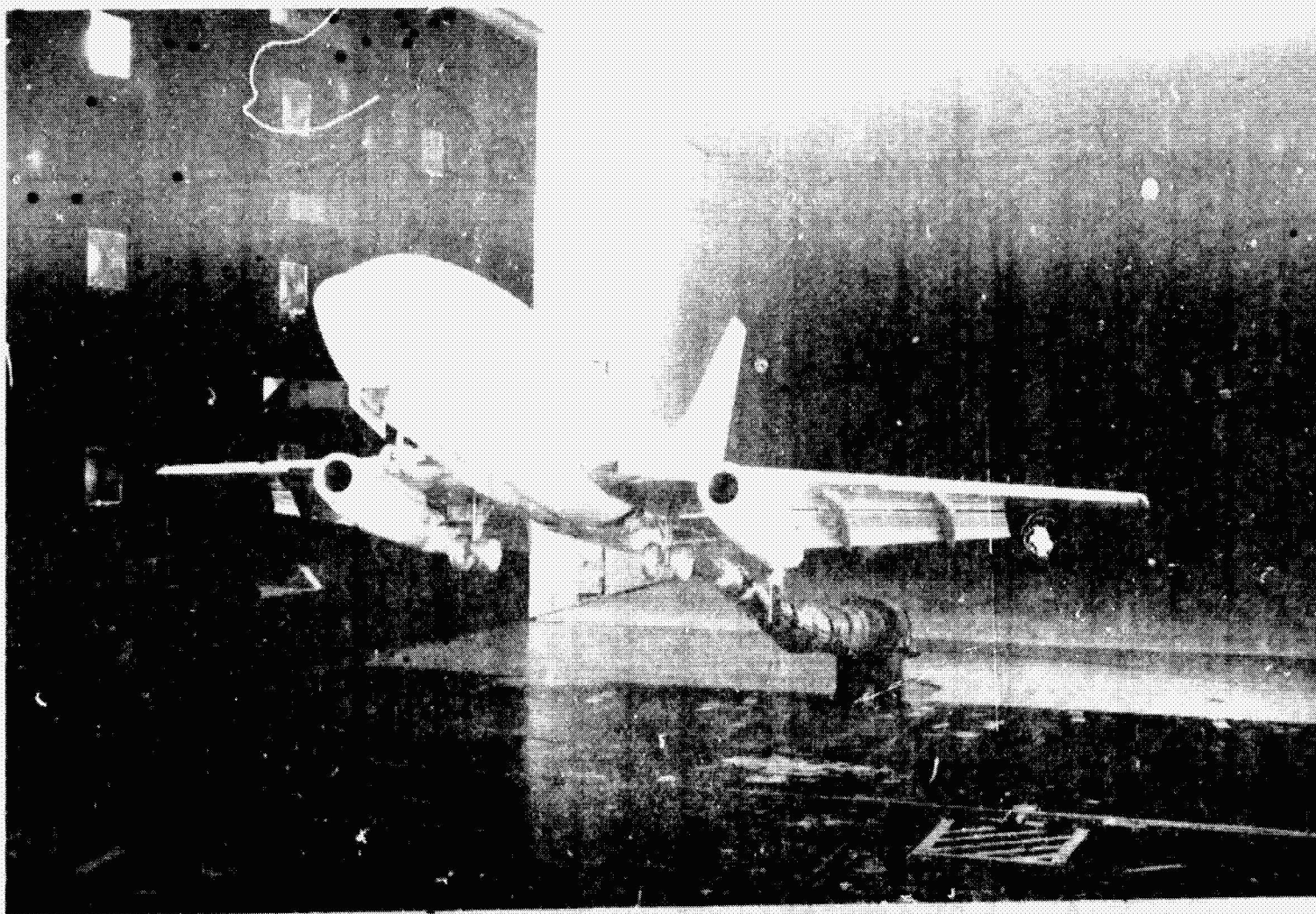


Figure 4. - Installation of 1/8-scale model of a twin-engine short-haul transport.

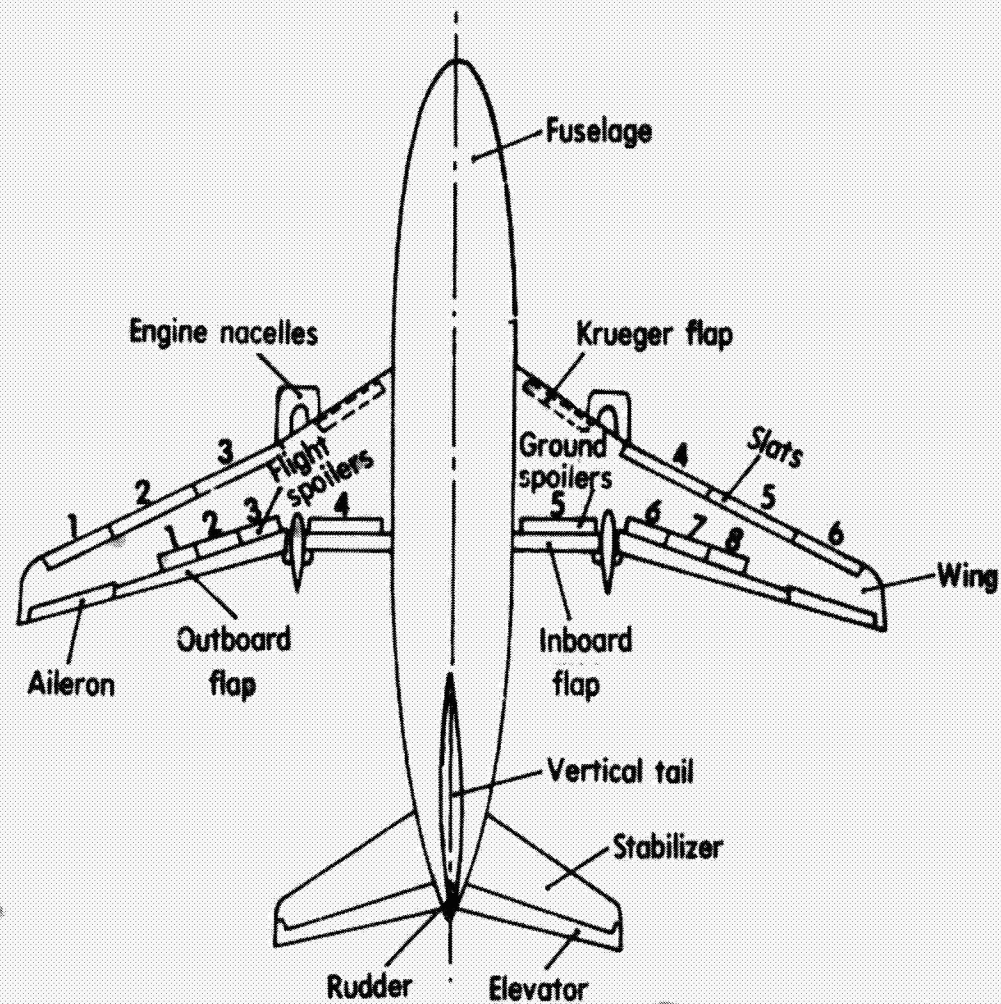


Figure 5. - Definition of components of 1/8-scale model of a twin-engine short-haul transport.

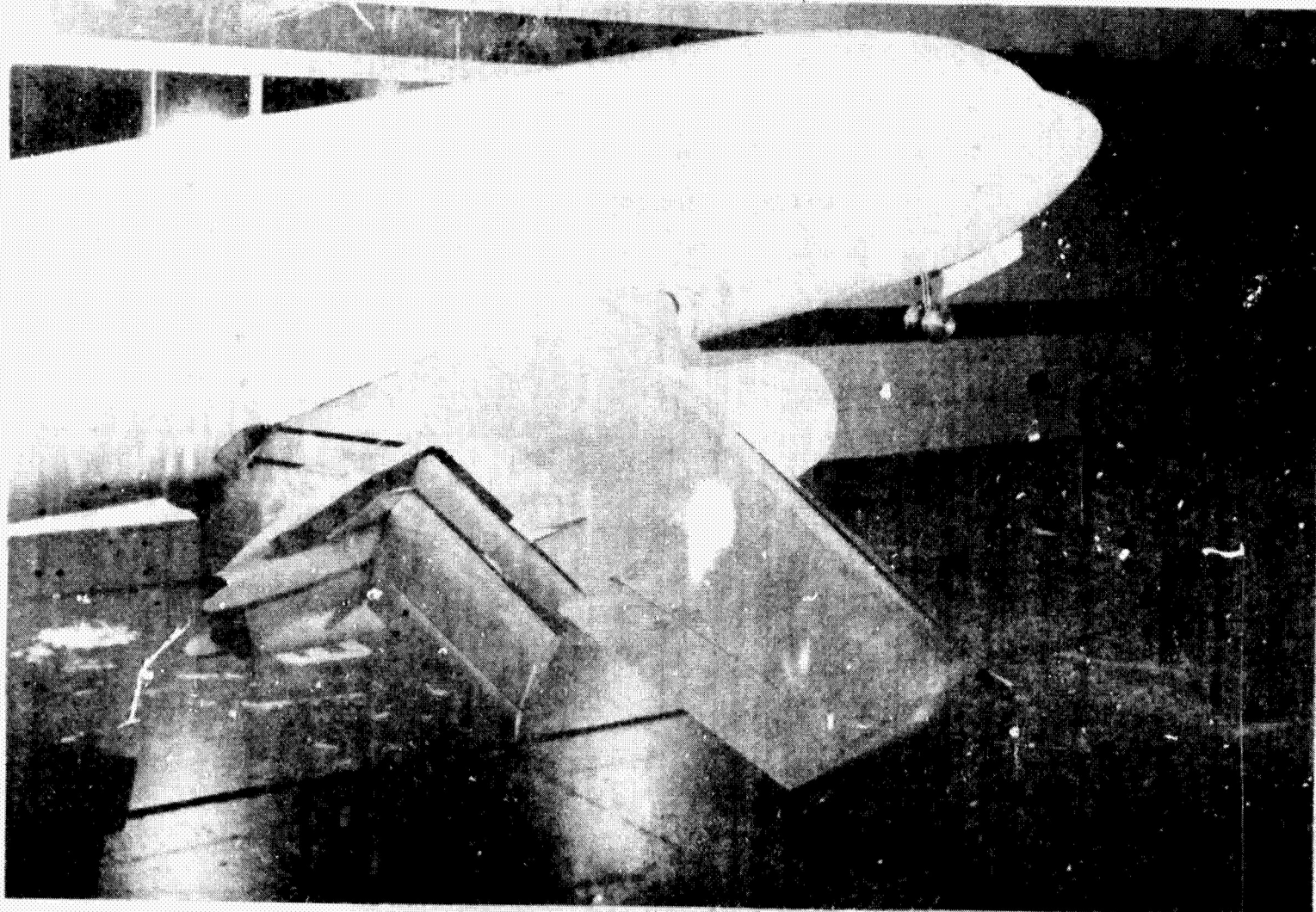


Figure 6. - Closeup of right wing of 1/8-scale model of a twin-engine short-haul transport showing approach flaps, Krueger flap, and leading-edge slat extended with spoilers 6, 7, 8 deflected.

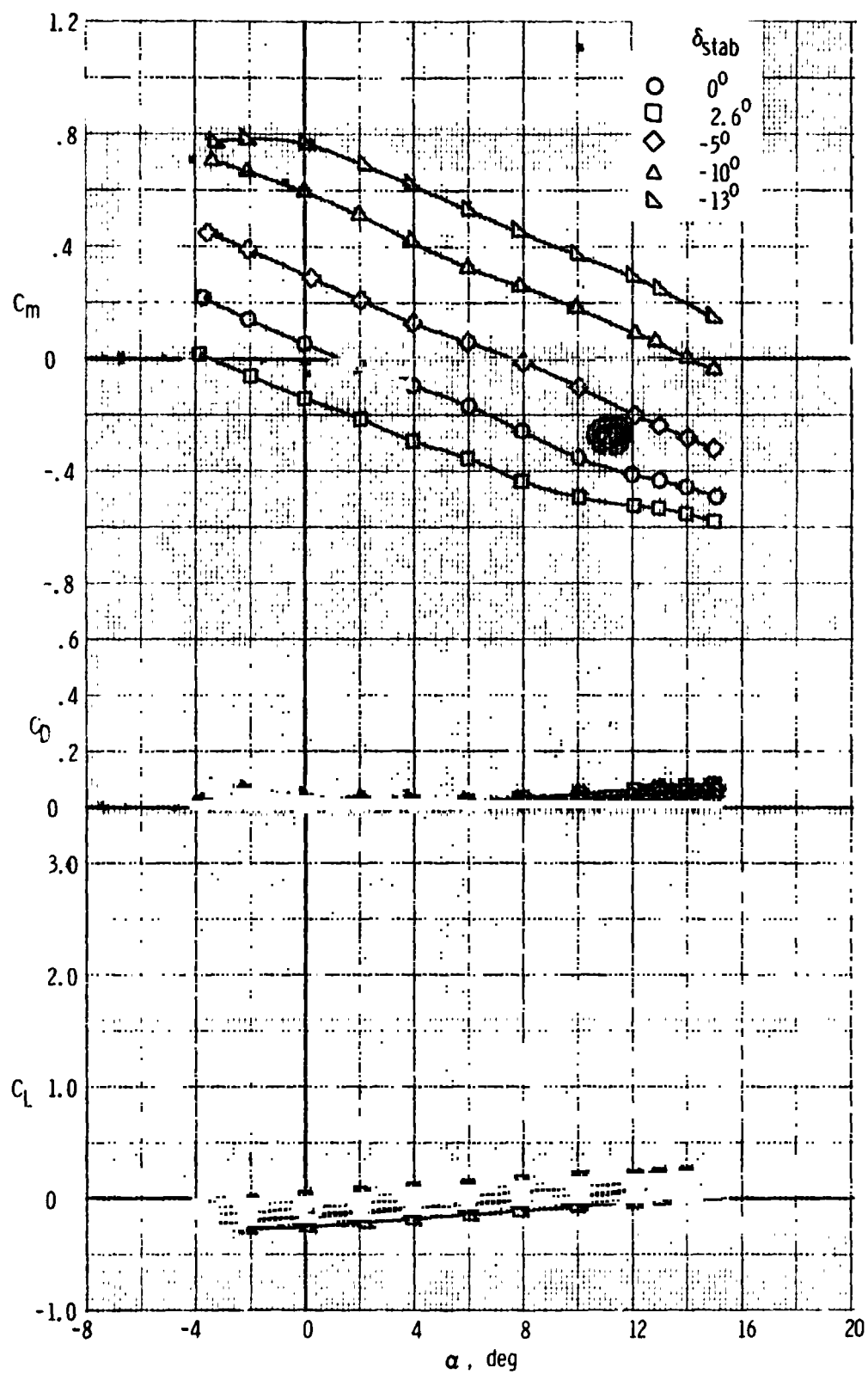
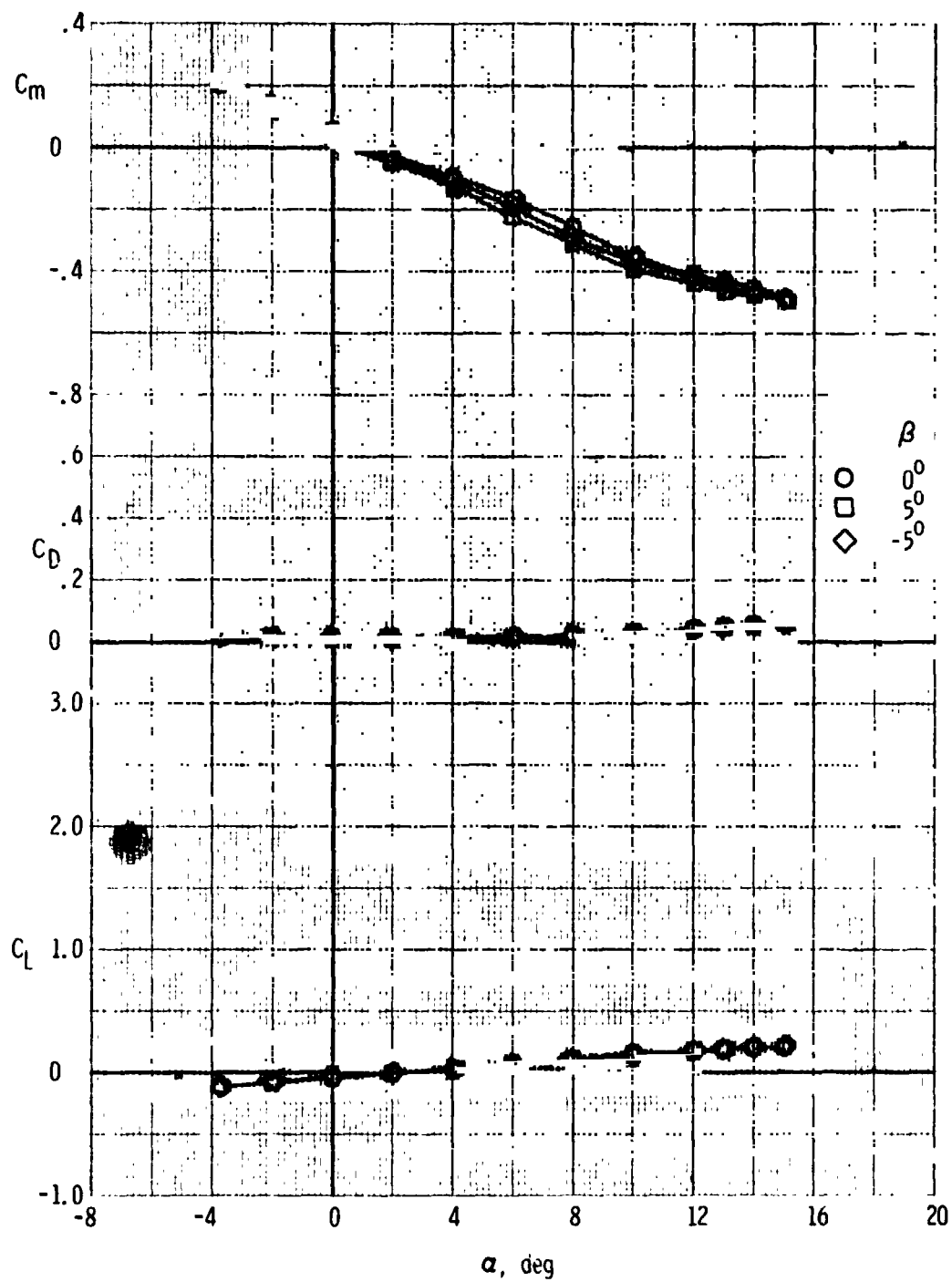
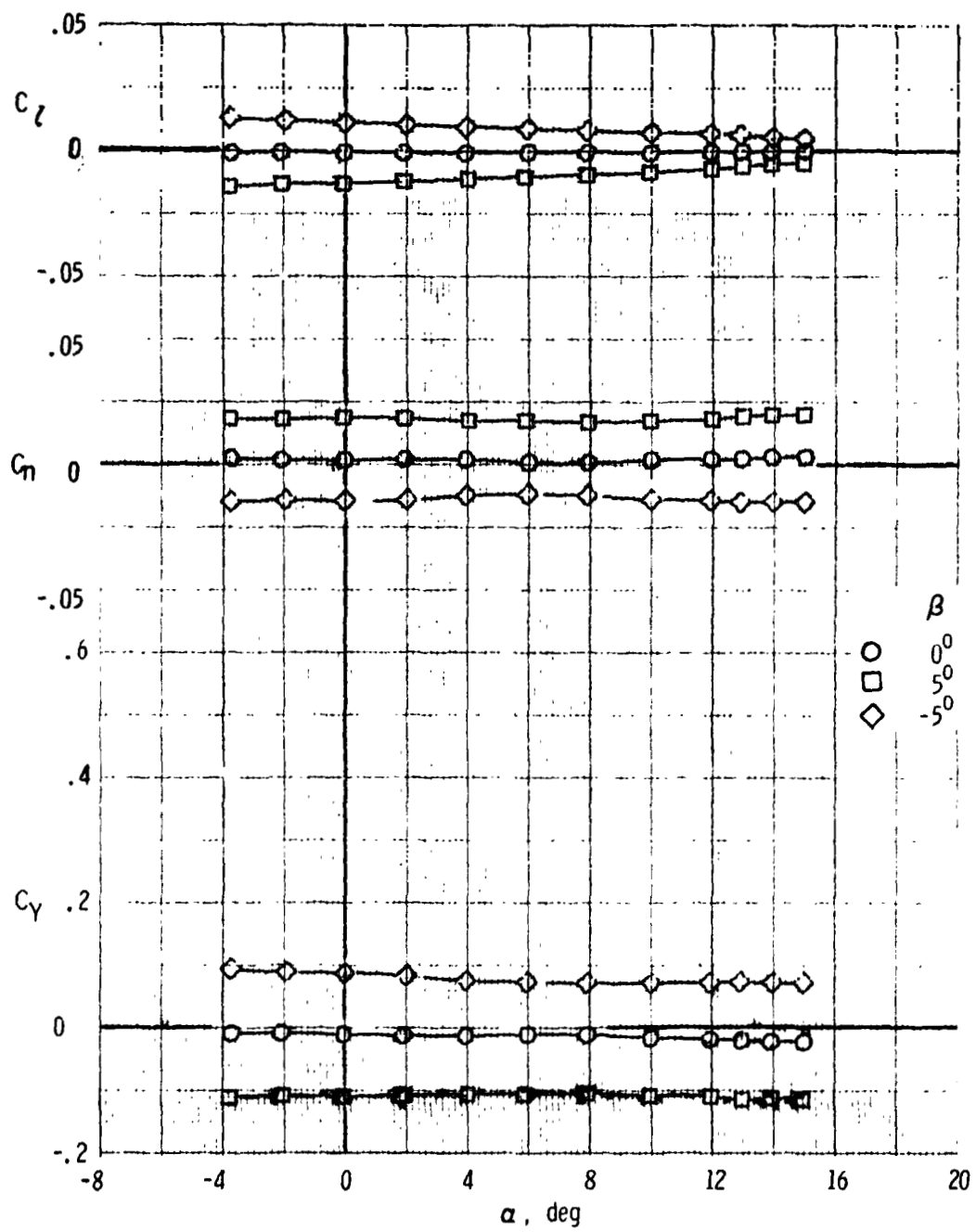


Figure 7. - Effects of stabilizer deflection on the longitudinal characteristics of the F, V_T, H_T configuration.

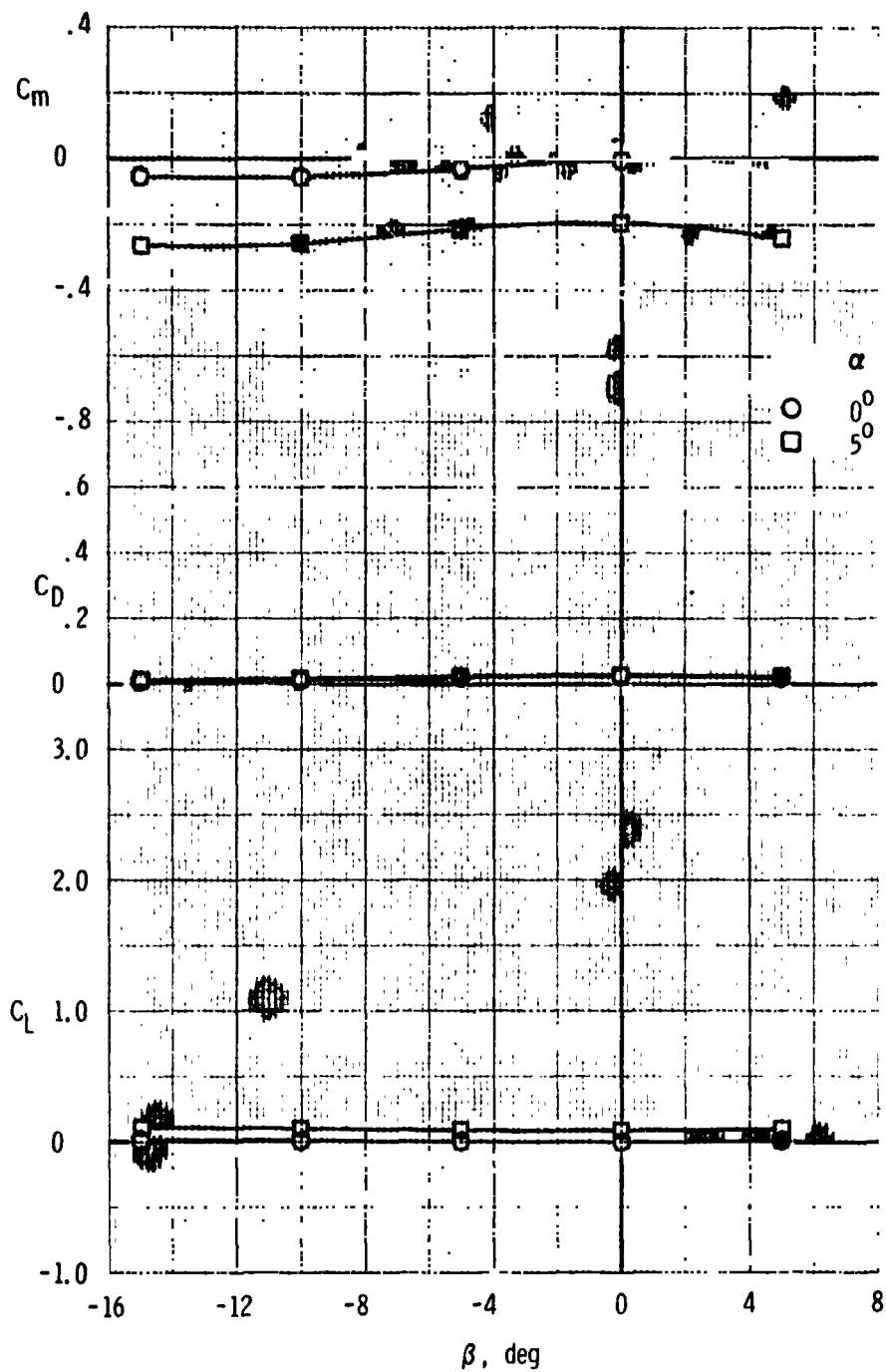


(a) Variation of longitudinal characteristics with angle of attack.

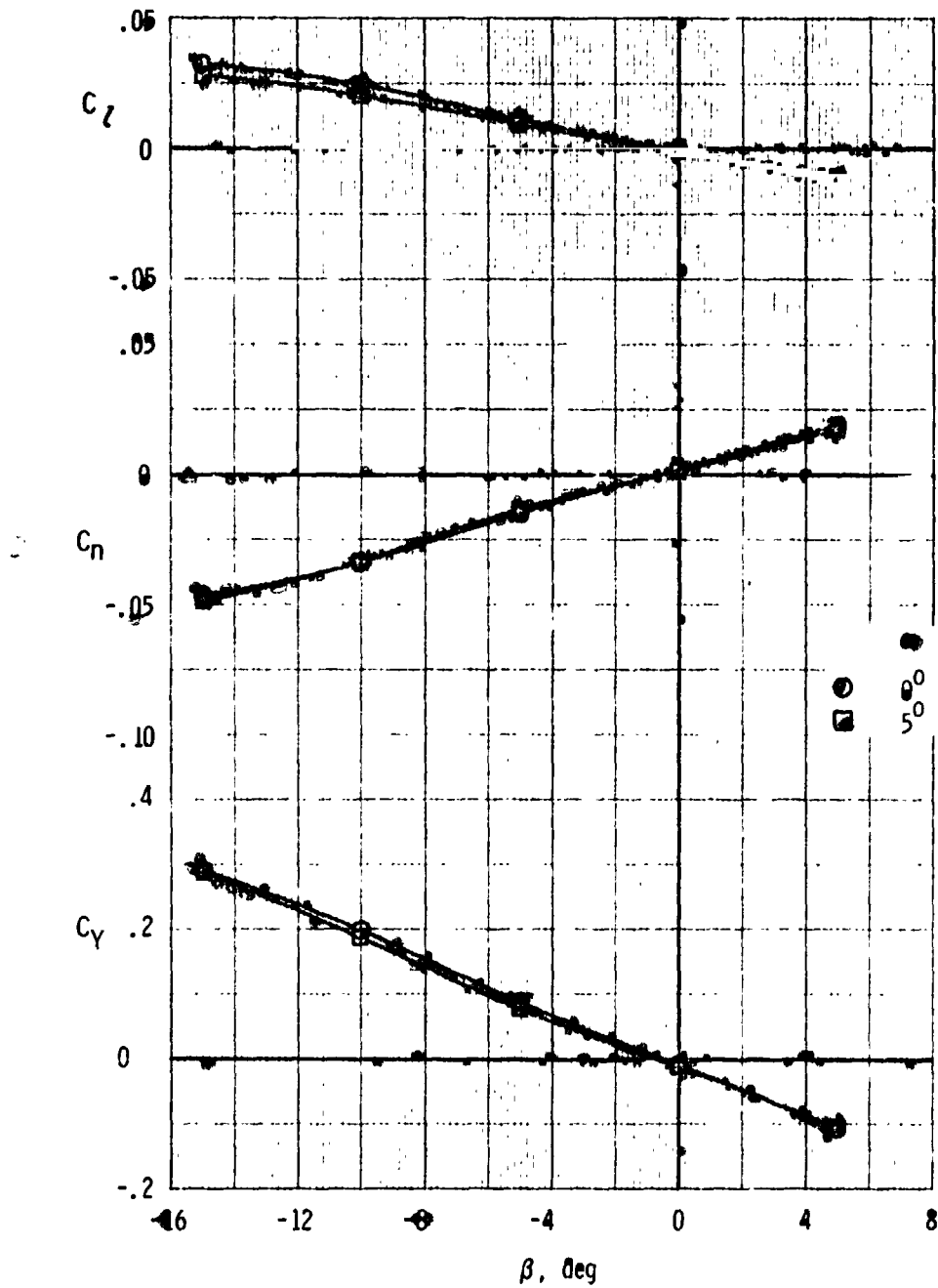
Figure 8. - Effect of sideslip on the aerodynamic characteristics of the F, V_T, N_T configuration.



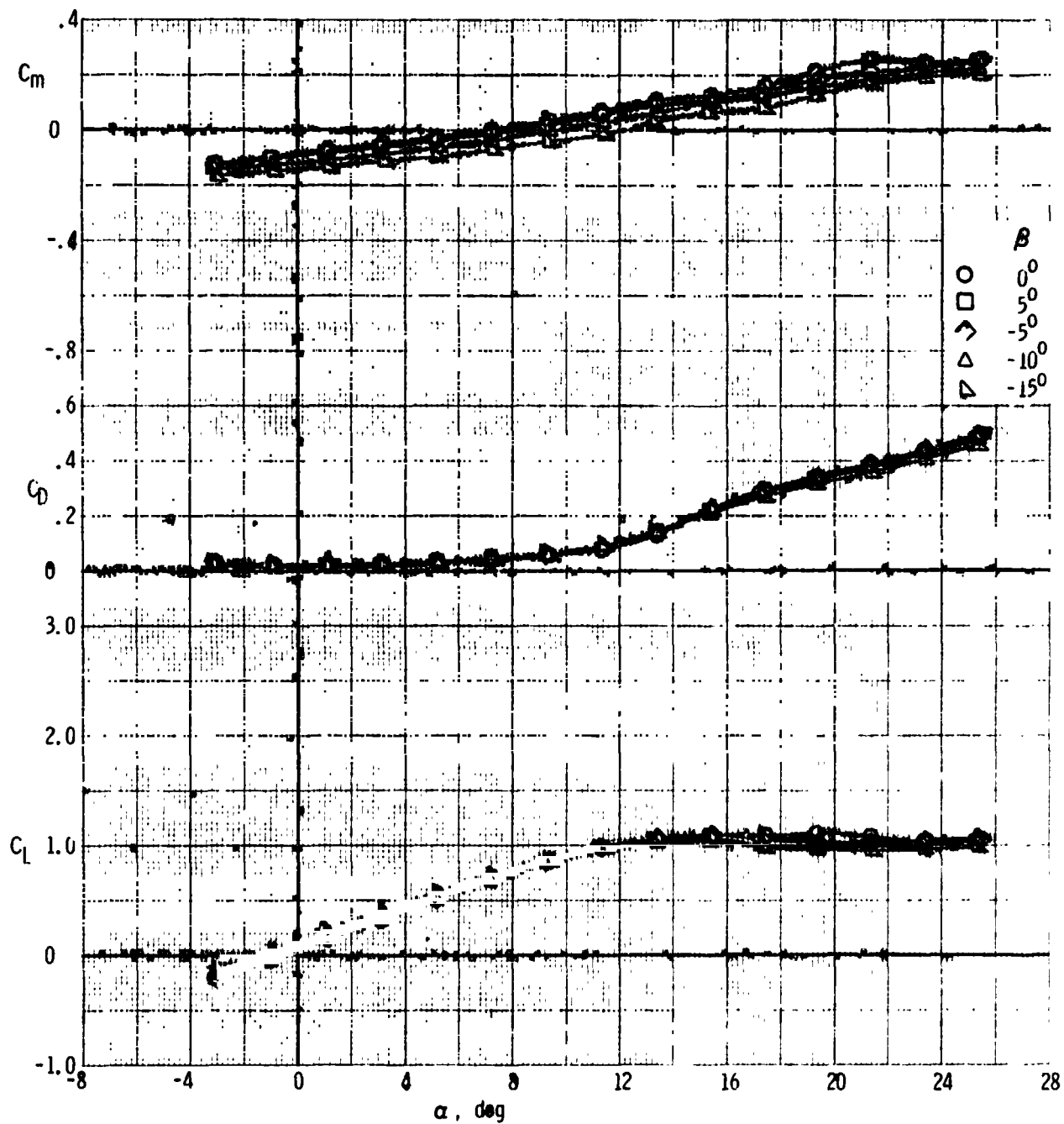
(b) Variation of lateral-directional characteristics with angle of attack.
Figure 8. - Continued.



(c) Variation of longitudinal characteristics with sideslip angle.
Figure 8. - Continued.

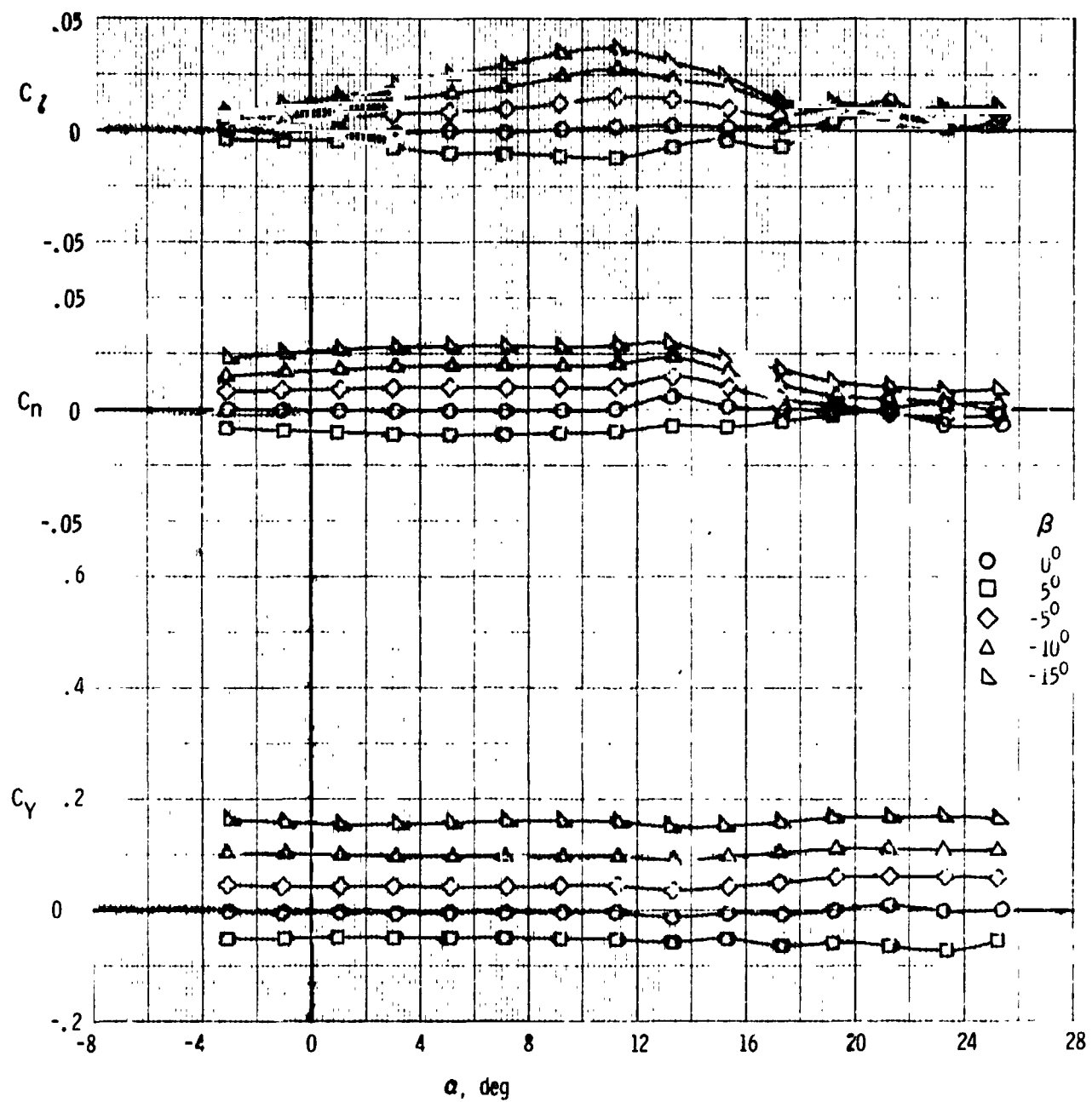


(d) Variation of lateral-directional characteristics with sideslip angle.
Figure 8 - Concluded.



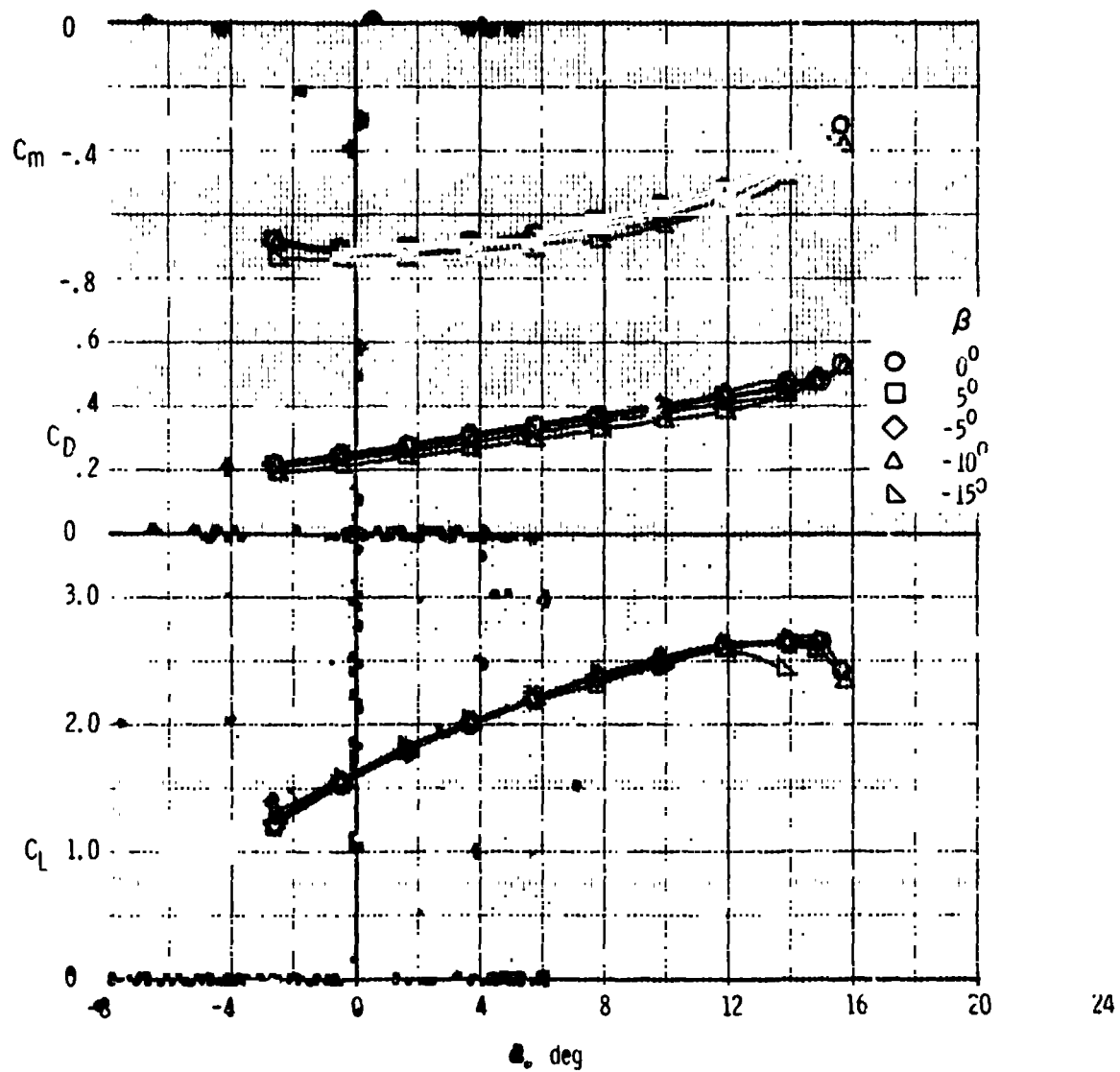
(a) Longitudinal characteristics

Figure 9. - Effect of sideslip on the aerodynamic characteristics of the F, W, F₀N configuration.



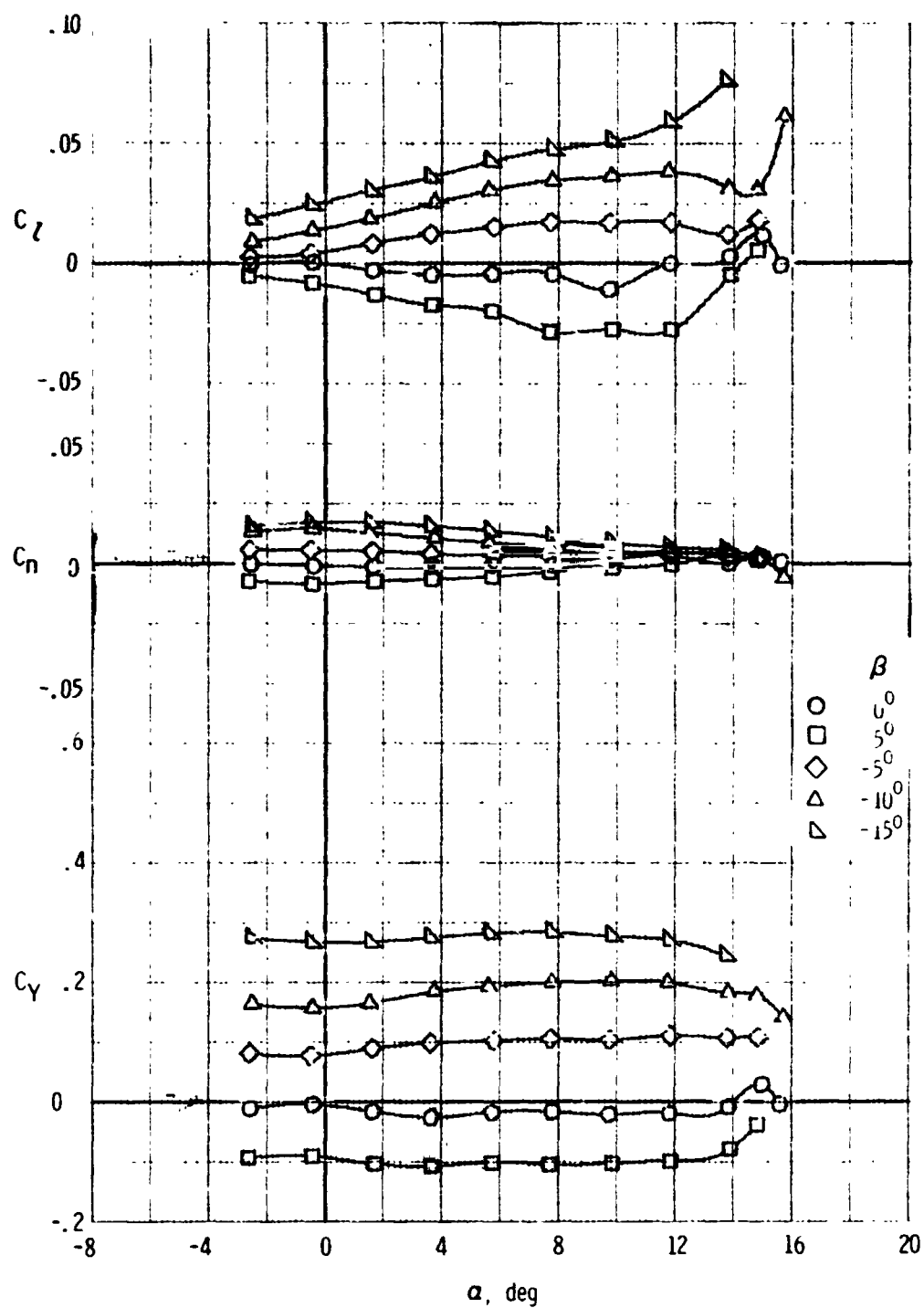
(b) Lateral-directional characteristics

Figure 9. - Concluded.



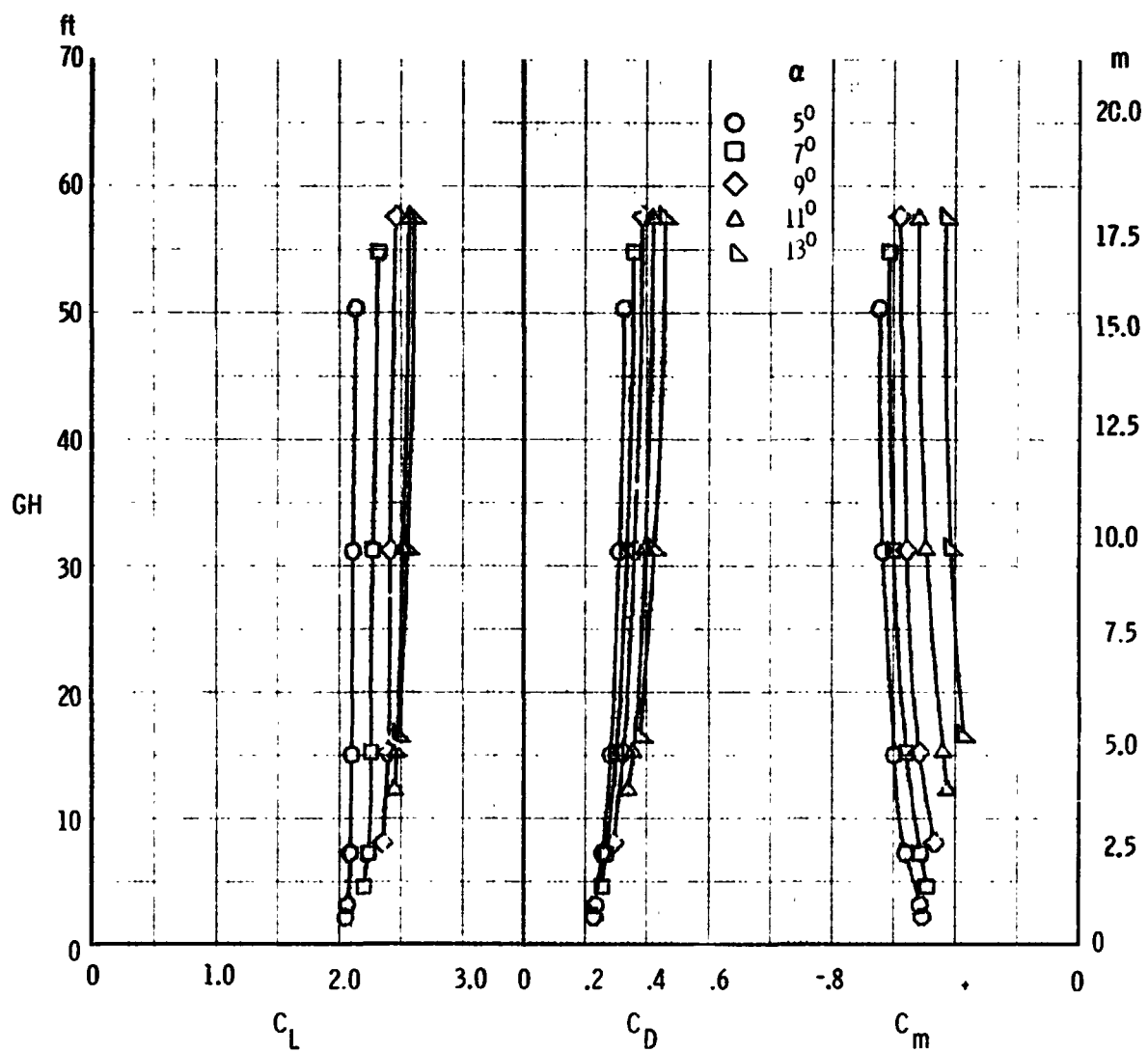
(a) Longitudinal characteristics

Figure 10. - Effect of sideslip on the aerodynamic characteristics of the F.W.F₄₀N configuration.



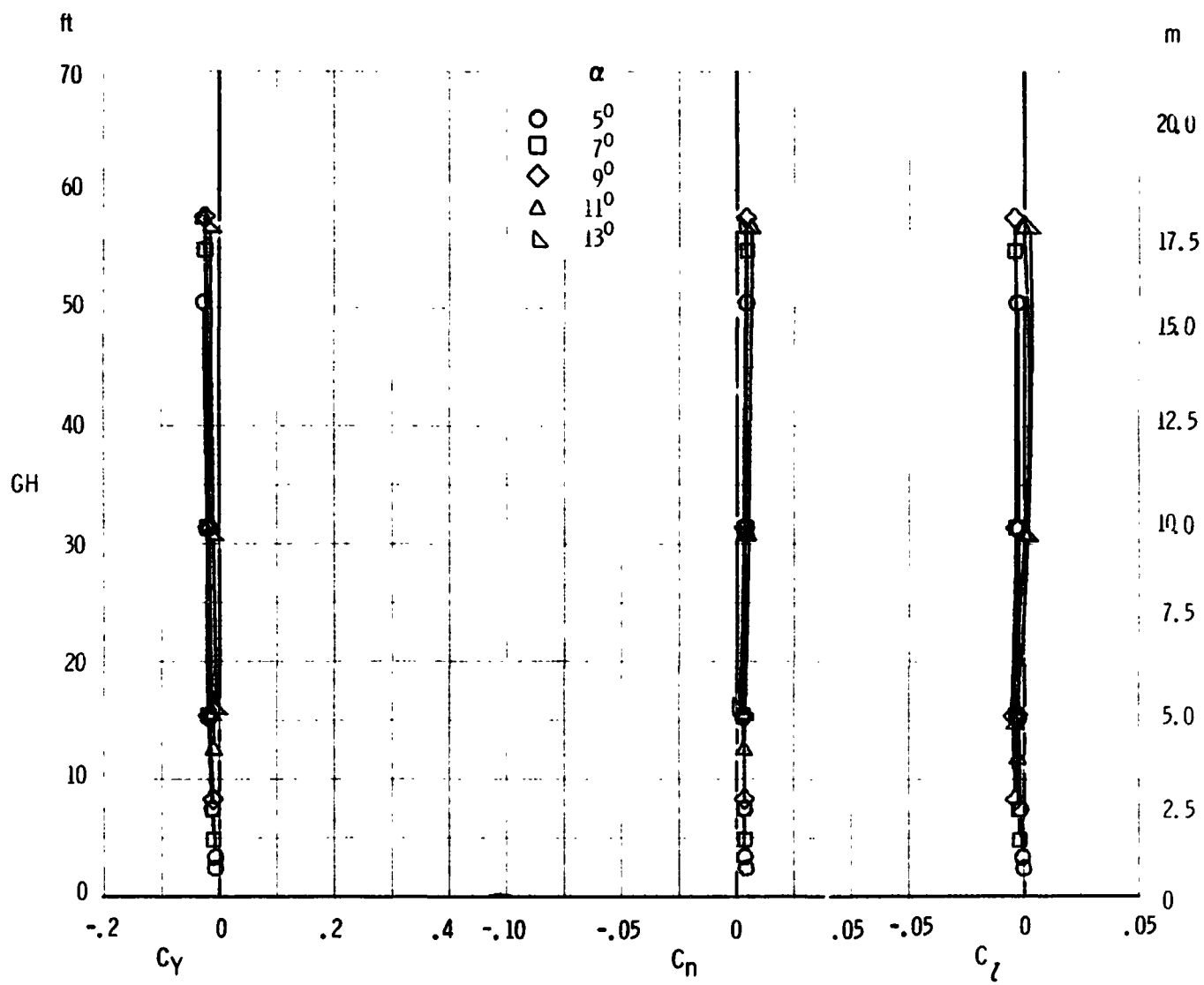
(b) Lateral-directional characteristics

Figure 10. - Concluded.



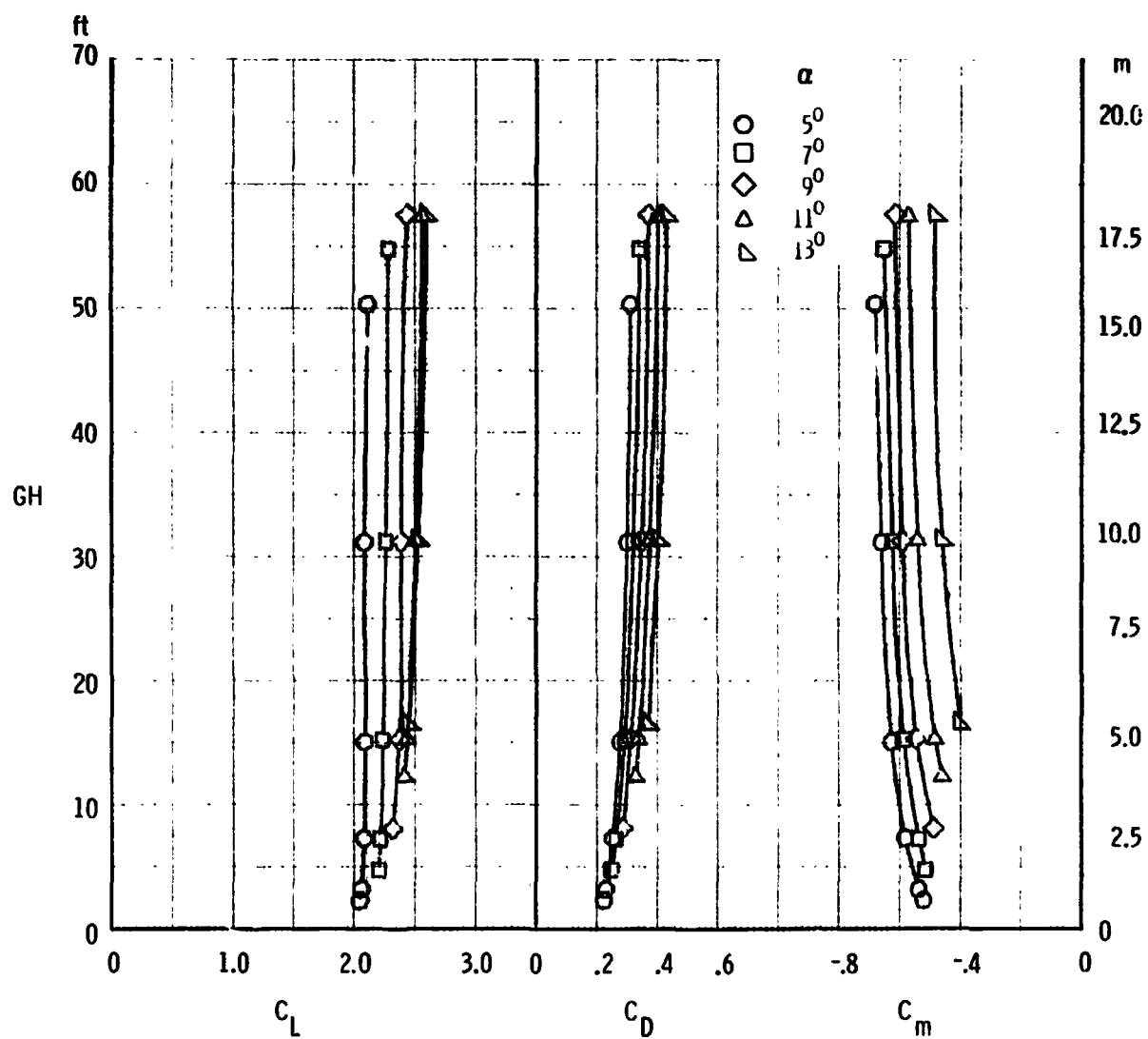
(a) Longitudinal characteristics, $\beta = 0^\circ$

Figure 11. - Effect of ground height on the aerodynamic characteristics of the F, W, F_{40°}N configuration at several values of β .



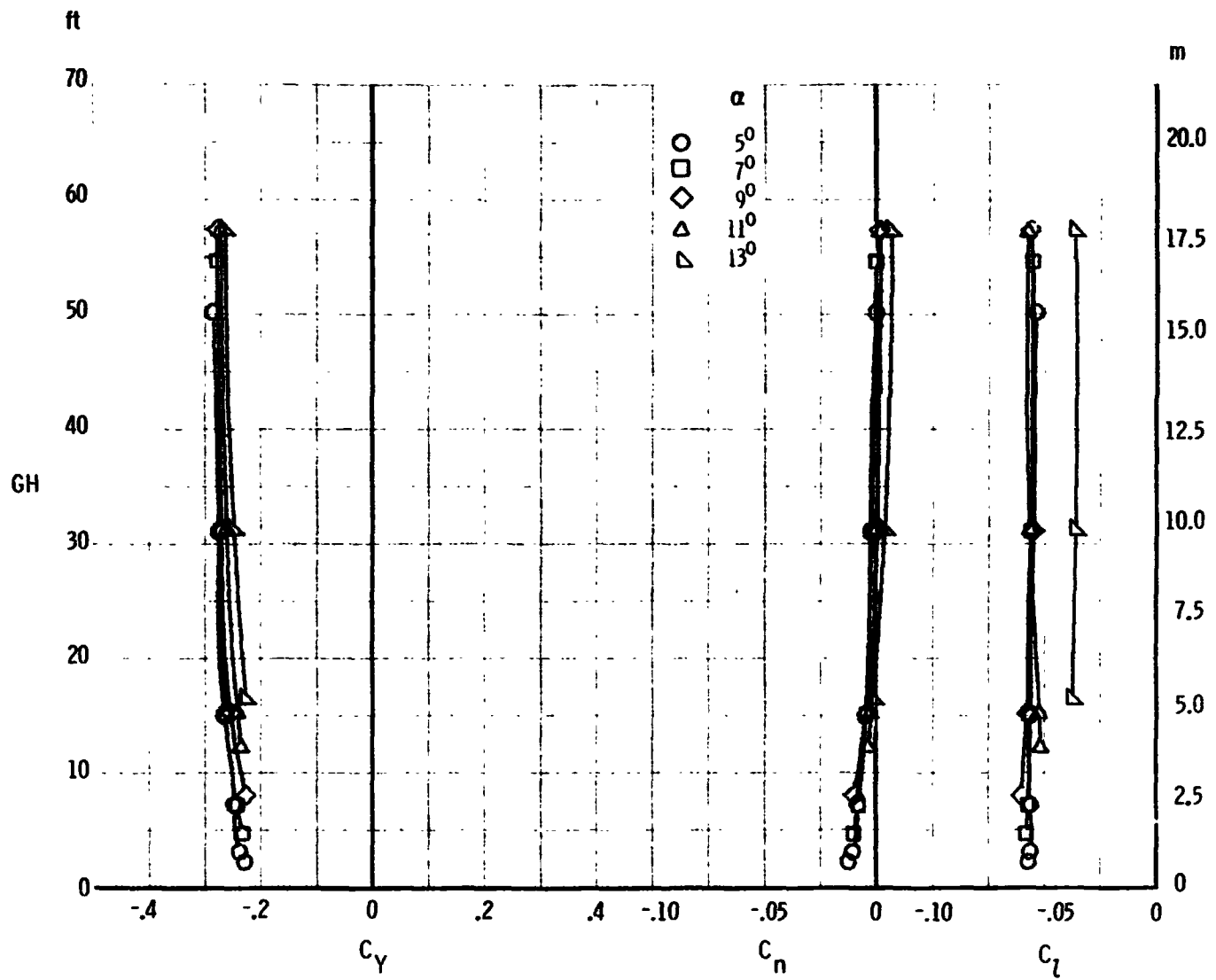
(b) Lateral-directional characteristics, $\beta = 0^\circ$

Figure 11. - Continued.



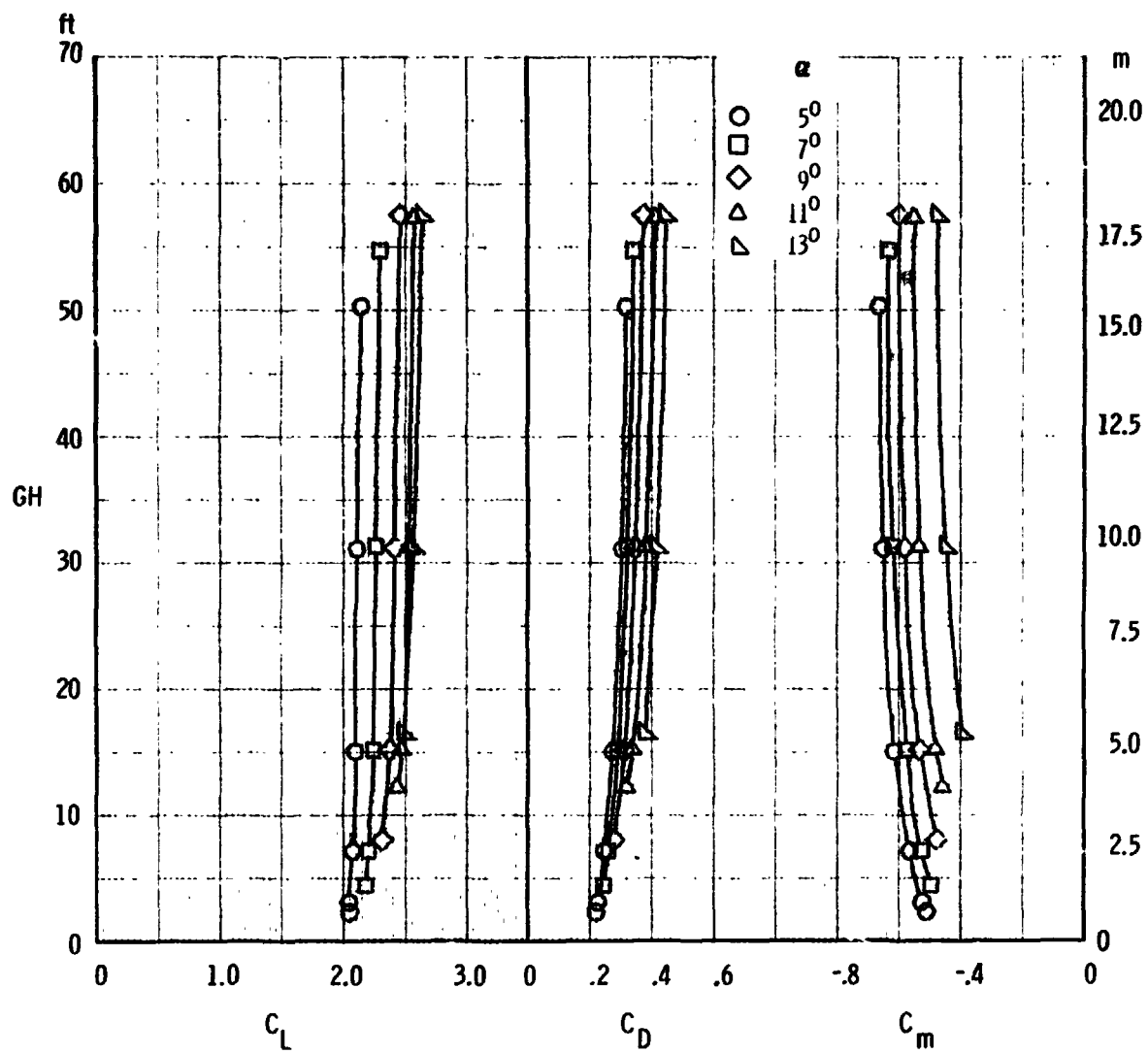
(c) Longitudinal characteristics, $\beta = 5^\circ$

Figure 11. - Continued.



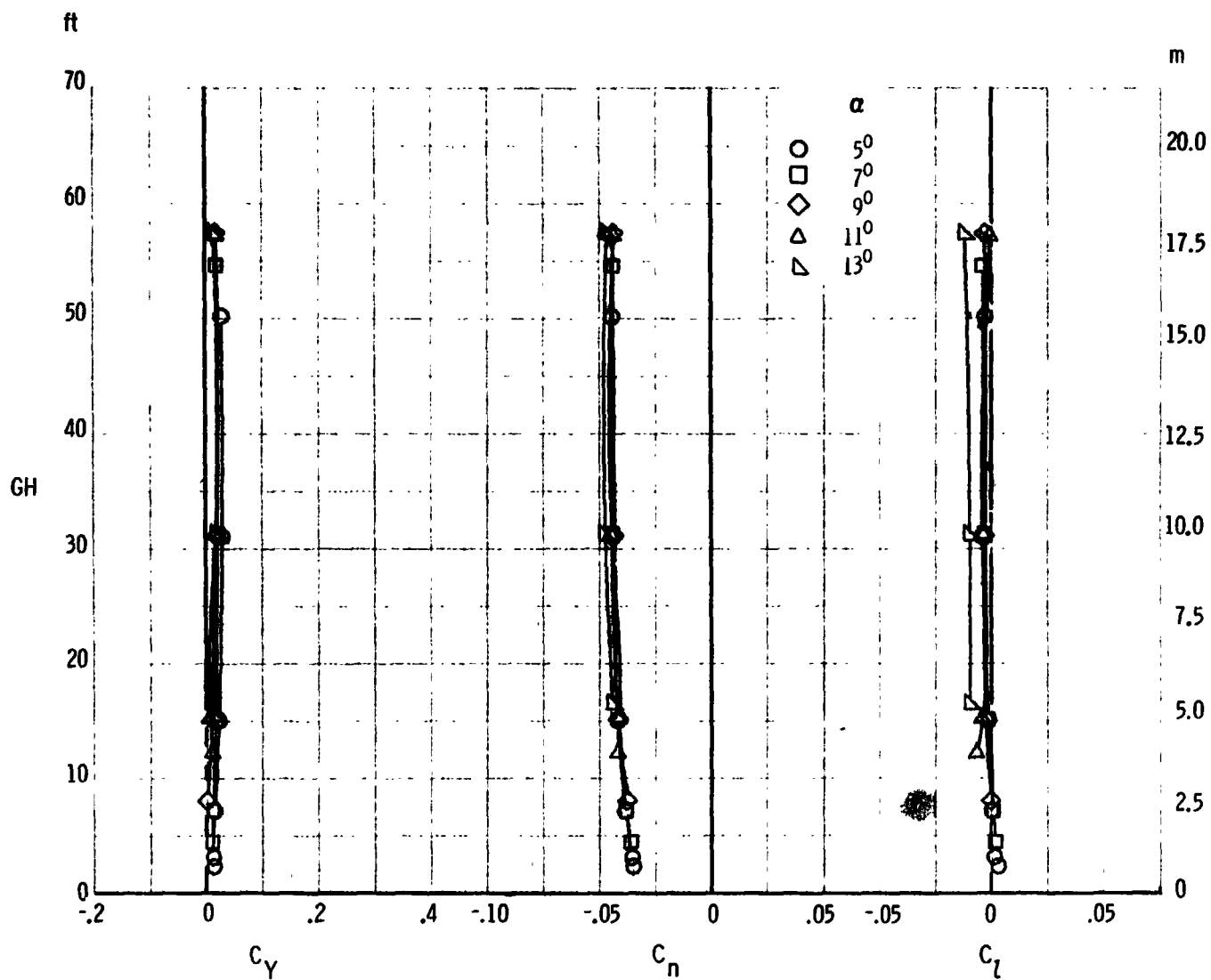
(d) Lateral-directional characteristics, $\beta = 5^\circ$

Figure 11. - Continued.



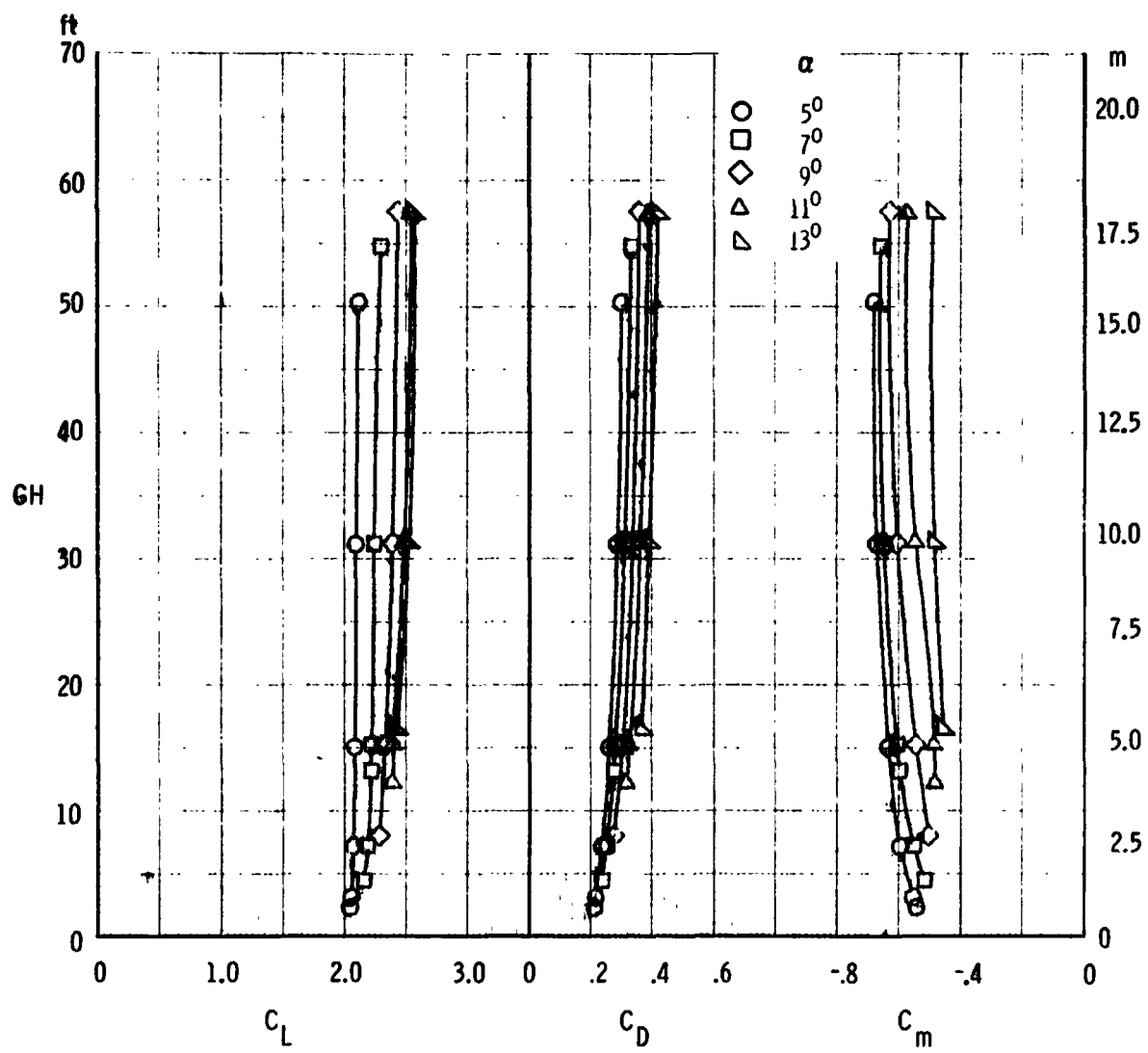
(e) Longitudinal characteristics, $\beta = -5^\circ$

Figure 11. - Continued.



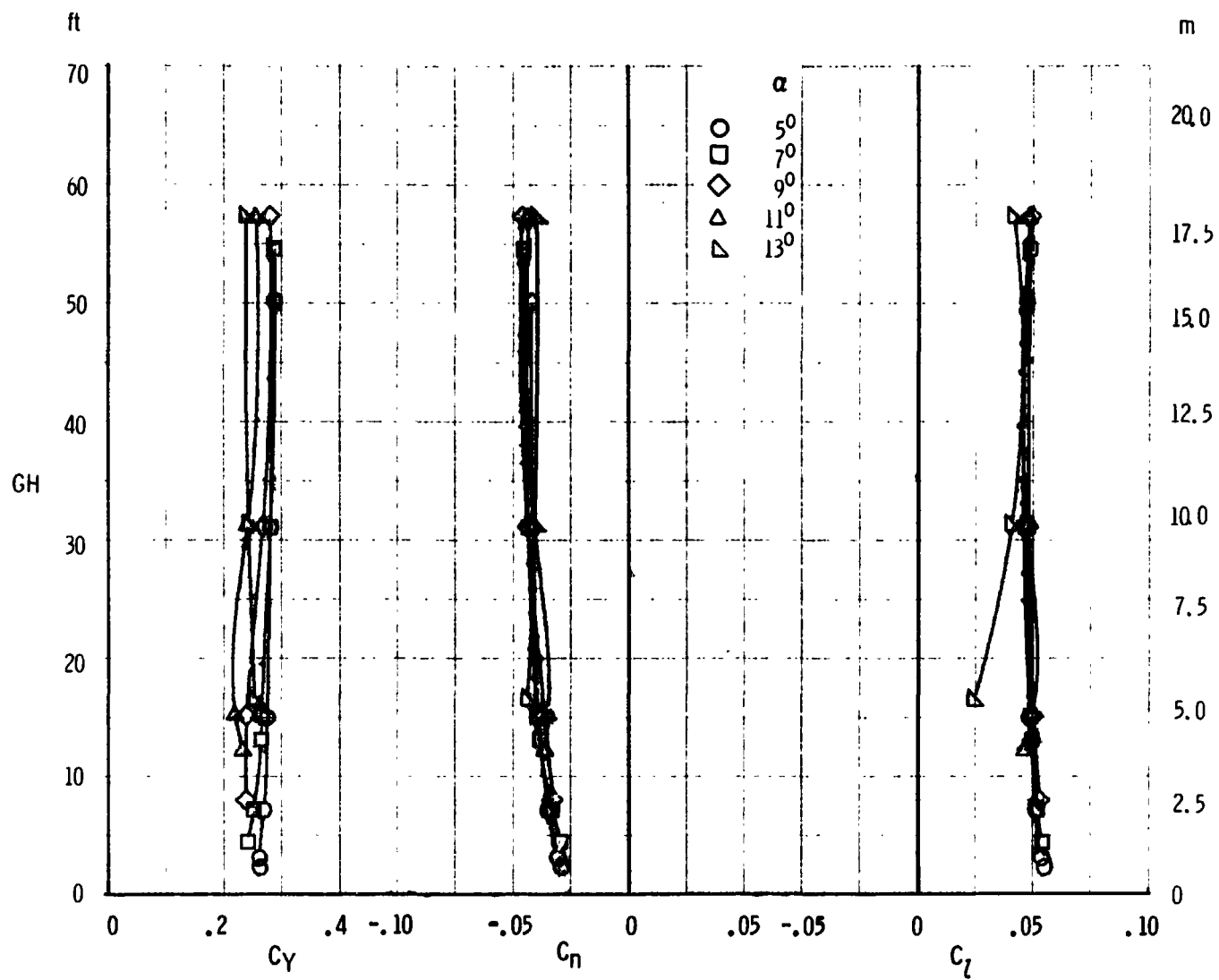
(f) Lateral-directional characteristics, $\beta = -5^\circ$

Figure 11. - Continued.



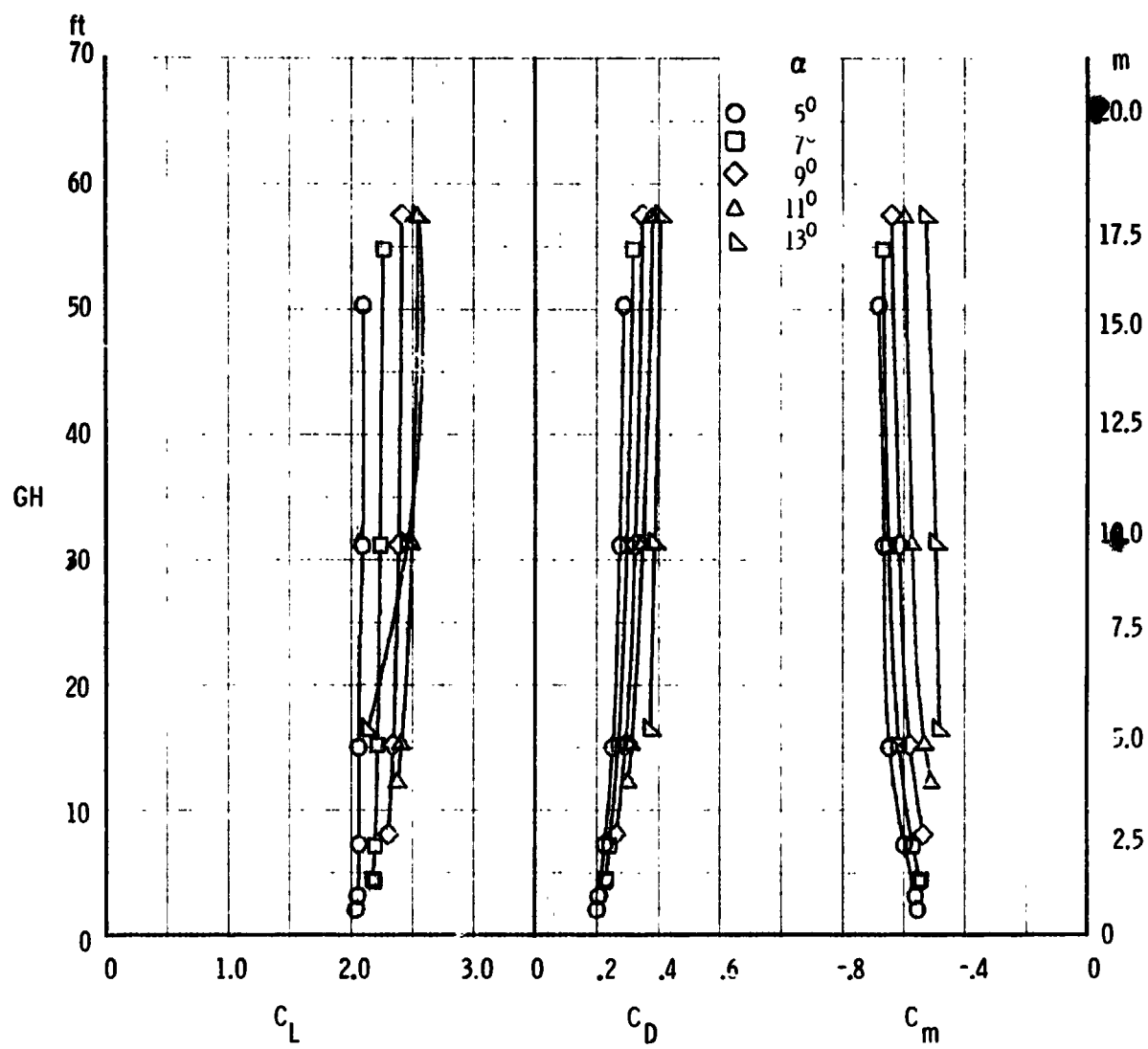
(g) Longitudinal characteristics, $\beta = 10^0$

Figure 11. - Continued.



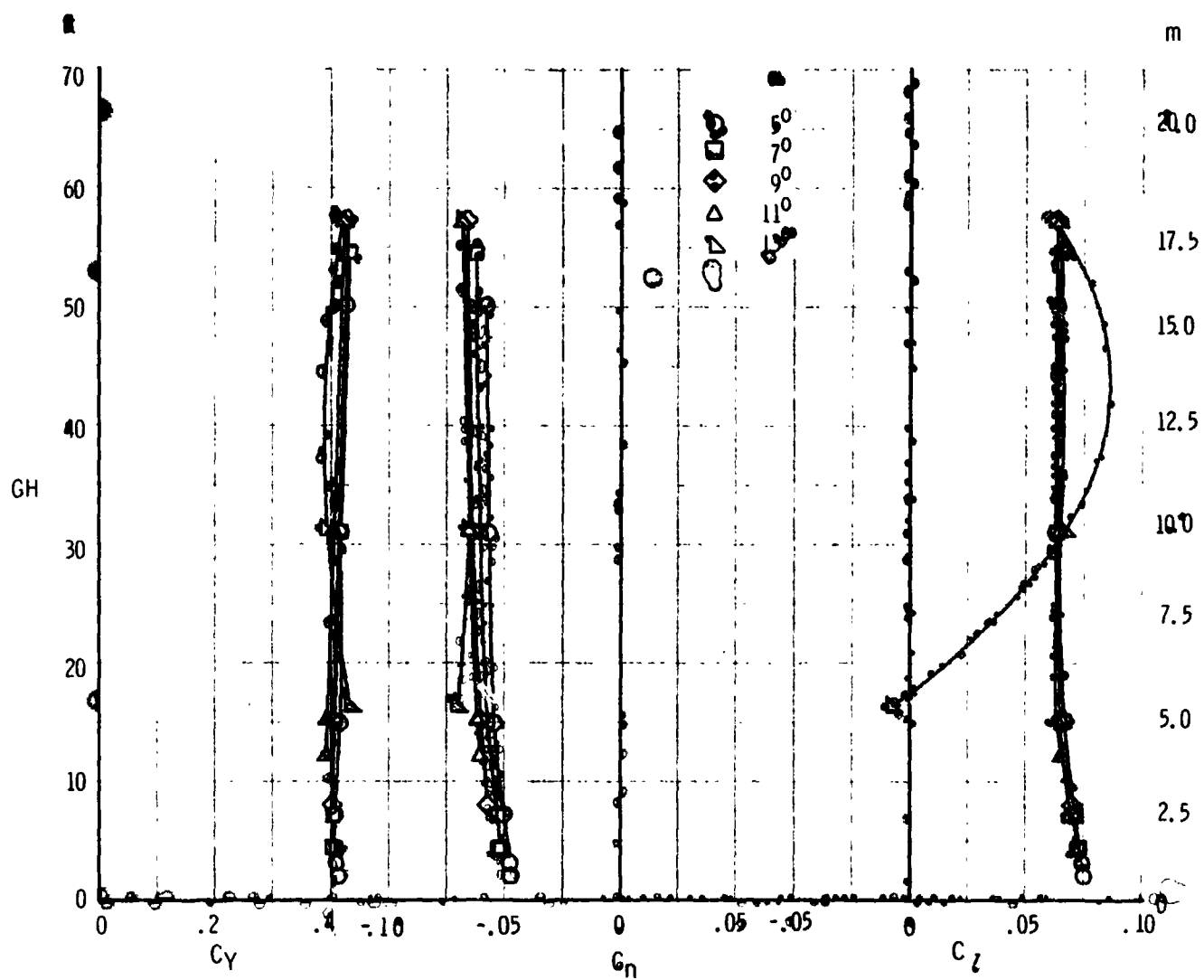
(h) Lateral-directional characteristics, $\beta = -10^\circ$

Figure 11. - Continued.



(i) Longitudinal characteristics, $\beta = -15^\circ$

Figure 11. - Continued.



(h) lateral-directional characteristics, $\beta = -15^\circ$

Figure 11 - Concluded.

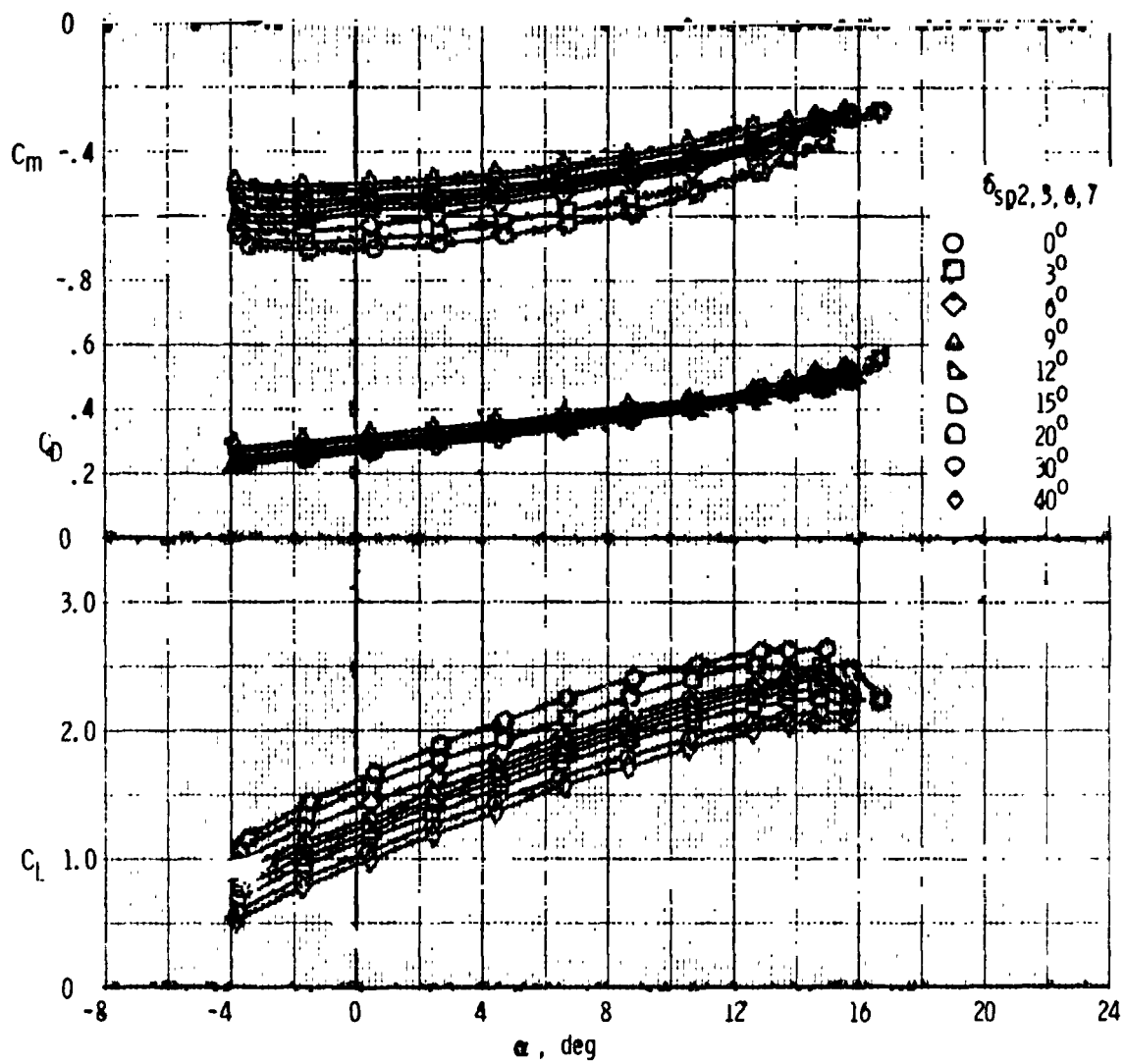
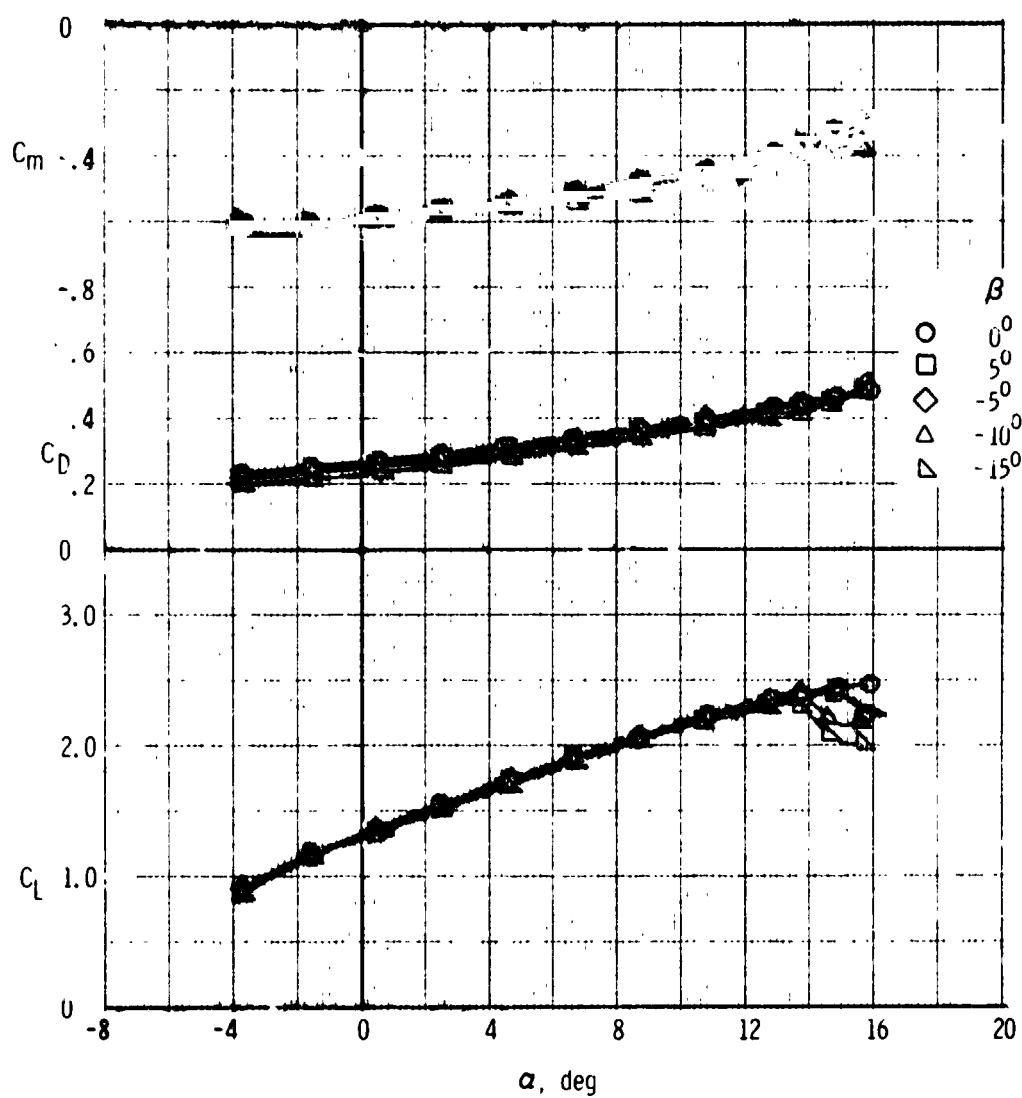
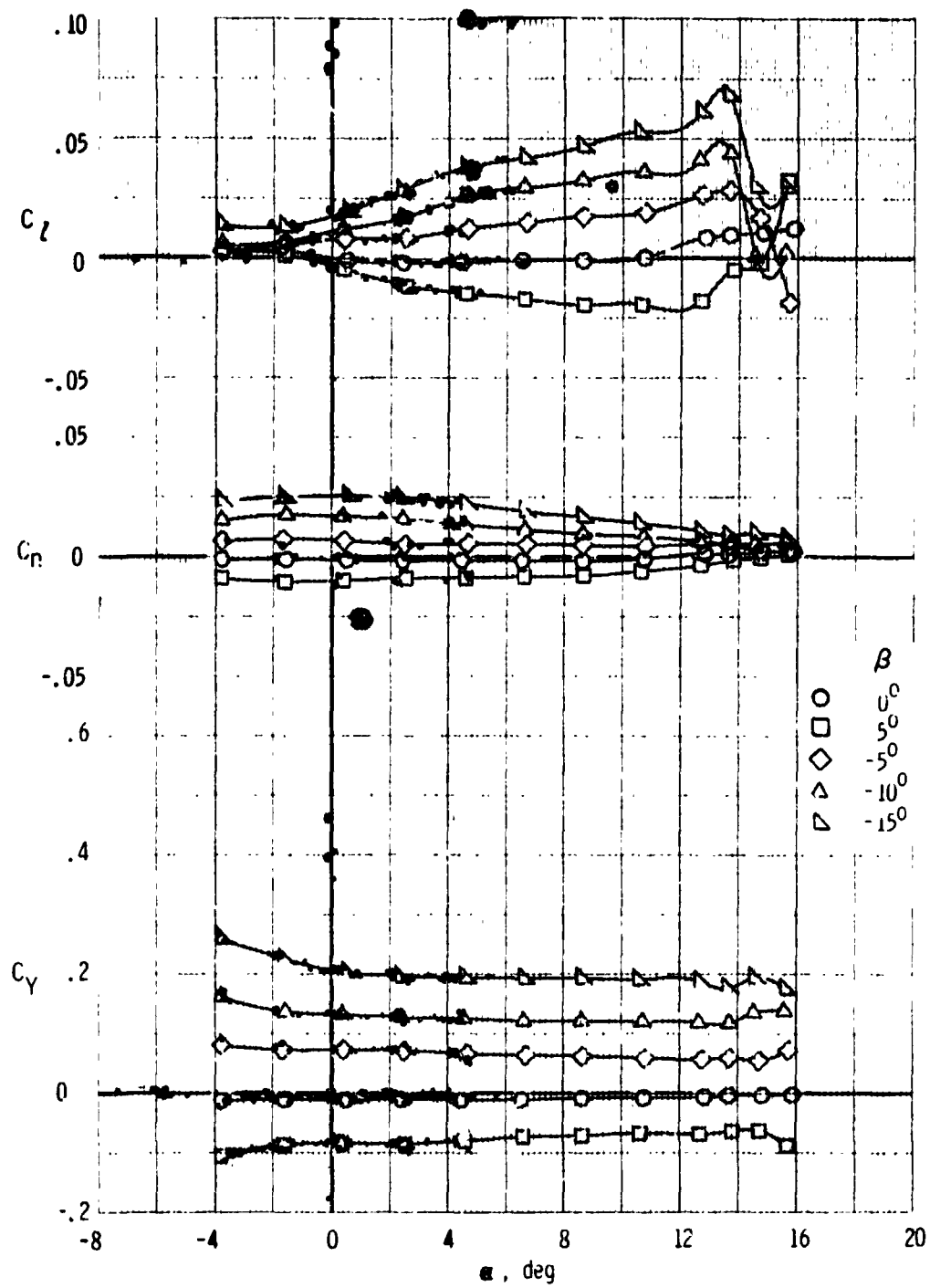


Figure 12. - Effect of DLC spoilers on the longitudinal aerodynamic characteristics of the F, W, F₄₀, N, G configuration.



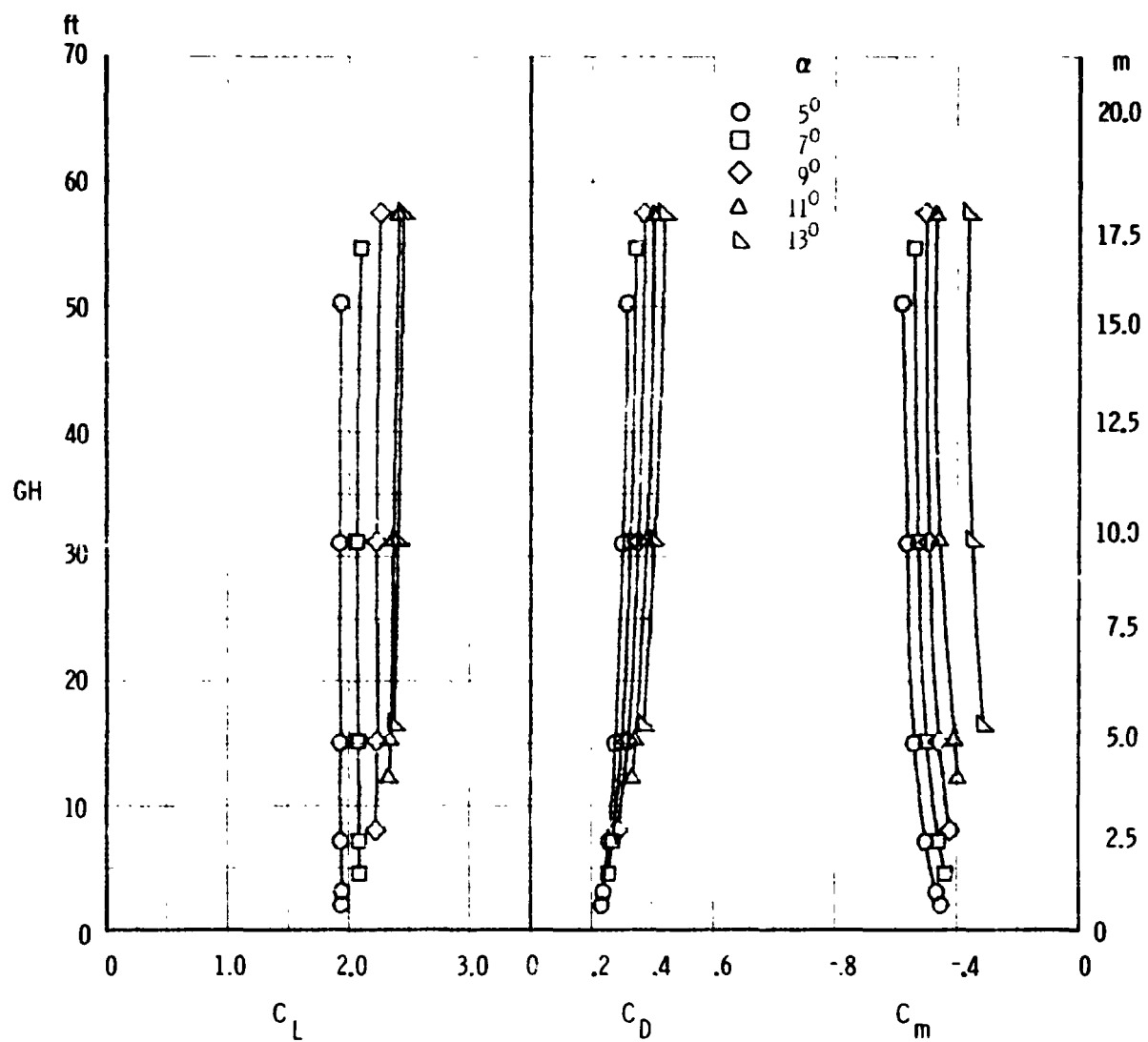
(a) Longitudinal characteristics, $\delta_{sp2,3,6,7} = 90^\circ$

Figure 13. - Effect of sideslip on the aerodynamic characteristics of the F.W.F.₄₀ N.G configuration with DLC spoilers.



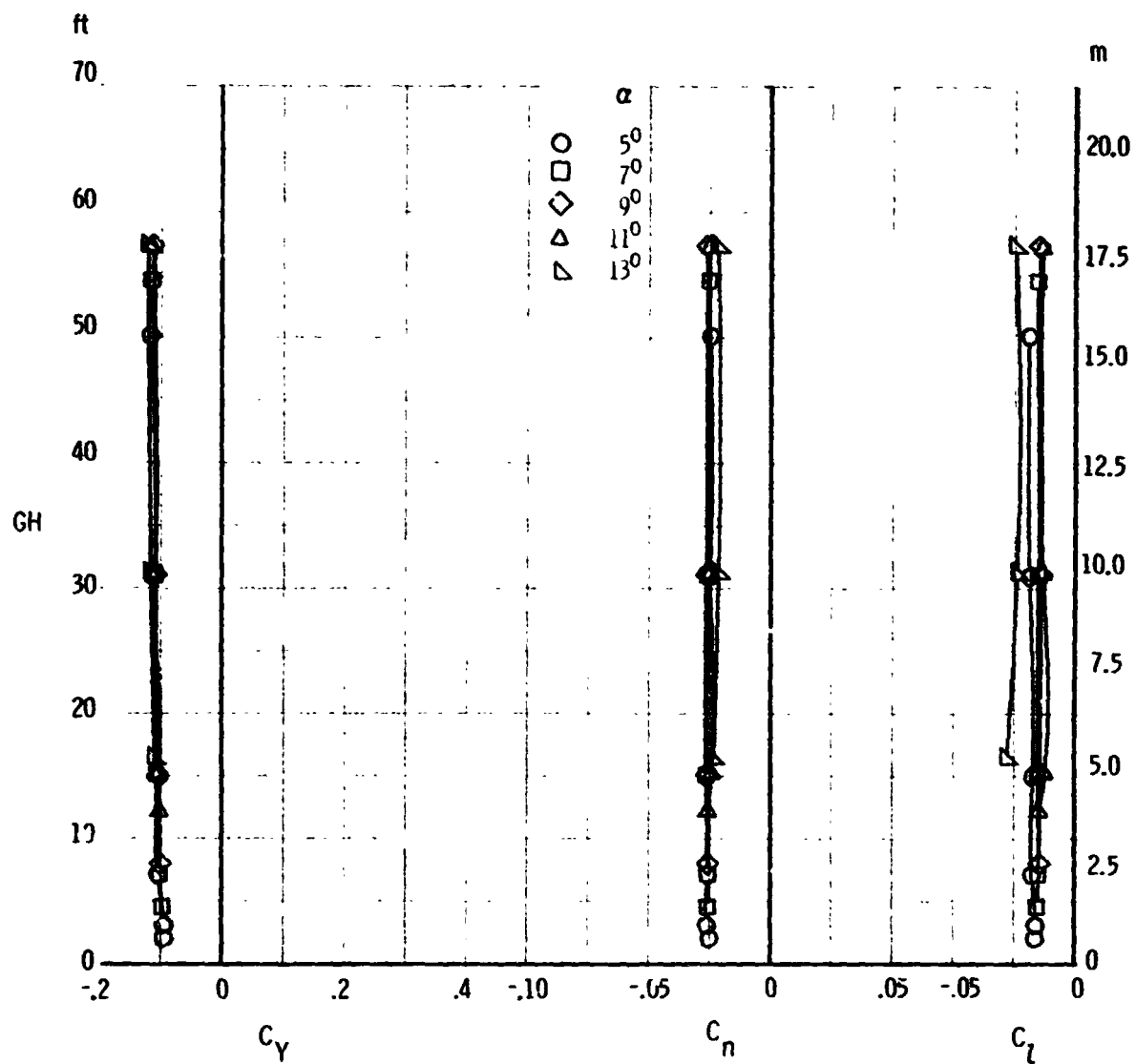
(b) Lateral-directional characteristics, $\delta_{sp2,3,6,7} = 9^\circ$

Figure 11 - Concluded.

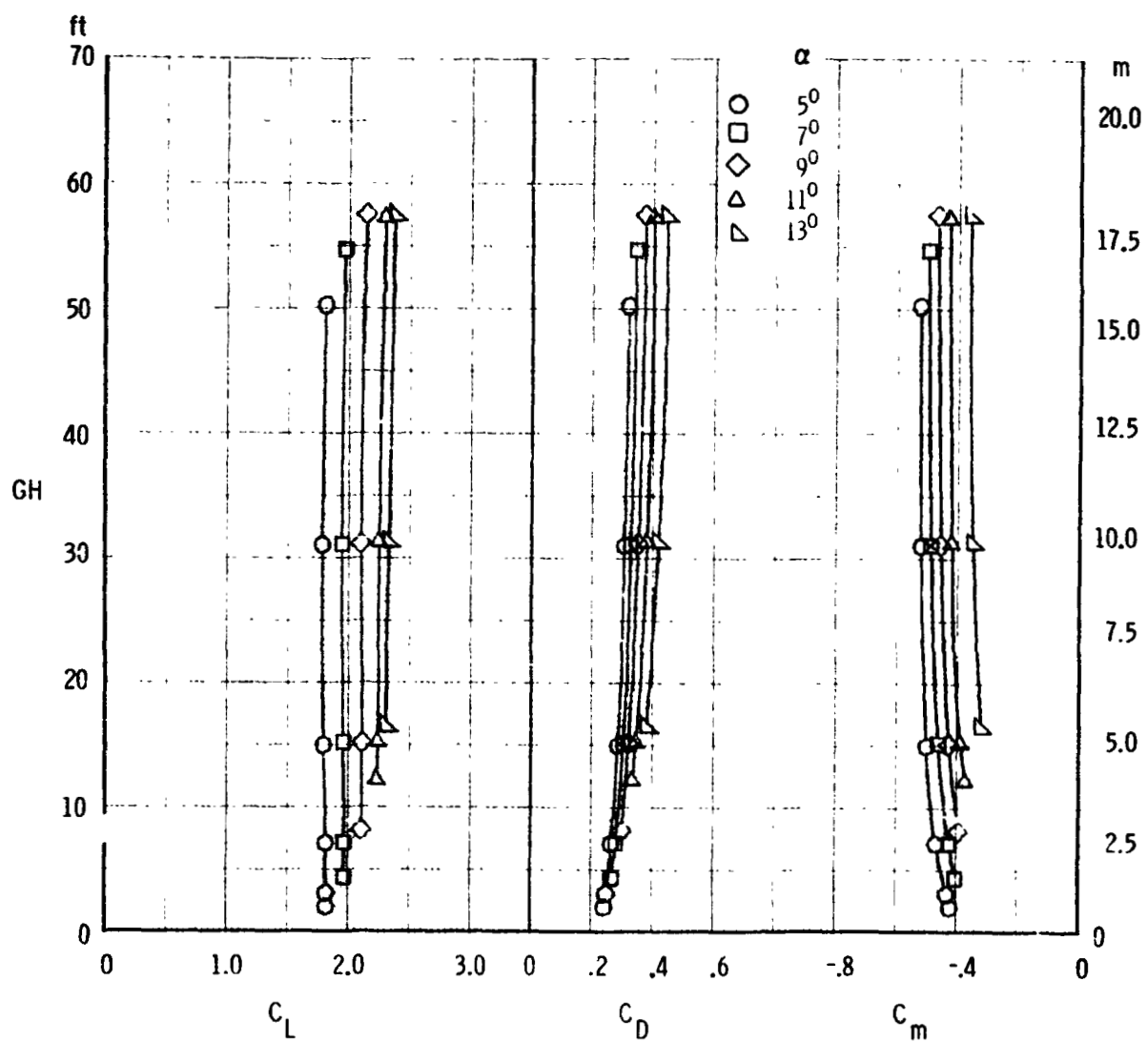


(a) Longitudinal characteristics, $\delta_{sp2,3,6,7} = 3^\circ$

Figure 14. - Effect of ground height on the aerodynamic characteristics of the $F_{40}N_GV_T$ configuration with several DLC spoiler deflections.

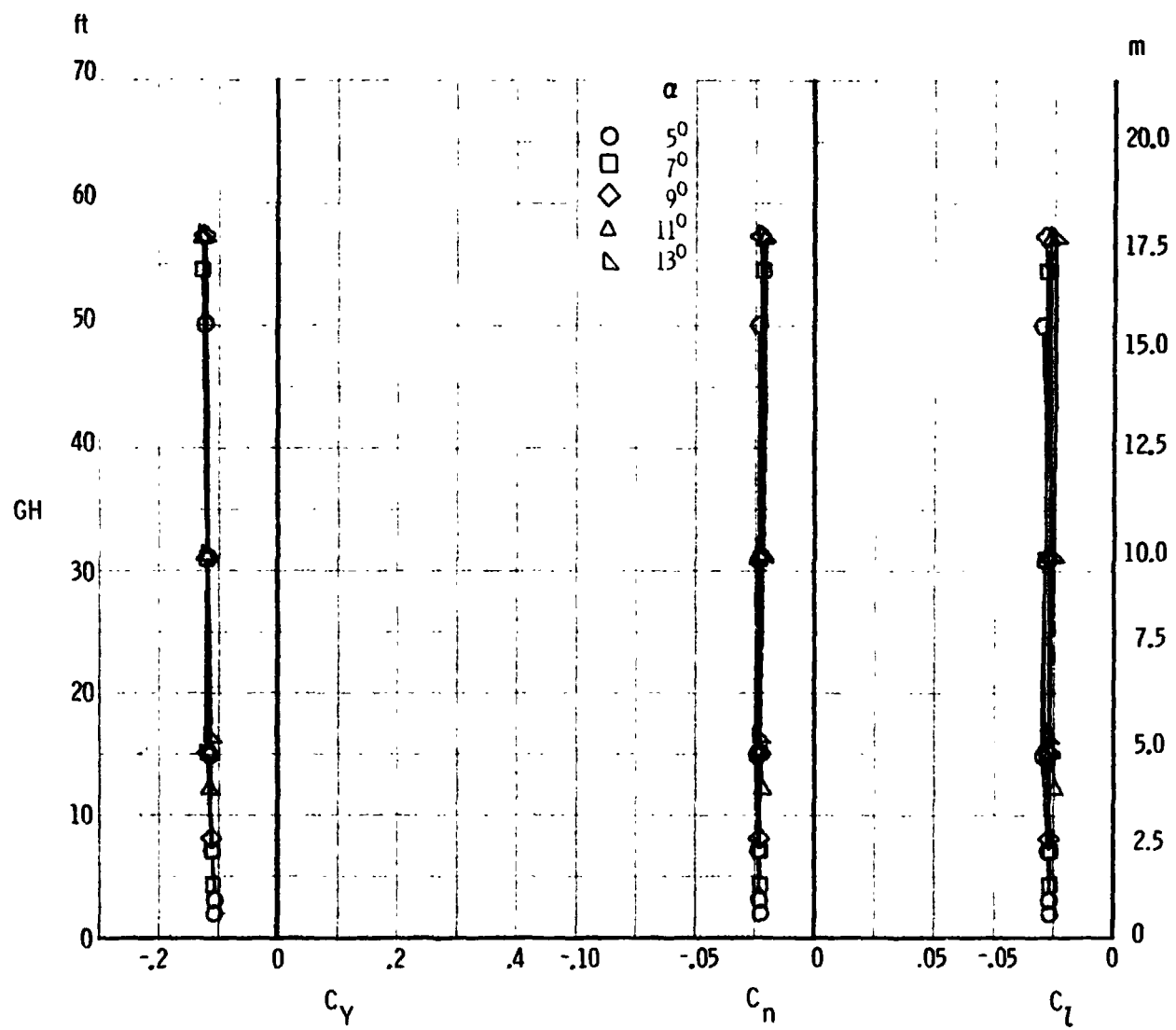


(b) Lateral-directional characteristics, $\delta_{sp2,3,6,7} = 3^\circ$
 Figure 14. - Continued.

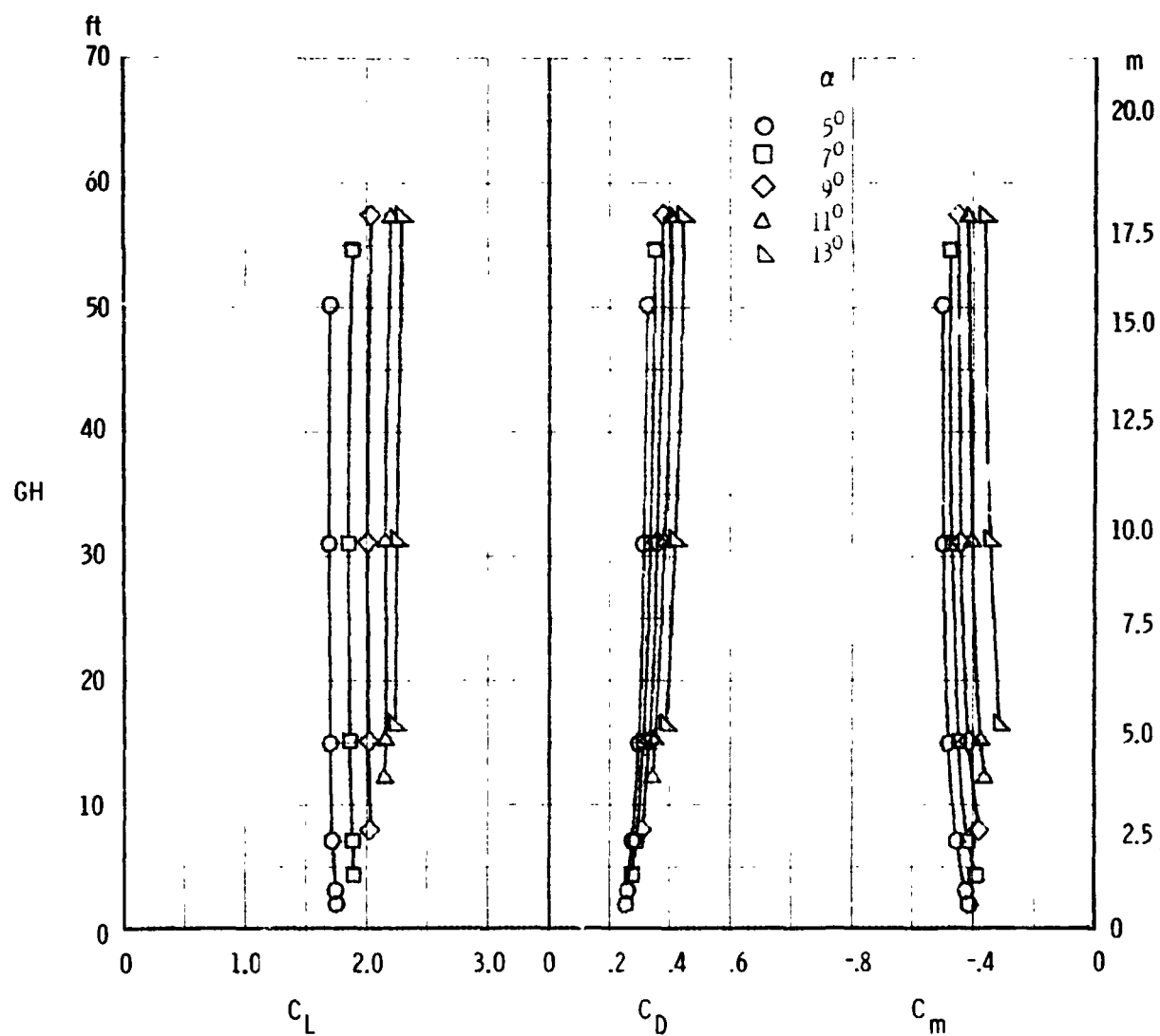


(c) Longitudinal characteristics, $\delta_{sp2,3,6,7} = 9^\circ$

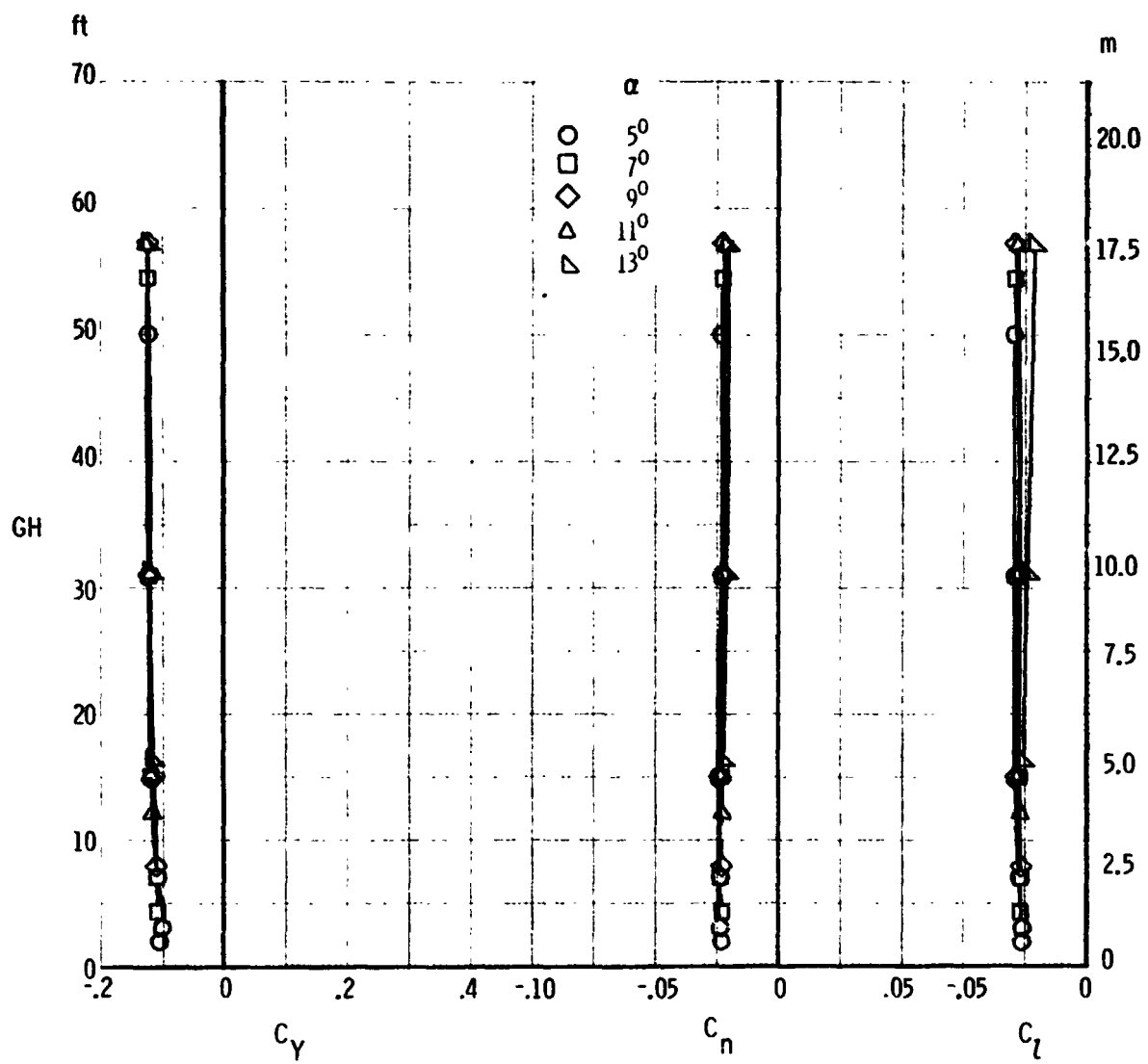
Figure 14. - Continued.



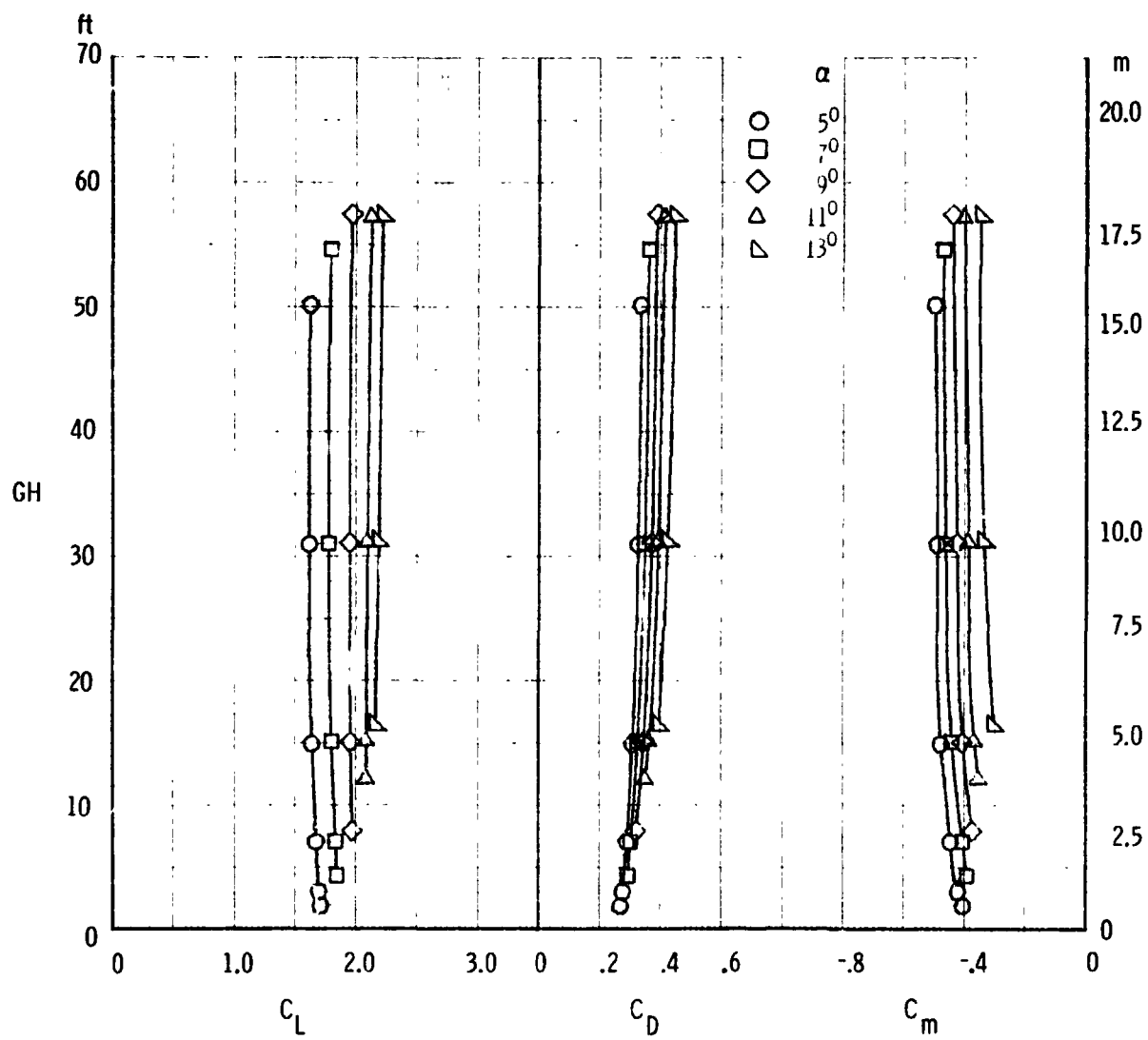
(d) Lateral-directional characteristics, $\delta_{sp2,3,6,7} = 9^\circ$
 Figure 14. - Continued.



(e) Longitudinal characteristics, $\delta_{sp2,3,6,7} = 15^\circ$
 Figure 14. - Continued.

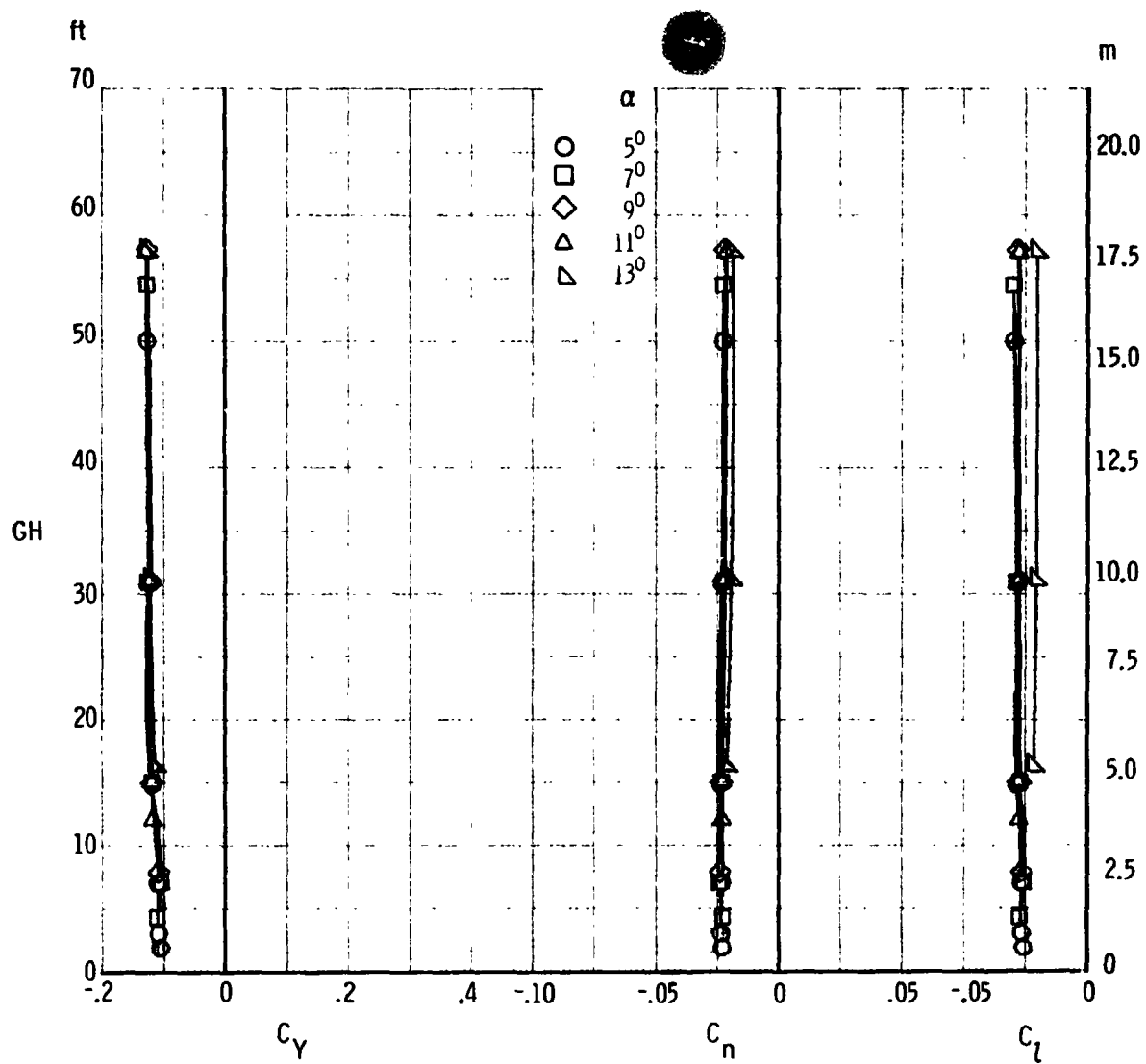


(f) Lateral-directional characteristics, $\delta_{sp2,3,6,7} = 15^\circ$
Figure 14. - Continued.

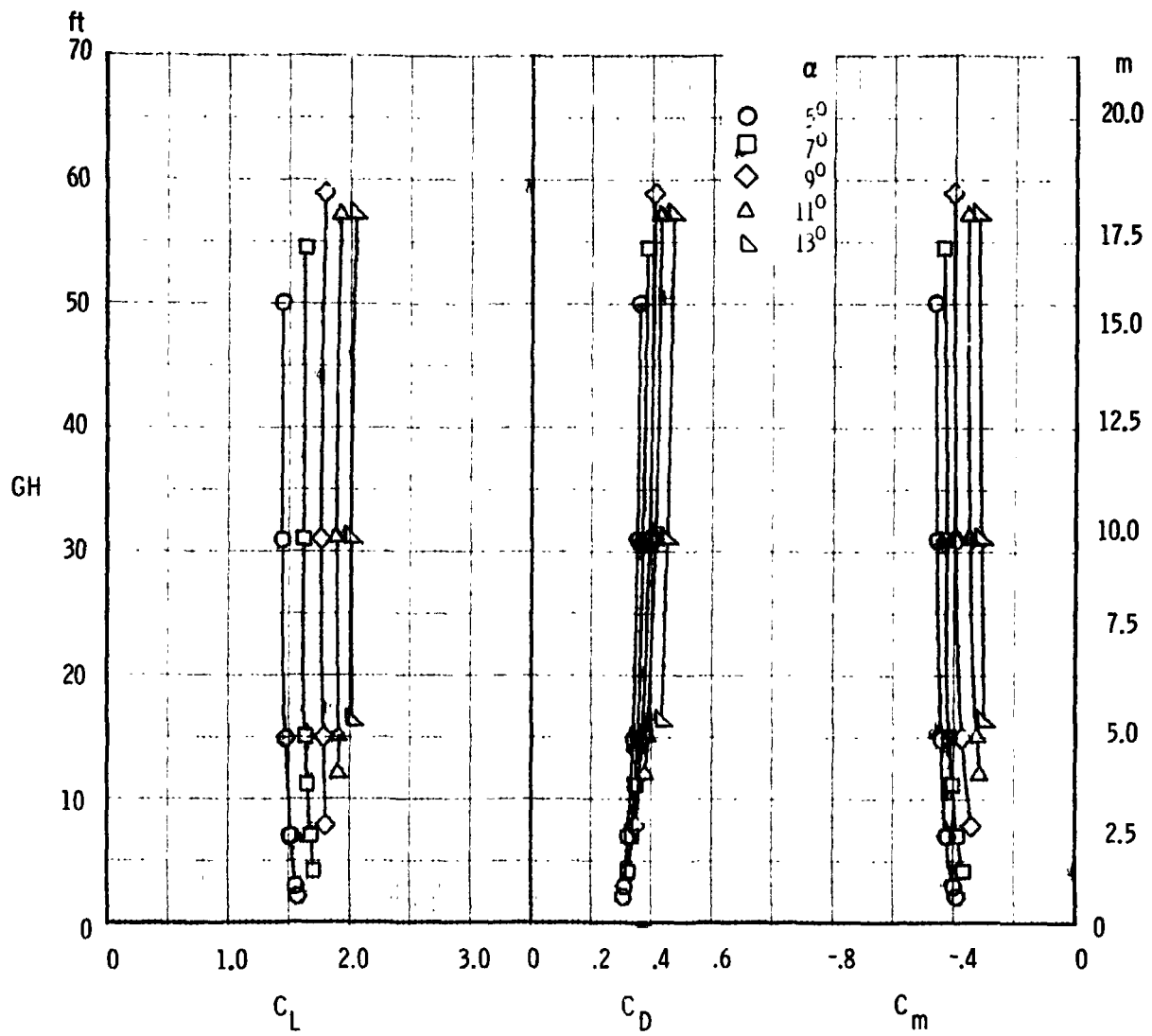


(g) Longitudinal characteristics, $\delta_{sp2,3,6,7} = 20^\circ$

Figure 14. - Continued.

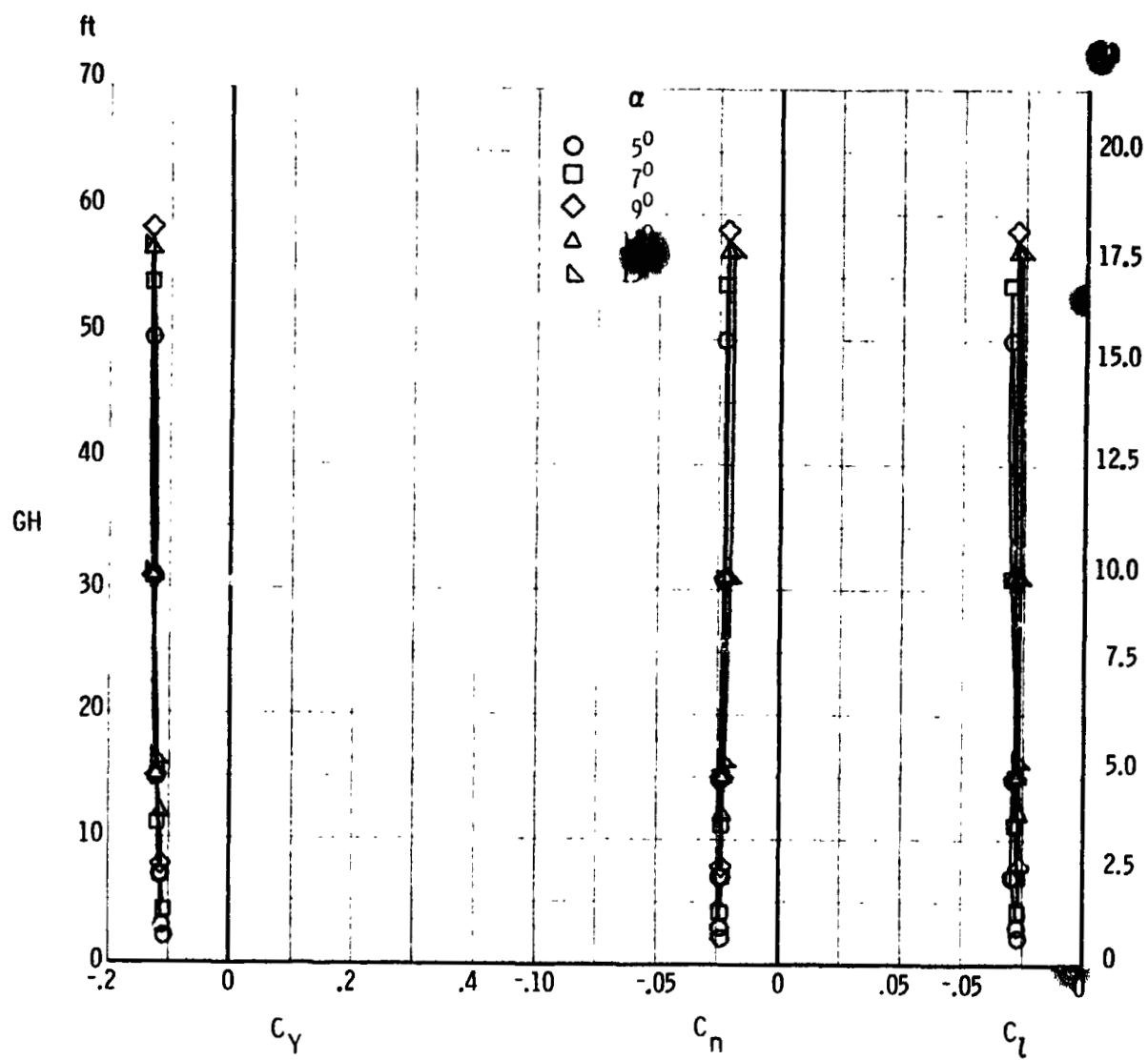


(h) Lateral-directional characteristics, $\delta_{sp2,3,6,7} = 20^\circ$
 Figure 14. - Continued.

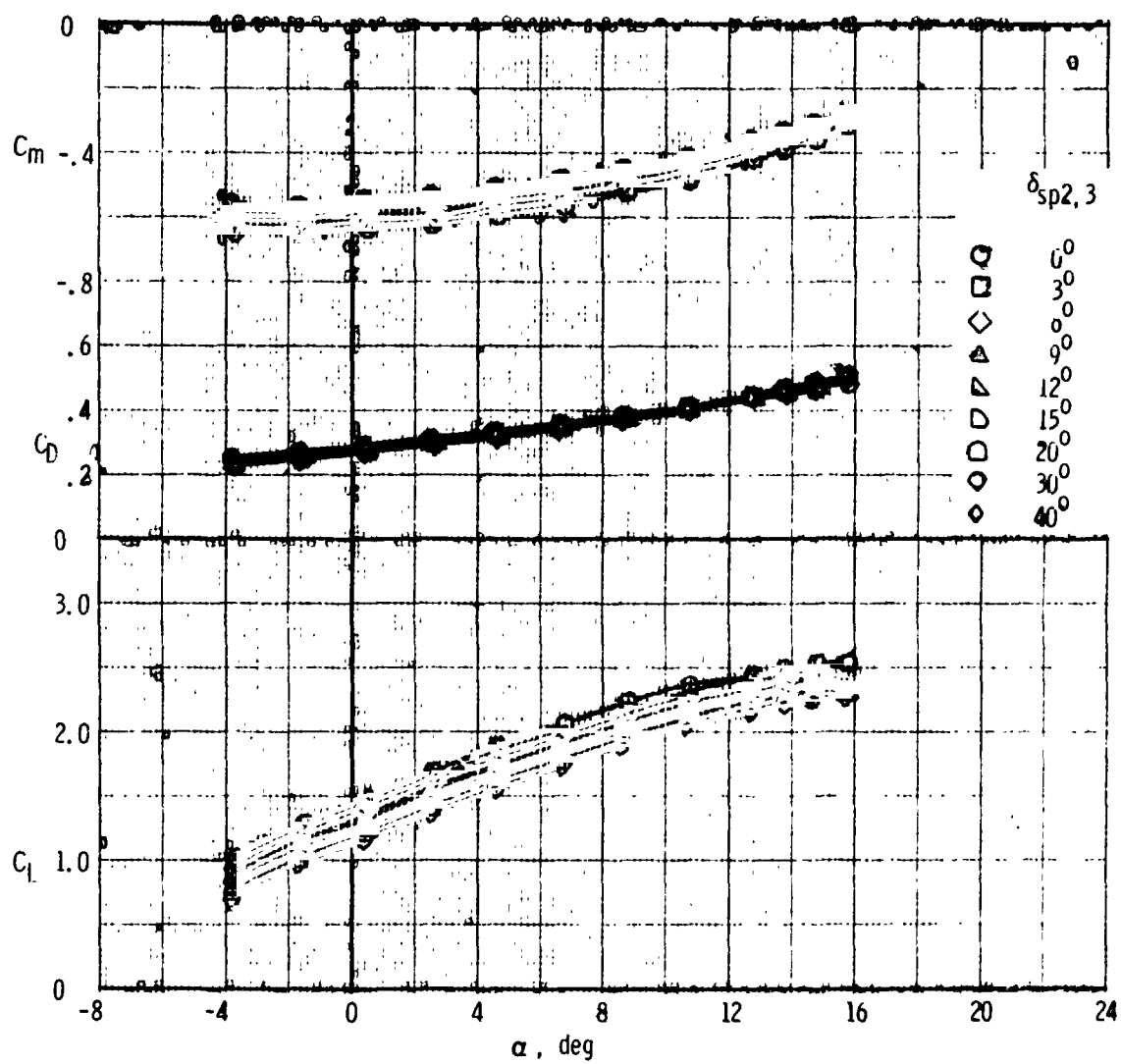


(ii) Longitudinal characteristics, $\delta_{sp2,3,6,7} = 40^\circ$

Figure 14. - Continued.

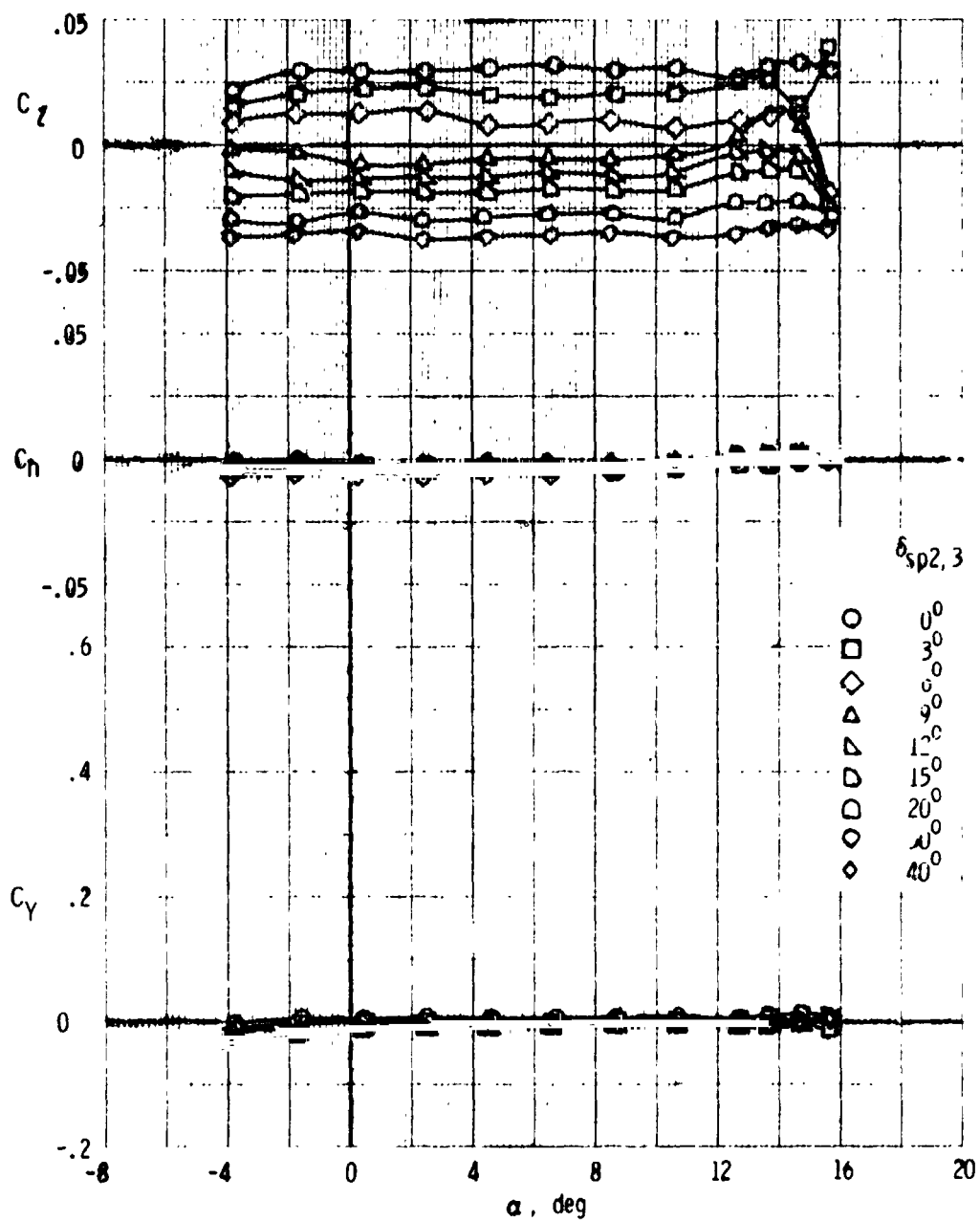


(j) Longitudinal characteristics, $\delta_{sp2,3,6,7} = 40^\circ$
 Figure 14. - Concluded.



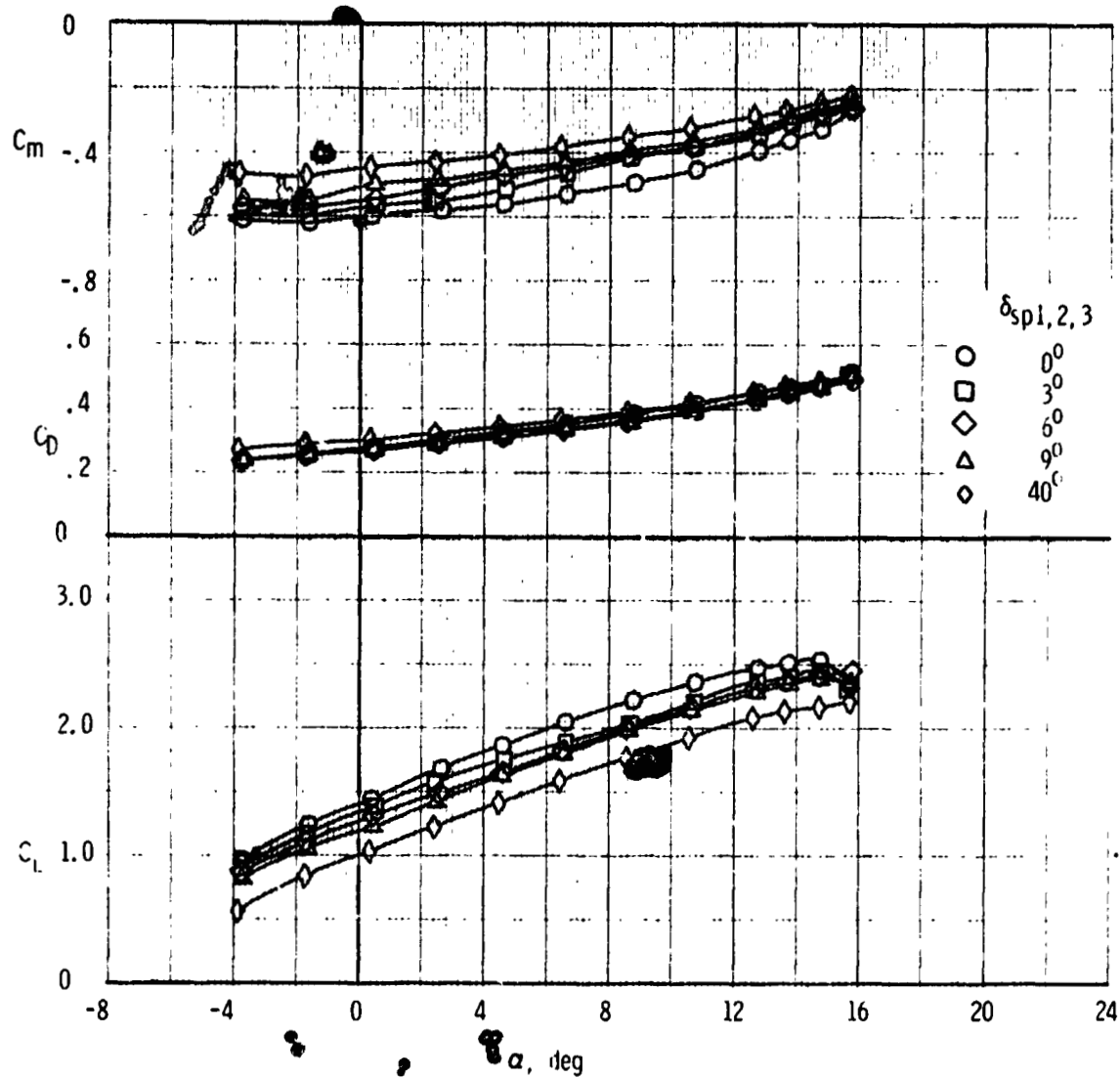
(a) Variation of longitudinal characteristics

Figure 15. - Effect of DLC roll control spoiler on the aerodynamic characteristics of the F, W, F₄₀, N, G configuration.



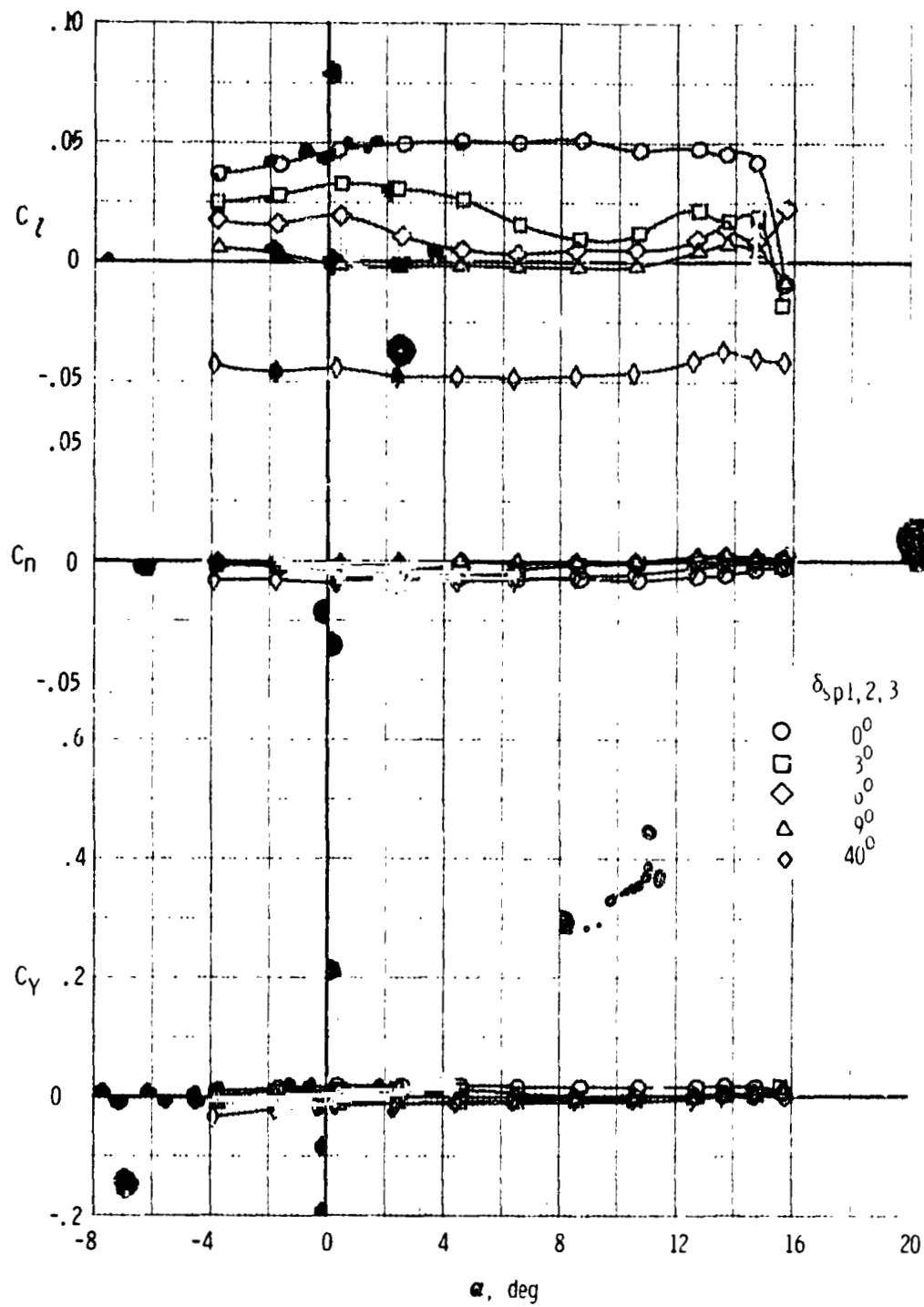
(b) Variation of lateral-directional characteristics

Figure 15. - Continued.



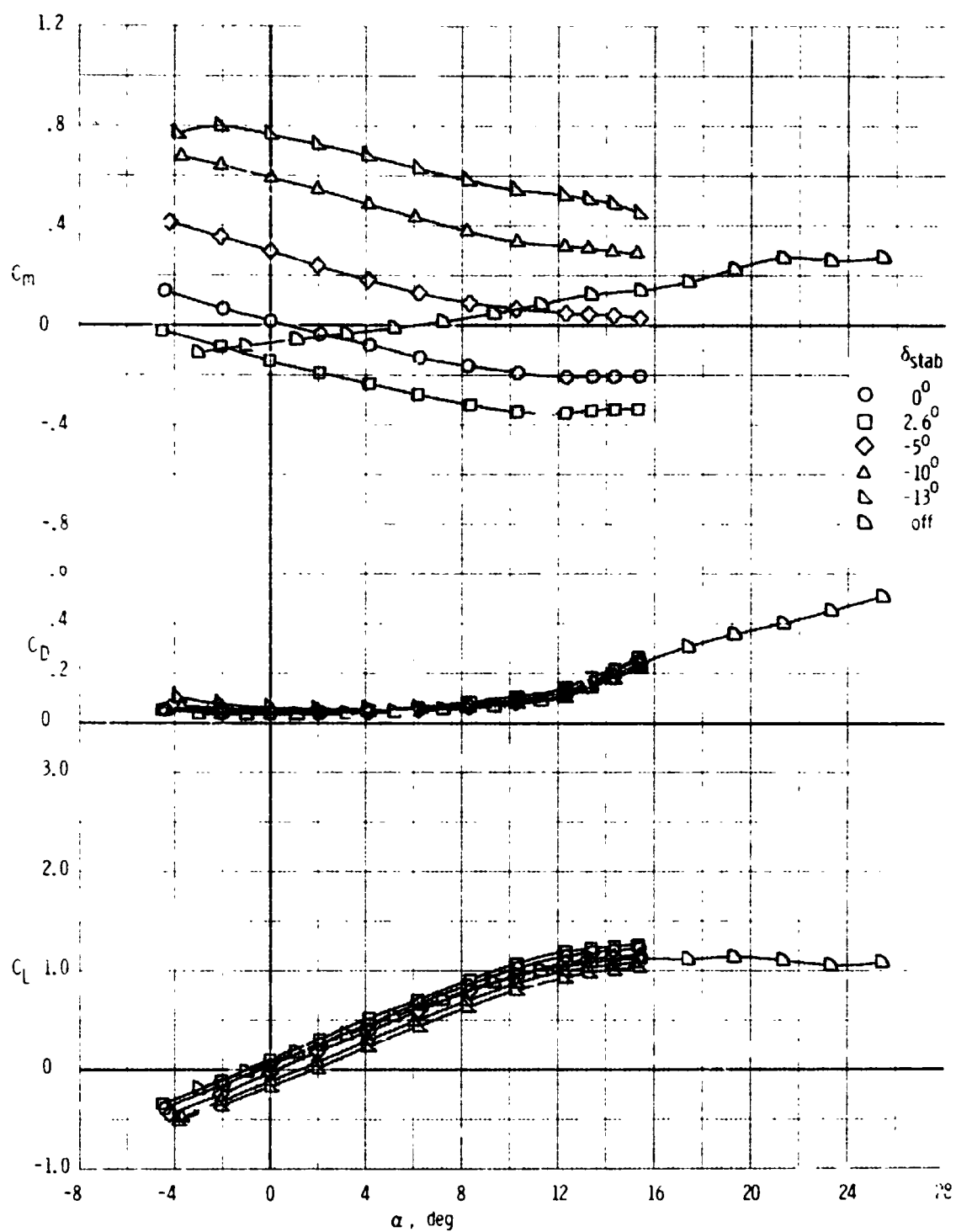
(c) Variation of longitudinal characteristics

Figure 15. - Continued.



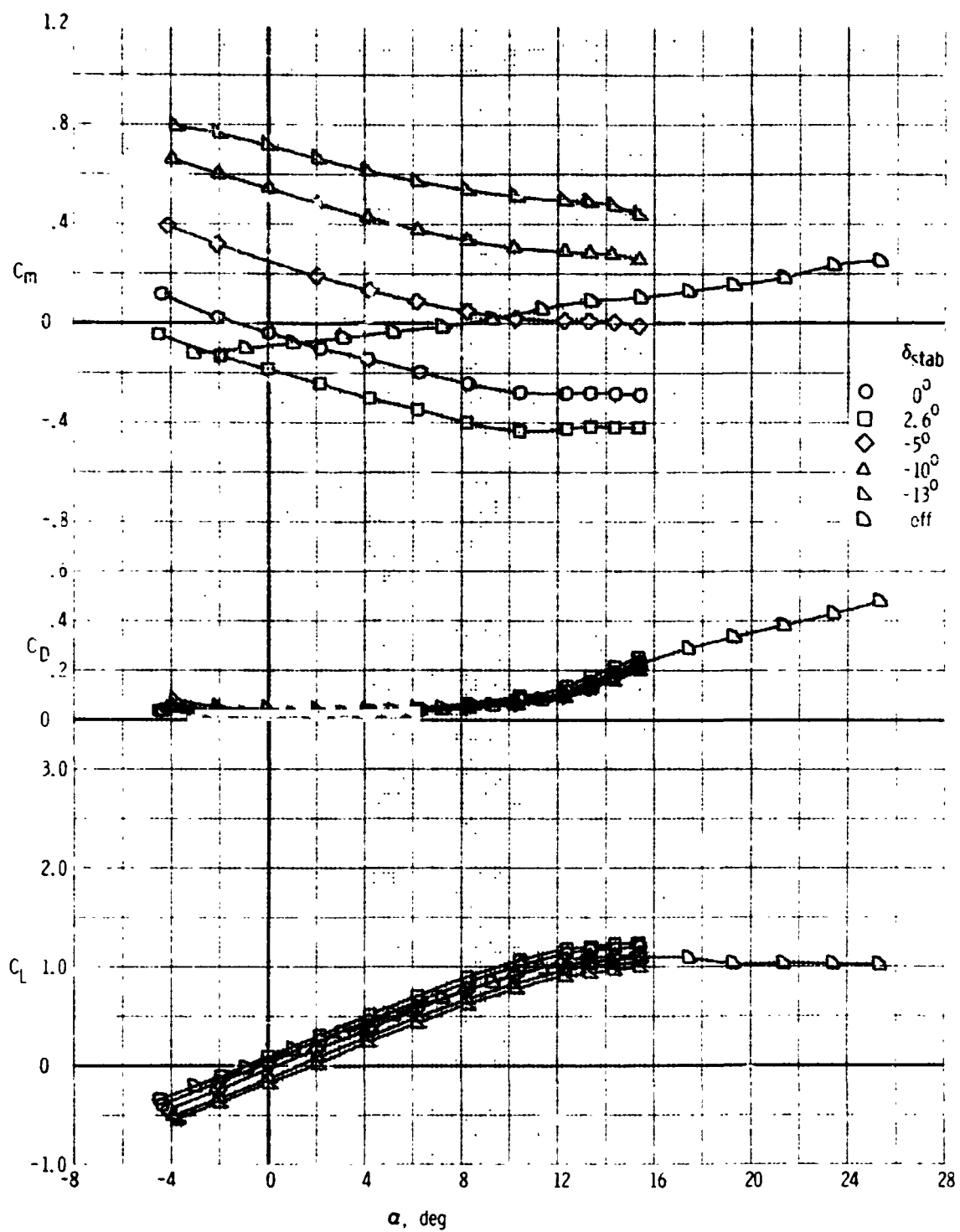
(d) Variation of lateral-directional characteristics

Figure 15. - Concluded.



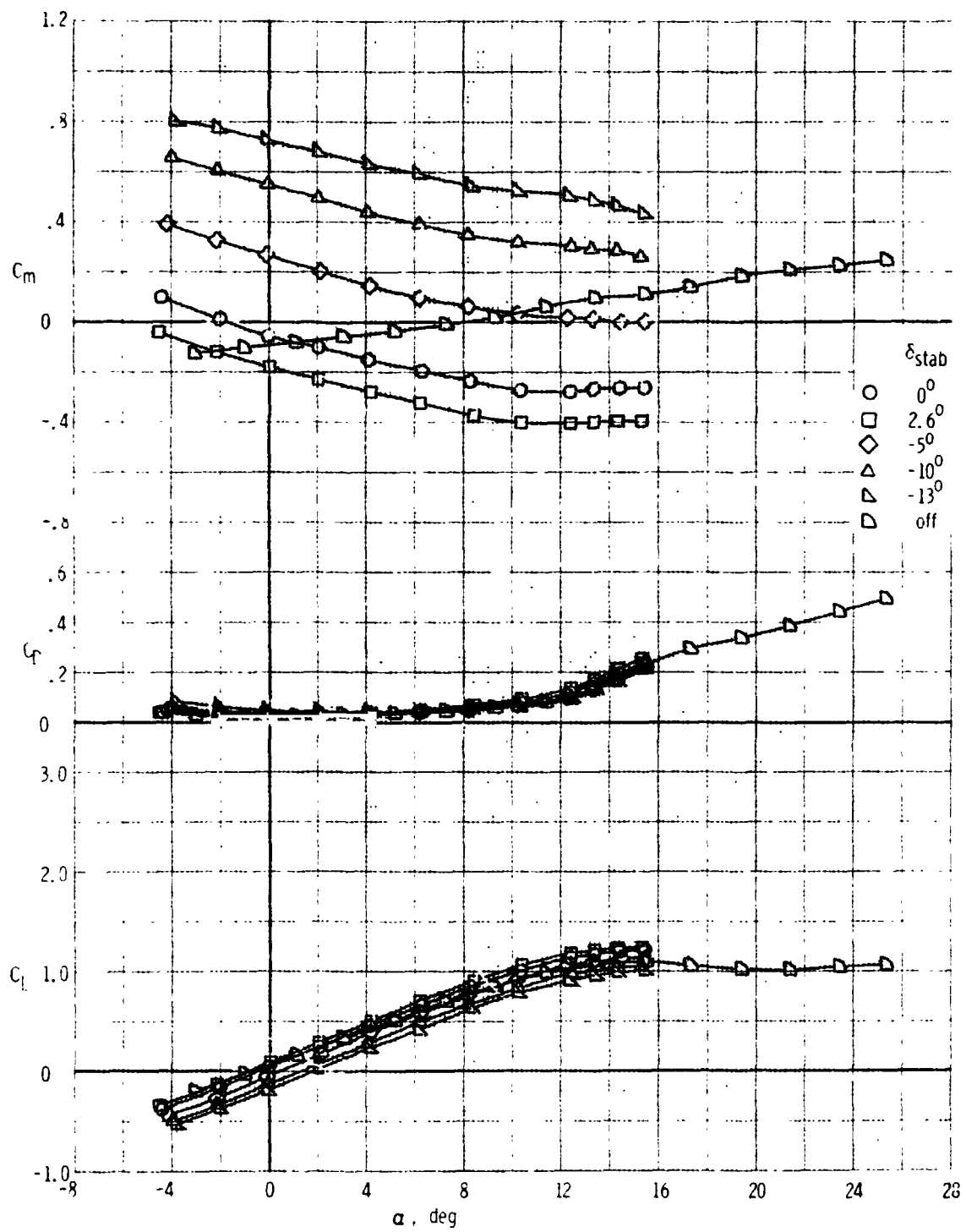
(a) $\beta = 0^\circ$

Figure 16. - Effect of stabilizer deflection on the longitudinal aerodynamic characteristics of the F, W, F_0, N, H_T, V_T configuration at various sideslip angles.



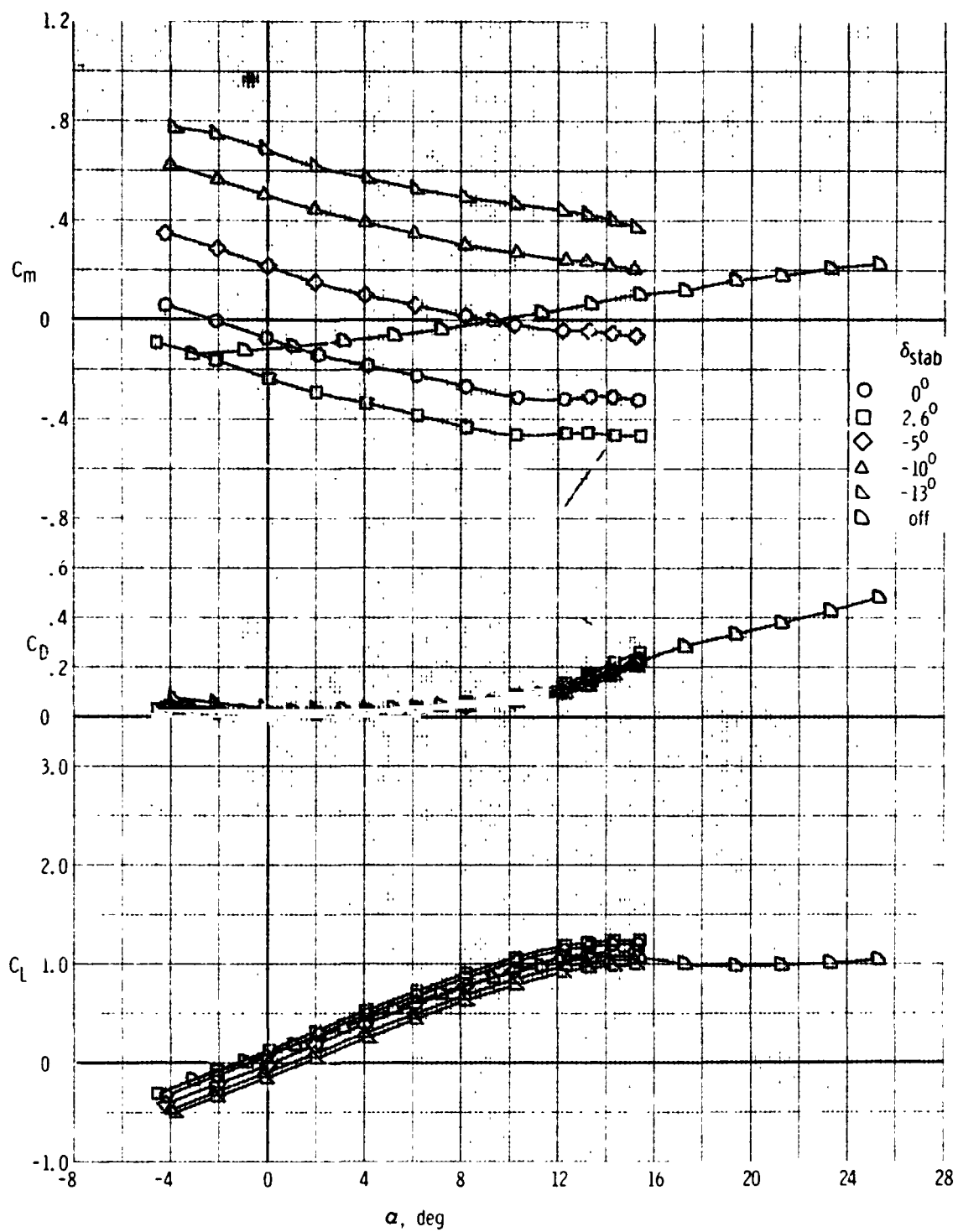
(b) $\beta = 5^\circ$

Figure 16. - Continued.



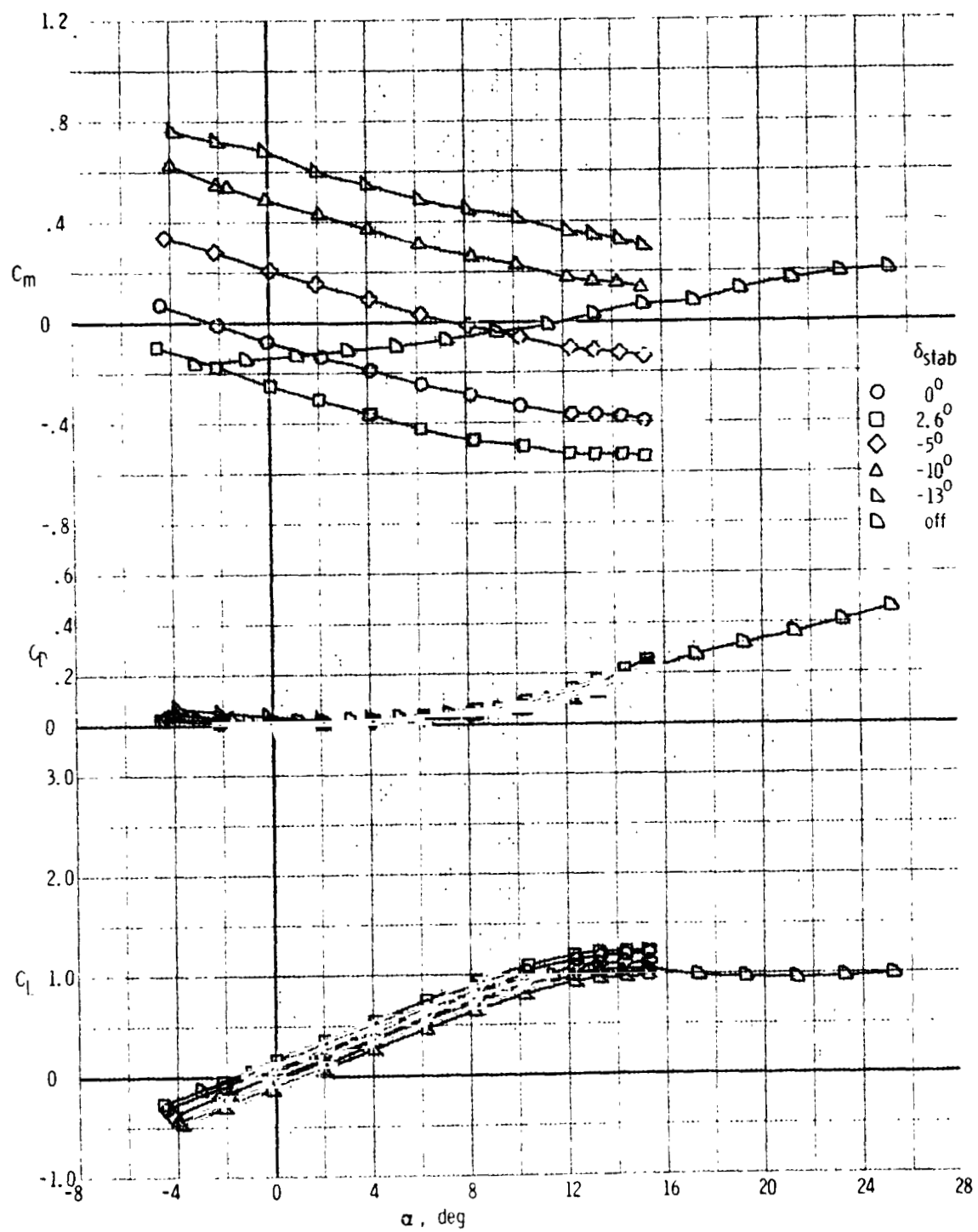
(c) $\beta = -5^\circ$

Figure 16. - Continued.



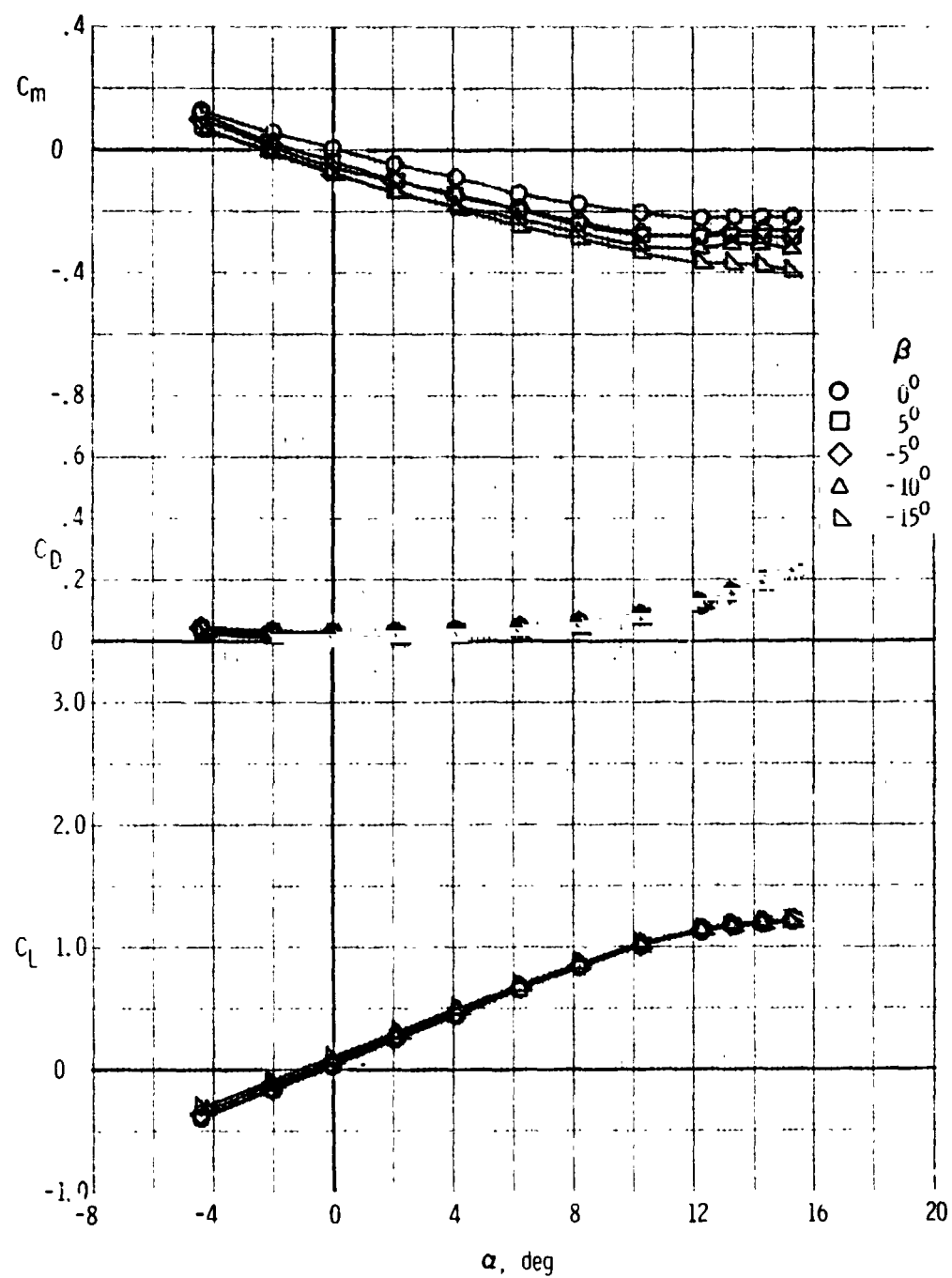
(d) $\beta = -10^\circ$

Figure 16. - Continued.



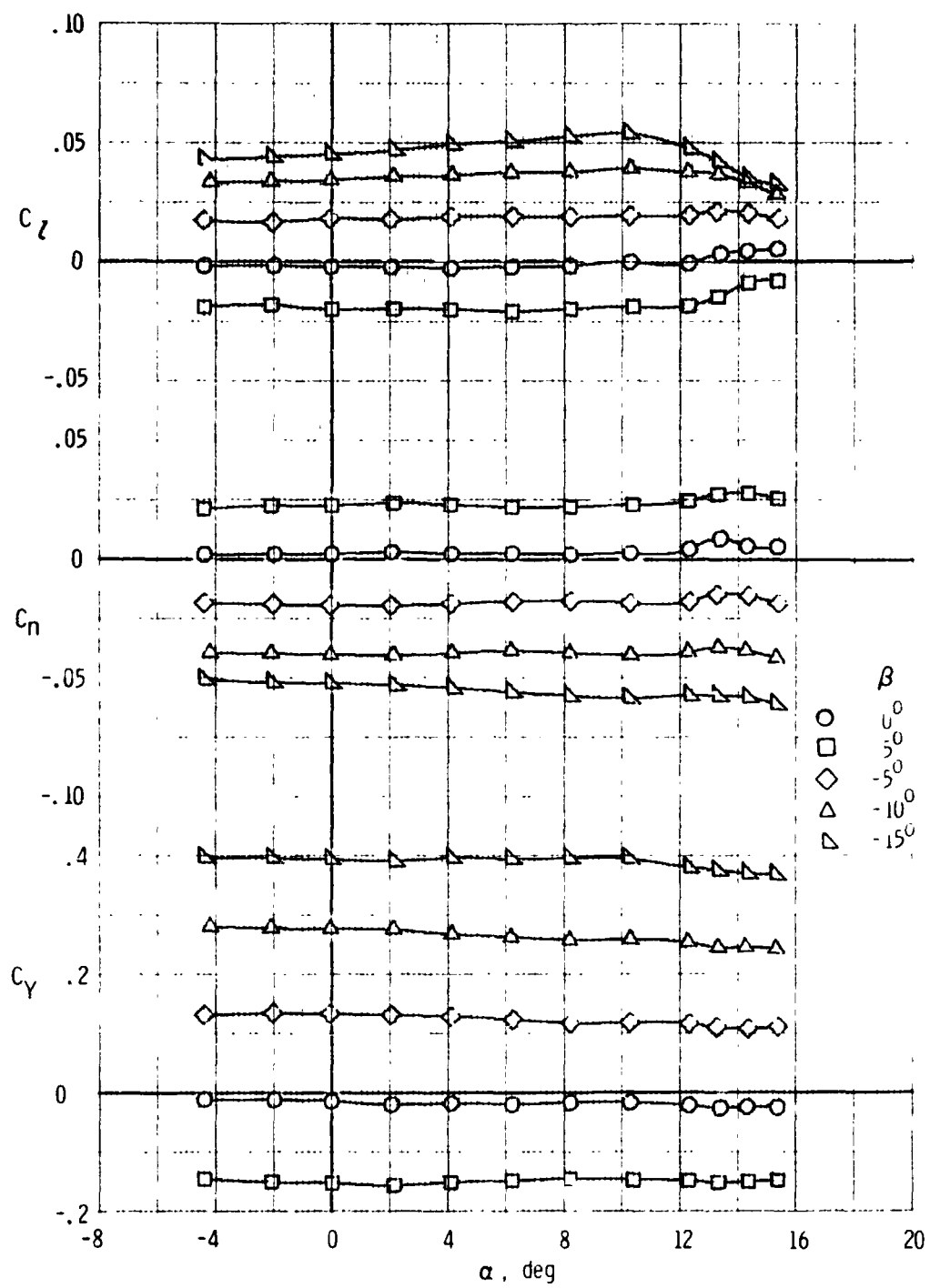
(e) $\beta = -15^\circ$

Figure 16. - Concluded.



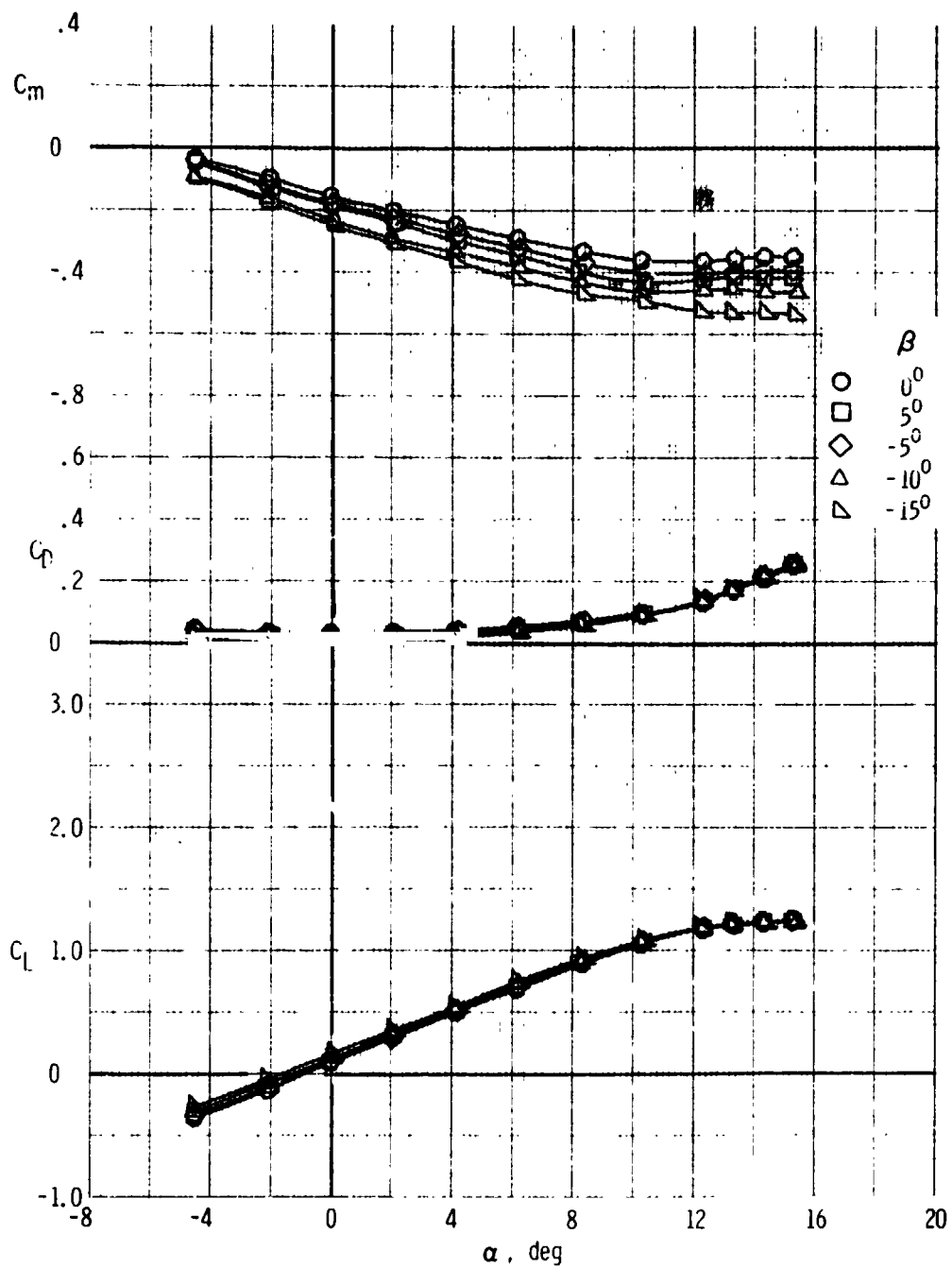
(a) Longitudinal characteristics, $\delta_{stab} = 0^\circ$

Figure 17. - Effect of sideslip on the aerodynamic characteristics of the F, W, F₀, N, H_T, V_T configuration with various stabilizer deflections.



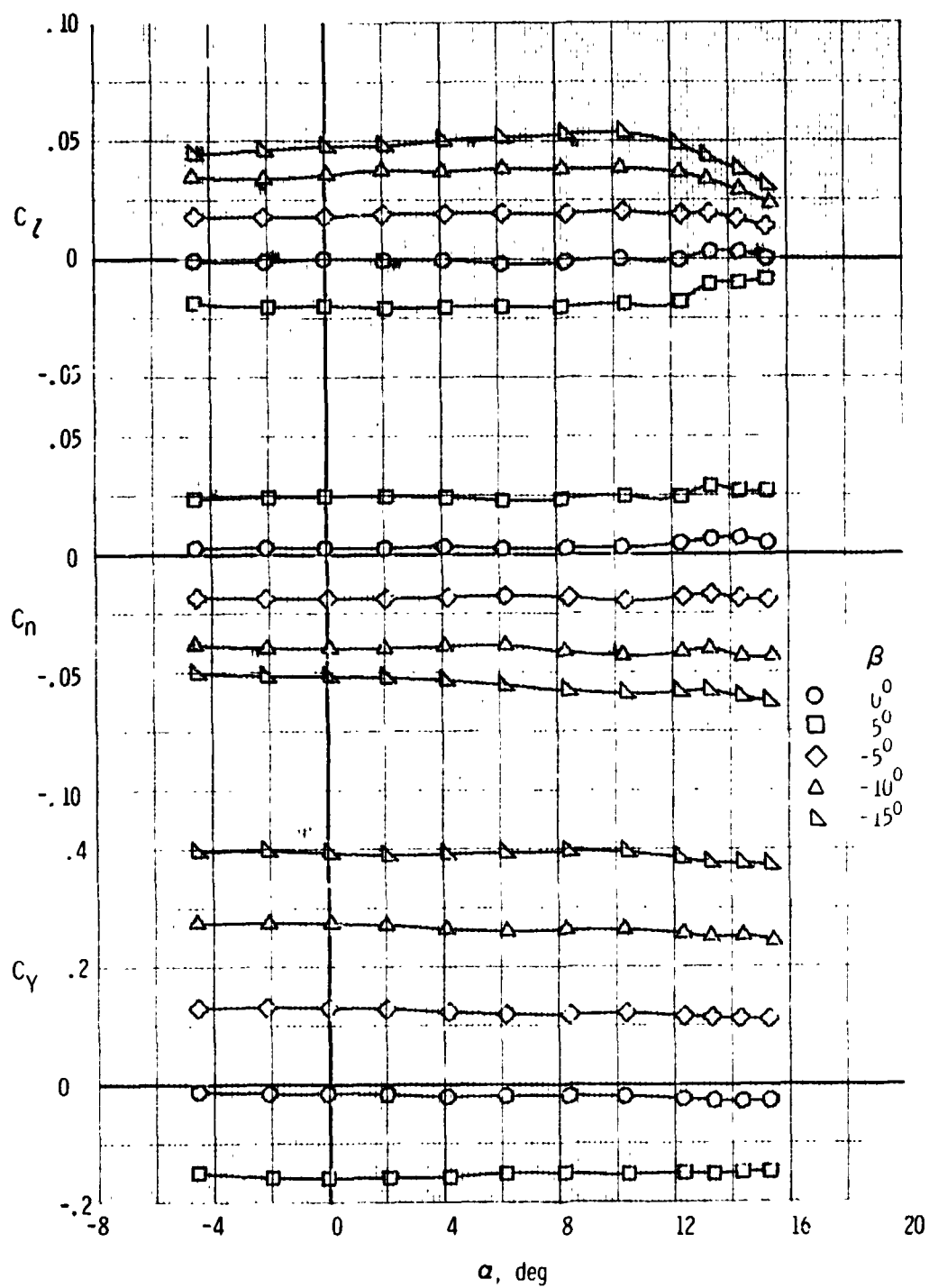
(b) Lateral-directional characteristics, $\delta_{stab} = 0^\circ$

Figure 17. - Continued.



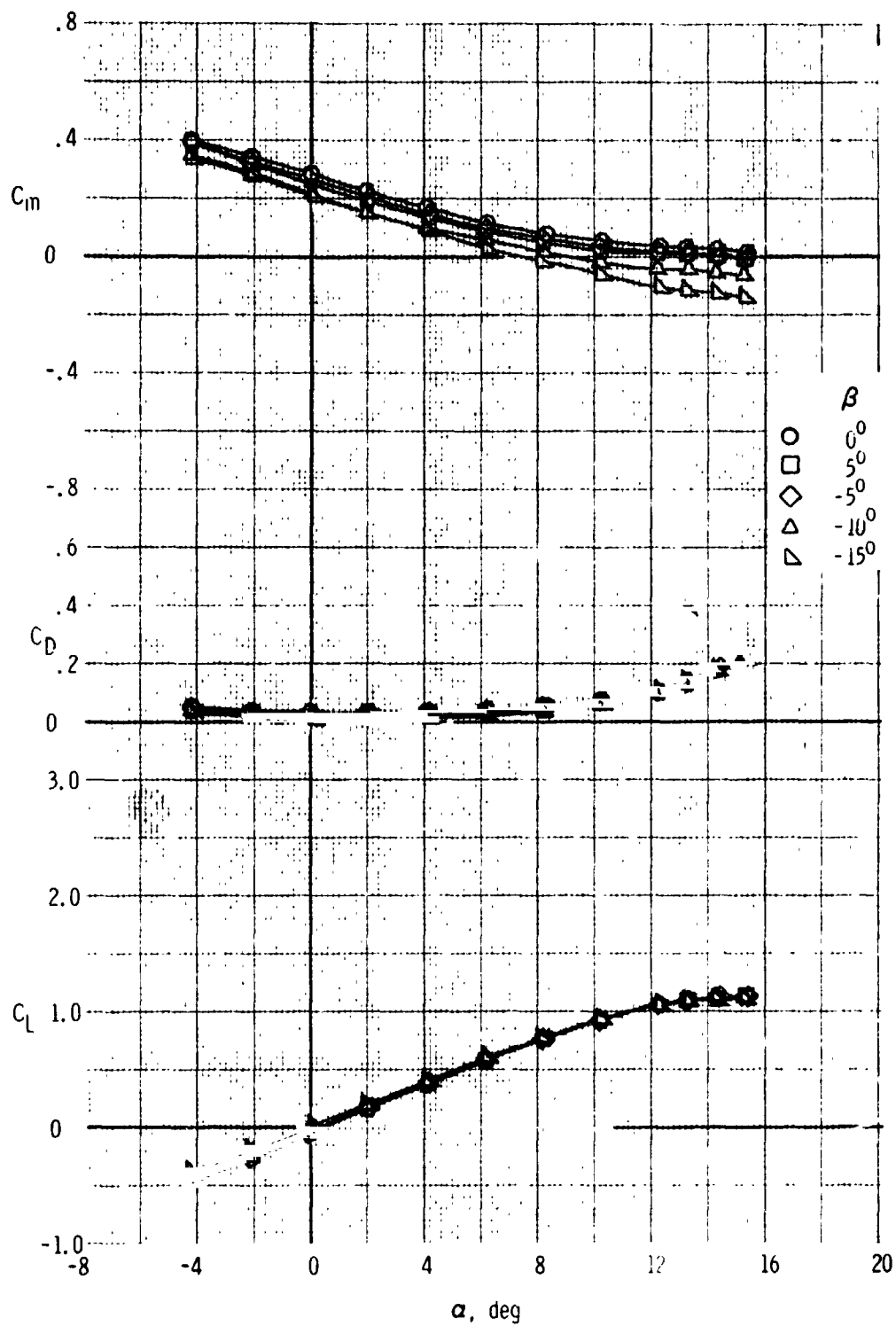
(c) Longitudinal characteristics, $\delta_{stab} = 2.6^\circ$

Figure 17. - Continued.



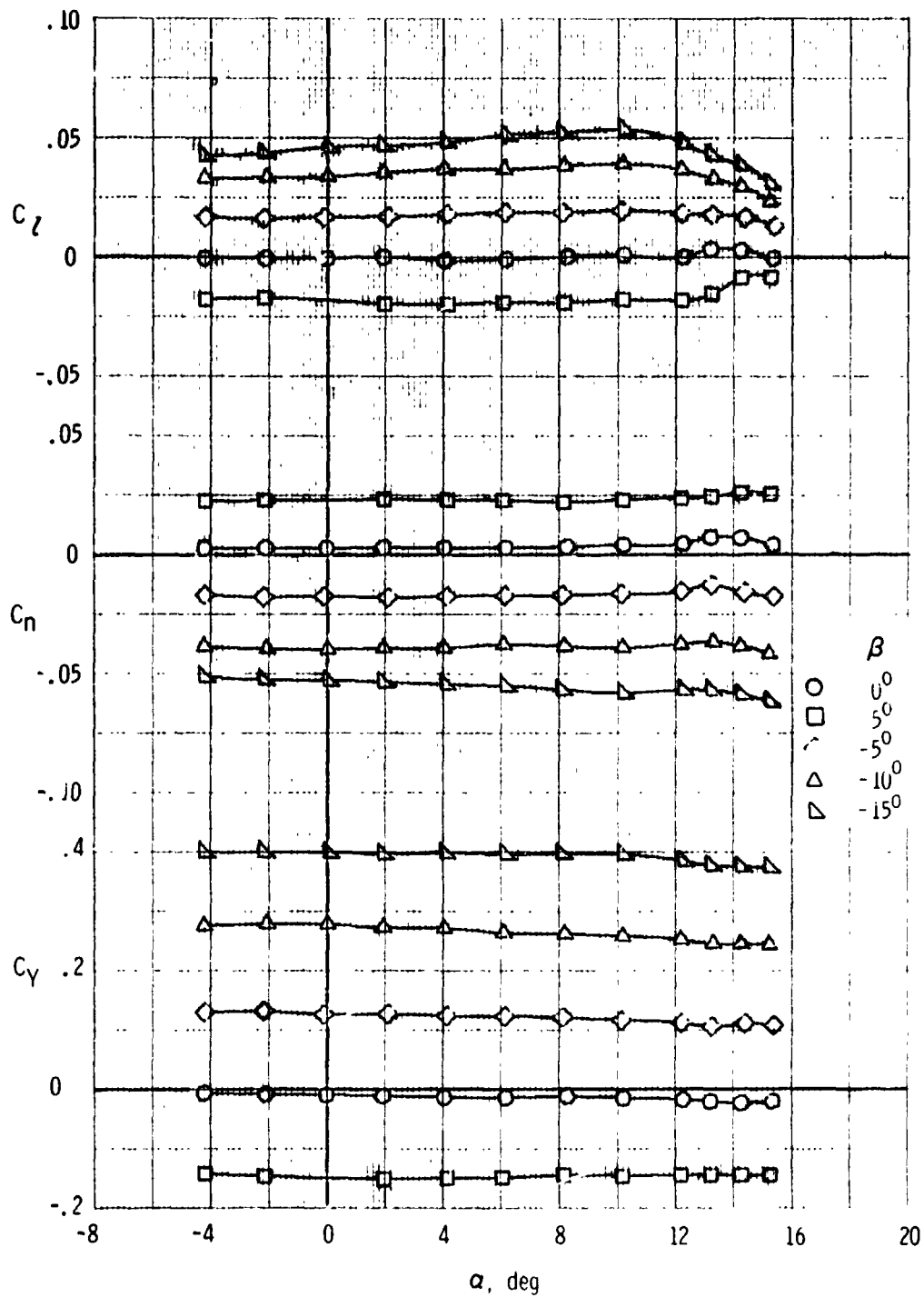
(d) Lateral-directional characteristics, $\delta_{stab} = 2.2^\circ$

Figure 17. - Continued.



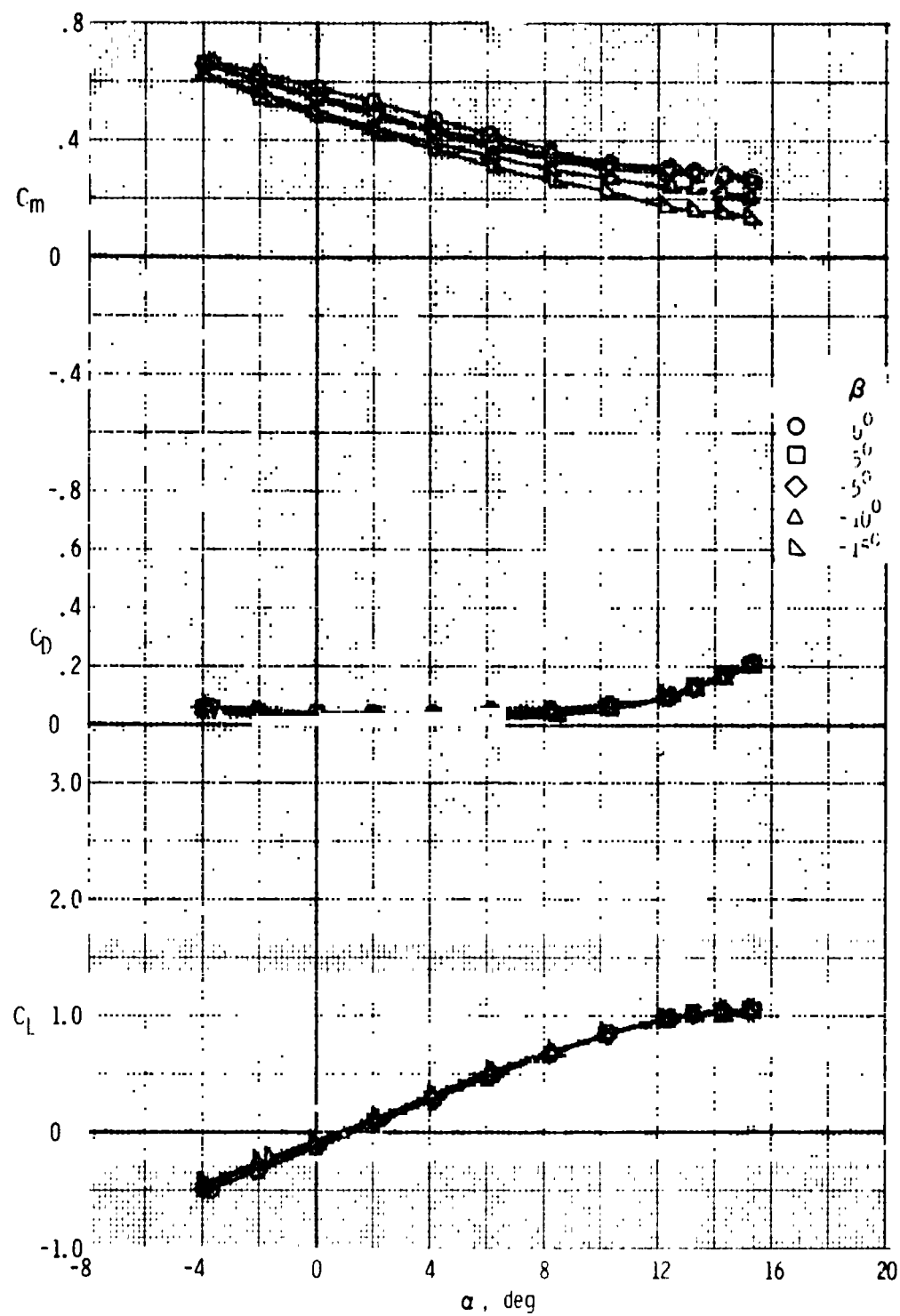
(e) Longitudinal characteristics, $\delta_{stab} = -5^\circ$

Figure 17. - Continued.

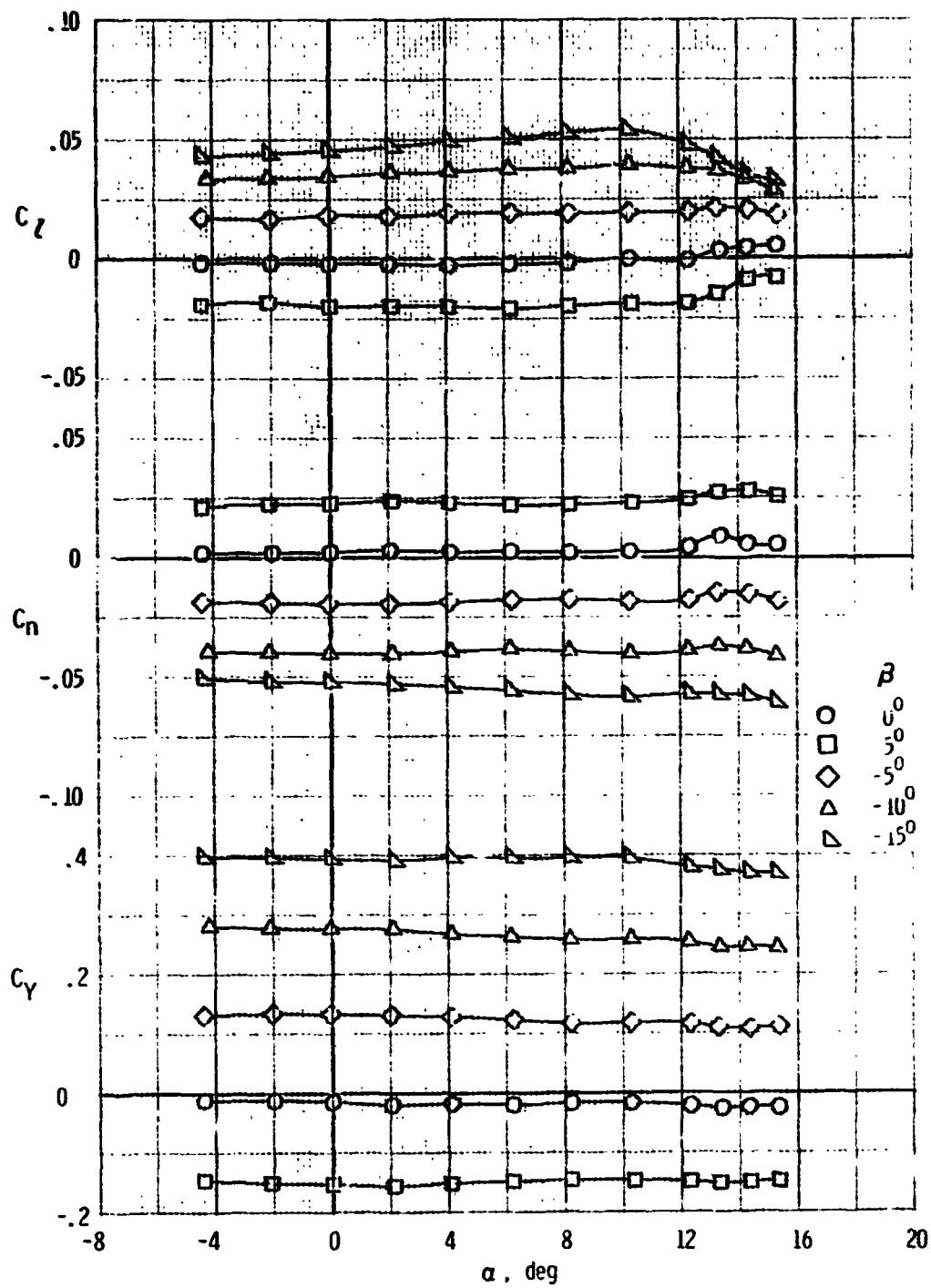


(f) Lateral-directional characteristics, $\delta_{stab} = -5^\circ$

Figure 17. - Continued.

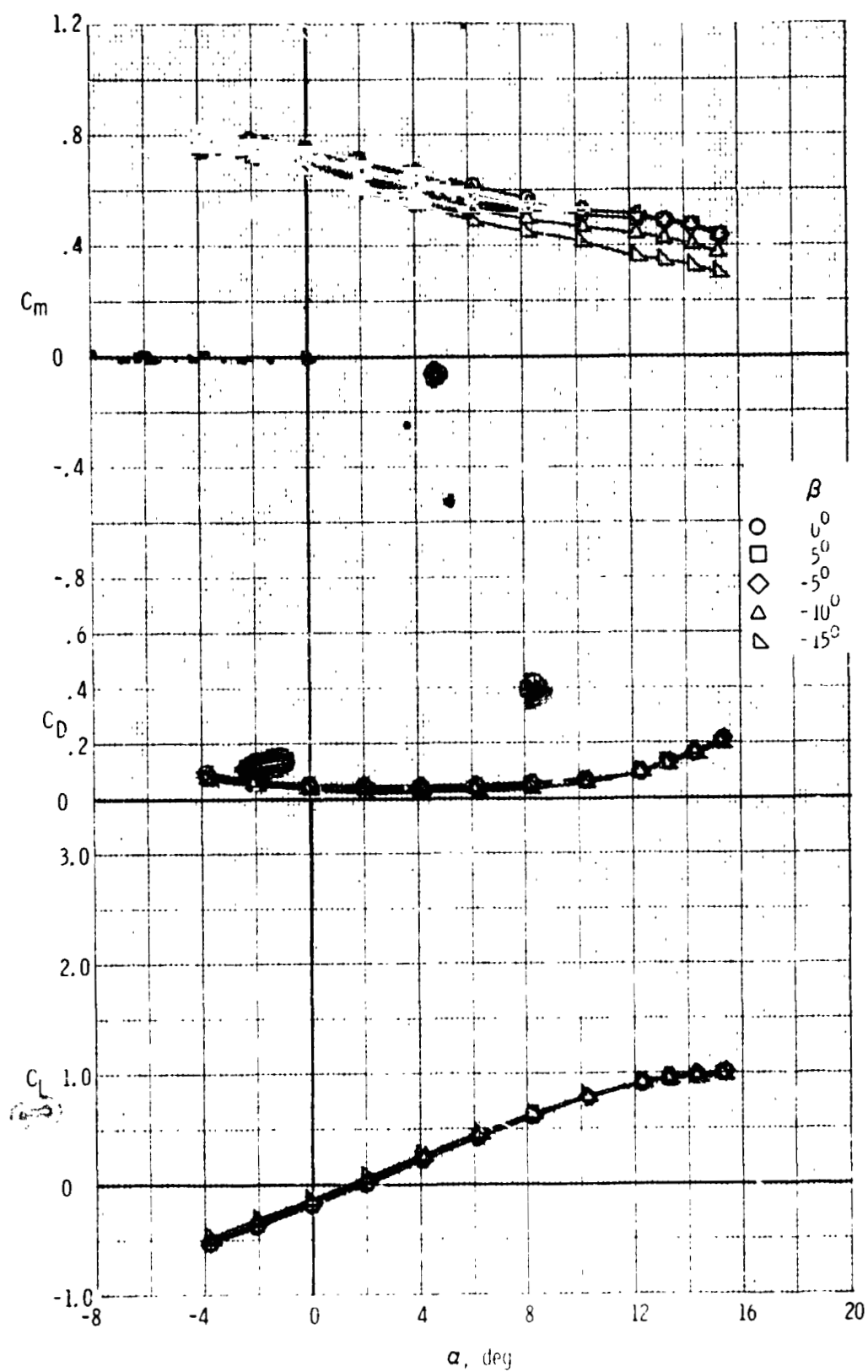


(g) Longitudinal characteristics, $\delta_{stab} = -10^\circ$
 Figure 17. - Continued.



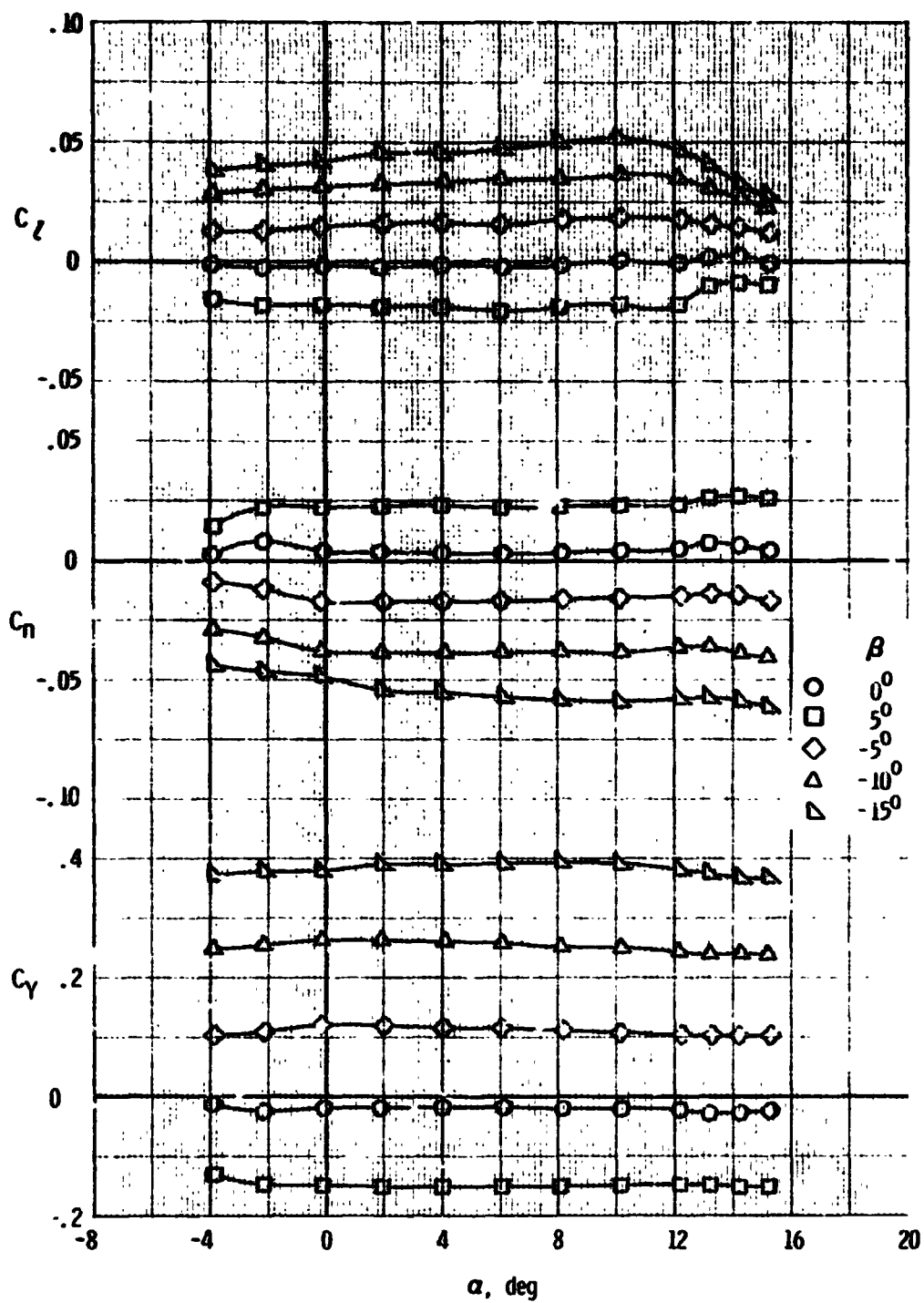
(b) Lateral-directional characteristics, $\delta_{stab} = 0^\circ$

Figure 17. - Continued.



(i) Longitudinal characteristics, $\delta_{stab} = -15^\circ$

Figure 17. - Continued.



(j) Lateral-directional characteristics, $\delta_{stab} = -15^\circ$

Figure 17. - Concluded.

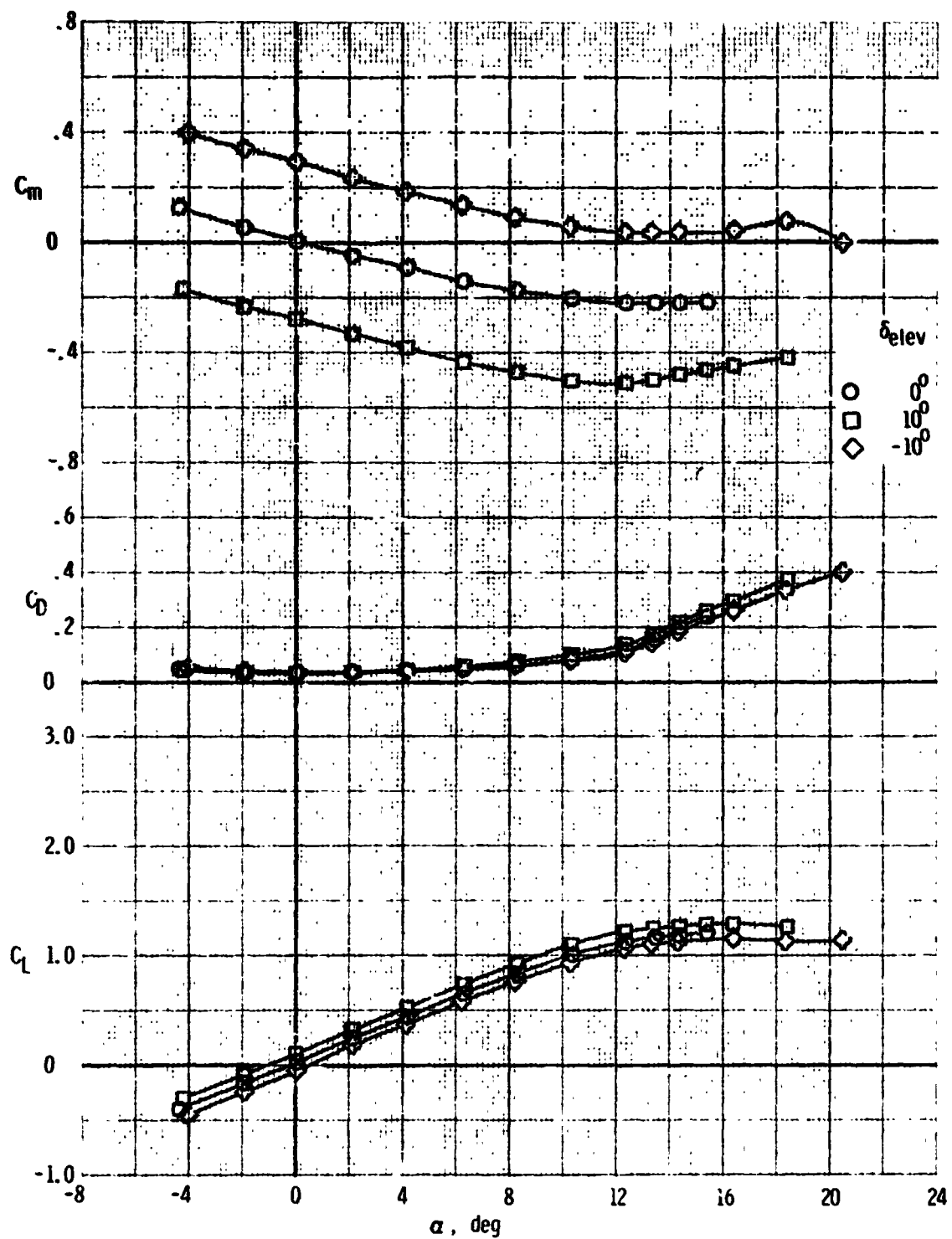
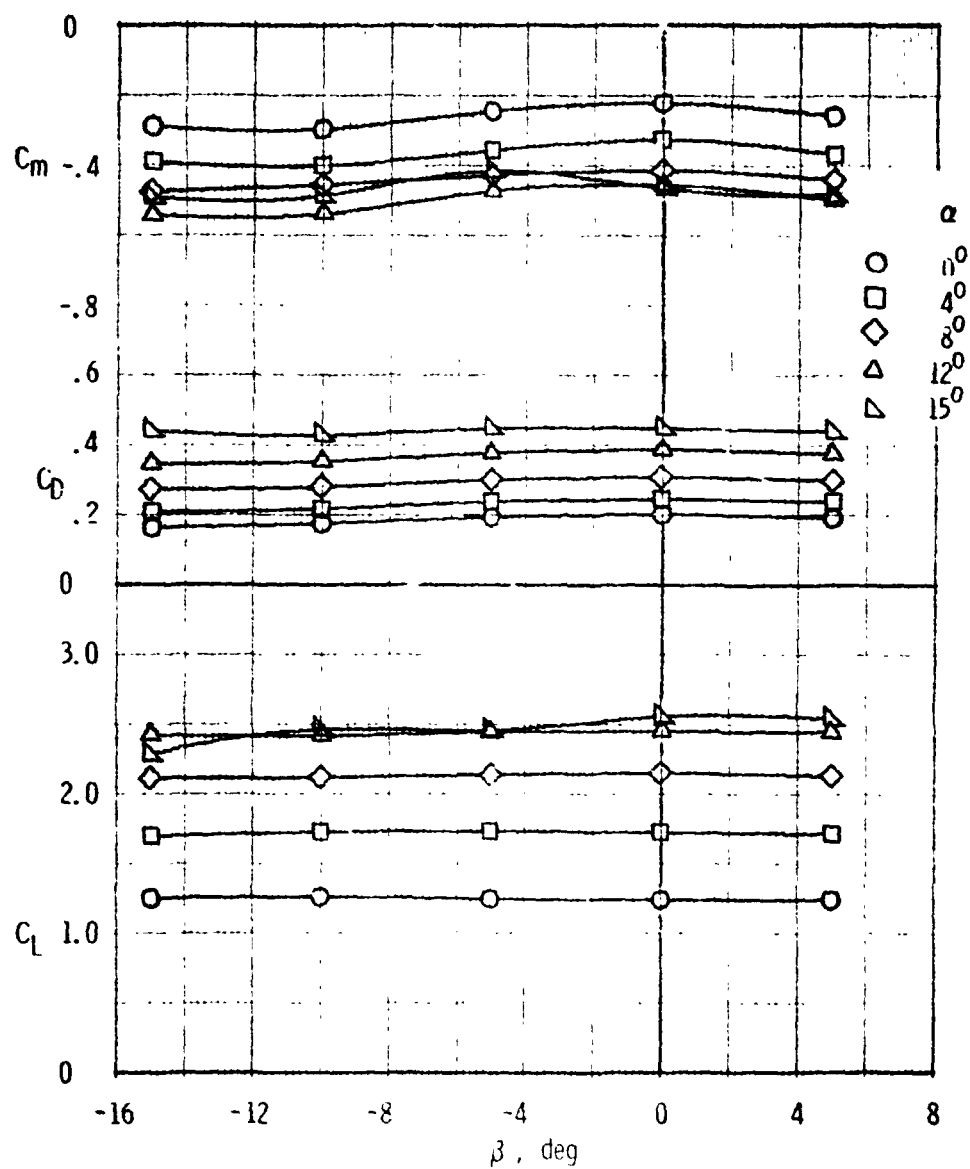


Figure 18. - Effect of elevator deflection on the longitudinal aerodynamic characteristics of the F, W, F₀, N, H_T, V_T configuration.

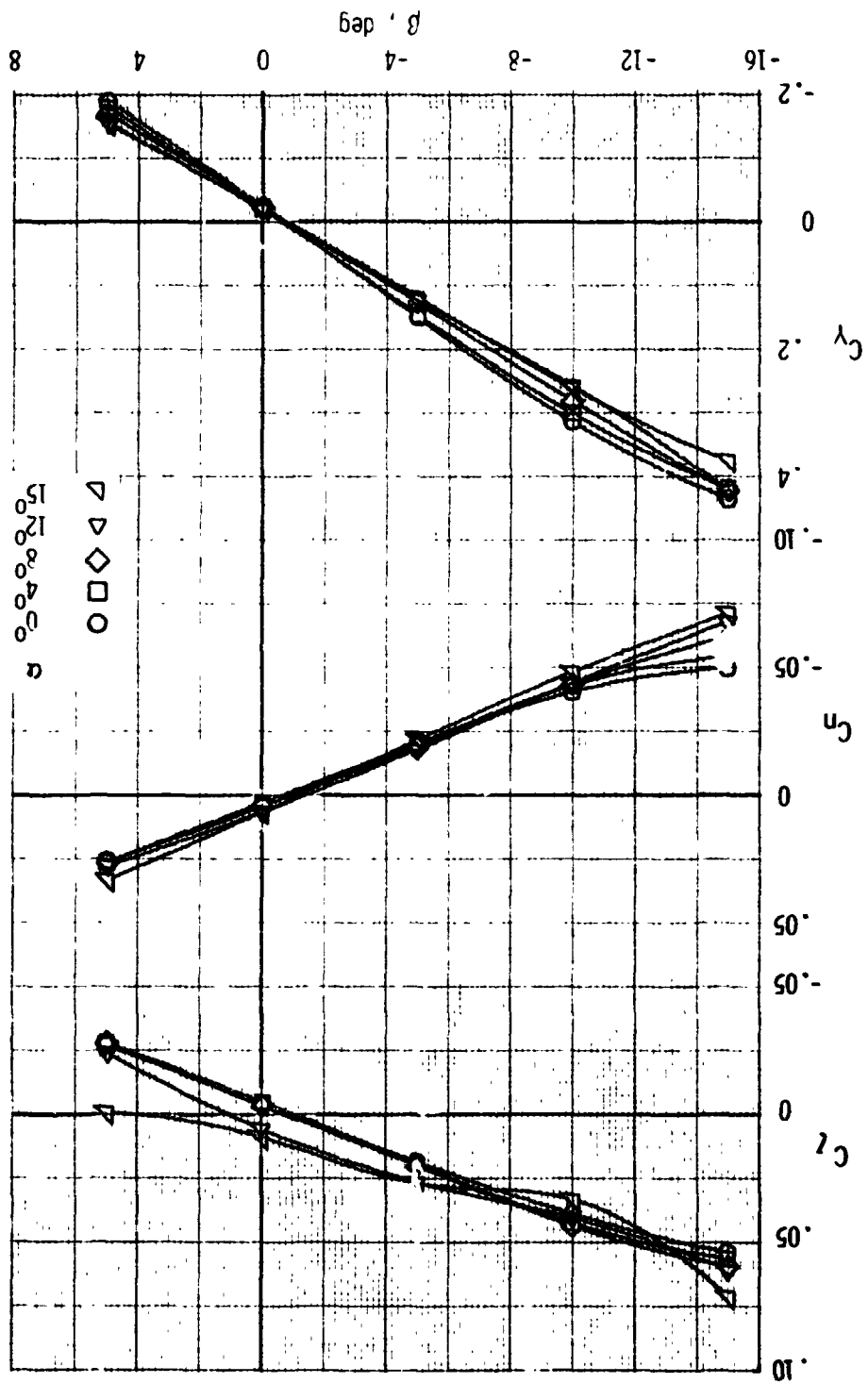


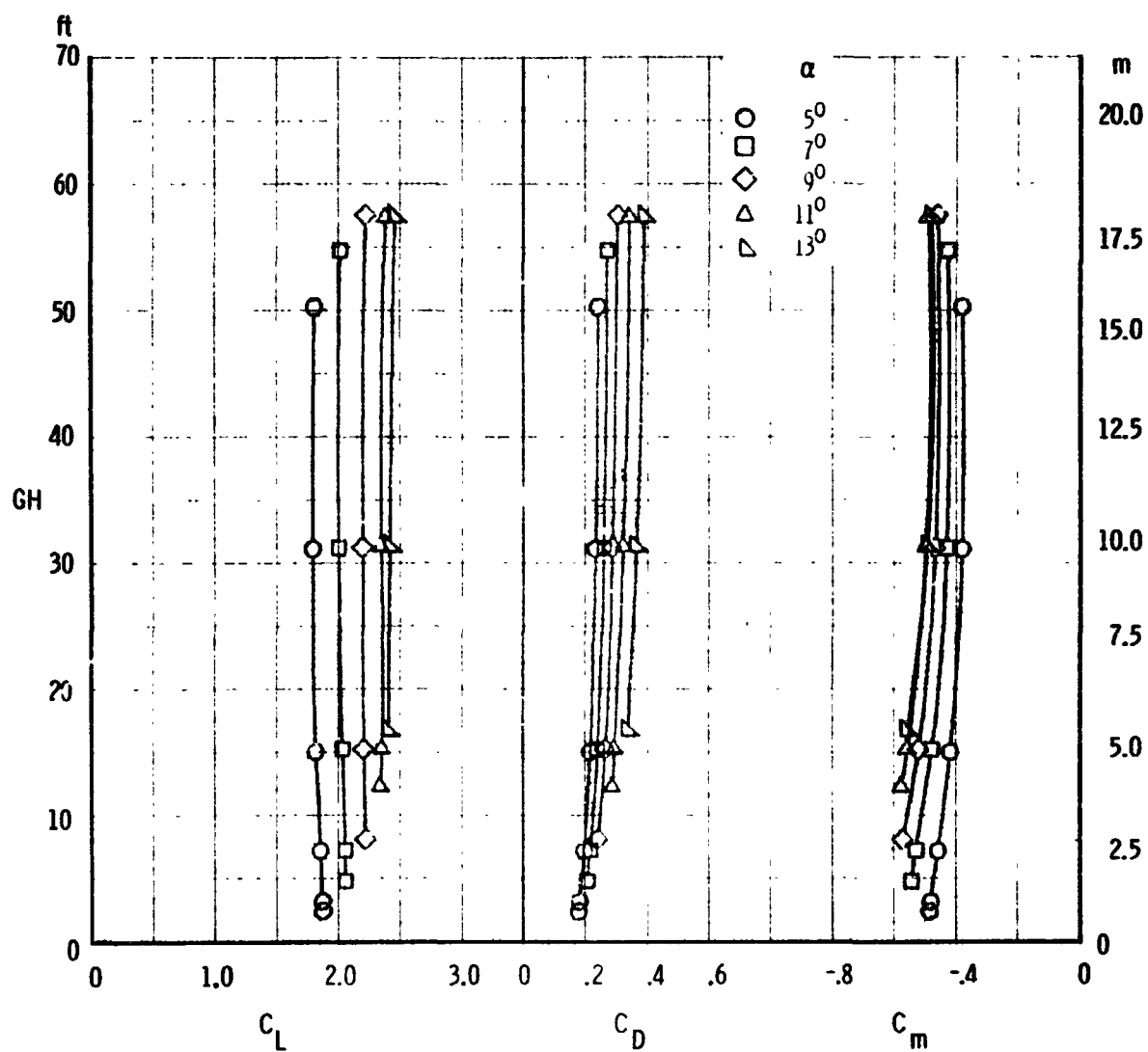
(a) Longitudinal characteristics

Figure 19. - Effect of sideslip angle on the aerodynamic characteristics of the F.W.F₃₀.N.G.H_T.V_T configuration.

(b) lateral-directional characteristics

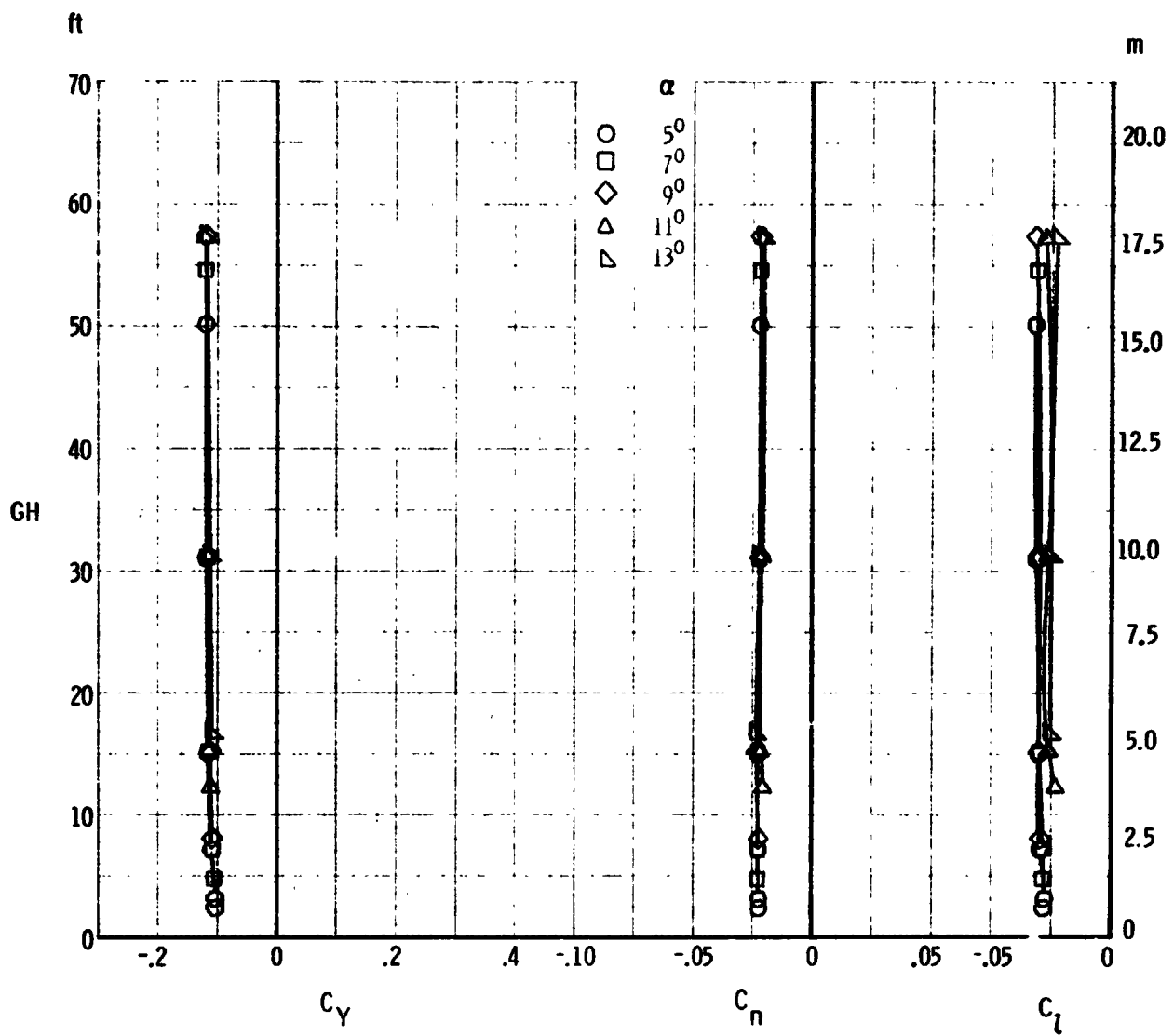
Figure 19. - Concluded.





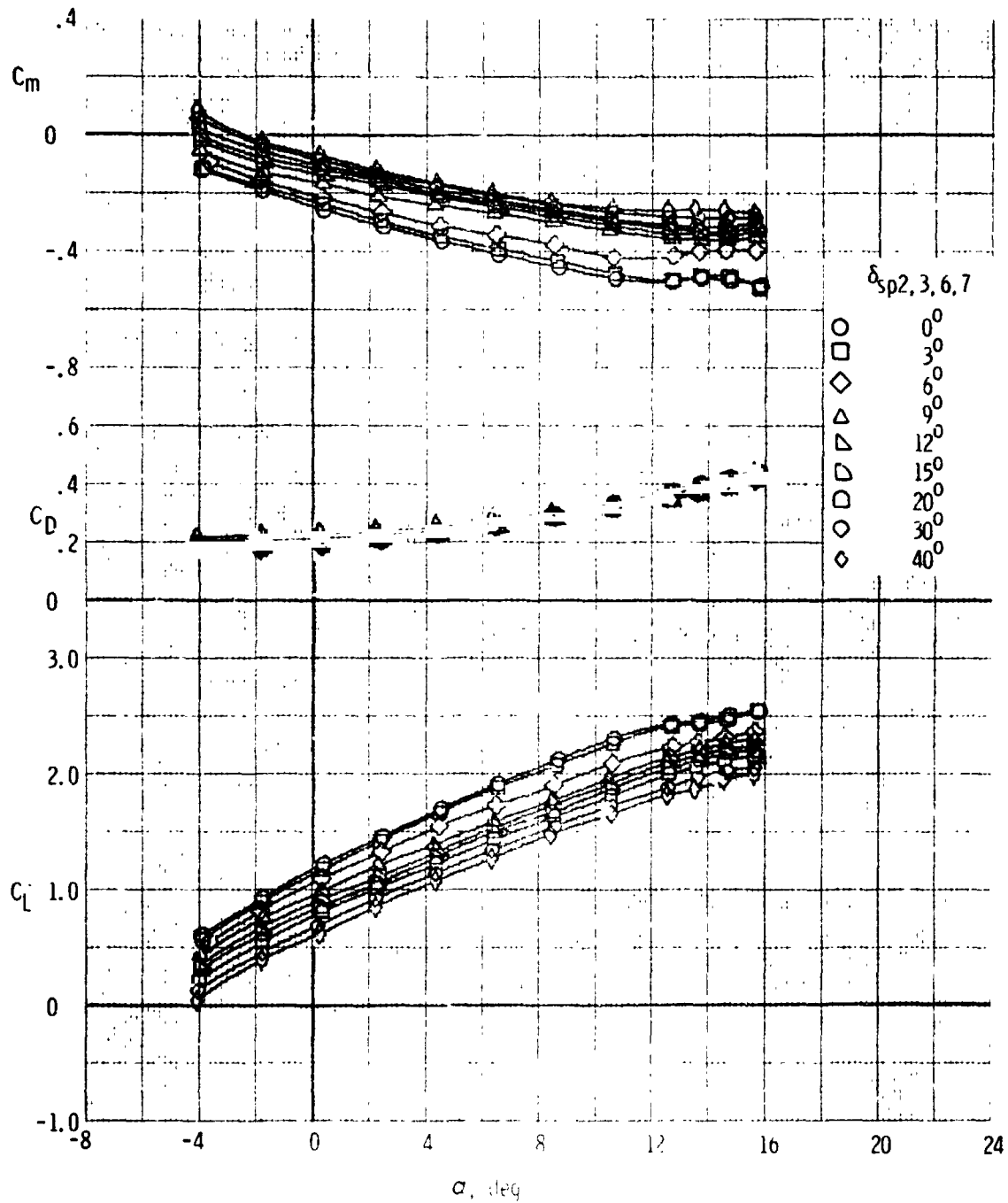
(a) Longitudinal characteristics

Figure 20. - Effect of ground height on the aerodynamic characteristics of the F, W, F₃₀, N, G, H_T, V_T configuration.



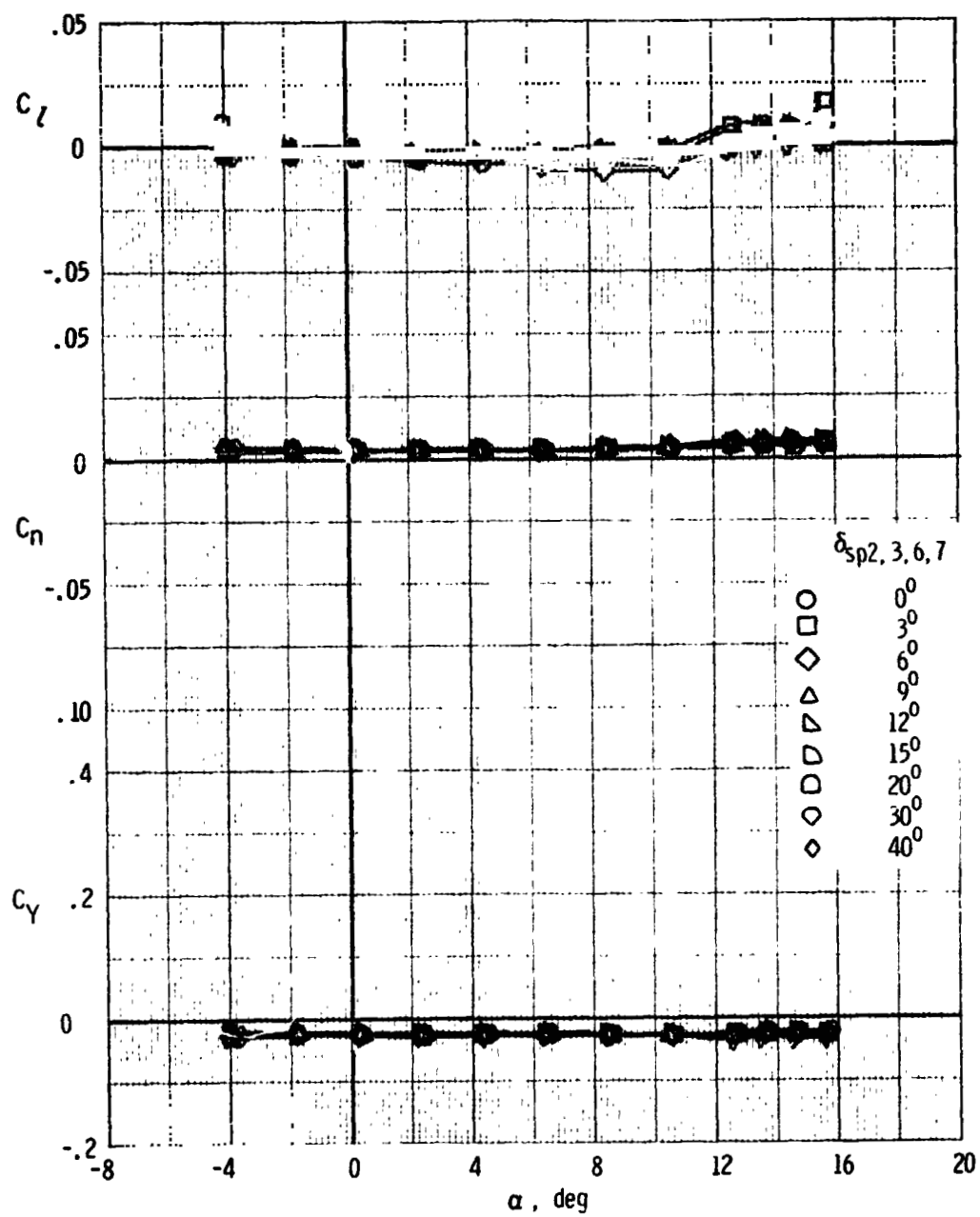
(b) Lateral-directional characteristics

Figure 20. - Concluded.



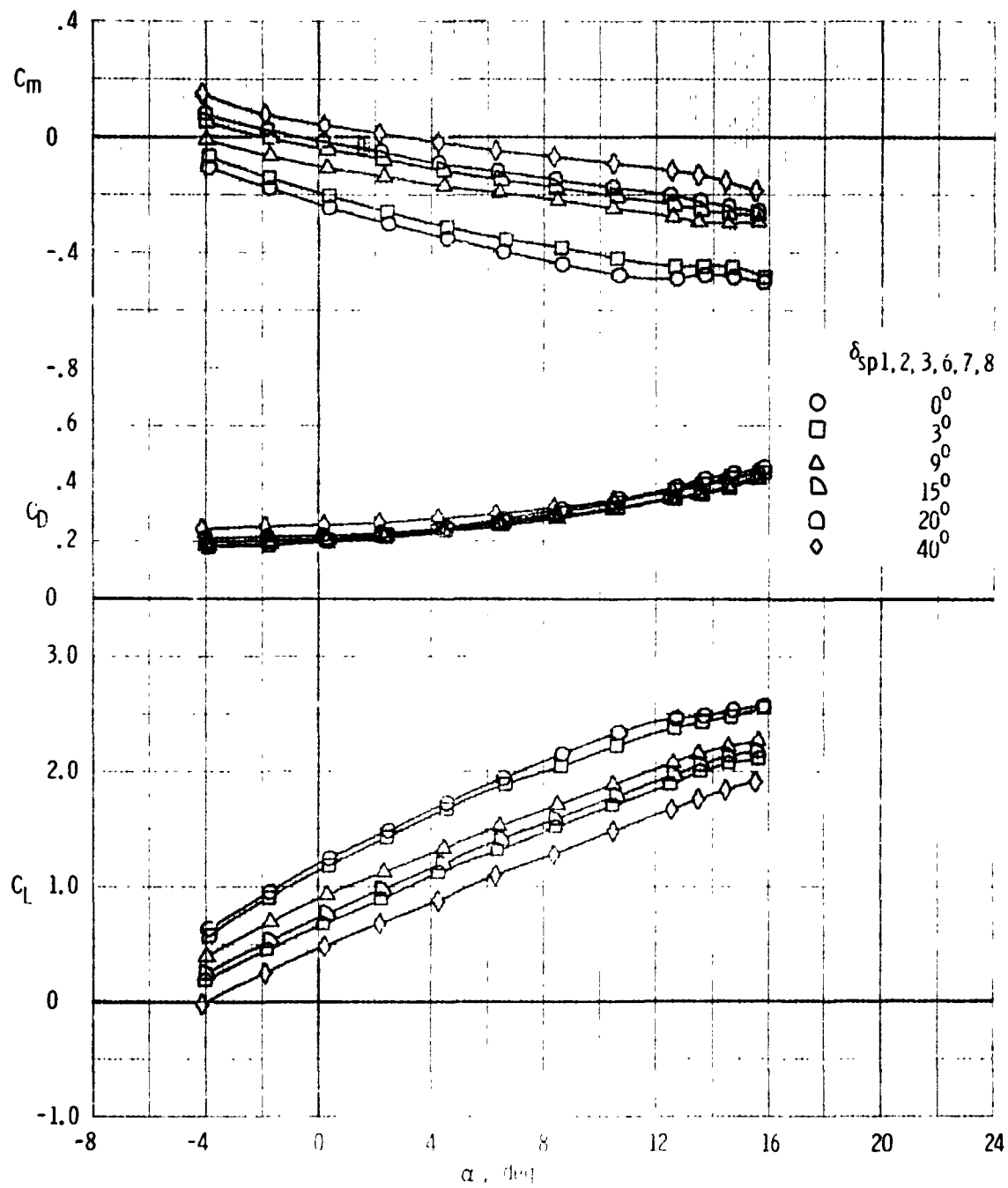
(a) Variation of longitudinal characteristics

Figure 21. - Effect of DLC spoiler deflection on the aerodynamic characteristics of the $F, W, F_{30}, N, G, H_T, V_T$ configuration.



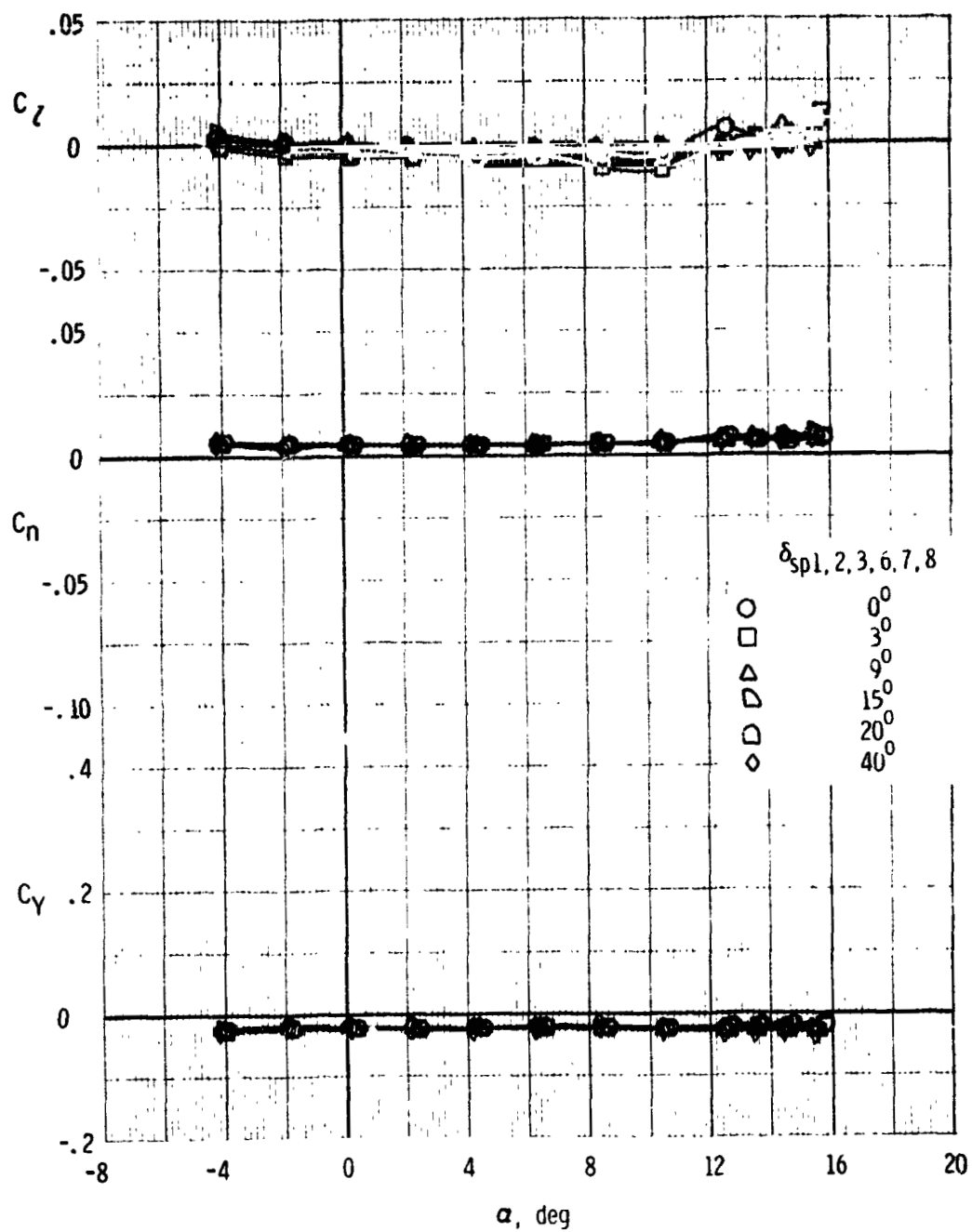
(b) Variation of lateral-directional characteristics

Figure 21. - Continued.



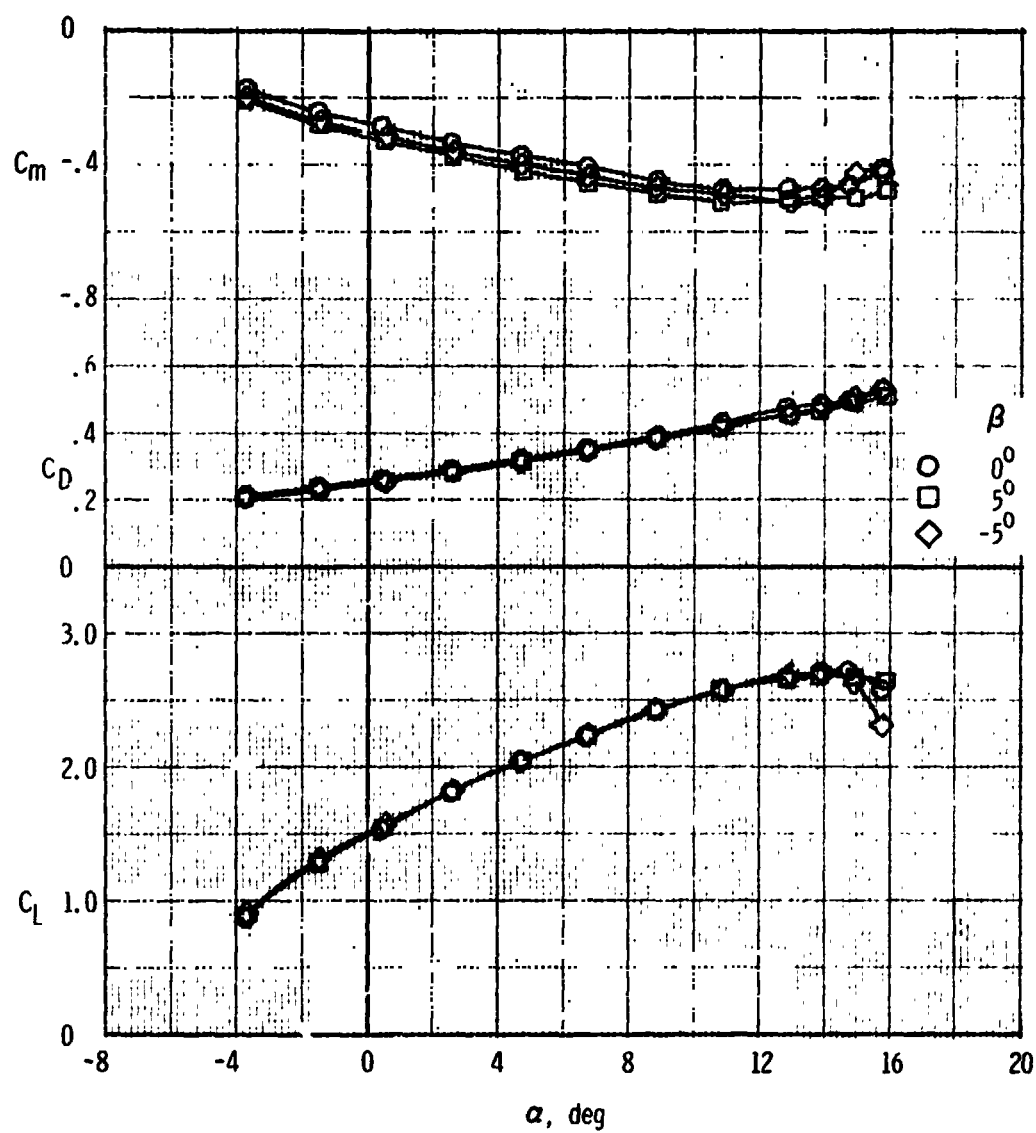
(c) Variation of longitudinal characteristics

Figure 21 - Continued.



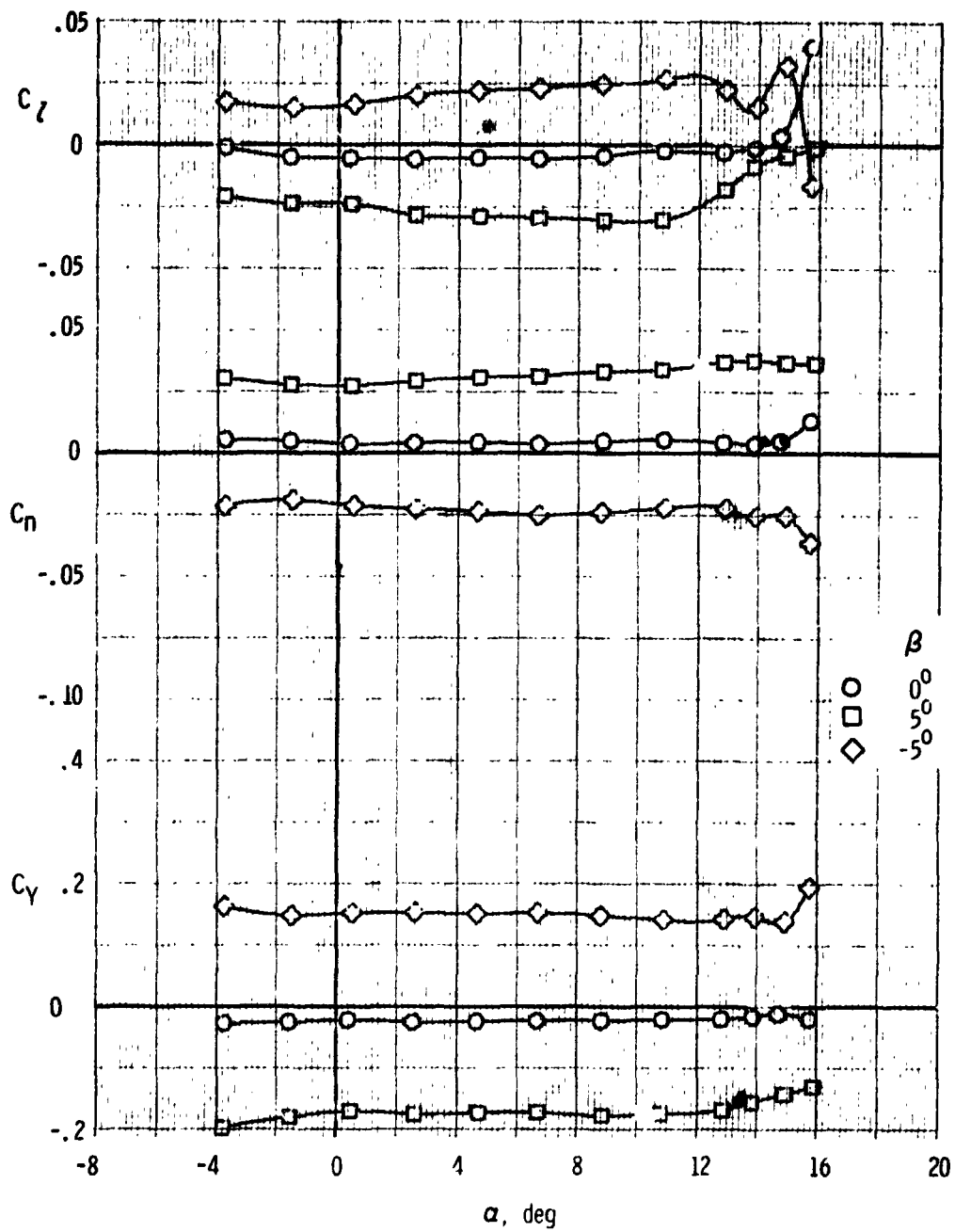
(d) Variation of lateral-directional characteristics

Figure 21. - Concluded.



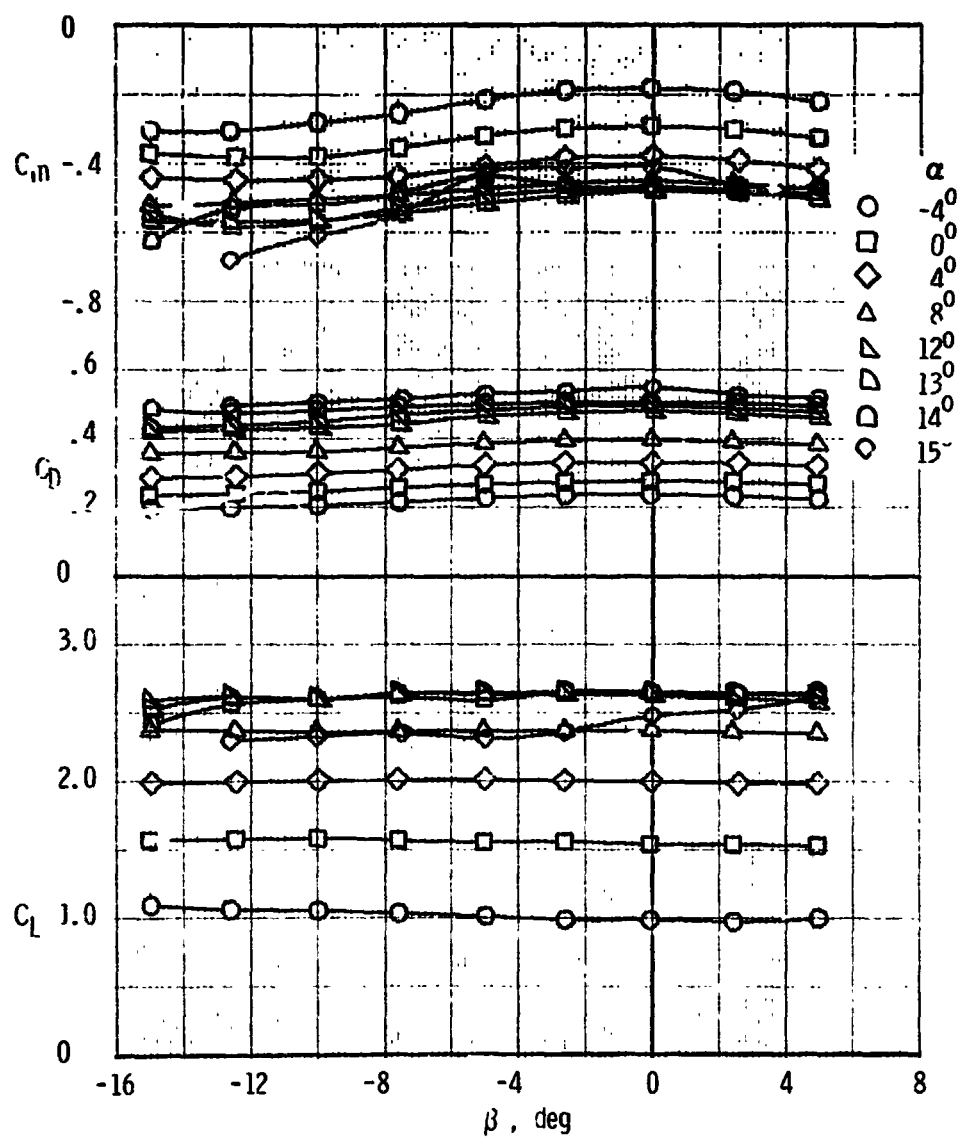
(a) Variation of longitudinal characteristics with angle of attack

Figure 22. - Effect of sideslip angle on the aerodynamic characteristics of the $F, W, F_{40}, N, G, H_T, V_T$ configuration.



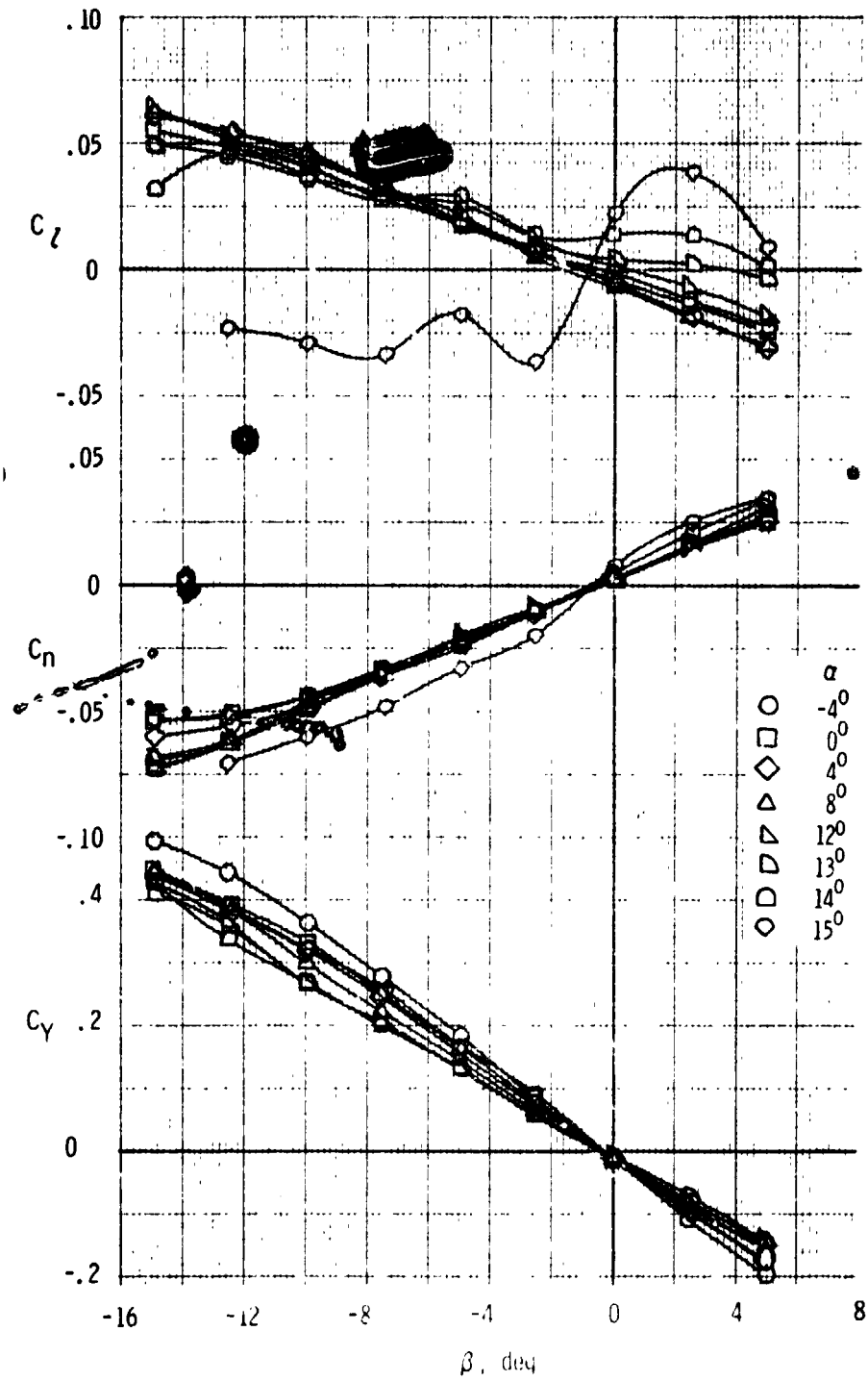
(b) Variation of lateral-directional characteristics with angle of attack

Figure 22. - Continued.



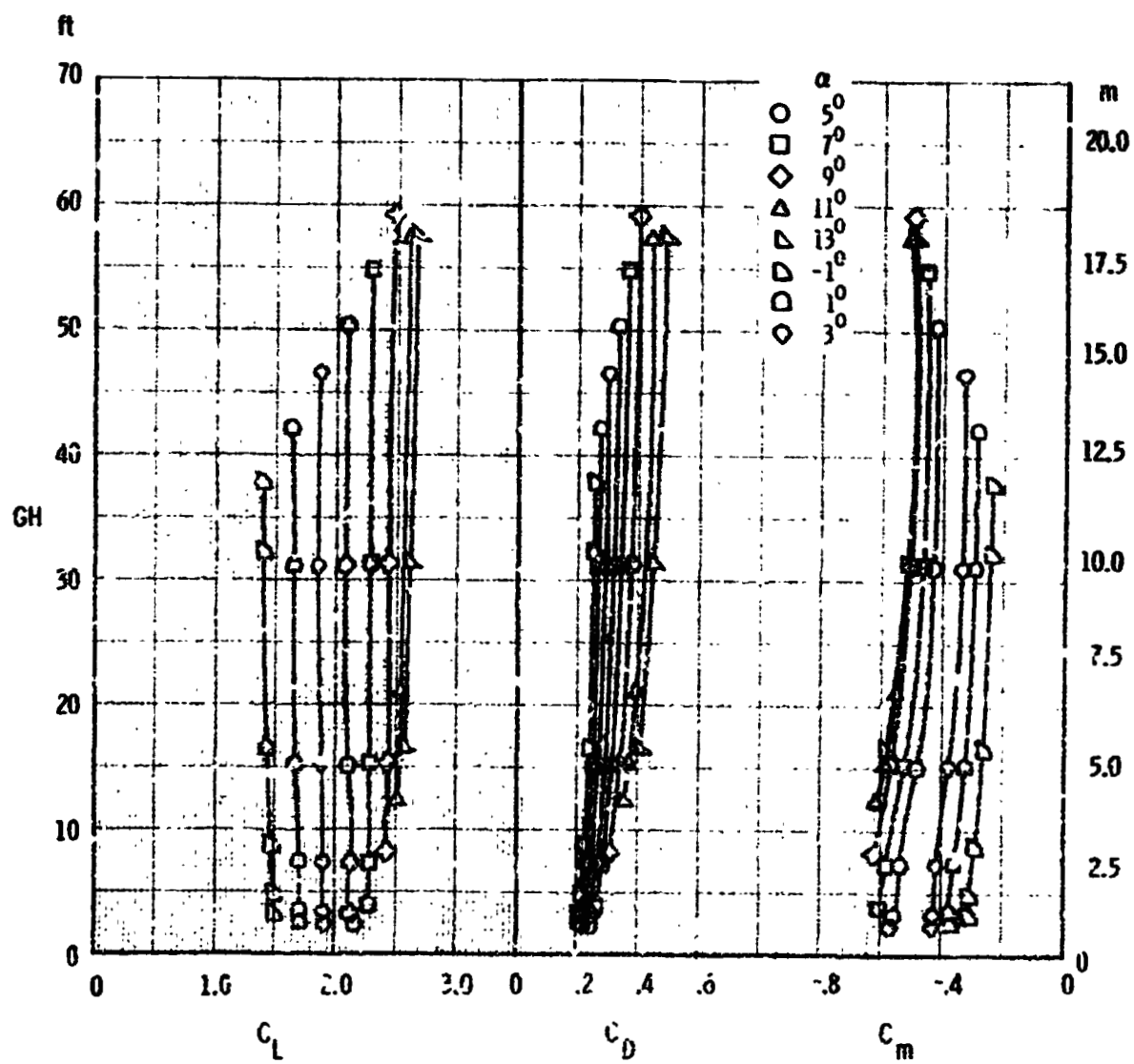
(c) Variation of longitudinal characteristics with sideslip angle

Figure 22. - Continued.



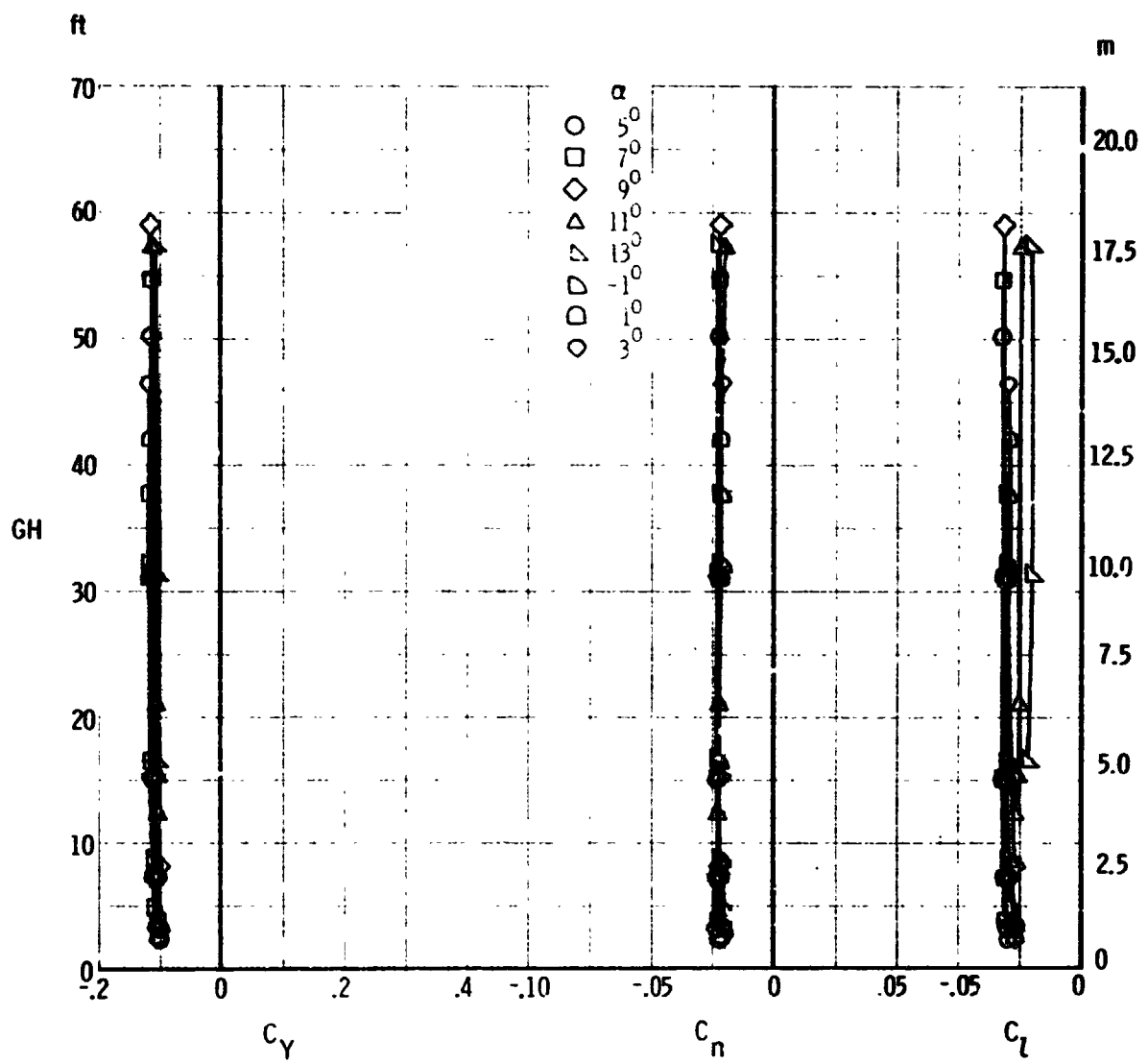
(b) Variation of lateral-directional characteristics with sideslip angle

Figure 22. - Concluded.



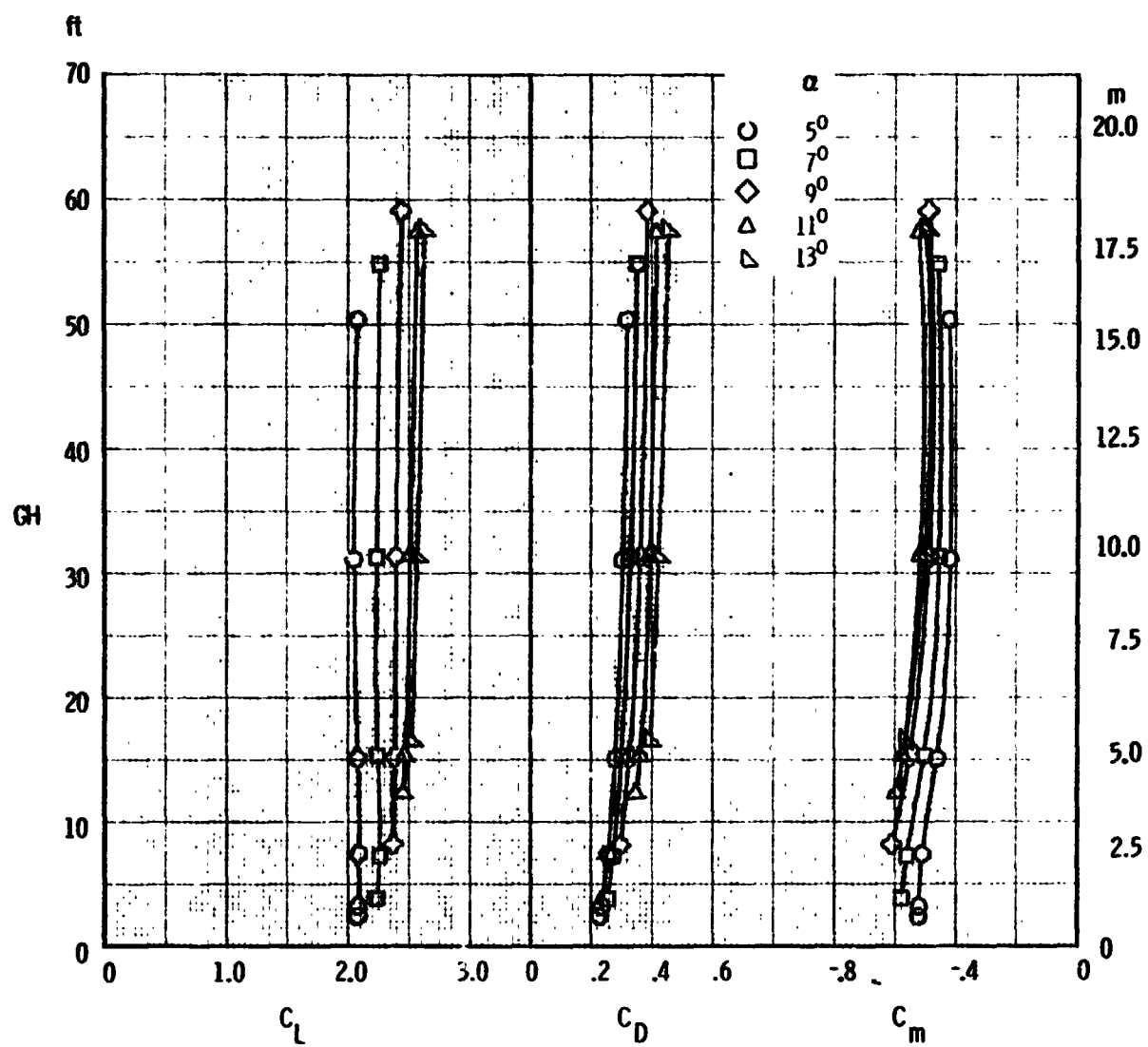
(a) Longitudinal characteristics, $\beta = 0^\circ$

Figure 23. - Effect of ground height on the aerodynamic characteristics of the F-40, N, G, H_T, V_T configuration at various sideslip angles.



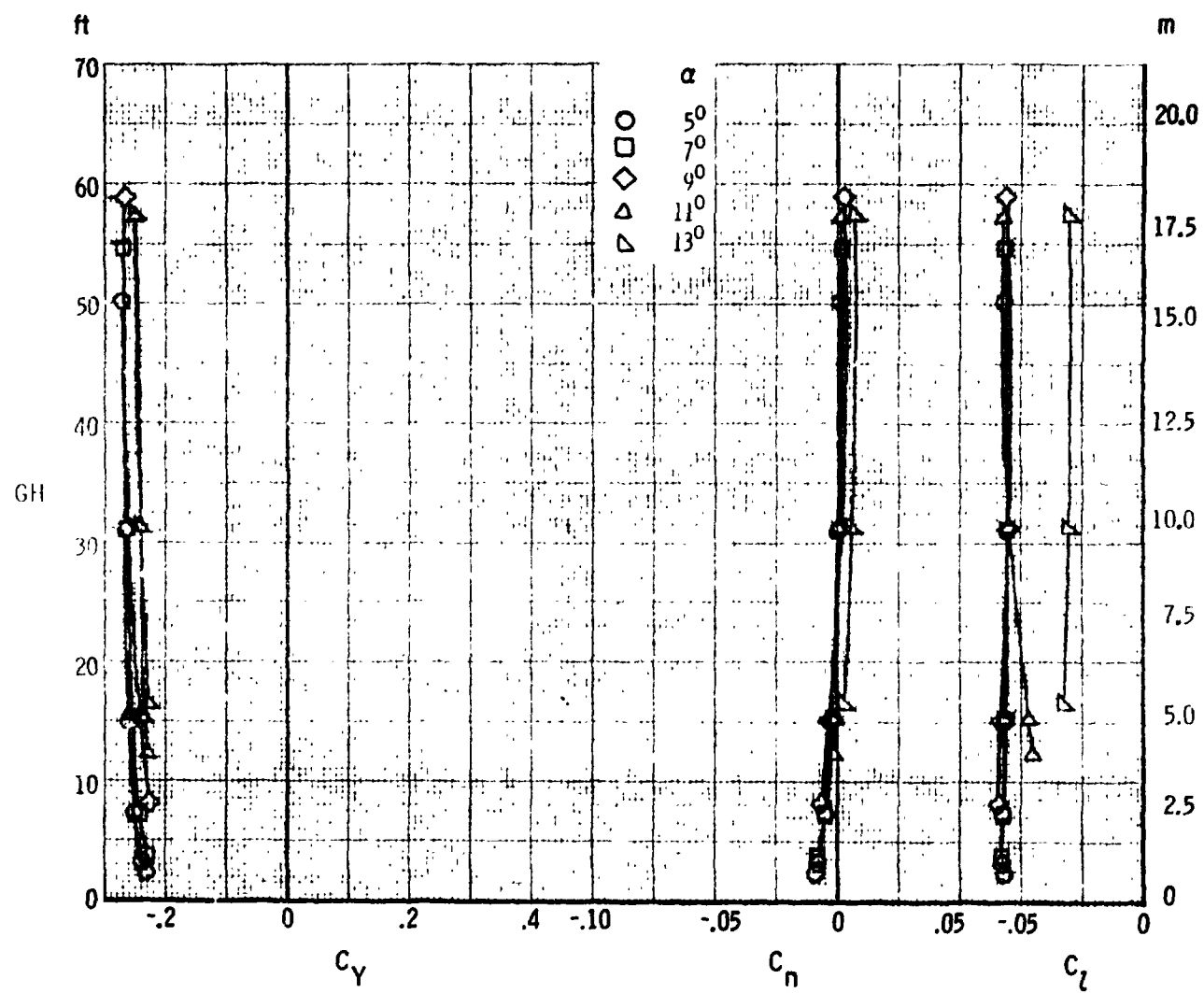
(b) Lateral-directional characteristics, $\beta = 0^\circ$

Figure 2a. - Continued.



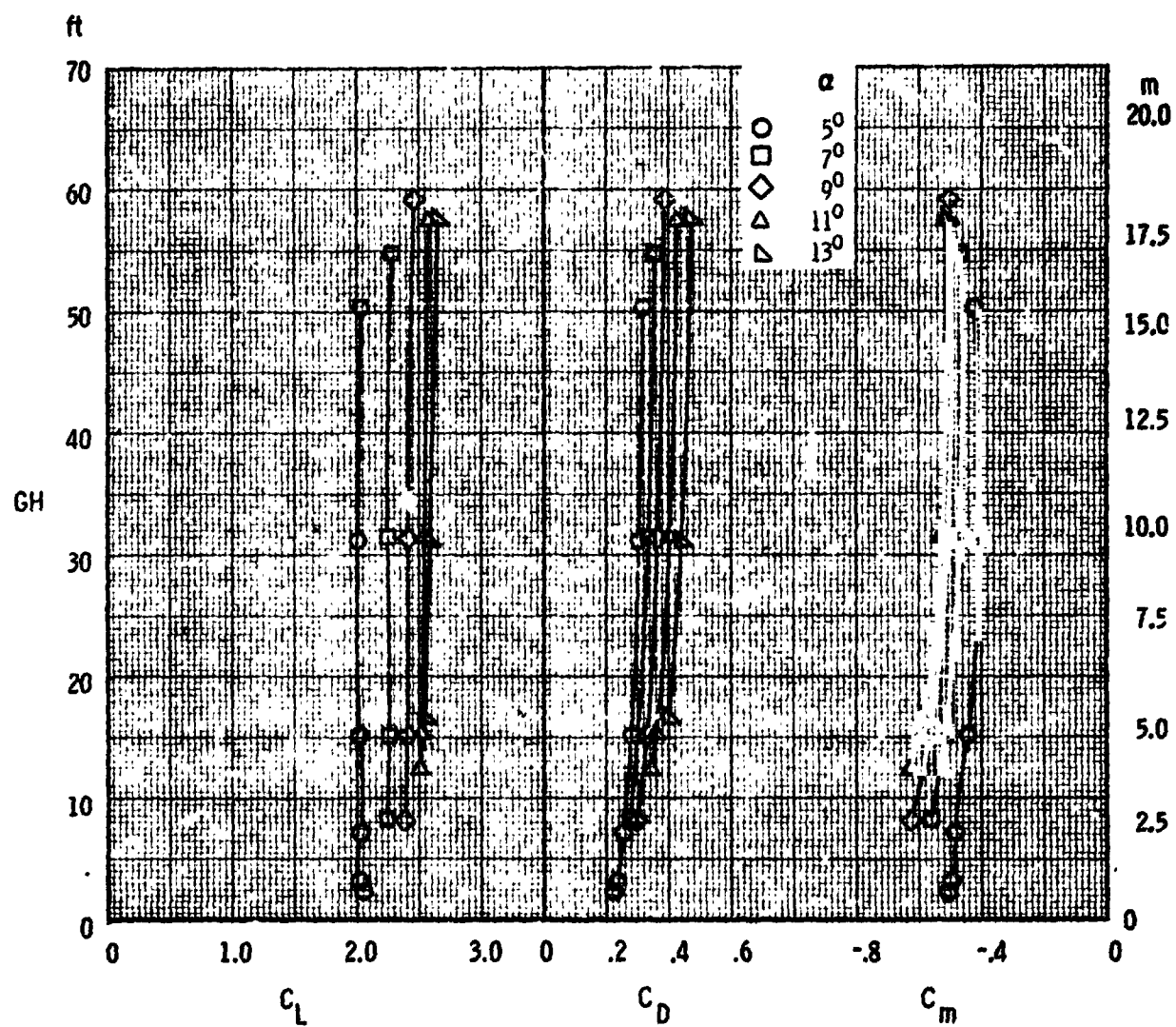
(c) Longitudinal characteristics, $\beta = 5^\circ$

Figure 23. - Continued.



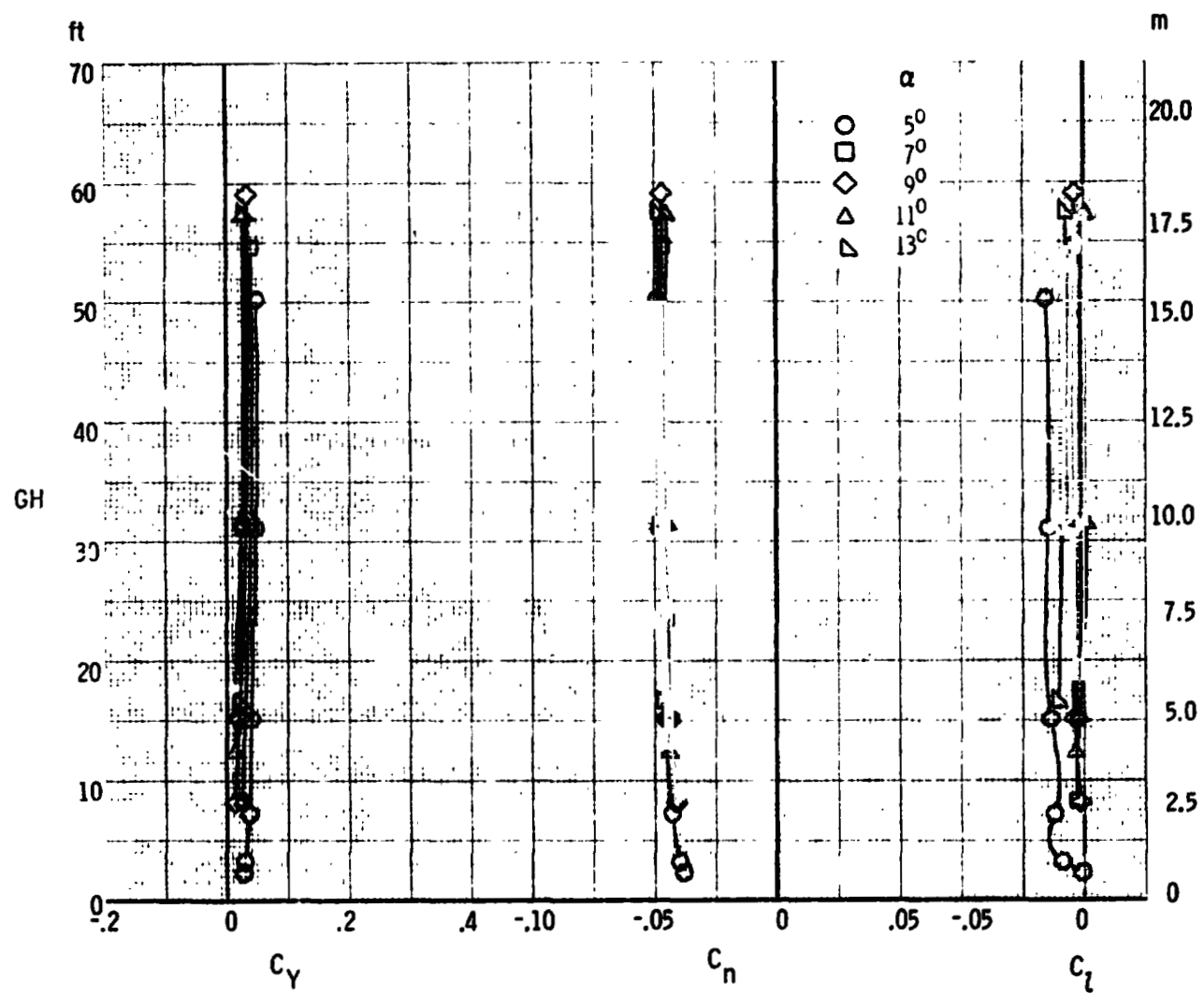
(d) Lateral-directional characteristics, $\beta = 5^\circ$

Figure 23. - Continued.



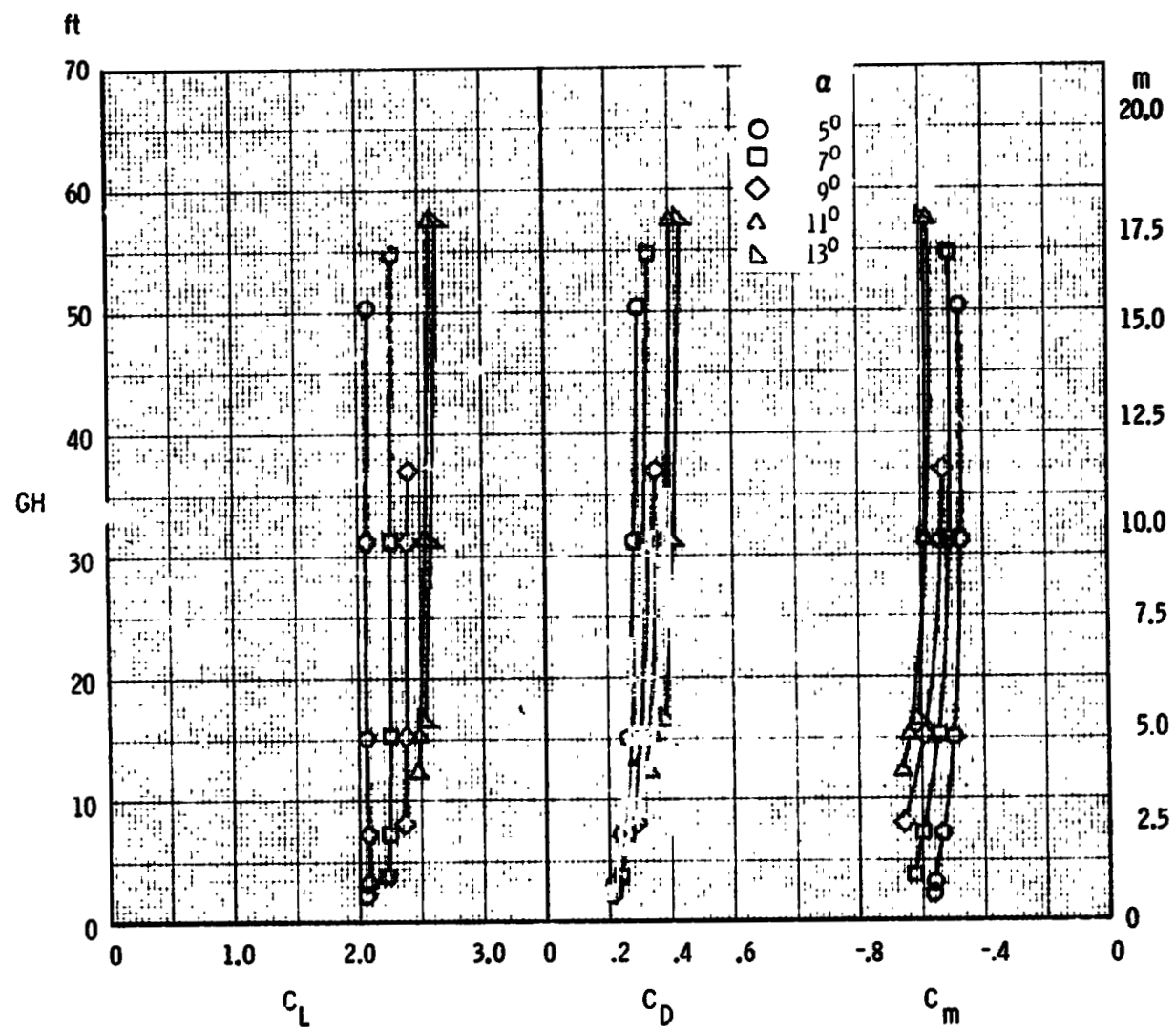
(e) Longitudinal characteristics, $\beta = -5^\circ$

Figure 23. - Continued.



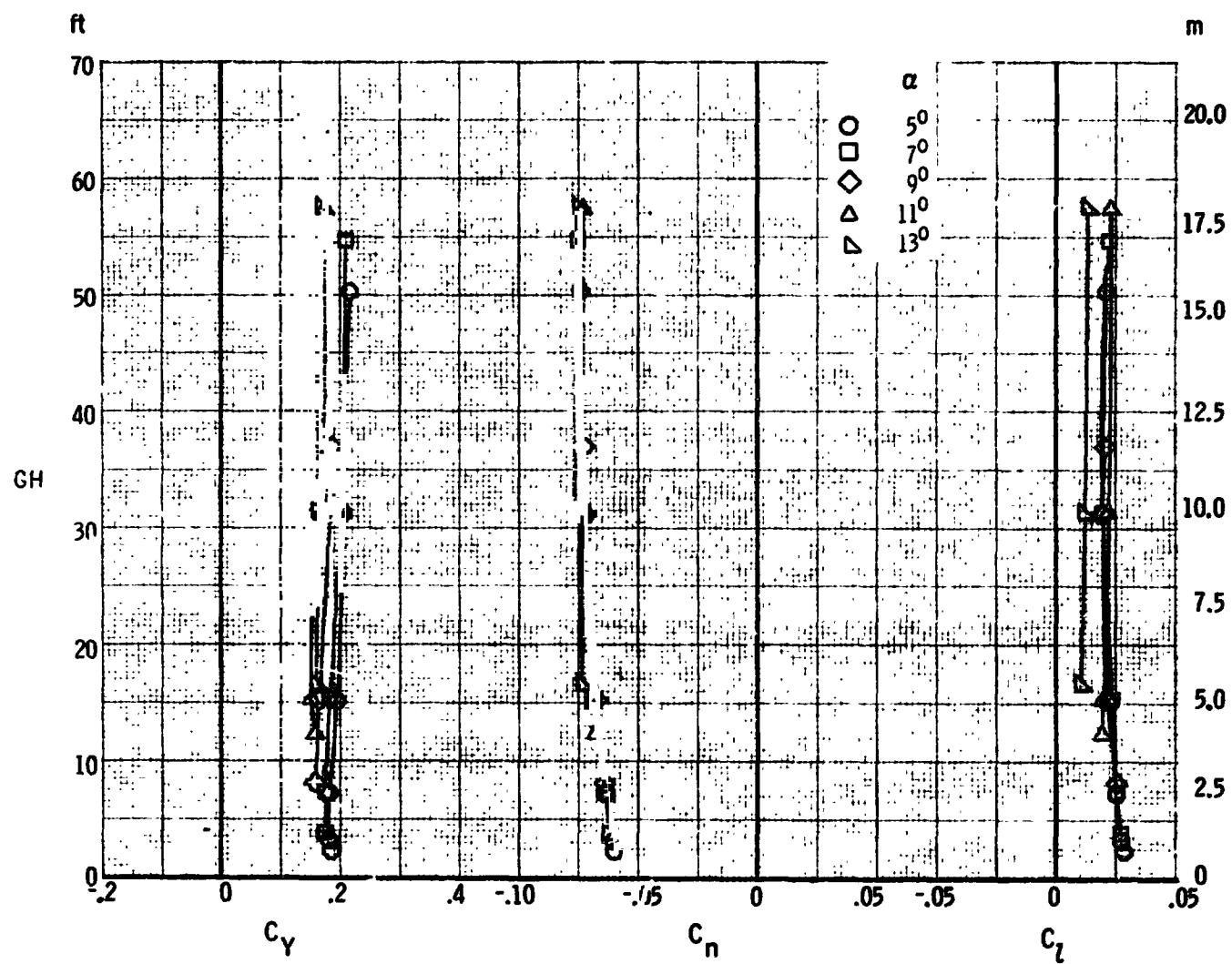
(f) Lateral-directional characteristics, $\beta = -5^\circ$

Figure 23. - Continued.



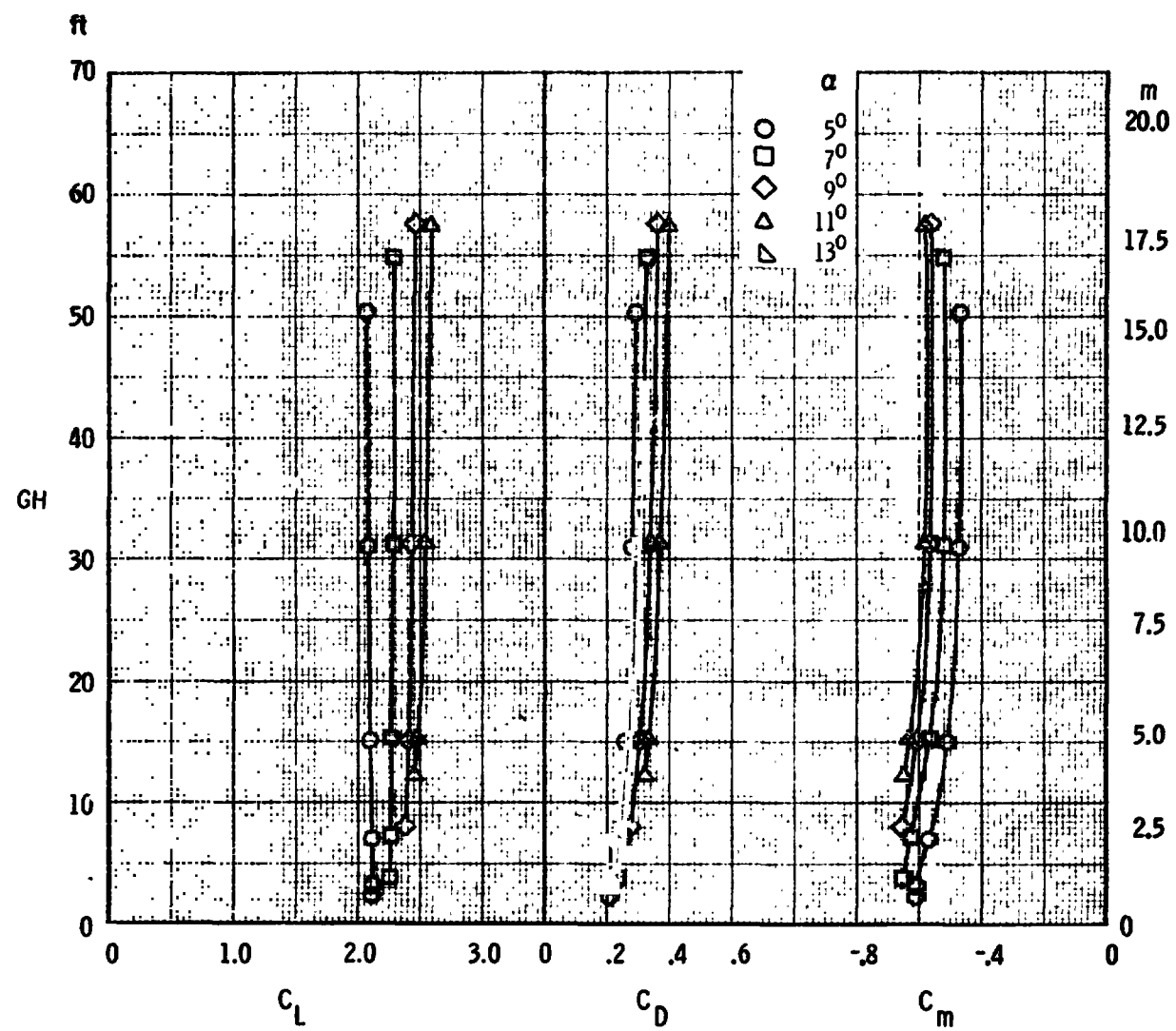
(g) Longitudinal characteristics, $\beta = -10^\circ$

Figure 23. - Continued.



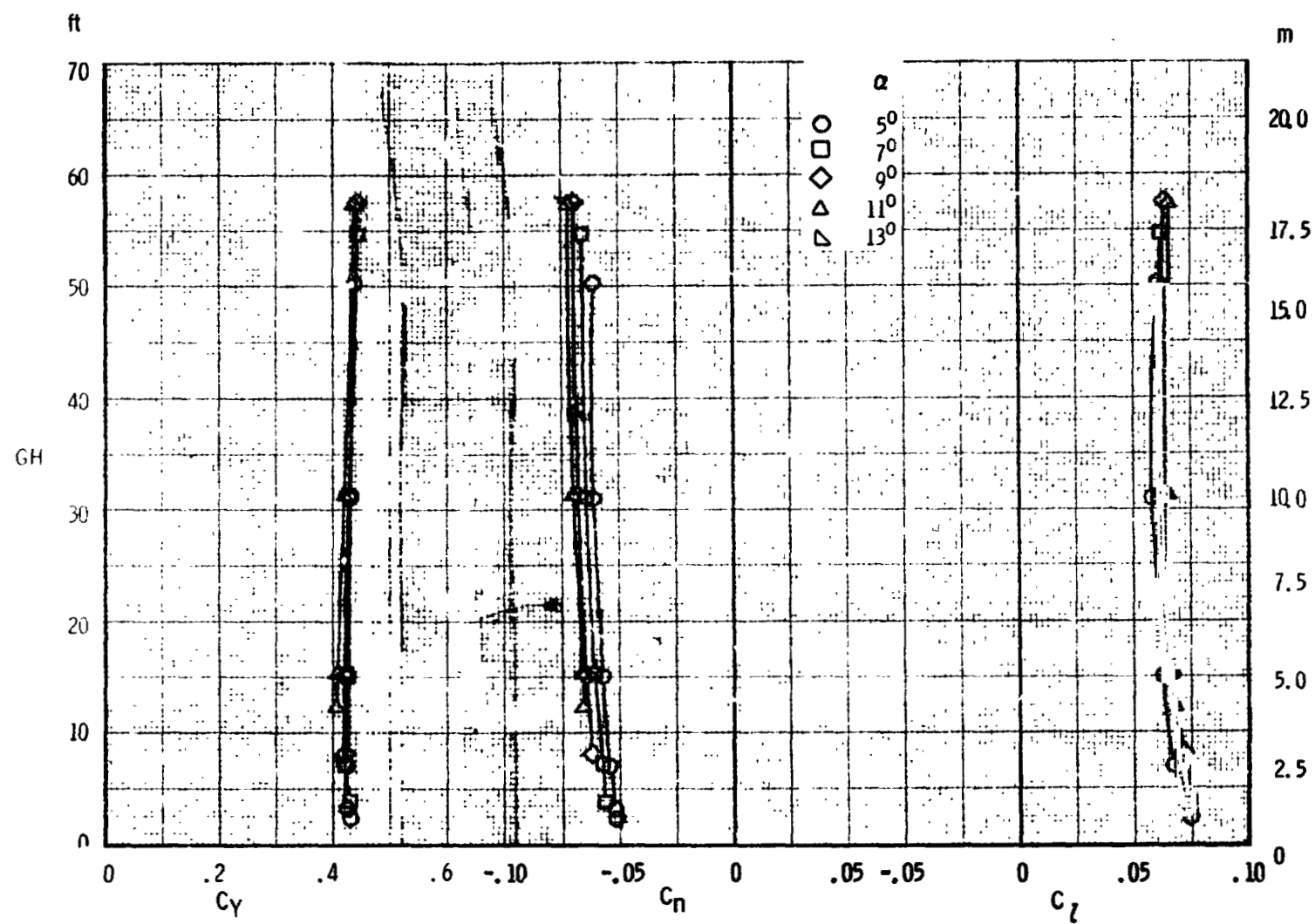
(h) Lateral-directional characteristics, $\beta = -10^\circ$

Figure 23. - Continued.



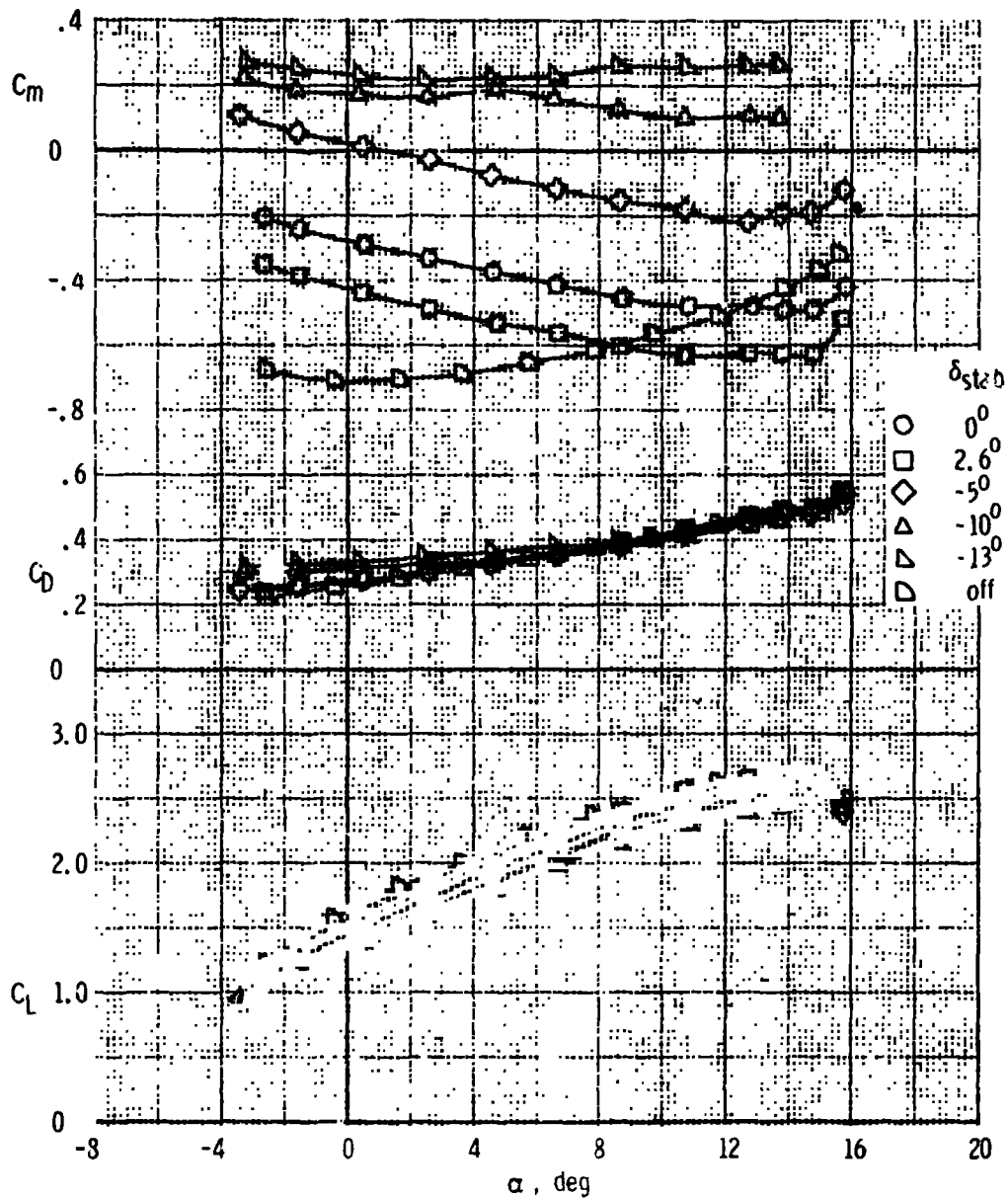
(i) Longitudinal characteristics, $\beta = -15^\circ$

Figure 23. - Continued.



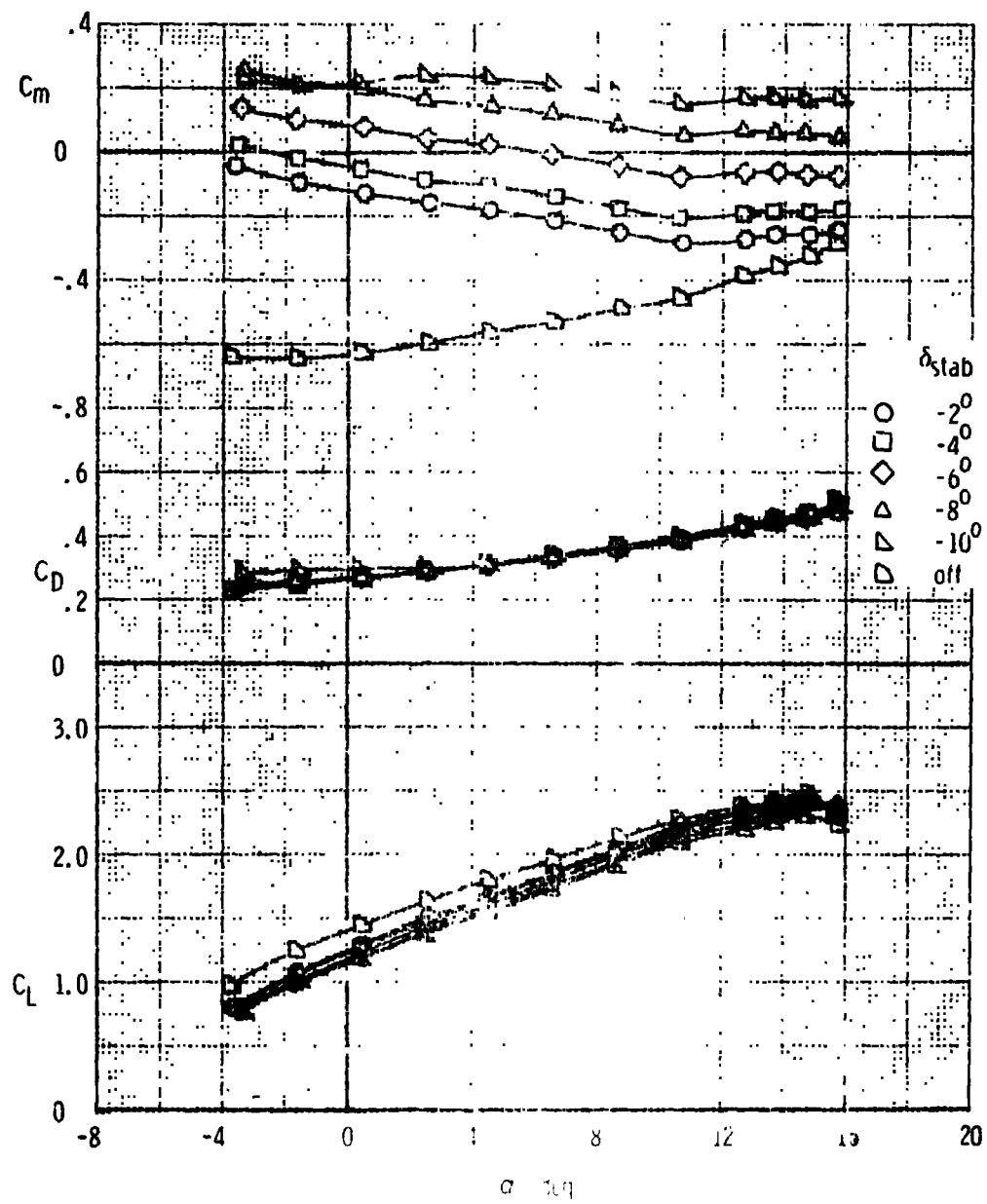
(j) Lateral-directional characteristics, $\beta = -15^\circ$

Figure 23. - Concluded.

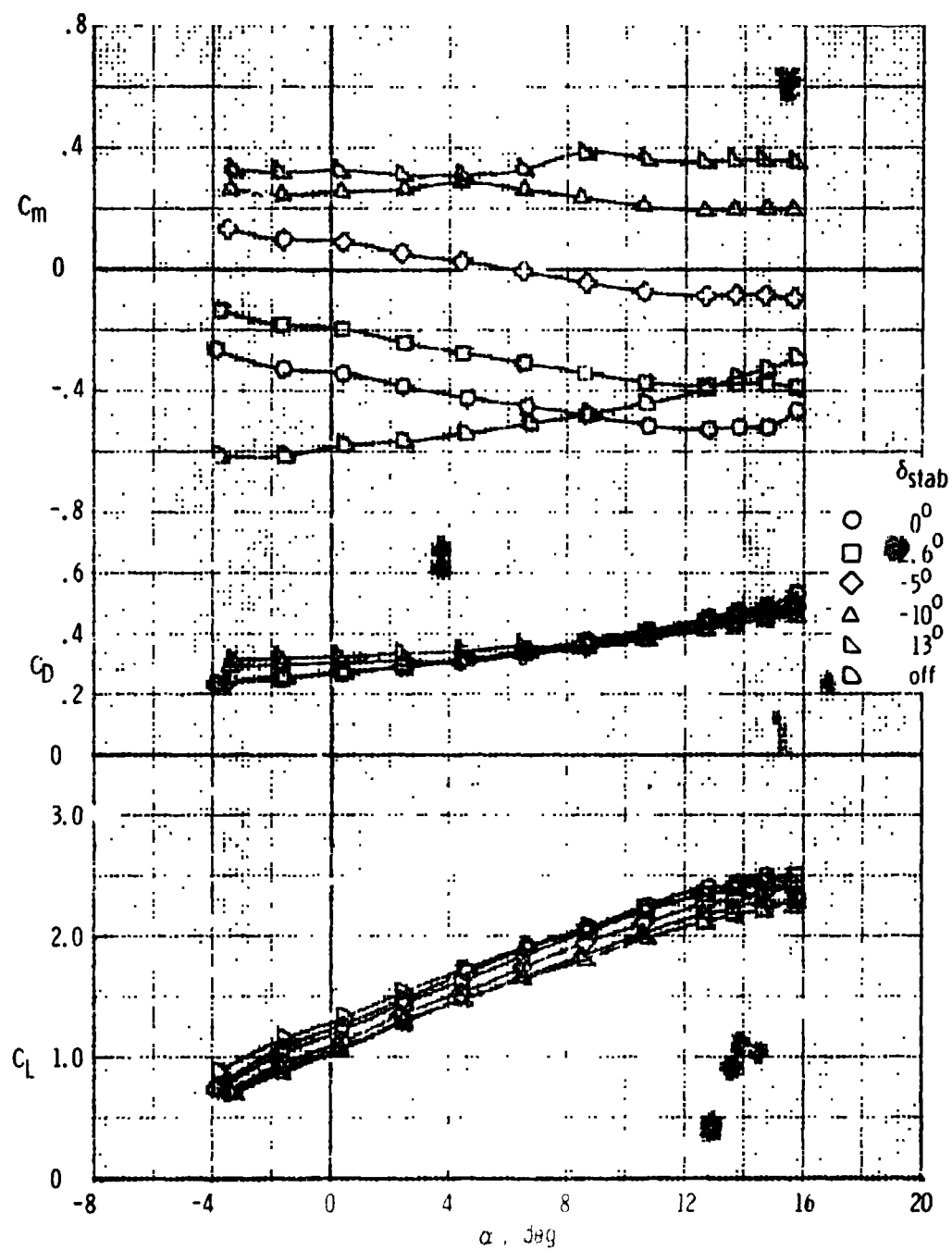


(a) $\delta_{sp2,3,6,7} = 0^\circ$

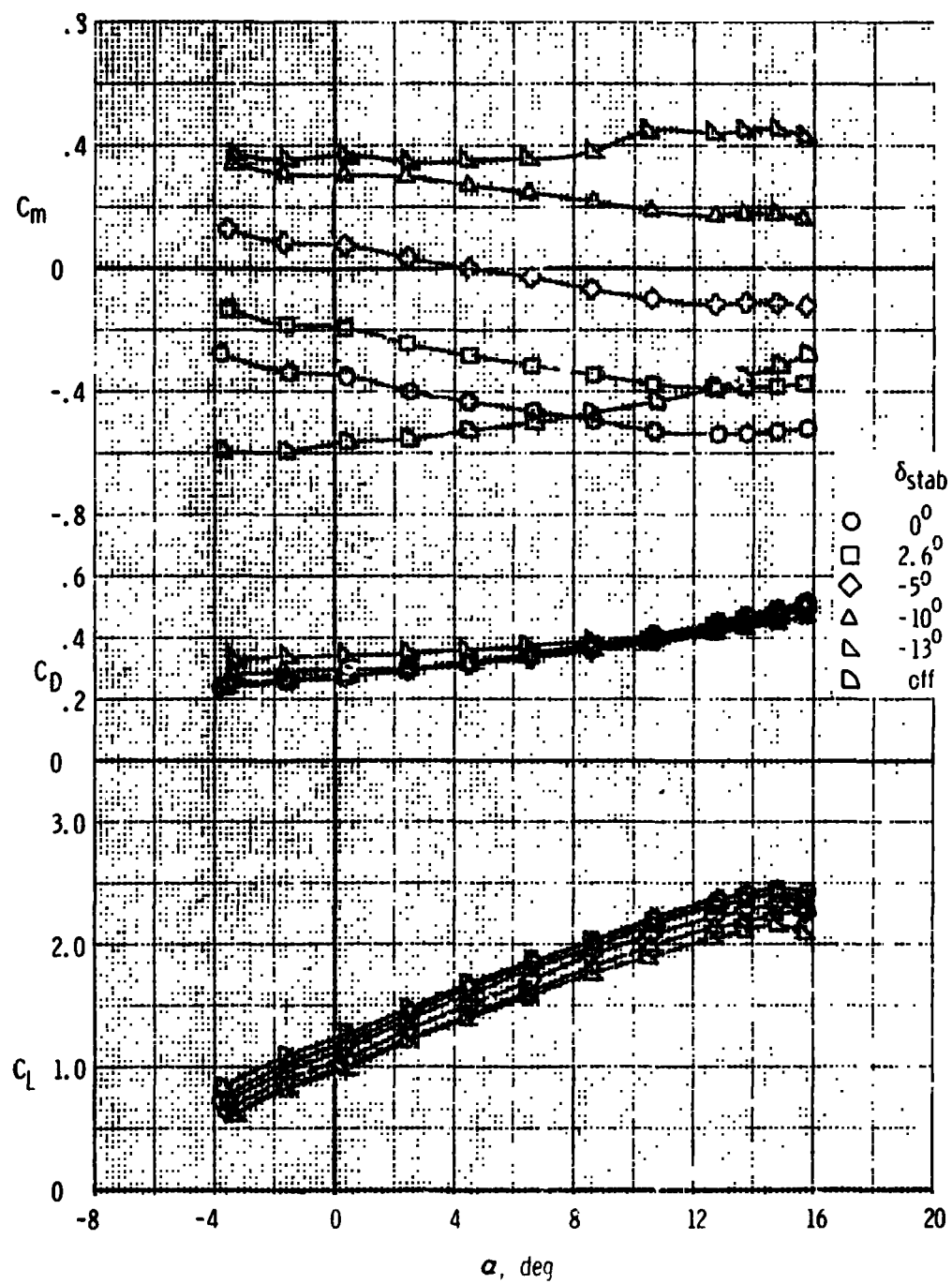
Figure 24. - Effect of stabilizer deflection on the longitudinal aerodynamic characteristics of the F, W, F₄₀, N, G, H_T, V_T configuration with various DLC spoiler deflections.



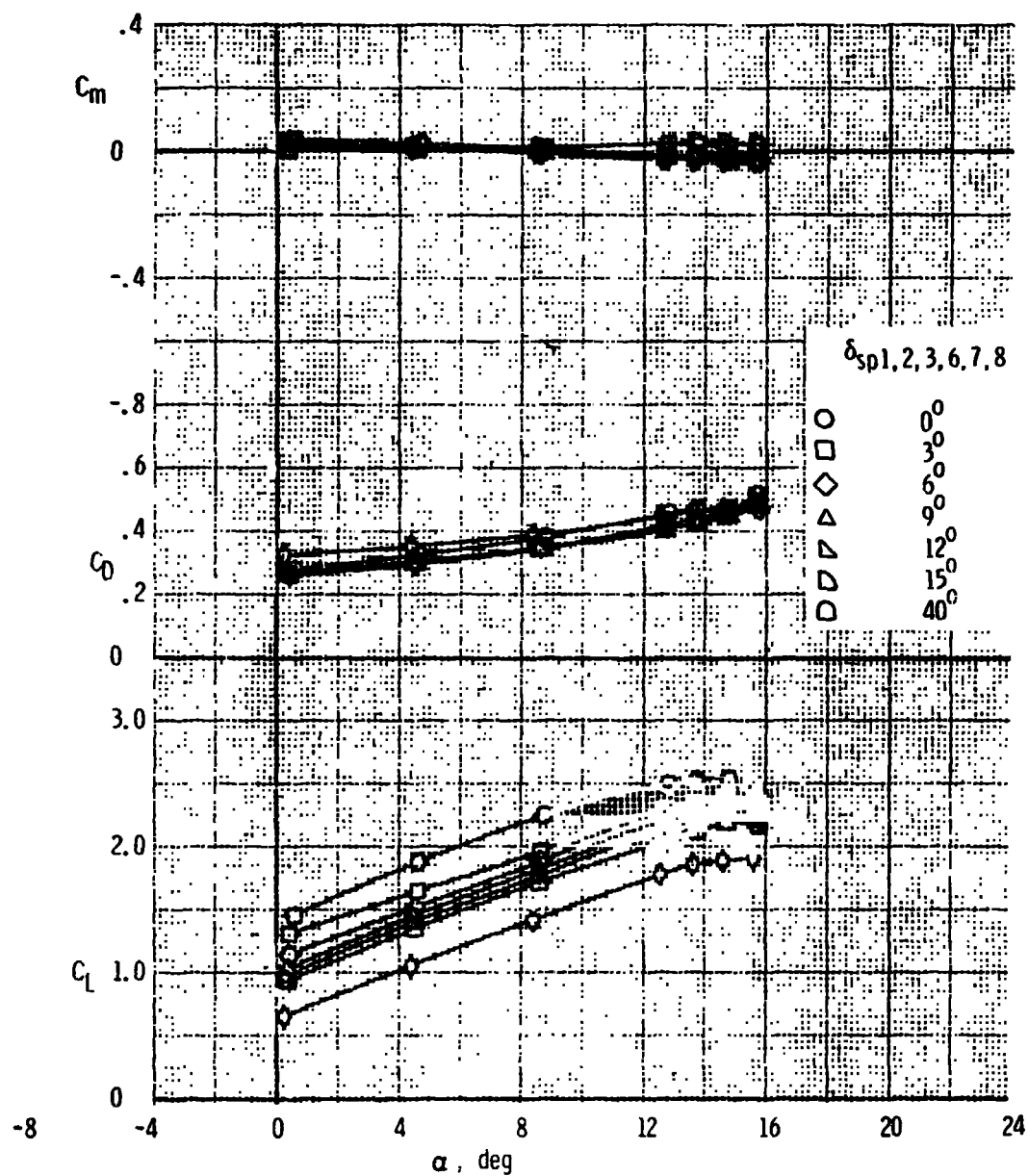
(b) $\delta_{stab} = -100^\circ$
Figure 24. - Cont'd.



(c) $\delta_{sp2,3,6,7} = 9^\circ$
 Figure 24. - Continued.



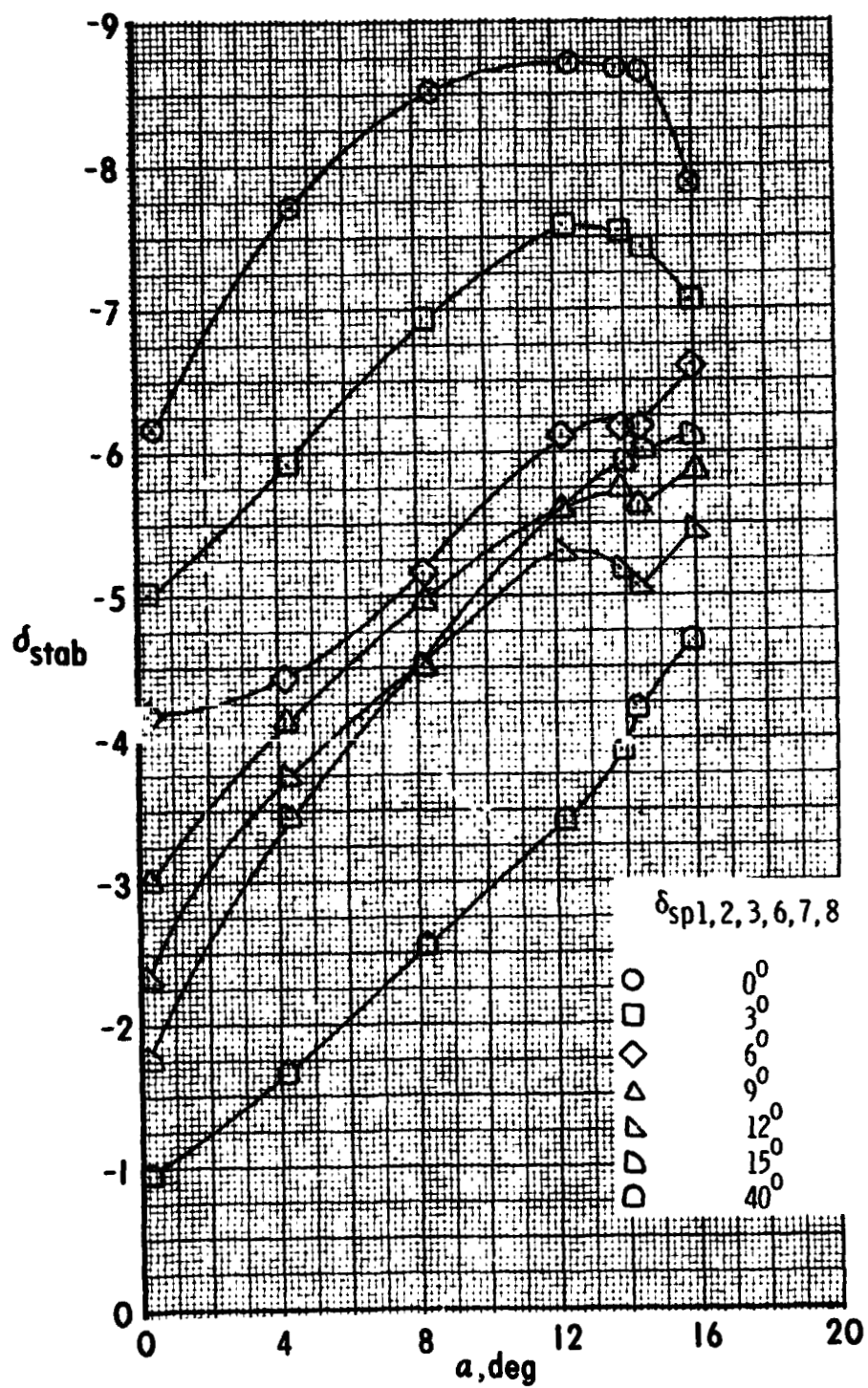
(d) $\delta_{sp2,3,6,7} = 12^\circ$
Figure 24. - Concluded.



(a) Variation of longitudinal characteristics with angle of attack

Figure 25. - Effect of Δ LC spoiler deflection on the trimmed longitudinal aerodynamic characteristics of the F, W, 40° N, G, H_T, V_T configuration.

2



(b) Variation of stabilizer setting for trim with angle of attack

Figure 25. - Concluded.

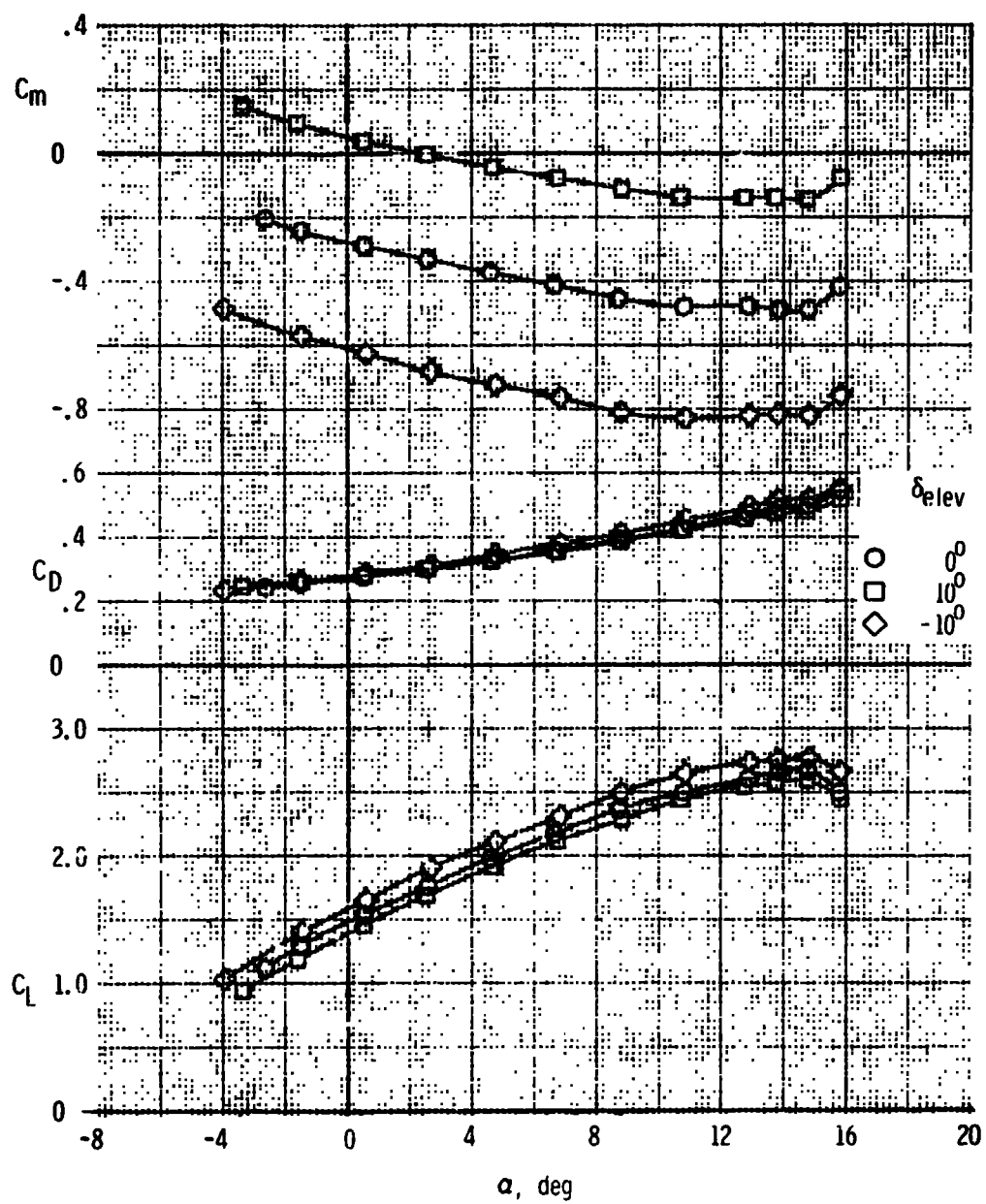


Figure 26. - Effect of elevator deflection on the longitudinal aerodynamic characteristics of the F, W, F₄₀, N, G, H, V_T, V_T configuration.

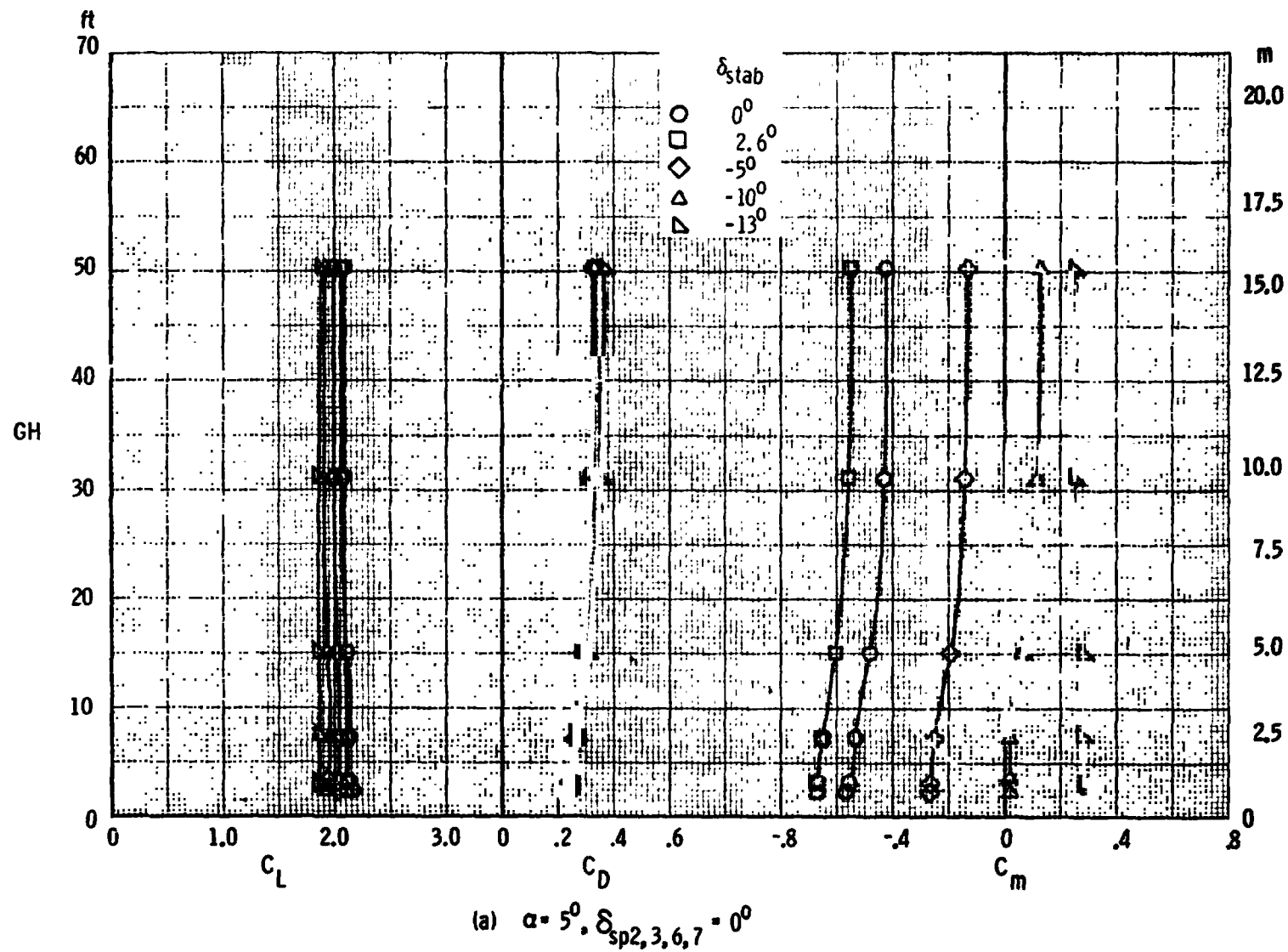
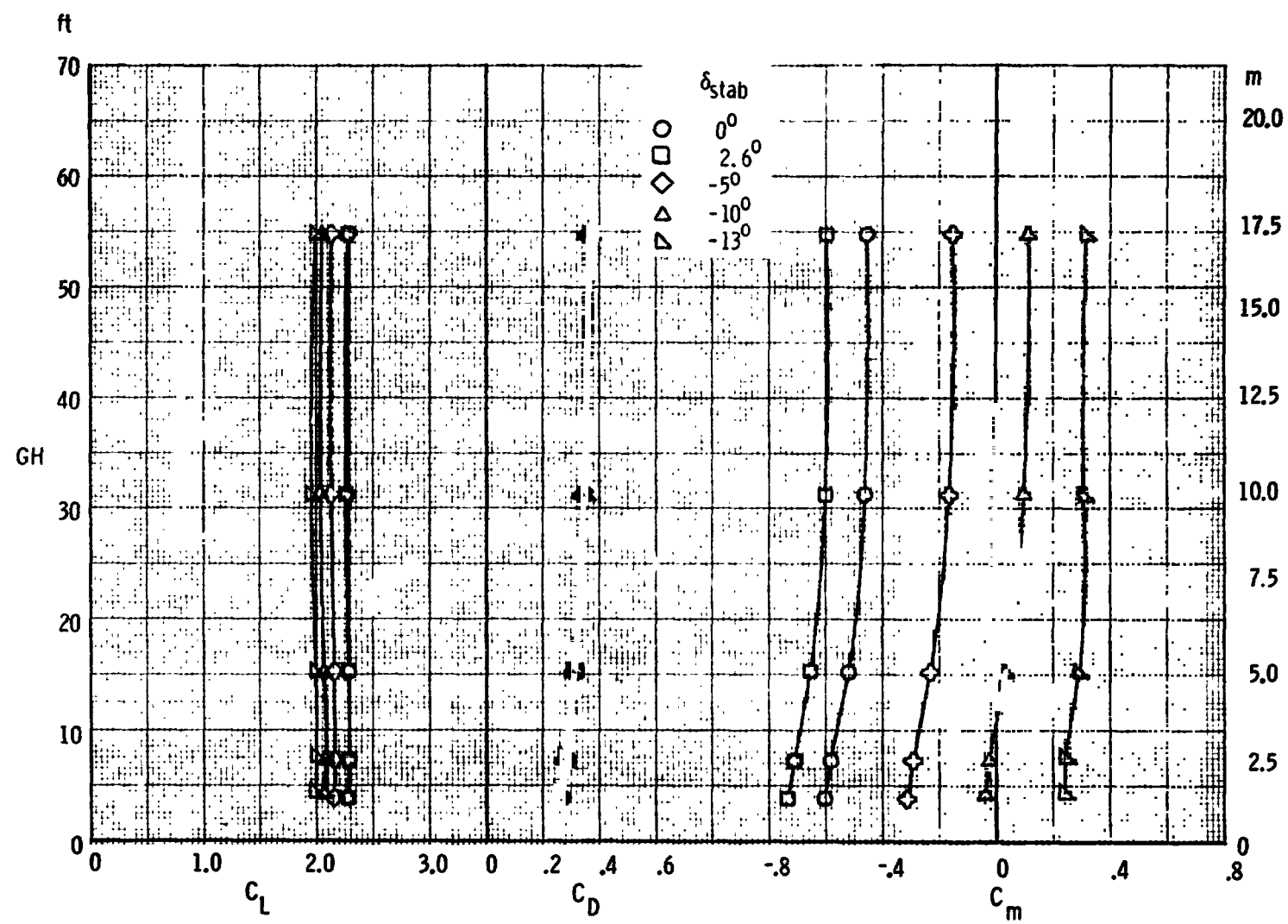
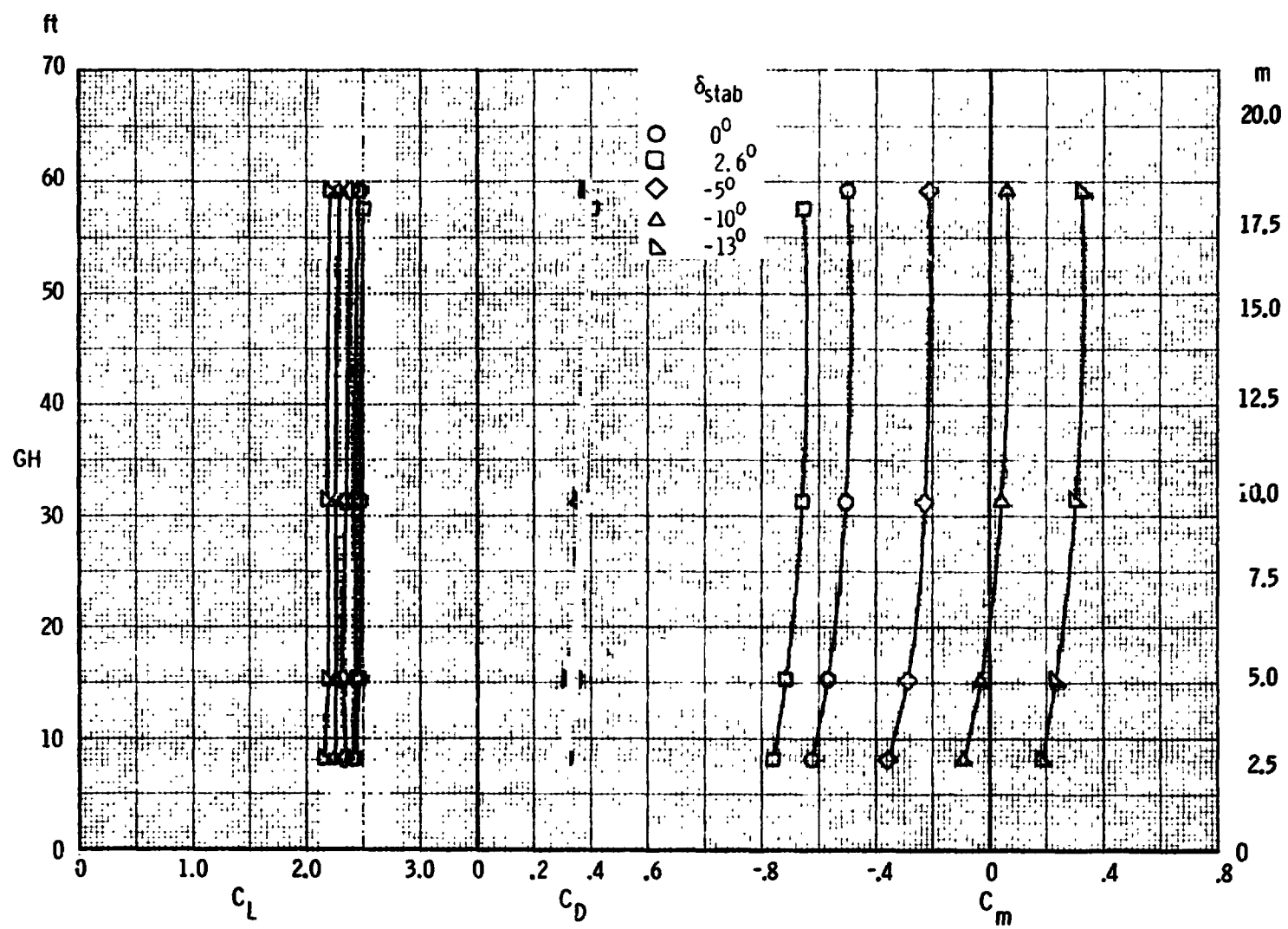


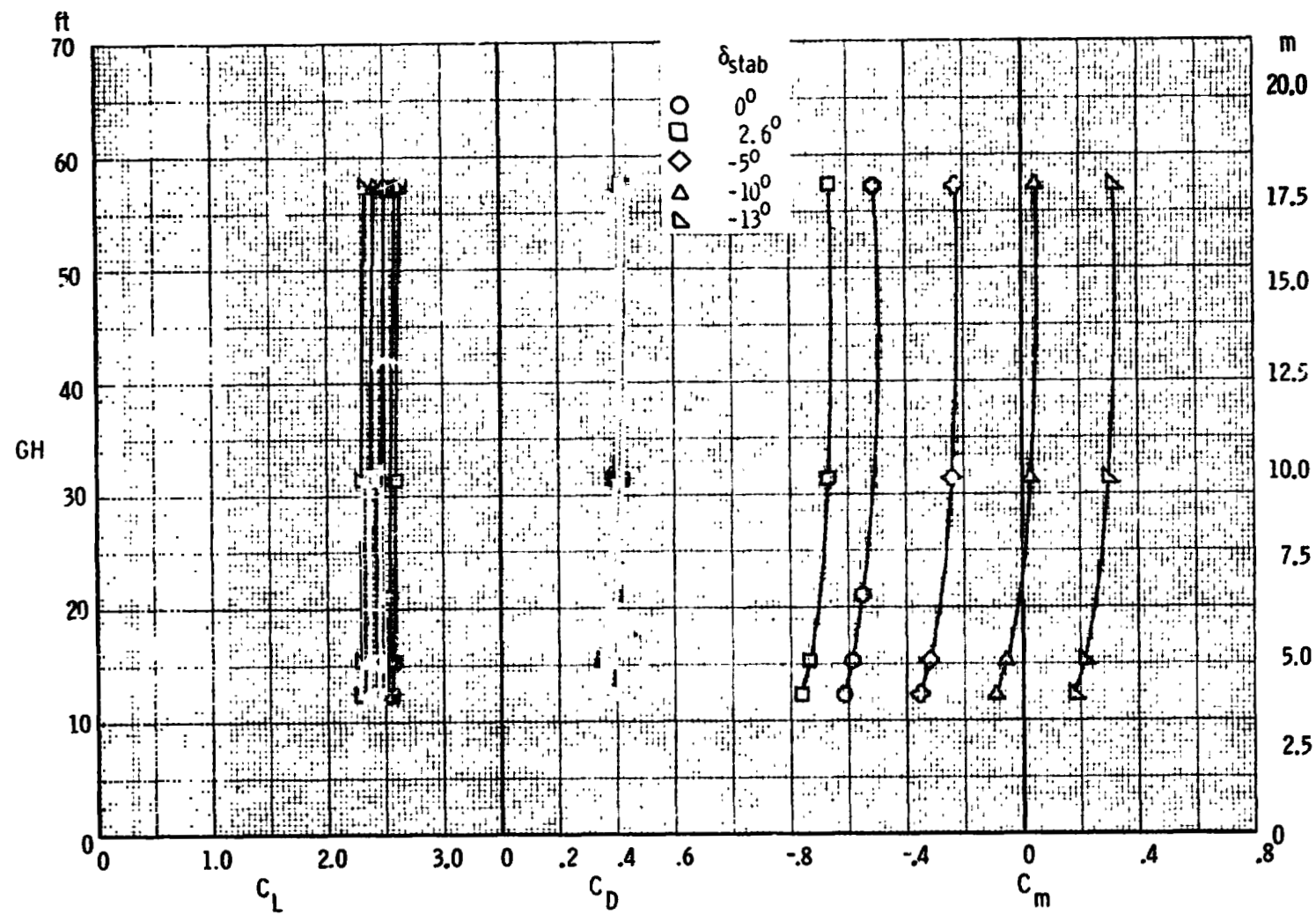
Figure 27. ~ Effect of ground height and stabilizer deflection on the longitudinal aerodynamic characteristics of the F.W.F₄₀ N,G,H_T,V_T configuration at various angles of attack and DLC spoiler deflections.



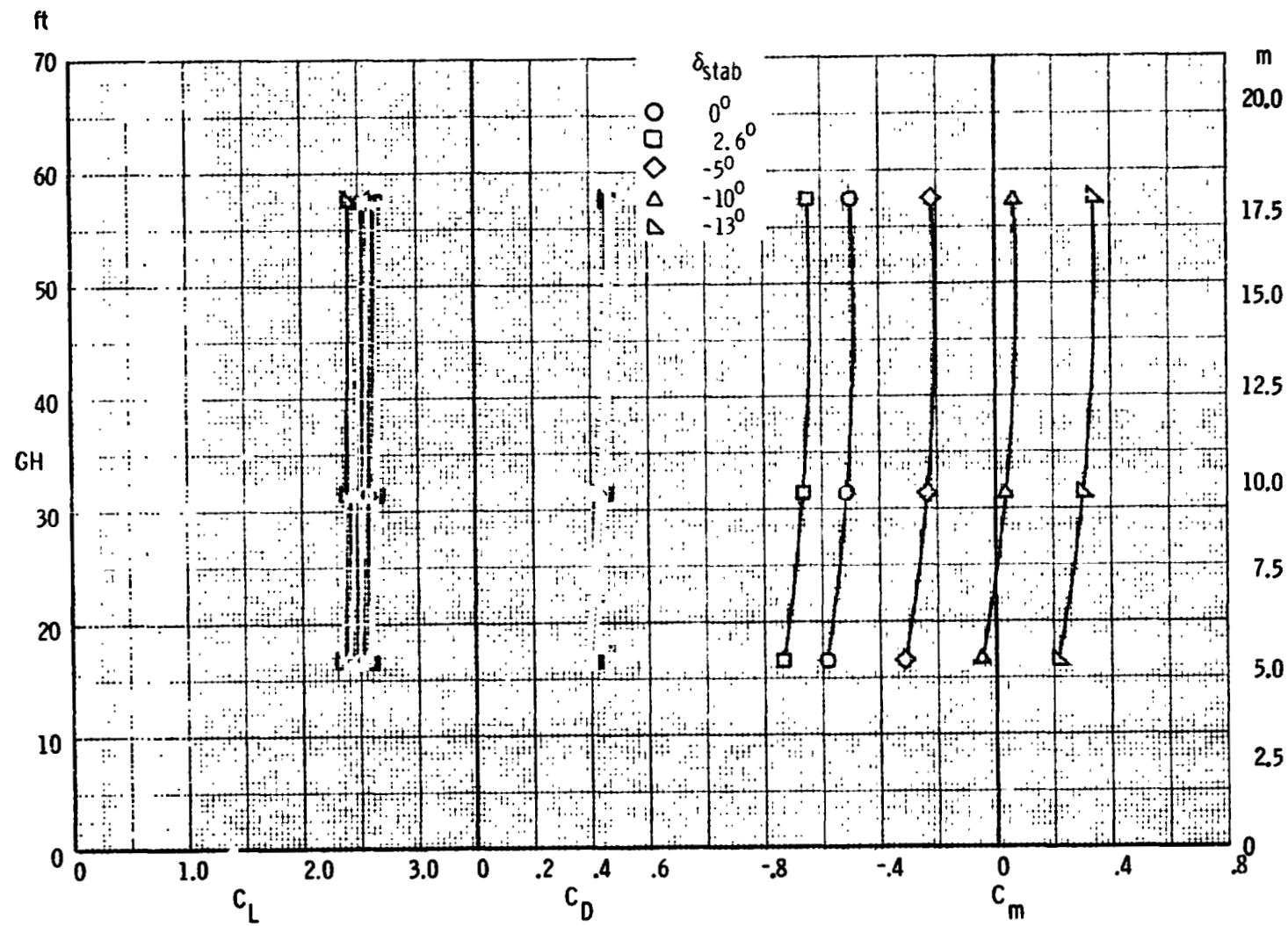
(b) $\alpha = 7^\circ$, $\delta_{sp2,3,6,7} = 0^\circ$
Figure 27. - Continued.



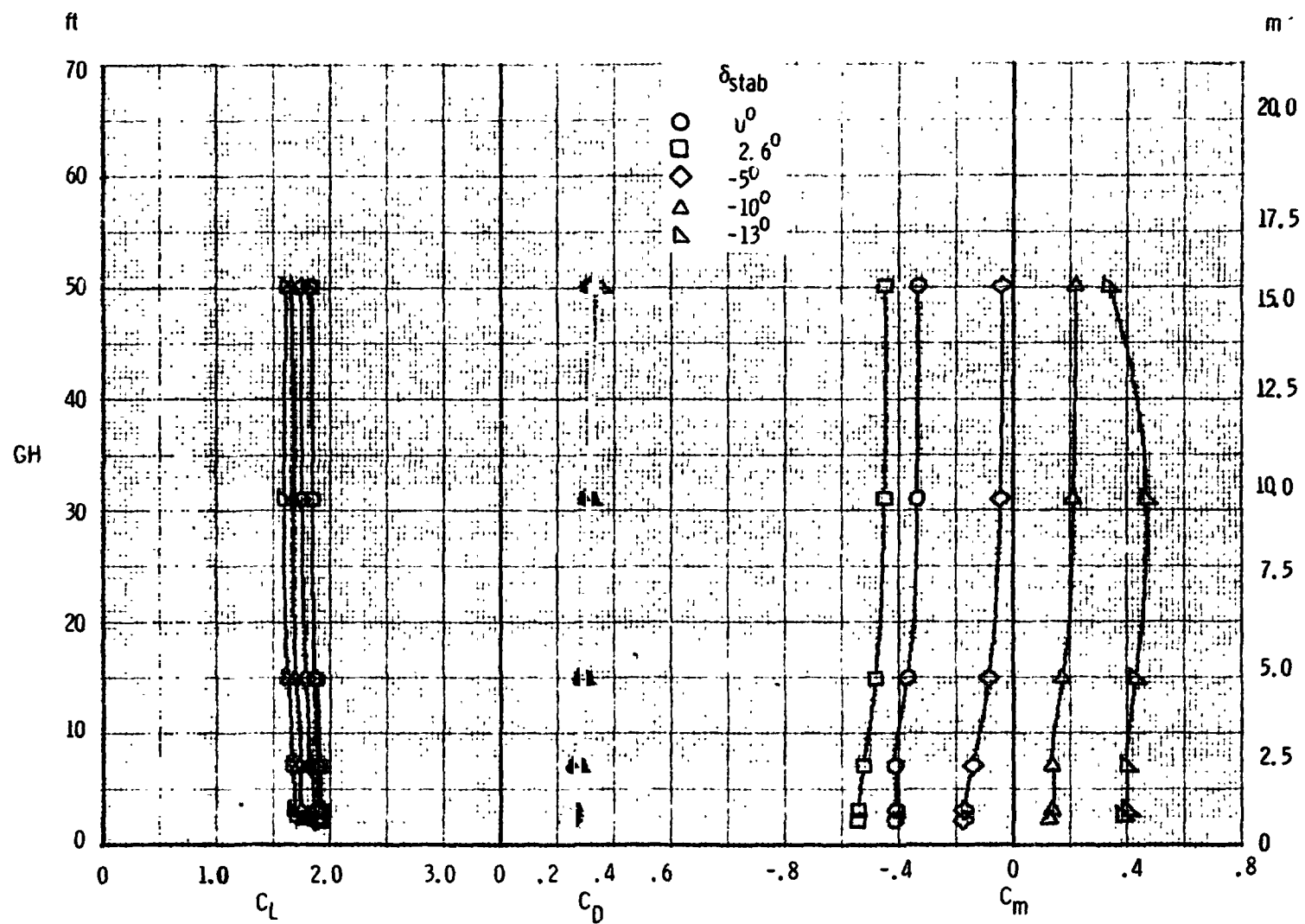
(c) $\alpha = 9^\circ$, $\delta_{sp2,3,6,7} = 0^\circ$
Figure 27. - Continued.



(d) $\alpha = 11^\circ$, $\delta_{sp2,3,6,7} = 0^\circ$
Figure 27. - Continued.

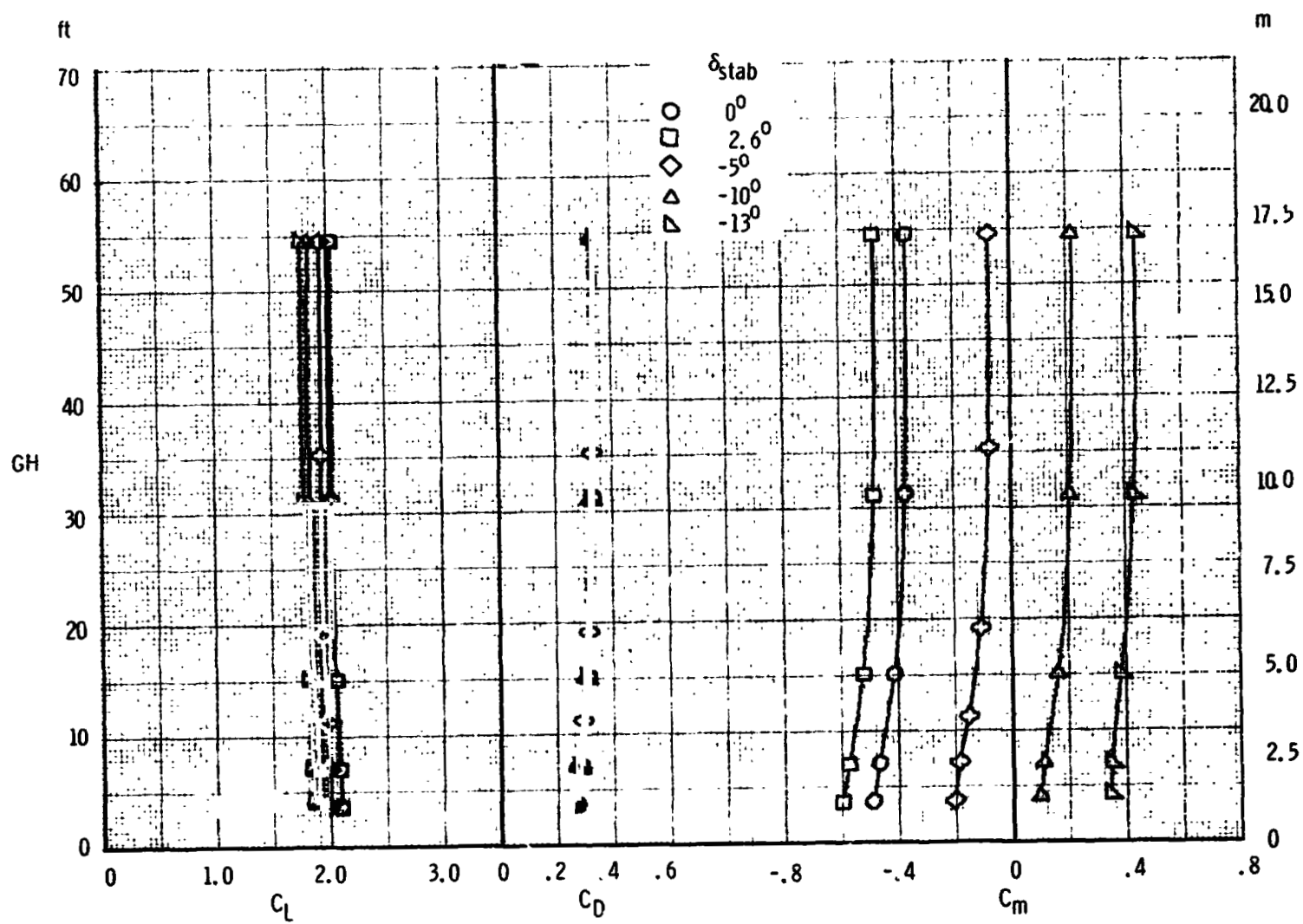


(e) $\alpha = 13^\circ$, $\delta_{sp2,3,6,7} = 0^\circ$
Figure 27. - Continued.

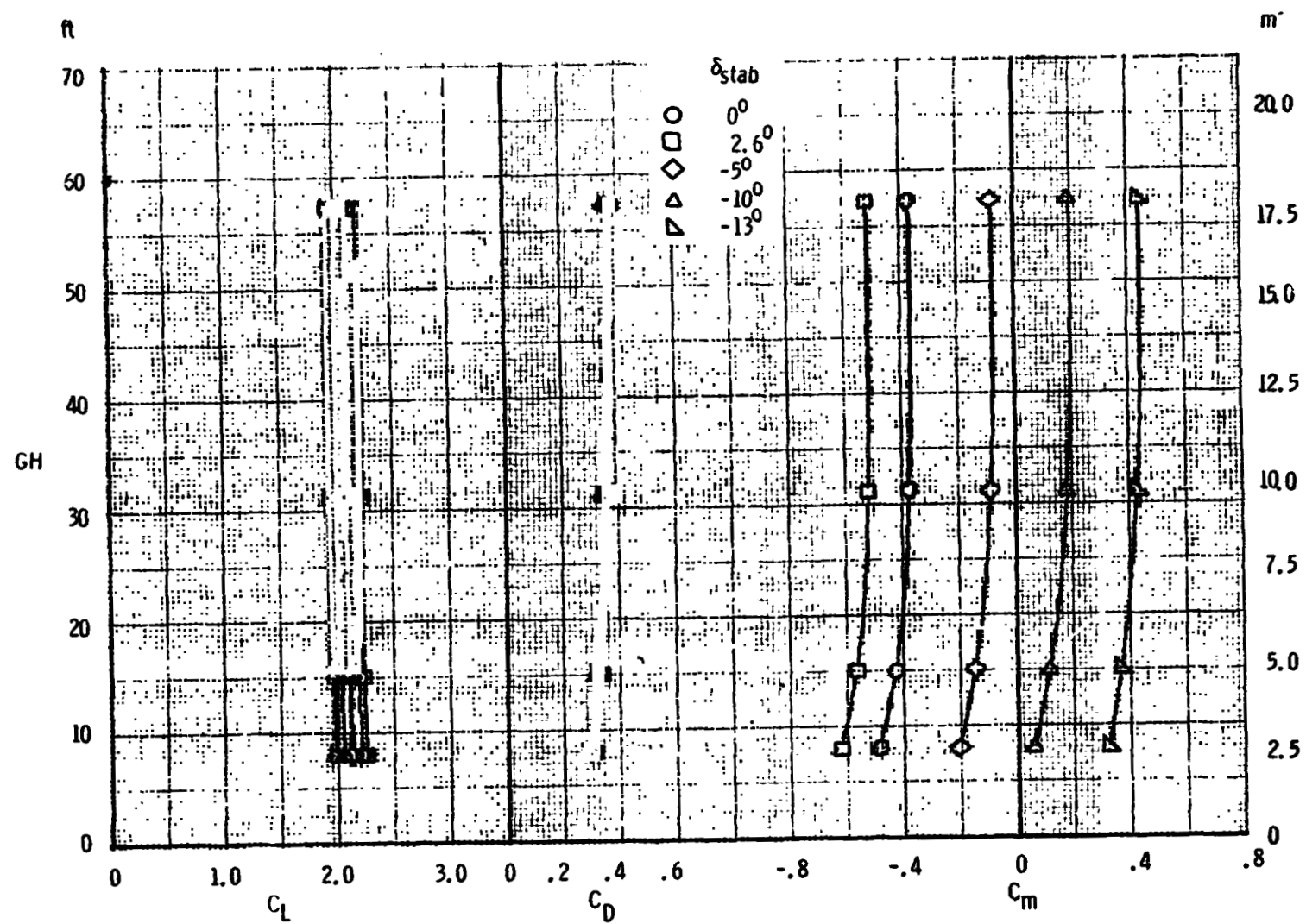


(f) $\alpha = 5^\circ$, $\delta_{sp2,3,6,7} = 6^\circ$

Figure 27. - Continued.

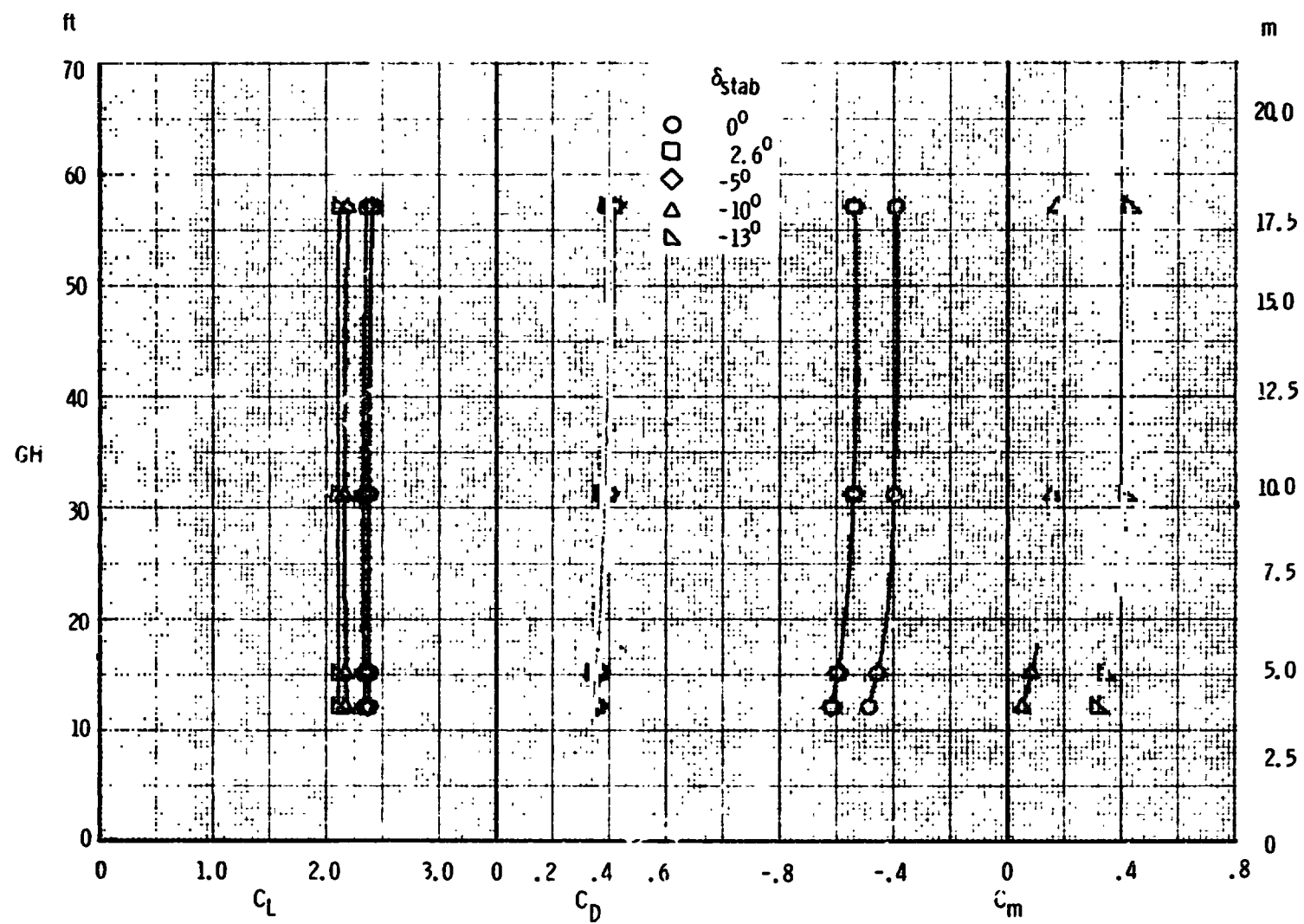


(g) $\alpha = 7^\circ$, $\delta_{sp2,3,6,7} = 6^\circ$
 Figure 27. - Continued.

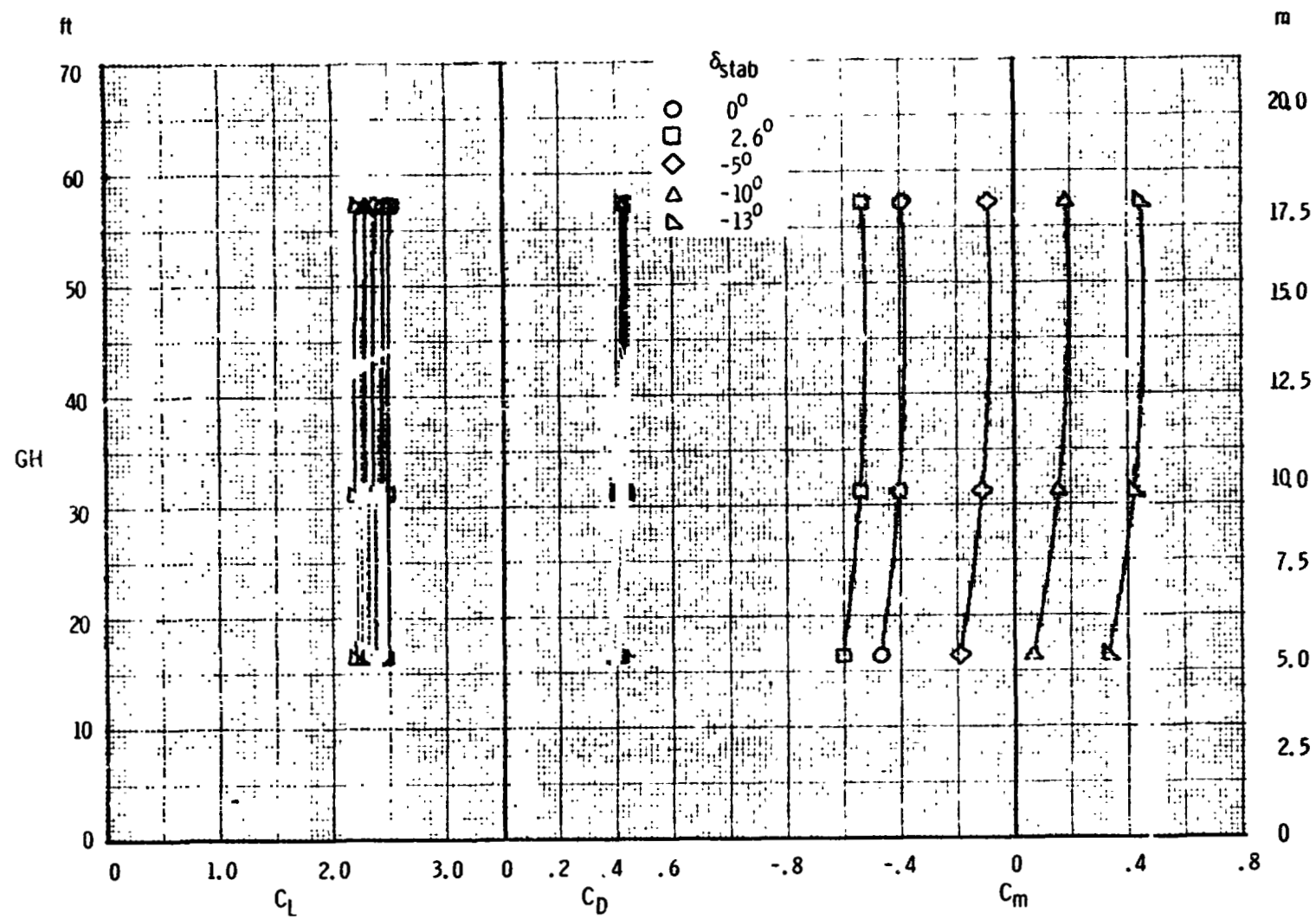


(h) $\alpha = 9^\circ$, $\delta_{sp2,3,6,7} = 6^\circ$

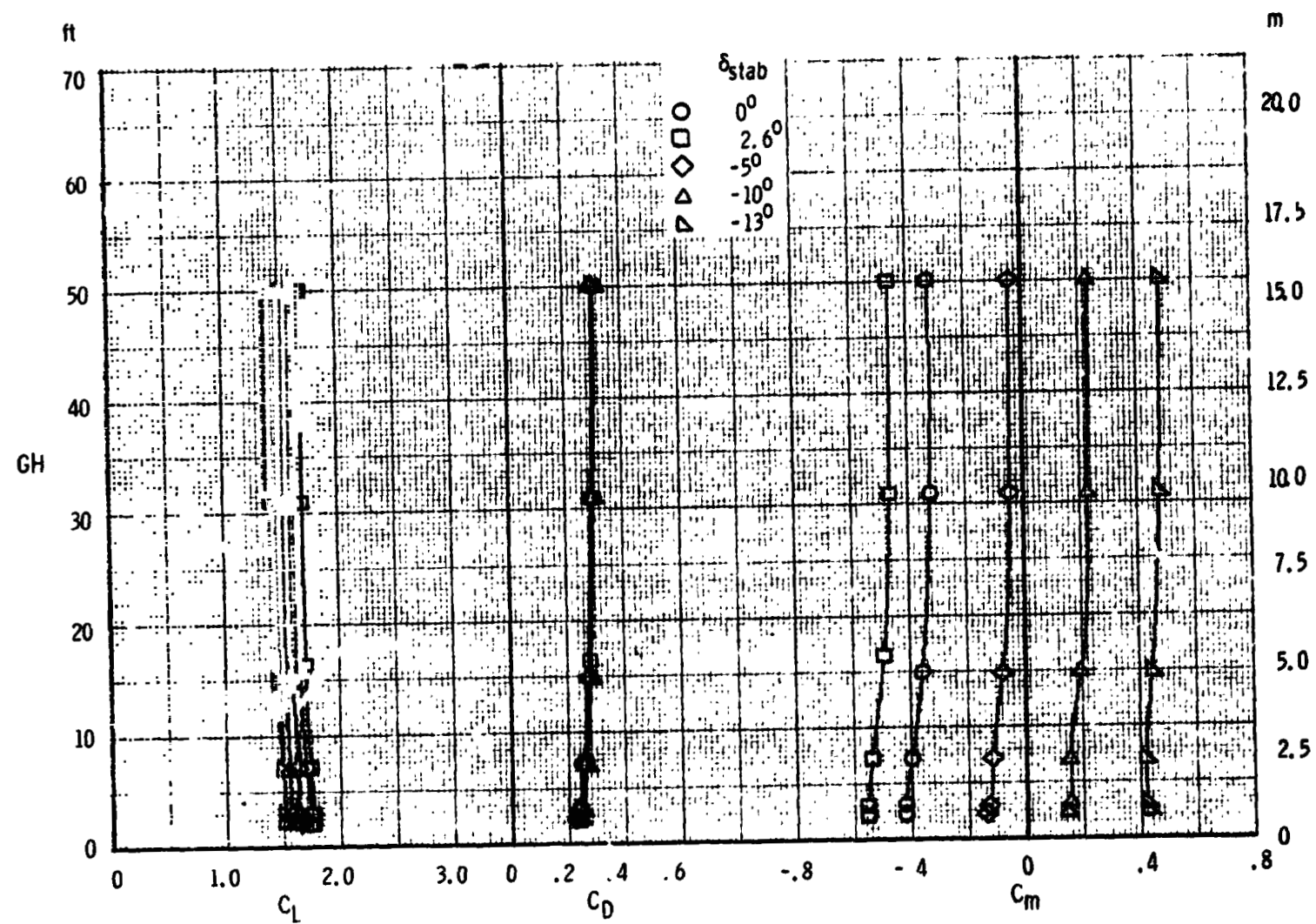
Figure 27. - Continued.



(ii) $\alpha = 11^\circ$, $\epsilon_{sp2,3,6,7} = 6^\circ$
Figure 27. - Continued.

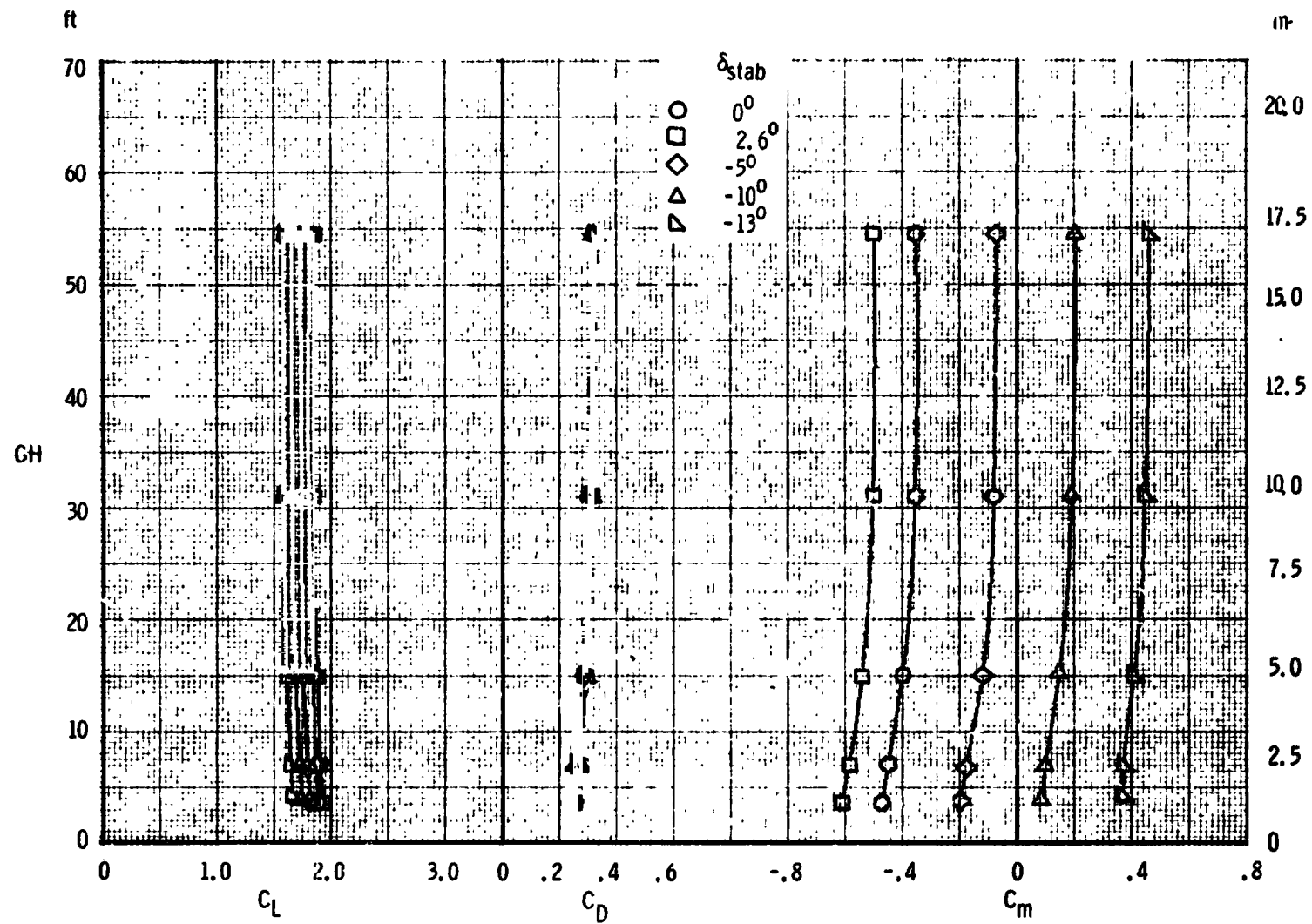


(j) $\alpha = 13^\circ$, $\delta_{sp2,3,6,7} = 6^\circ$
Figure 27. - Continued.

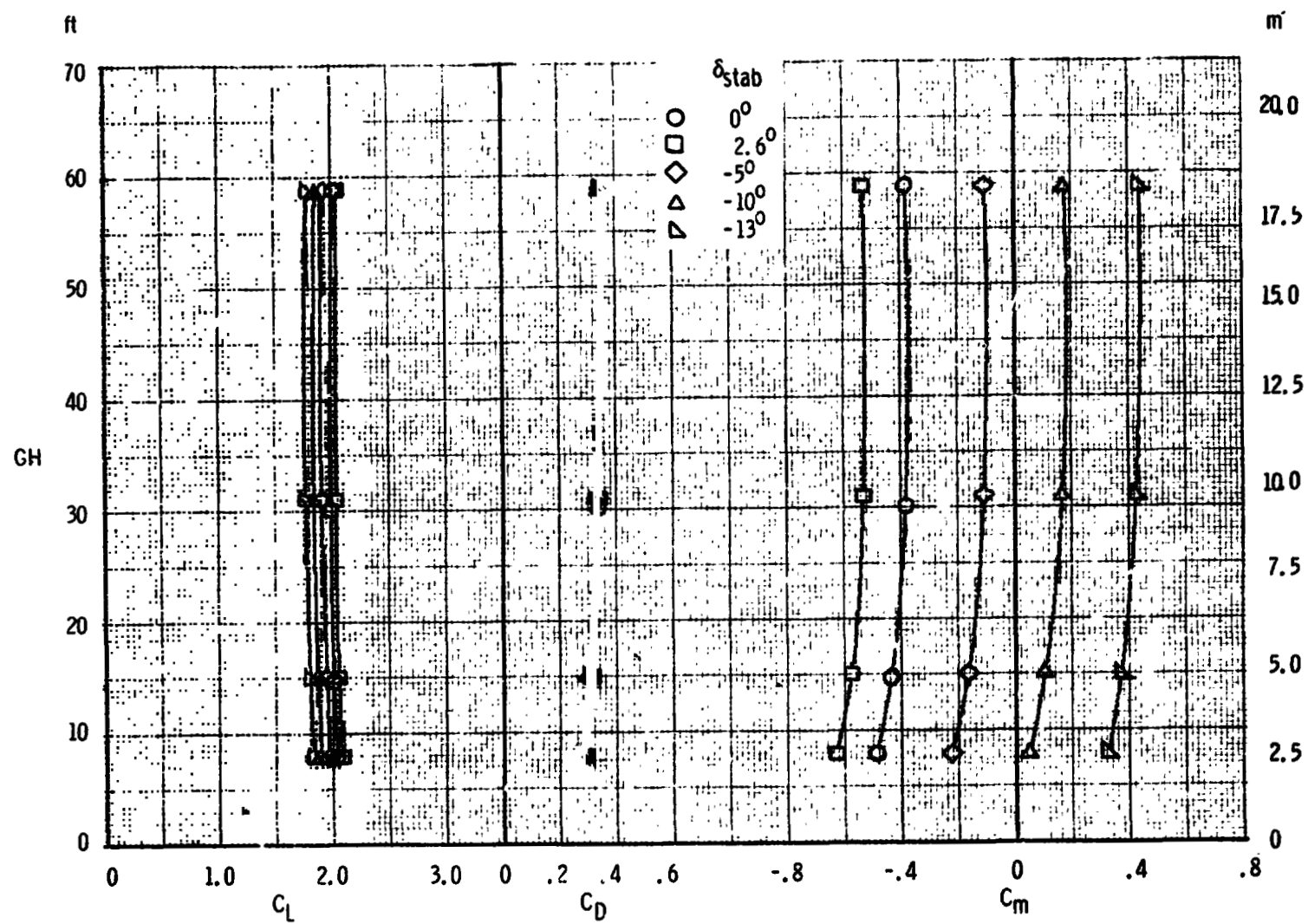


(k) $\alpha = 5^\circ$, $\delta_{sp2,3,6,7} = 9^\circ$

Figure 27. - Continued.

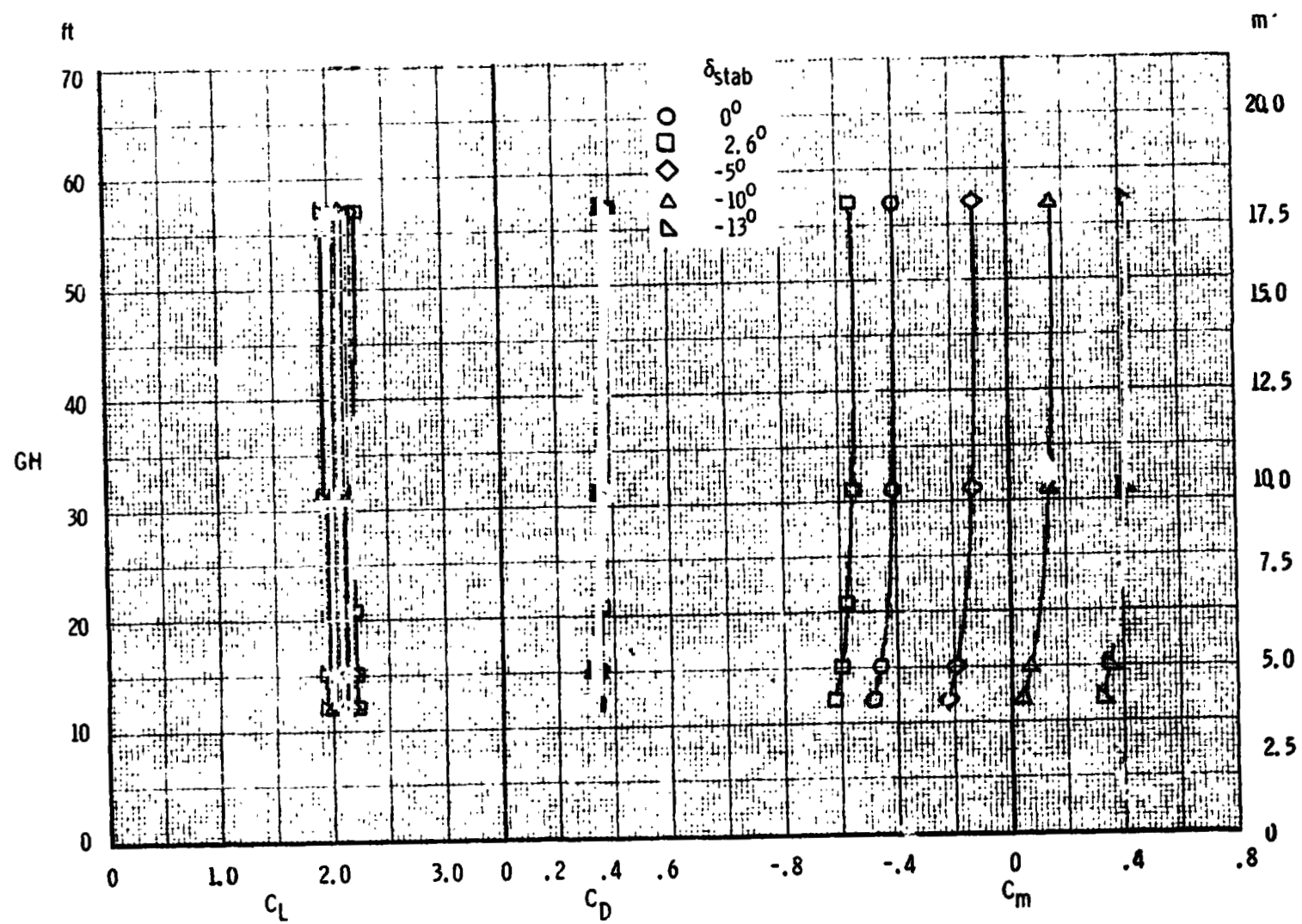


(1) $\alpha = 7^\circ$, $\delta_{sp2,3,6,7} = 9^\circ$
 Figure 27. - Continued.

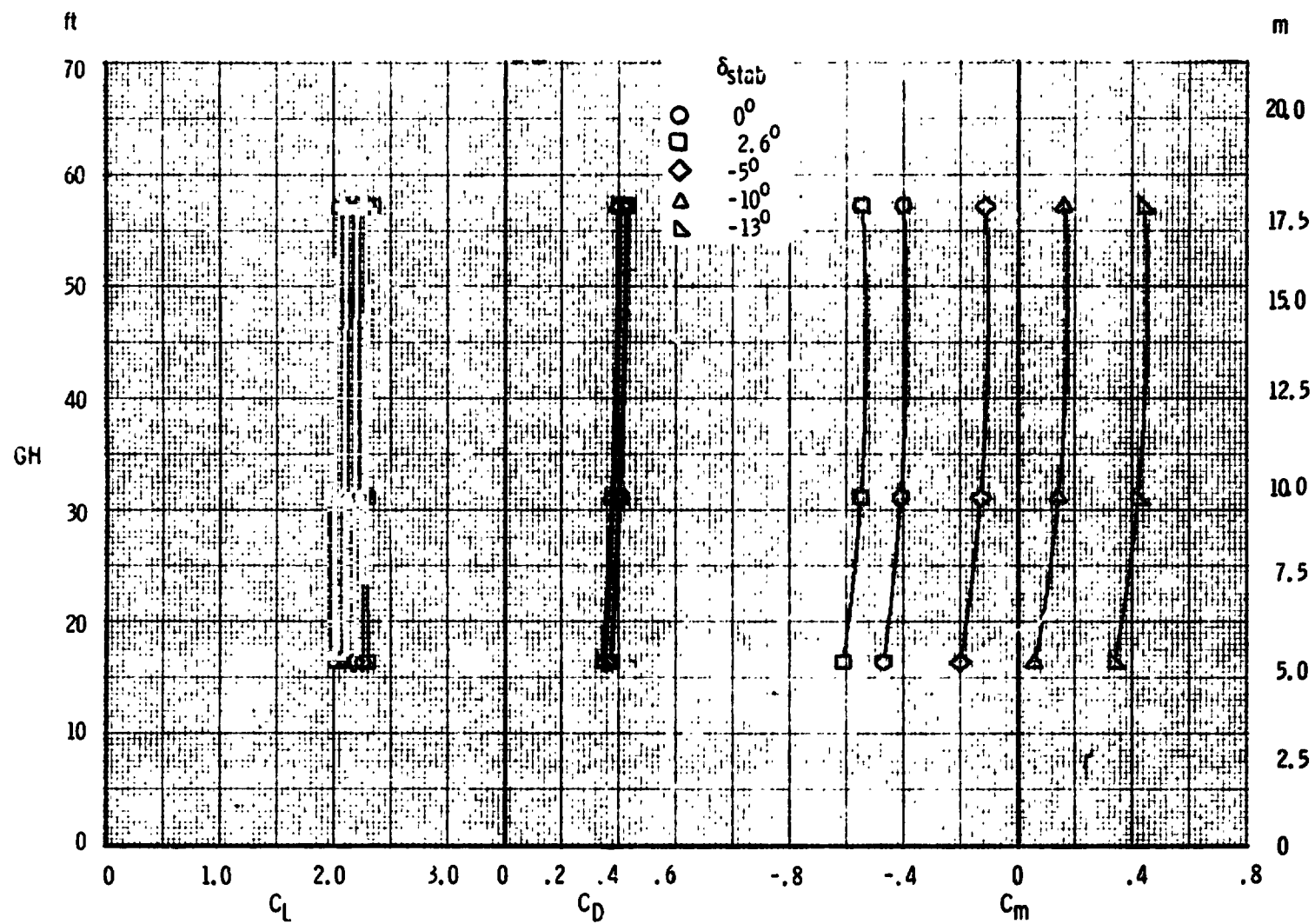


(m) $\alpha = 9^\circ$, $\delta_{sp2,3,6,7} = 9^\circ$

Figure 27. - Continued.

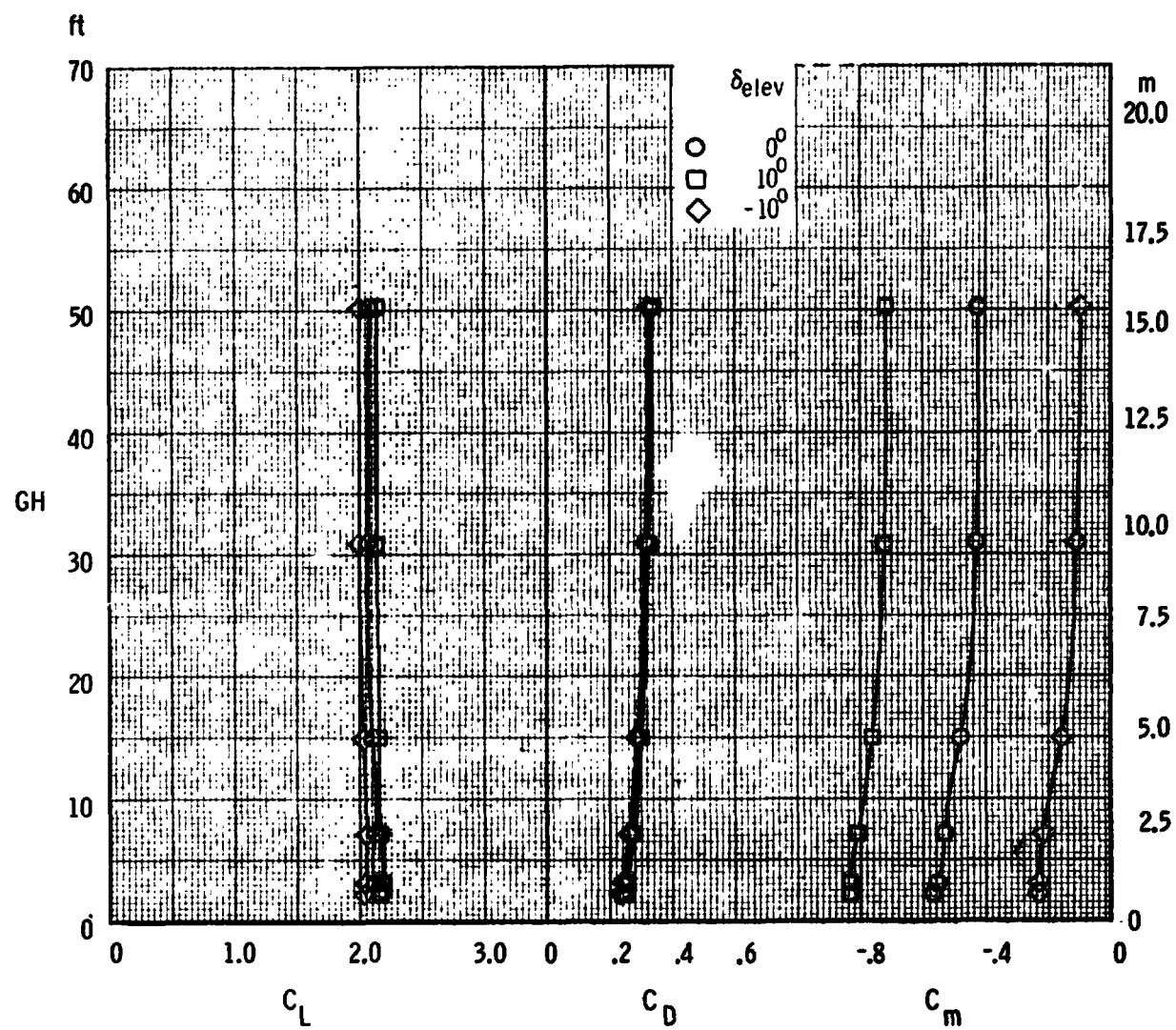


(n) $\alpha = 11^\circ$, $\delta_{sp2,3,6,7} = 9^\circ$
 Figure 27. - Continued.



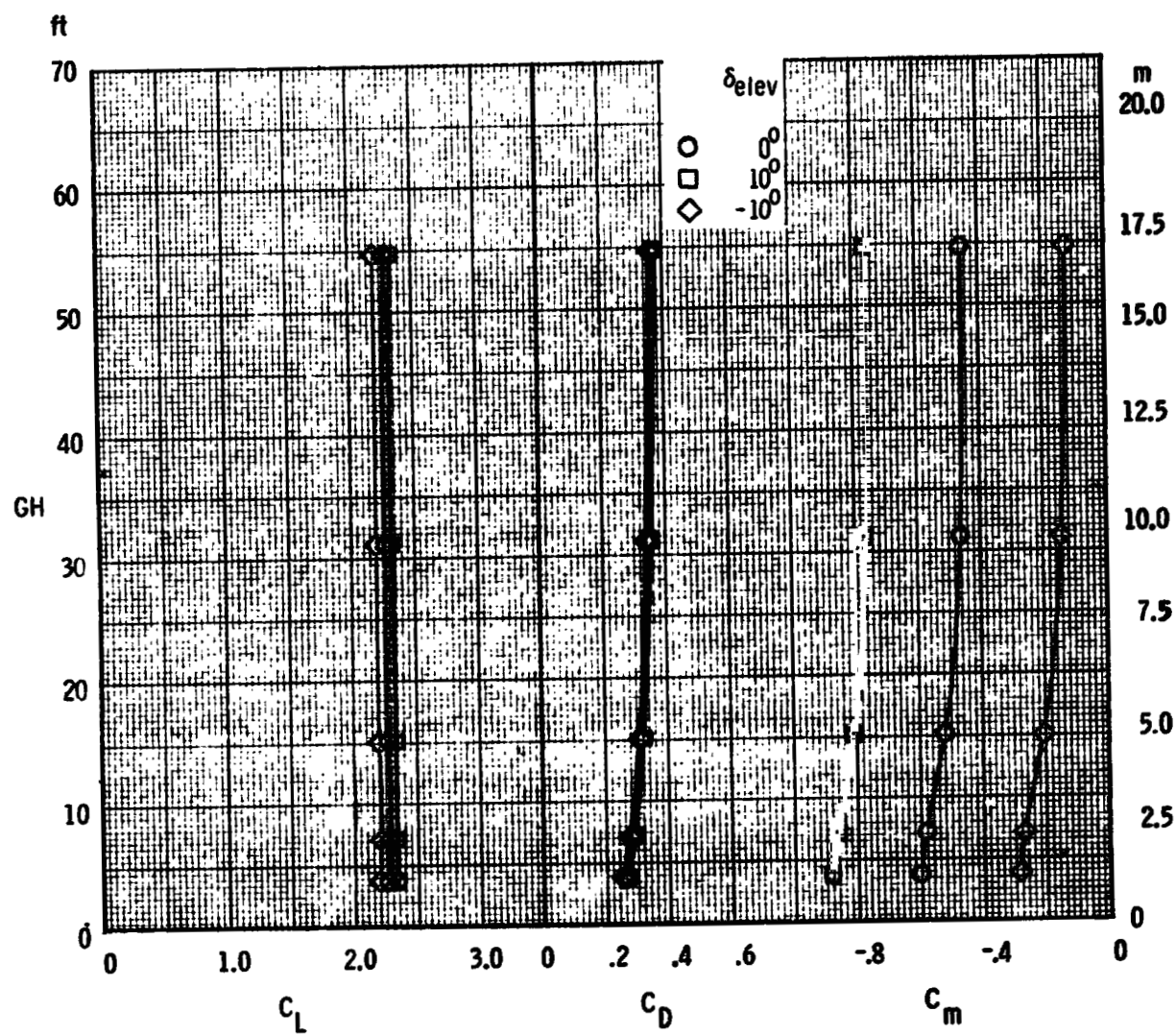
(a) $\alpha = 13^\circ$, $\delta_{sp2,3,6,7} = 9^\circ$

Figure 27. - Concluded

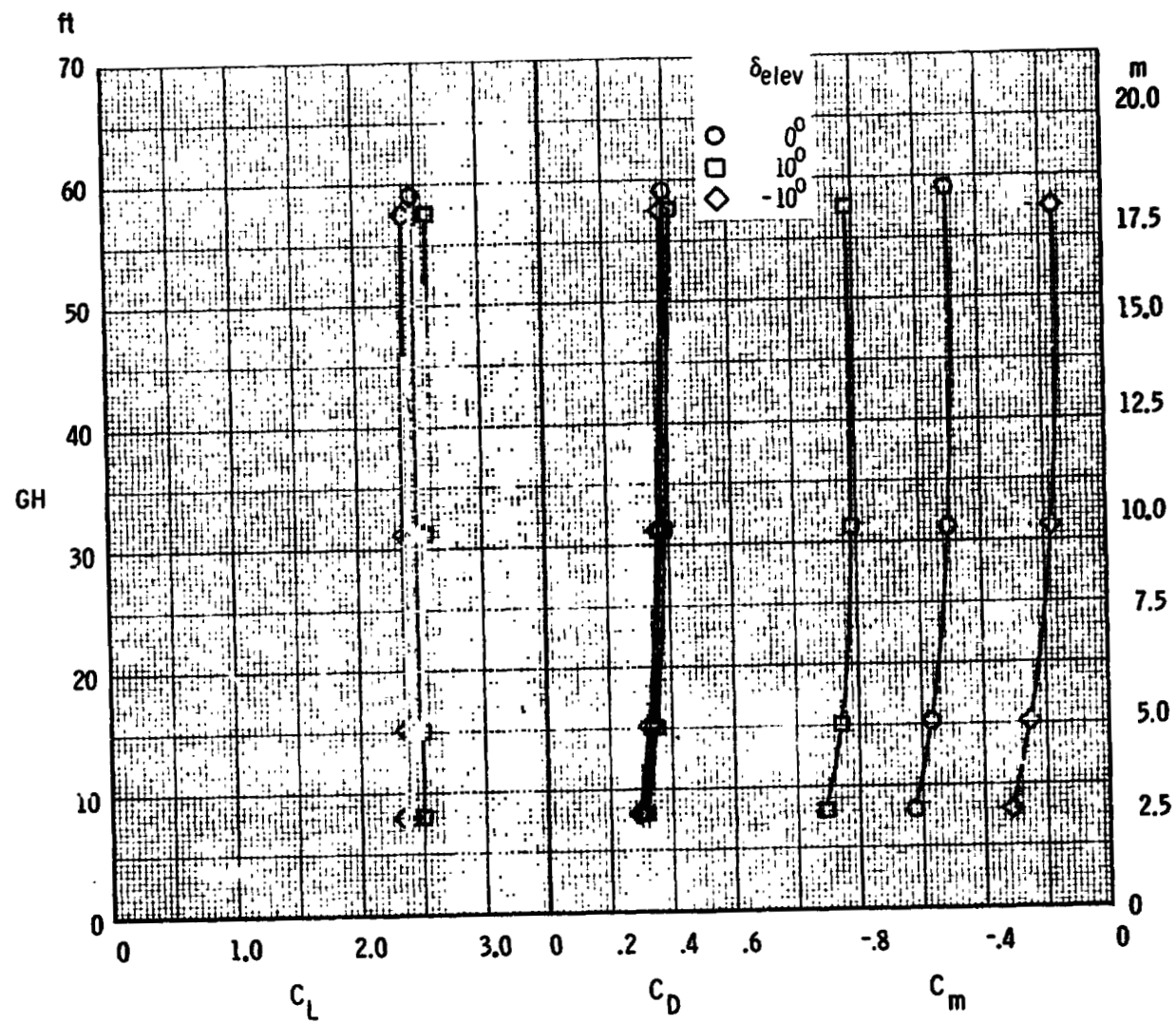


(a) $\alpha = 5^\circ$

Figure 28. - Effect of ground height and elevator deflection on the longitudinal aerodynamic characteristics of the F, W, F₄₀, N, G, H_T, V_T configuration at various angles of attack.

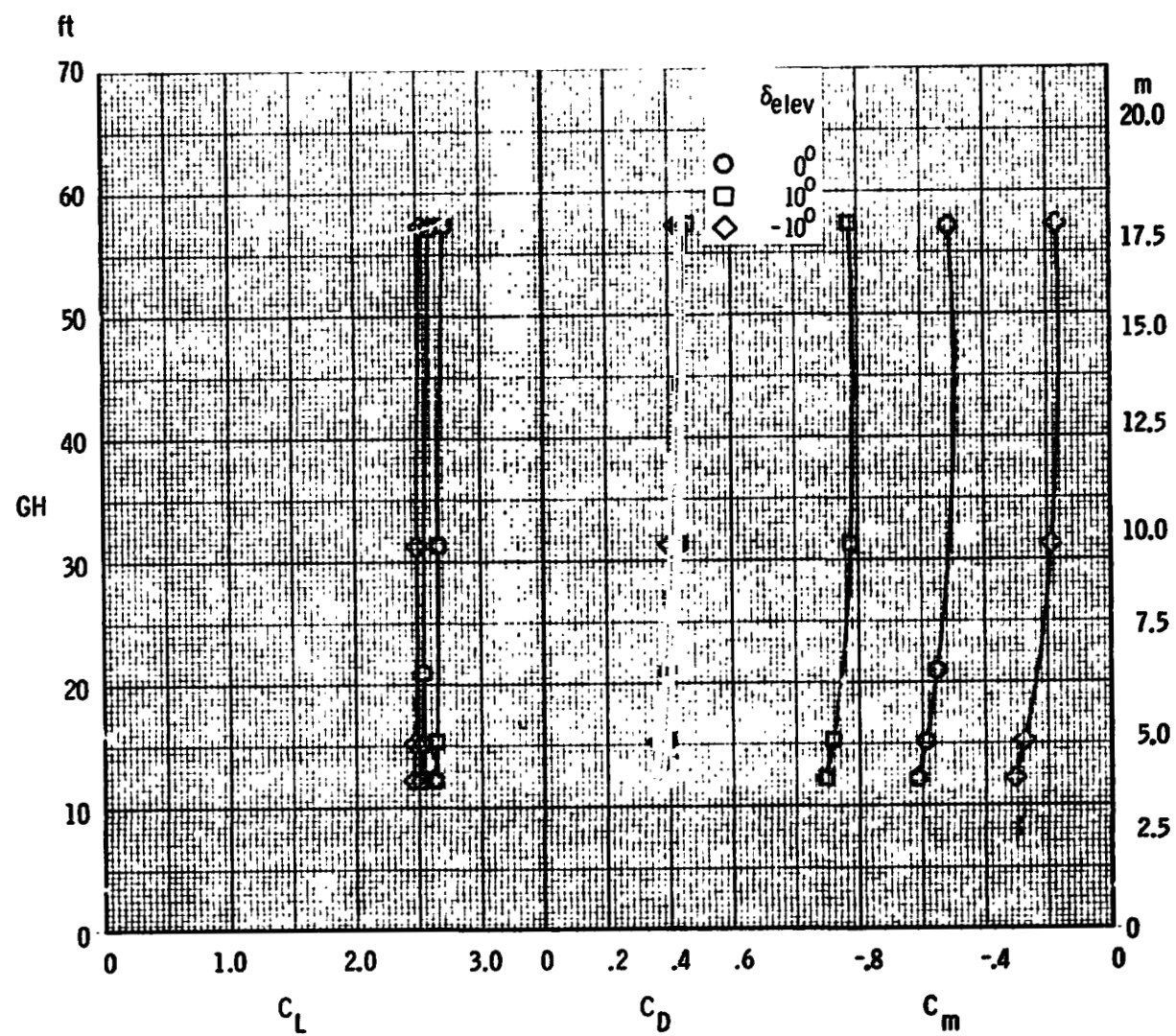


(b) $\alpha = 7^\circ$
Figure 28. - Continued.



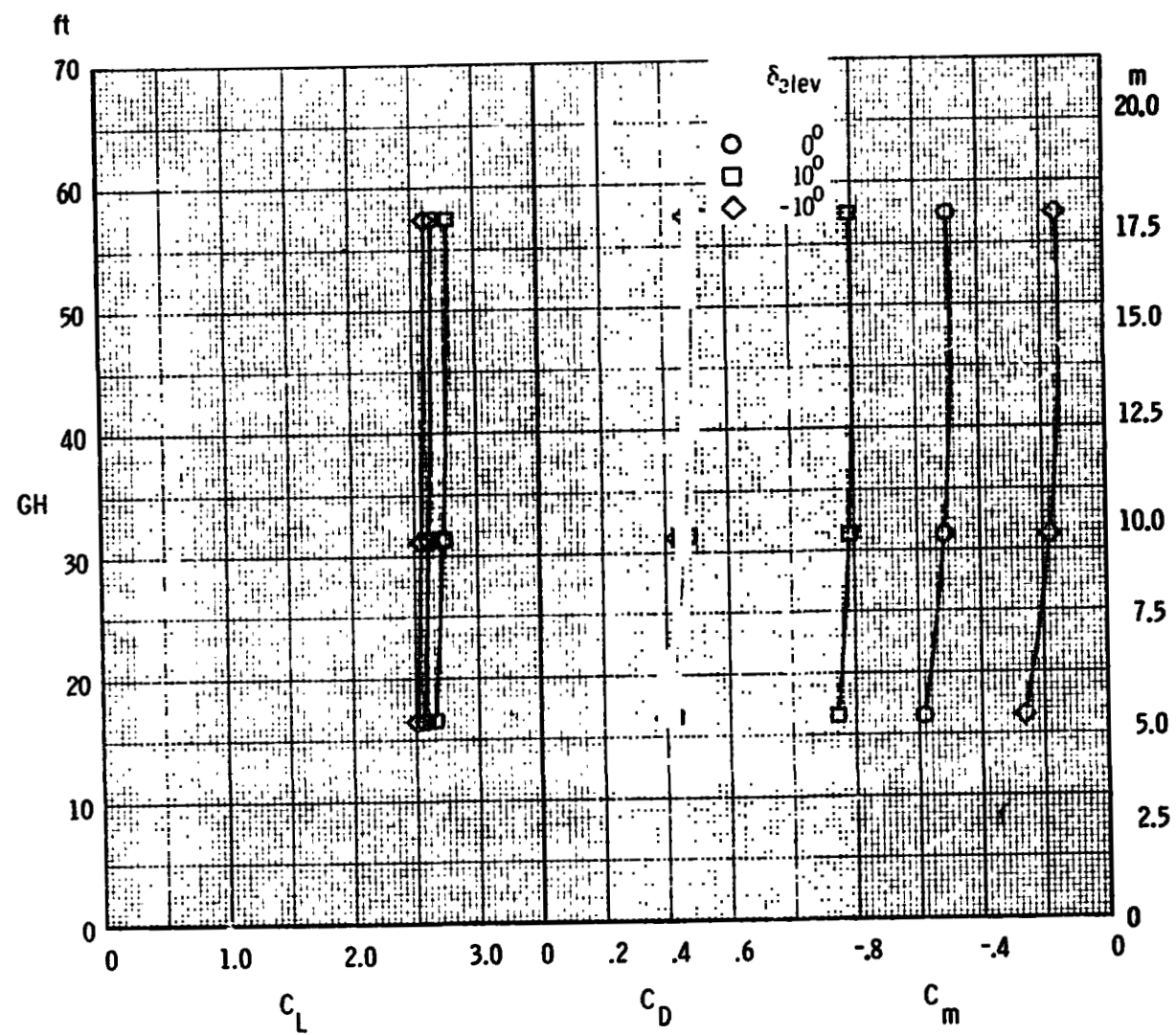
(c) $\alpha = 9^\circ$

Figure 28. - Continued.



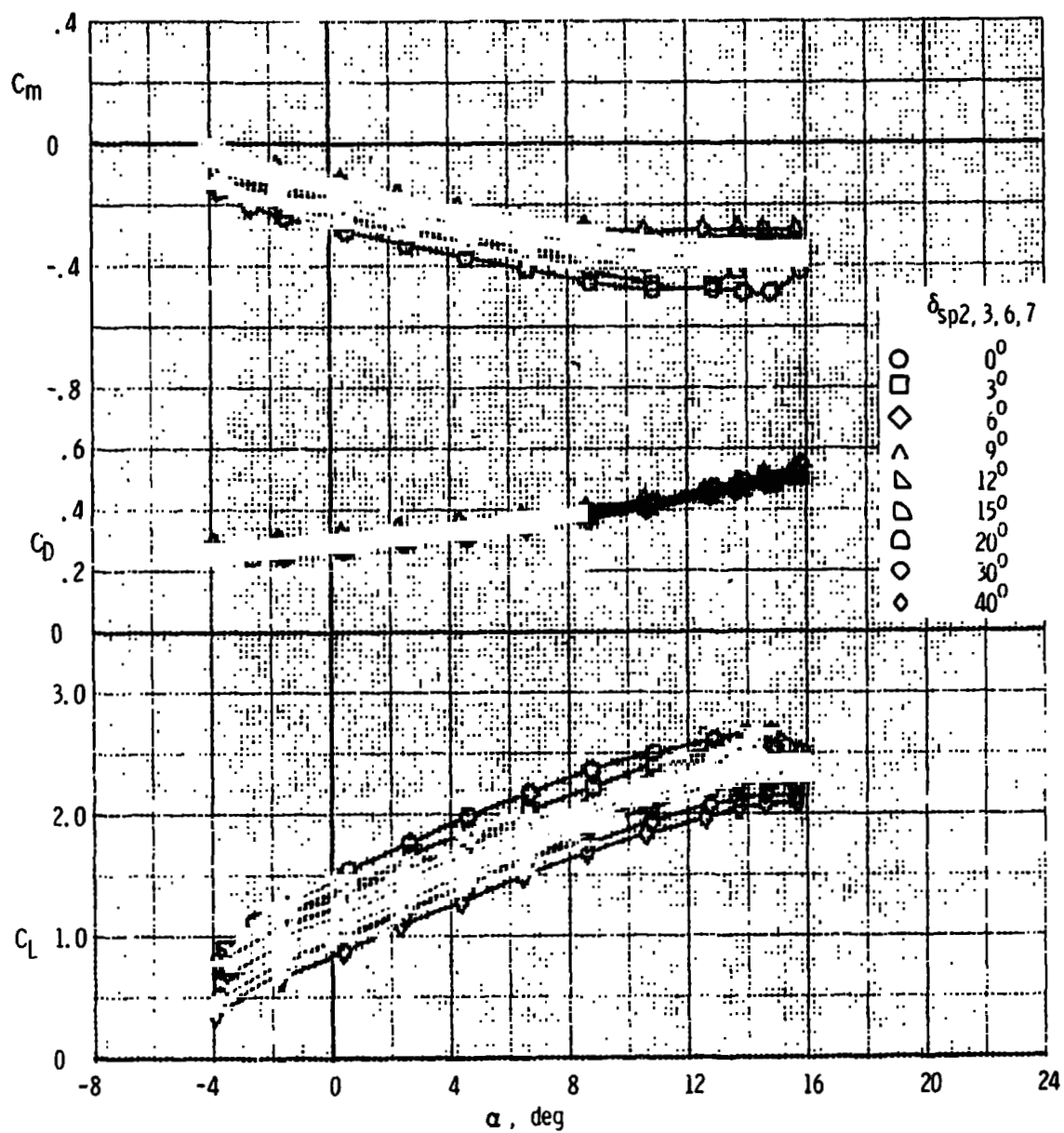
(d) $\alpha = 11^\circ$

Figure 28. - Continued.



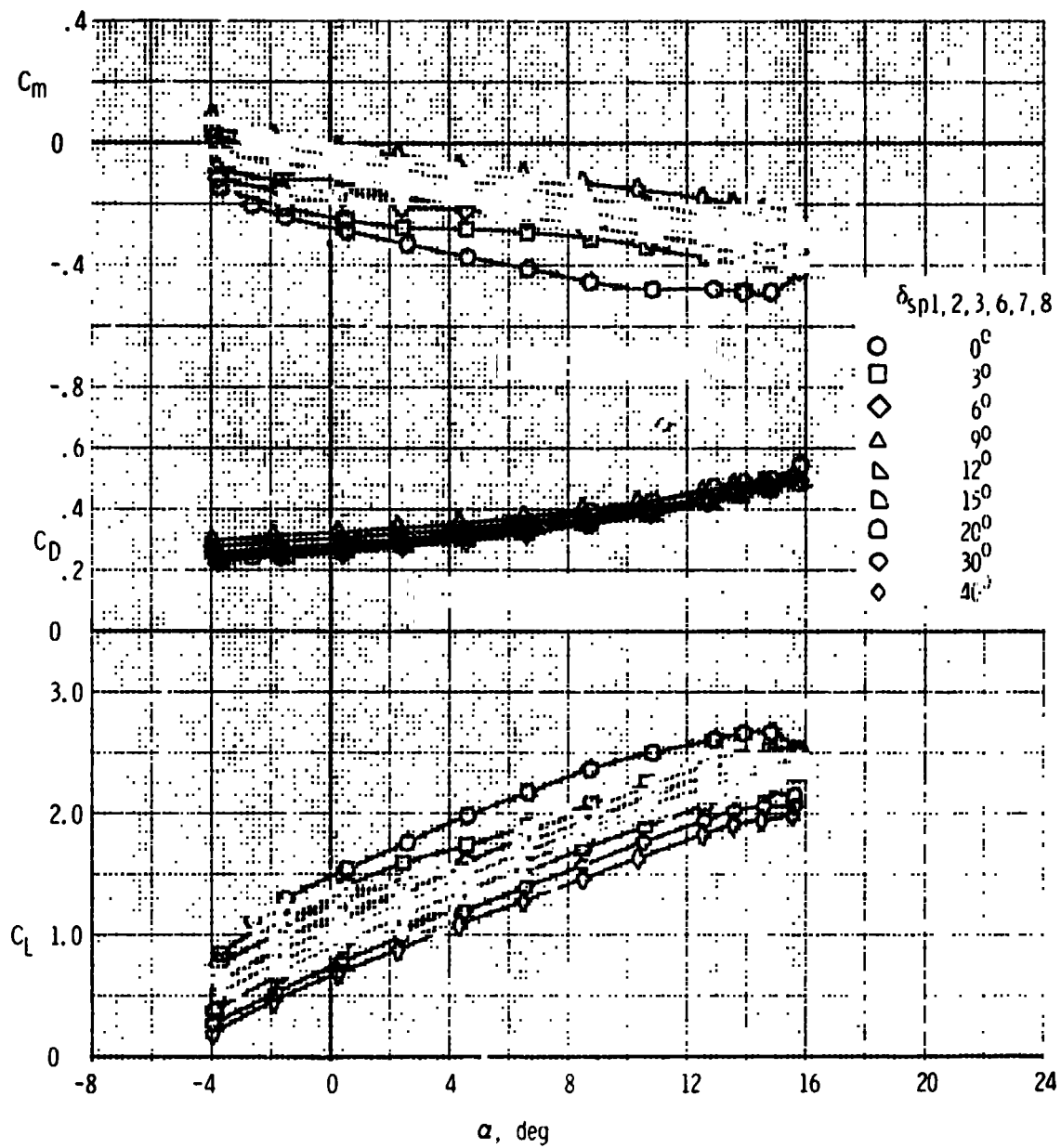
(e) $\alpha = 13^\circ$

Figure 28. - Concluded.



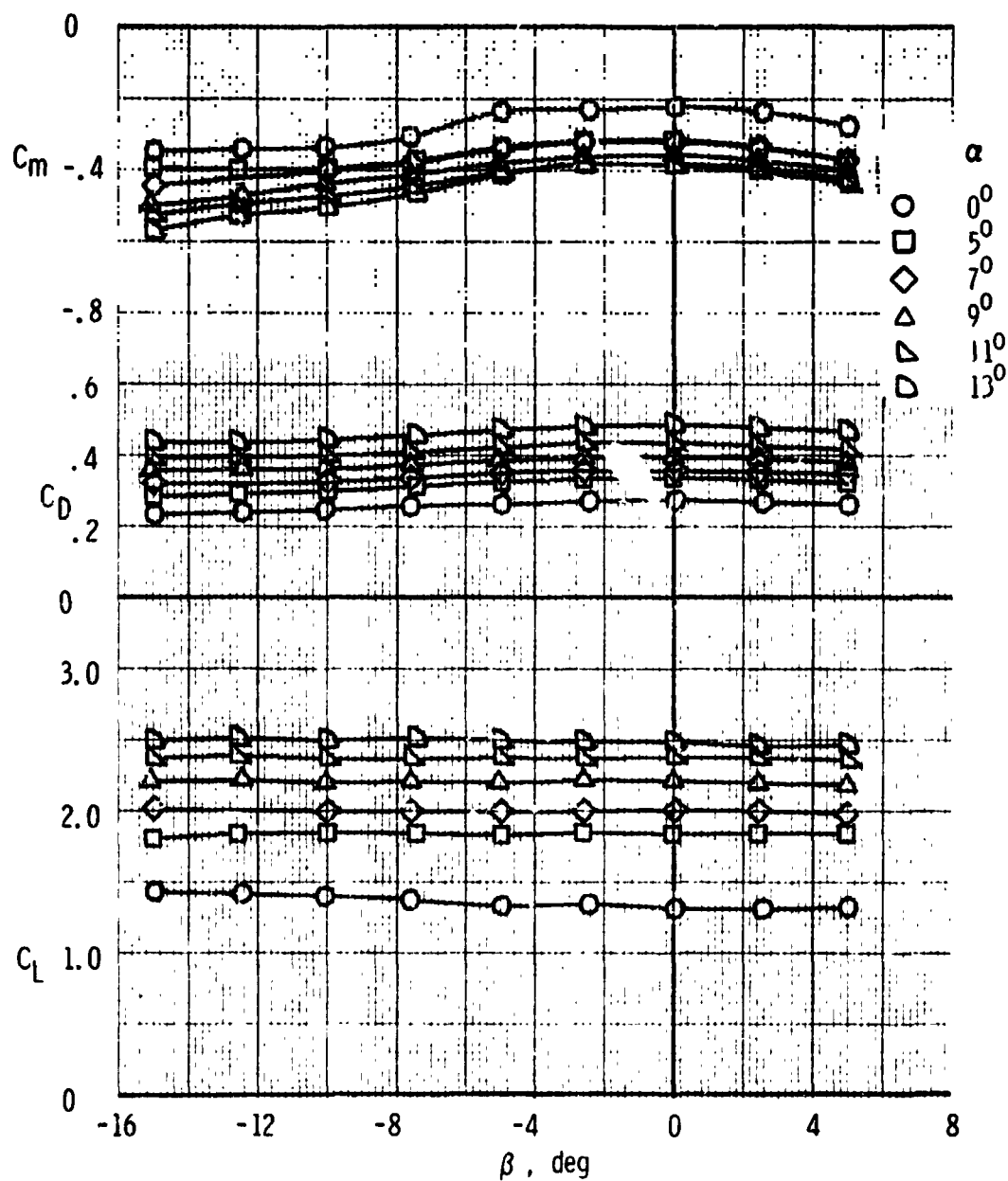
(a) Longitudinal characteristics

Figure 29. - Effect of DLC spoiler deflection on the longitudinal aerodynamic characteristics of the $F, W, F_{40^\circ N}, G, H_T, V_T$ configuration.



(b) Lateral-directional characteristics

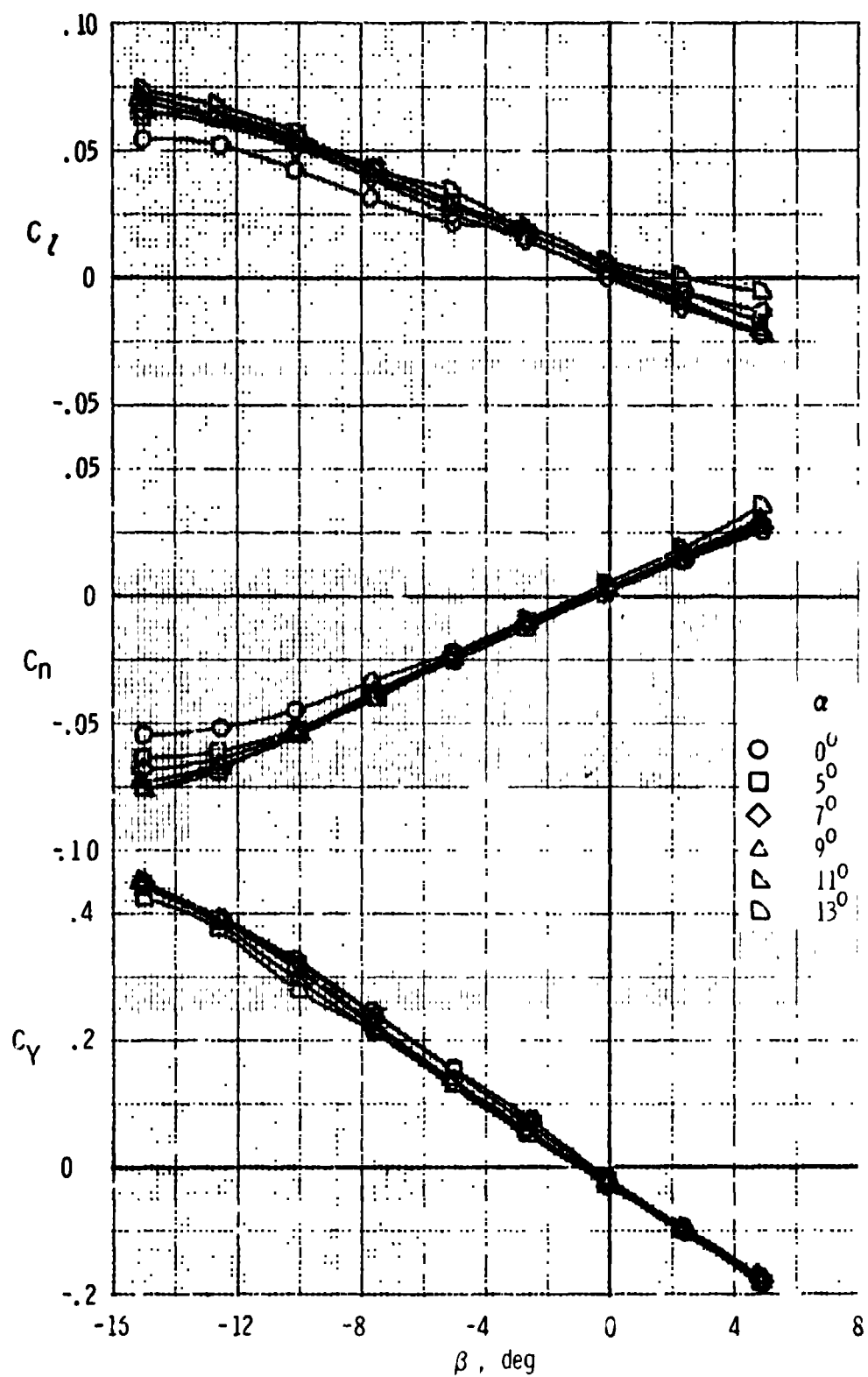
Figure 2^c - Concluded.



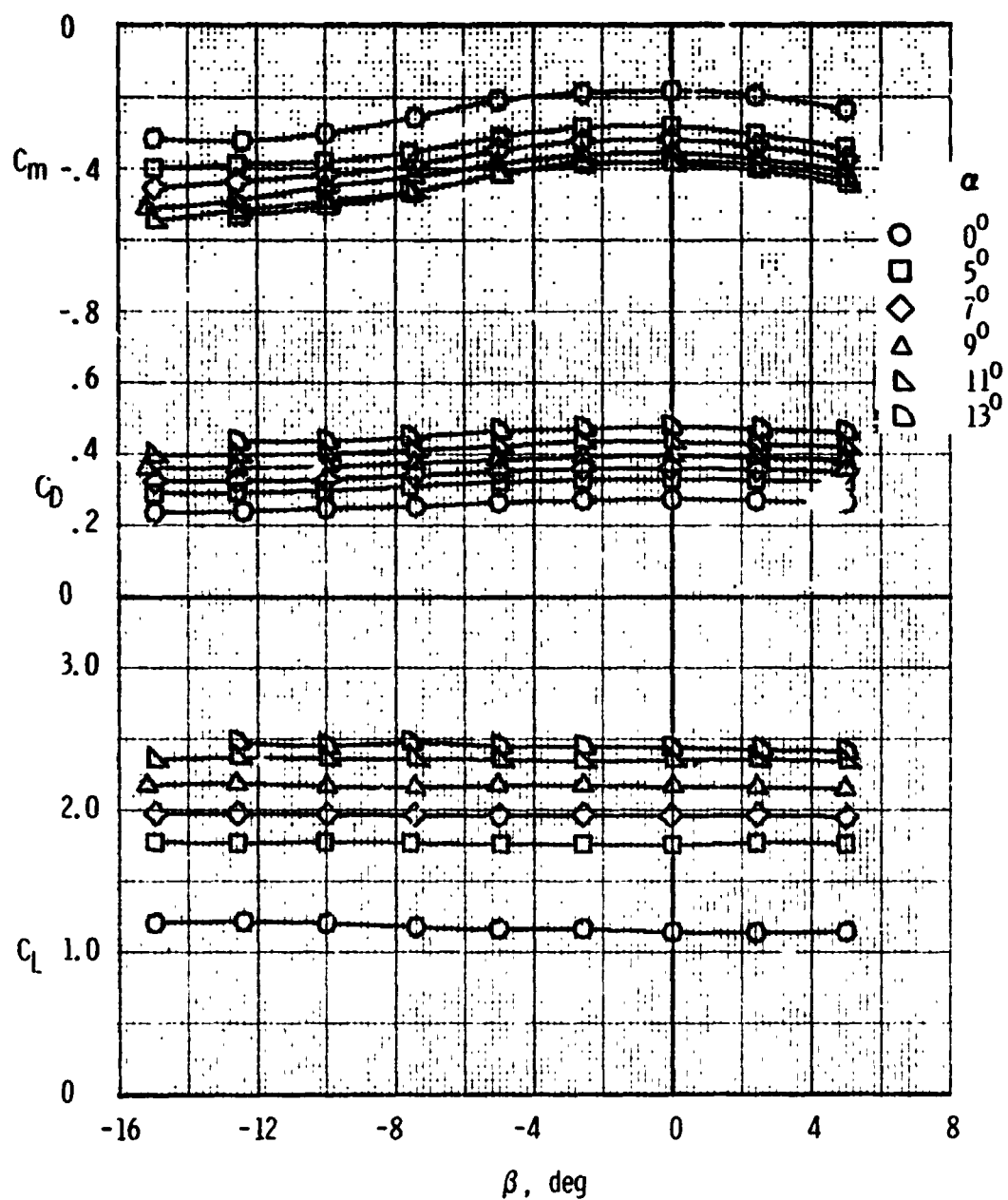
(a) Longitudinal characteristics, $\delta_{sp2,3,6,7} = 6^\circ$

Figure 30. - Effect of sideslip angle on the aerodynamic characteristics of the $F, W, F_{40}, N, G, H_T, V_T$ configuration at various DLC spoiler deflections.

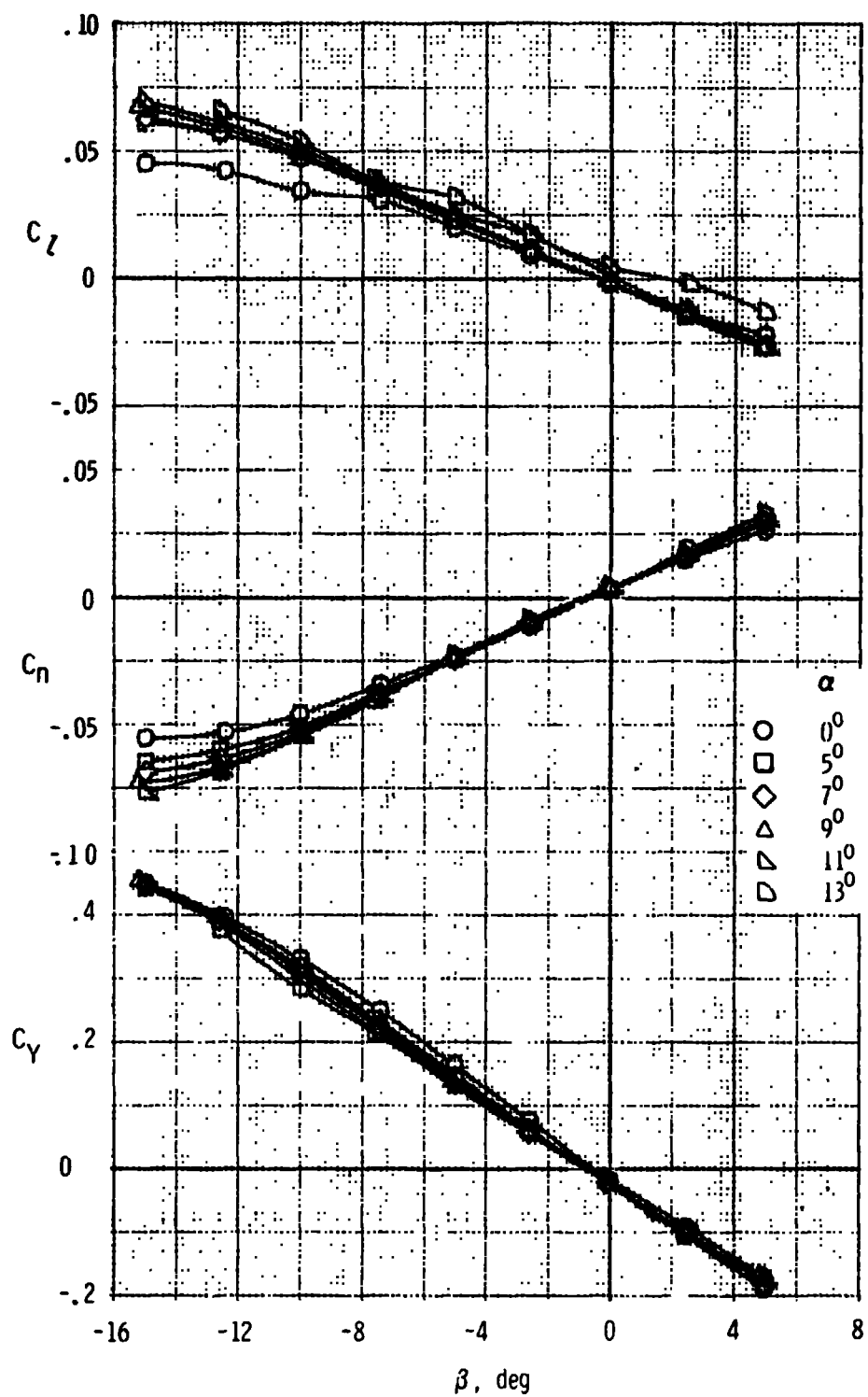
REPRODUCIBILITY OF THE
ORIGINAL PAGE IS POOR



(b) Lateral-directional characteristics, $\delta_{sp2,3,6,7} = 6^\circ$
 Figure 30. - Continued.

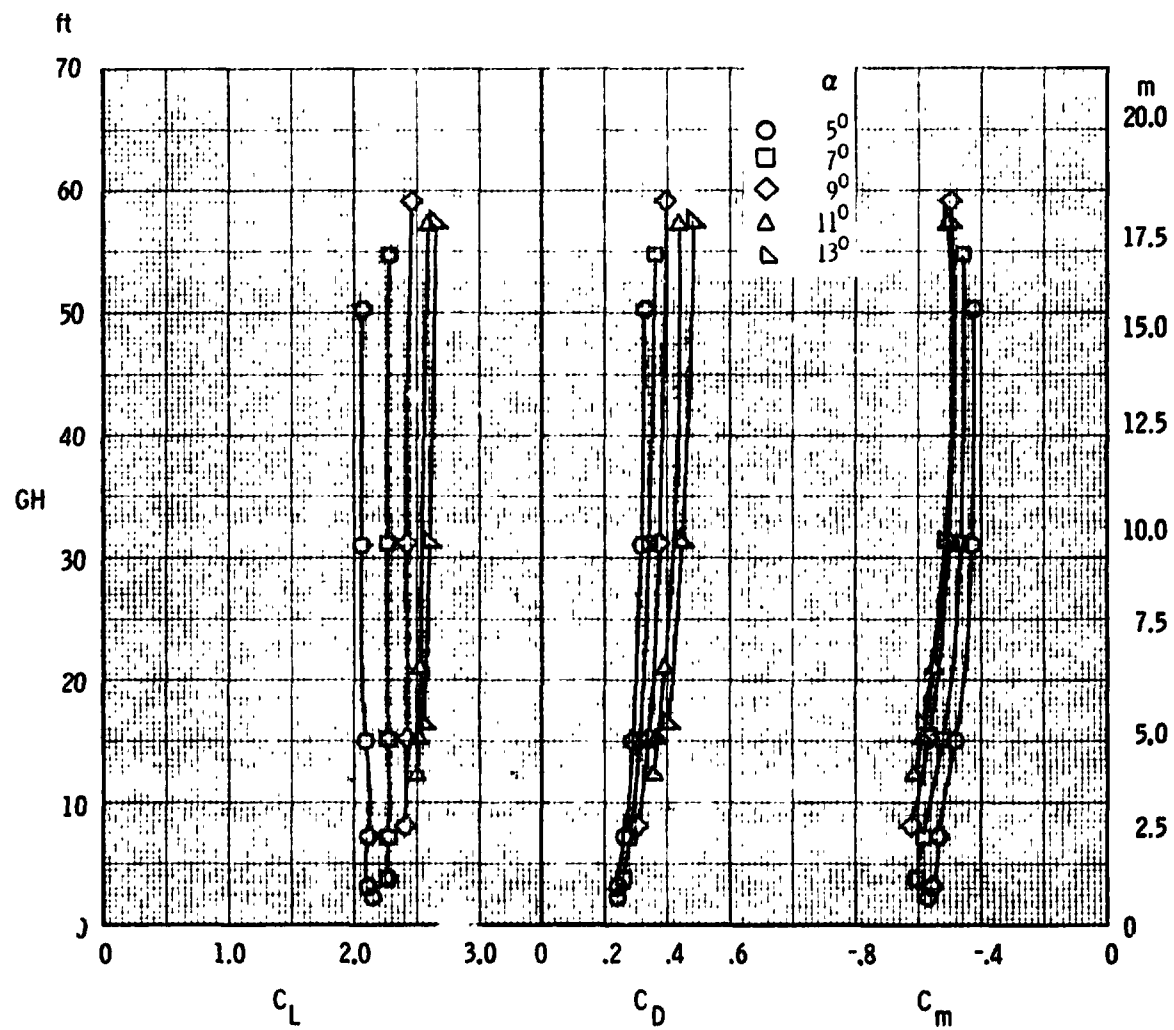


(c) Longitudinal characteristics, $\delta_{sp2,3,6,7} = 90^\circ$
 Figure 30. - Continued.



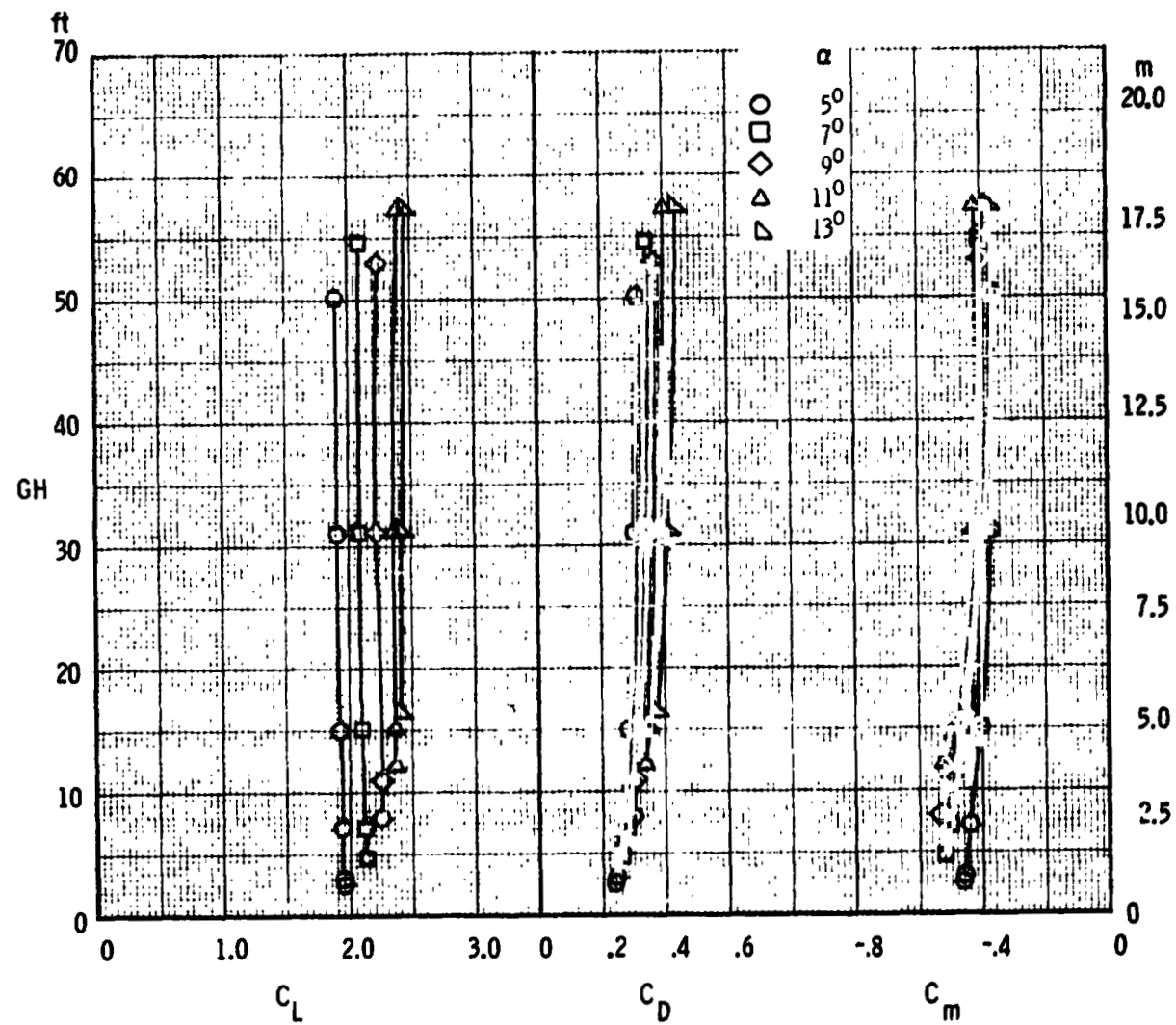
(d) Lateral-directional characteristics, $\delta_{sp2,3,6,7} = 0^\circ$

Figure 30. - Concluded.

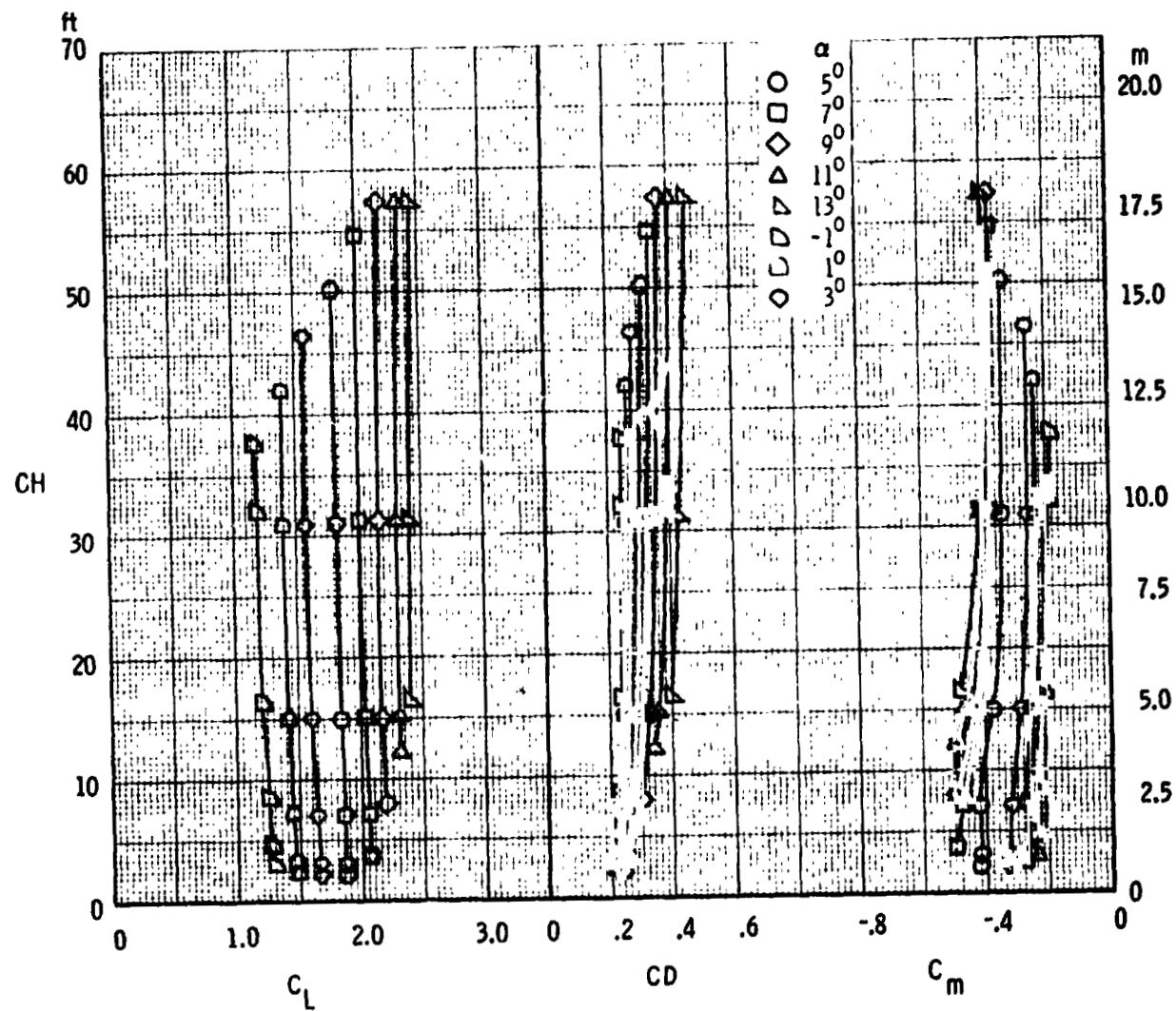


(a) $\delta_{sp2,3,6,7} = 0^\circ$

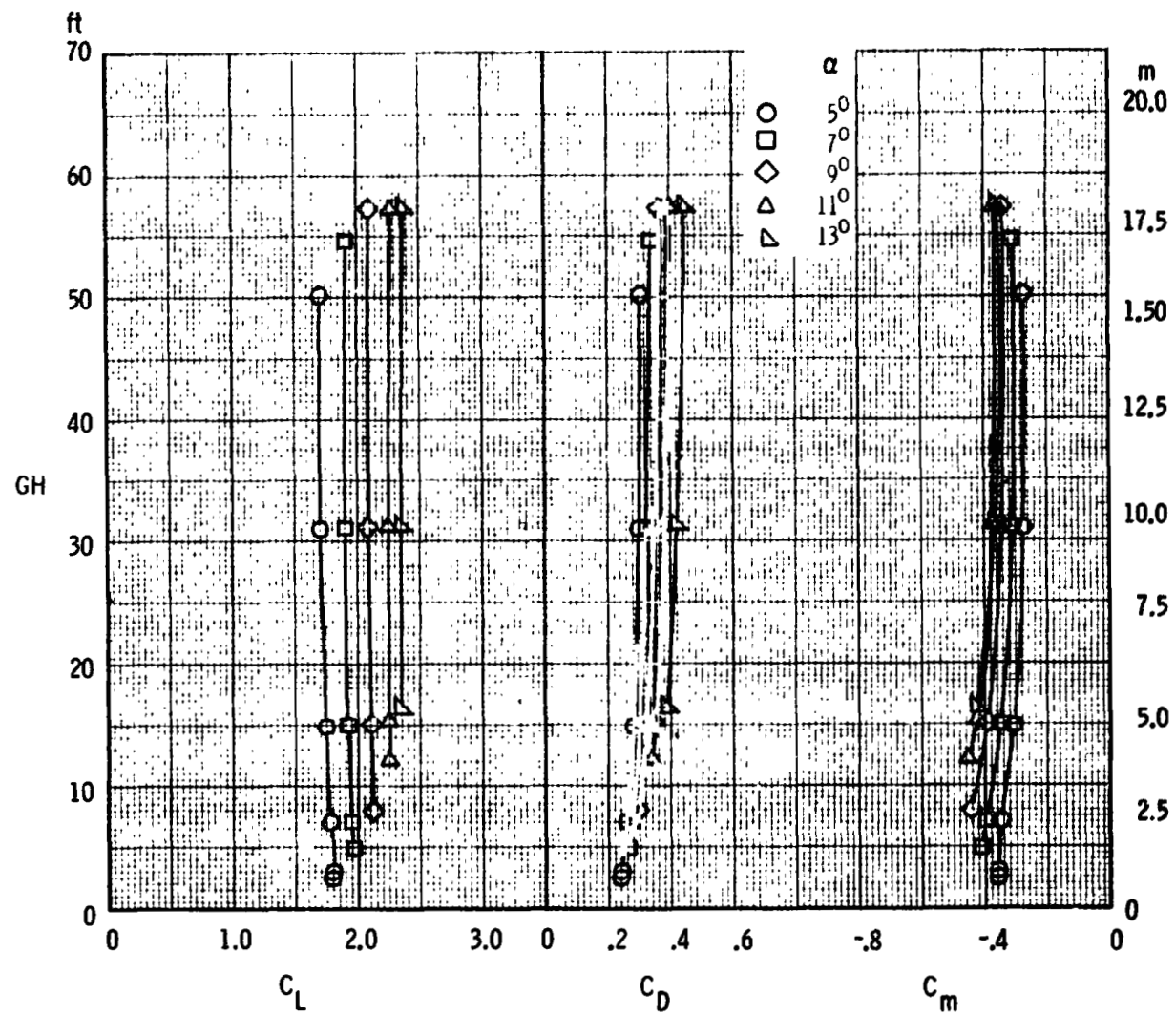
Figure 31. - Effect of ground height on the longitudinal aerodynamic characteristics of the F, W, F₄₀, N, G, H_T, V_T configuration with various DLC spoiler deflections.



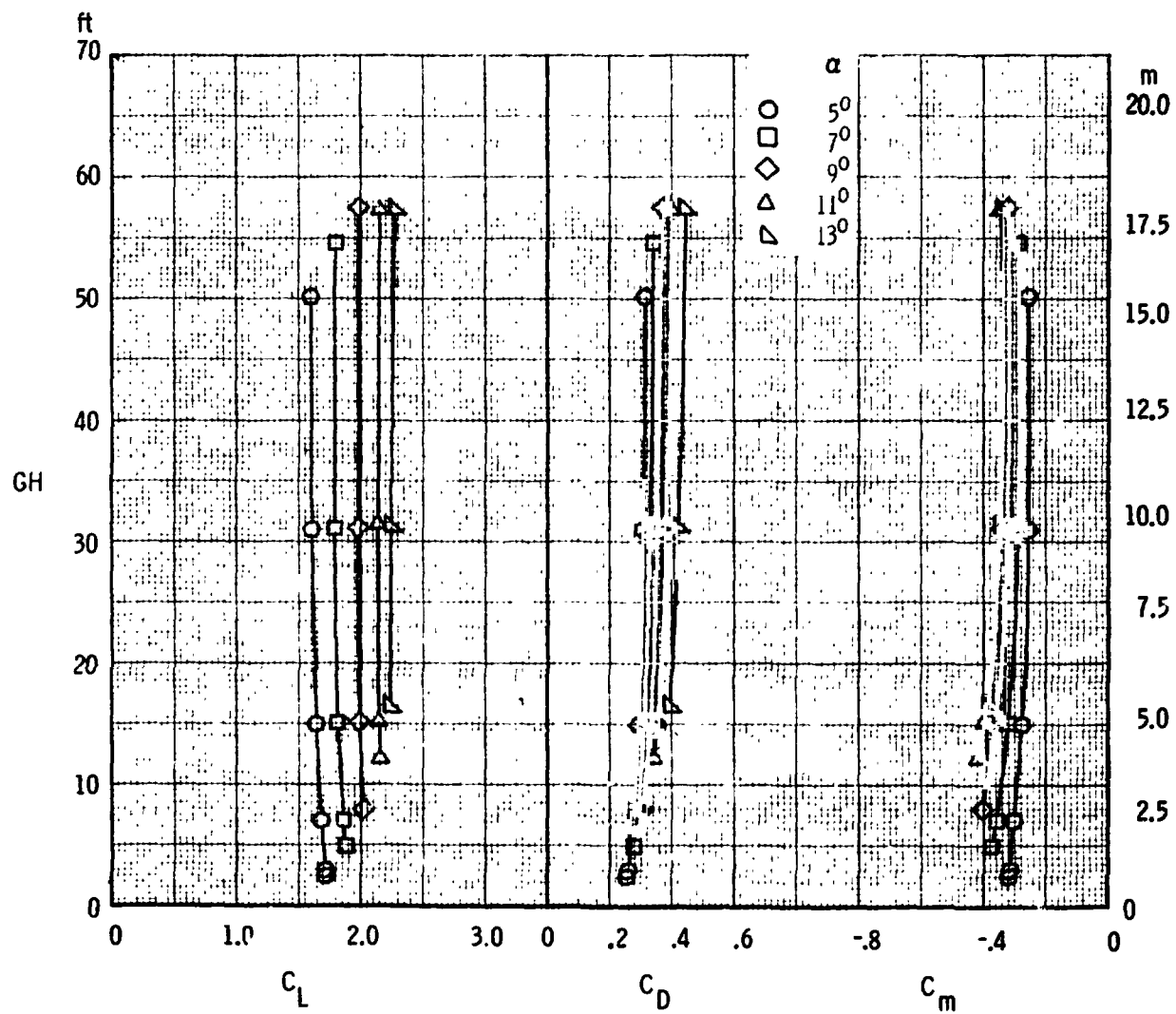
(b) $\delta_{sp2,3,6,7} = 3^\circ$
Figure 31. - Continued.



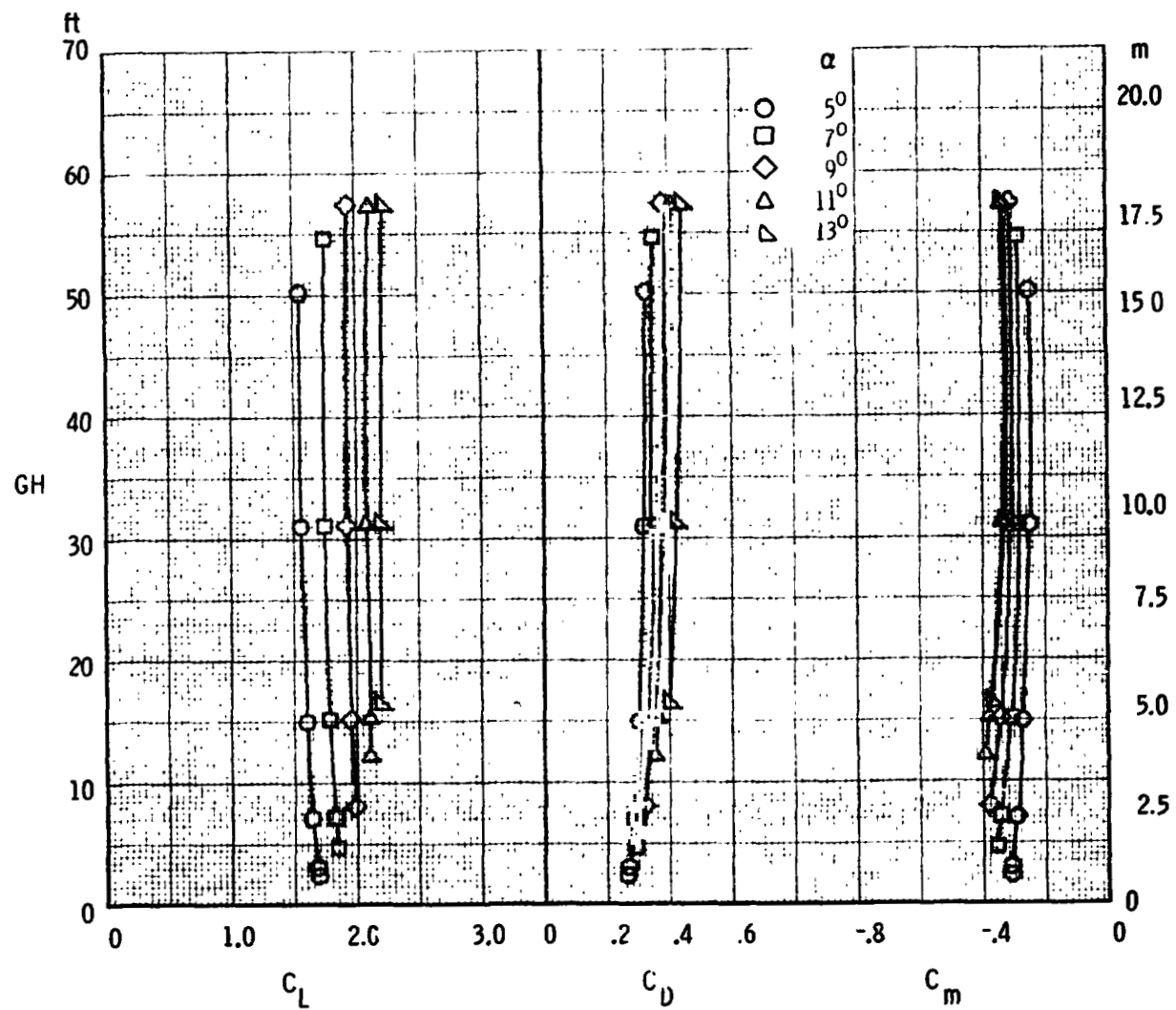
(c) $\delta_{sp2,3,6,7} = 6^\circ$
Figure 31. - Continued.



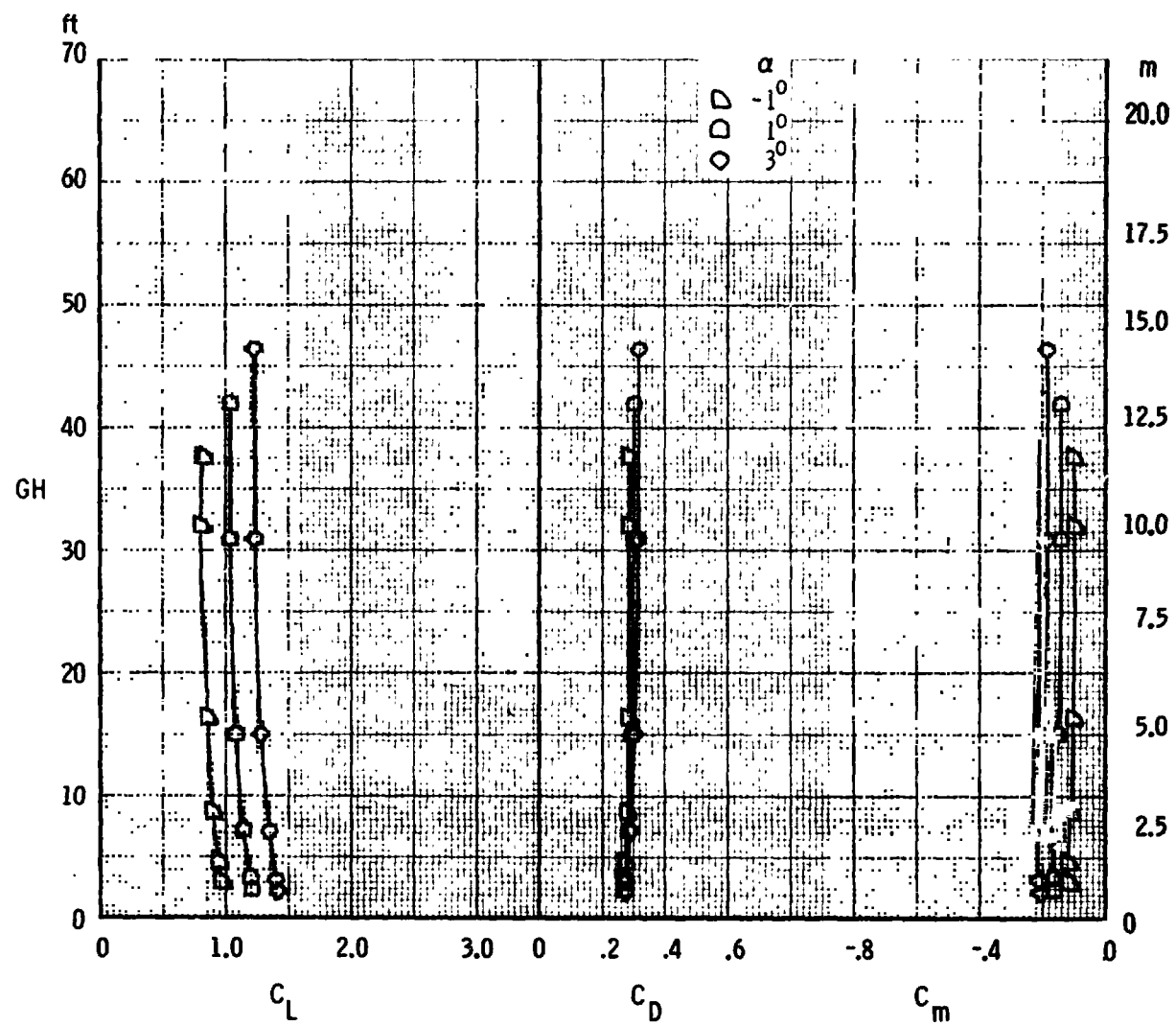
(d) $\delta_{sp2,3,6,7} = 9^\circ$
Figure 31. - Continued.



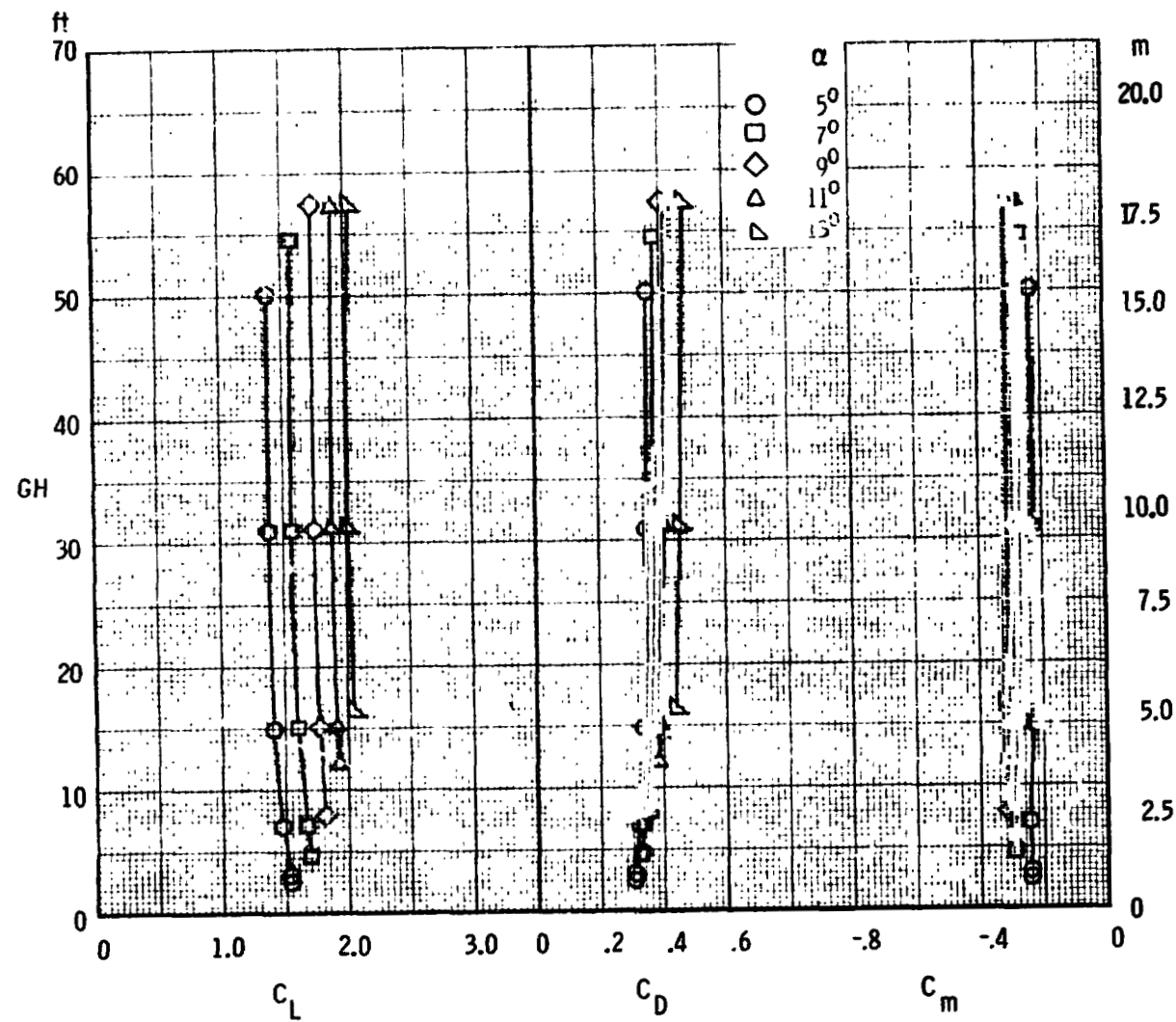
(e) $\delta_{sp2,3,6,7} = 15^\circ$
Figure 3L - Continued.



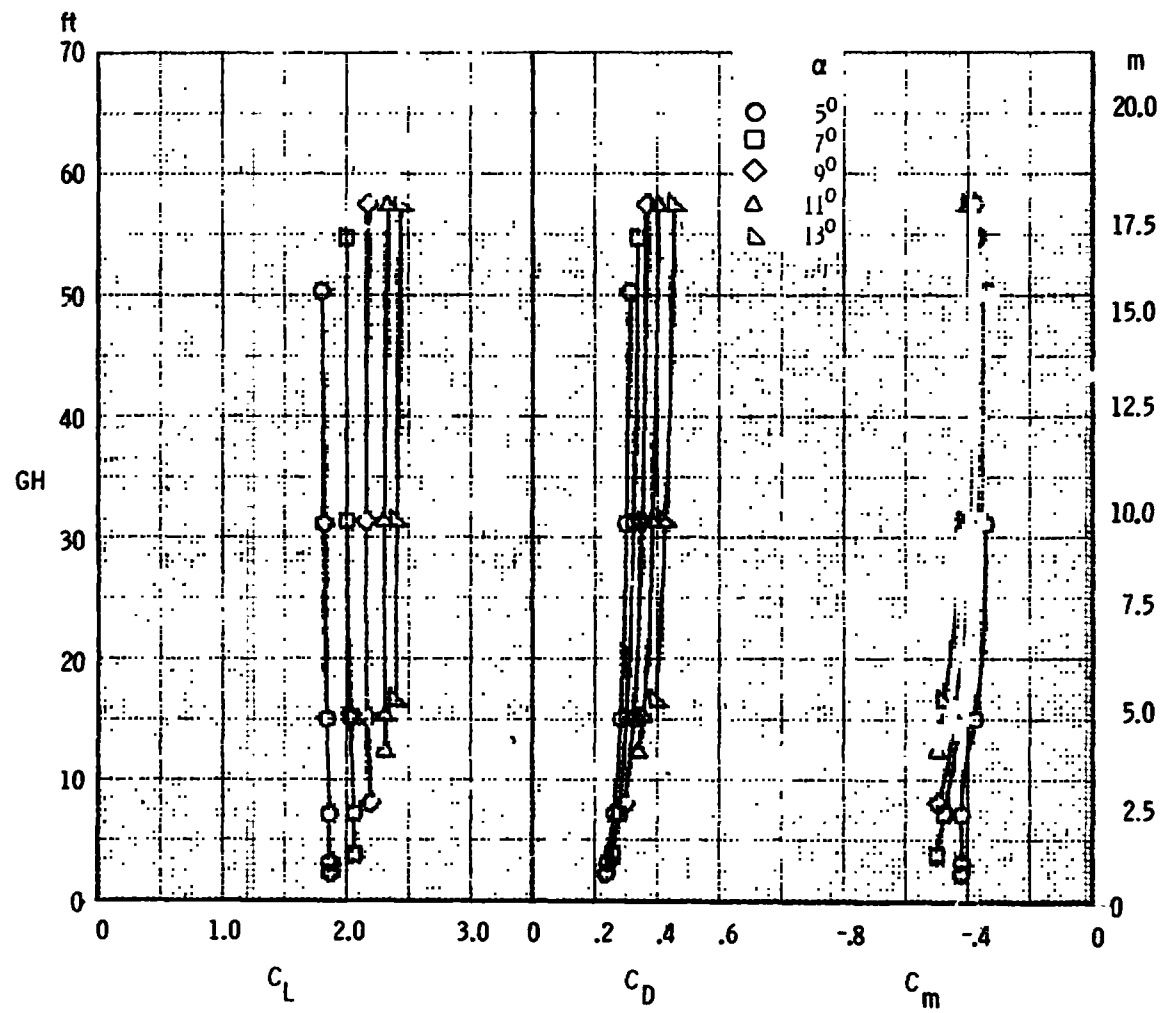
(f) $\epsilon_{sp2,3,6,7} = 20^\circ$
Figure 31. - Continued.



(g) $\delta_{sp2,3,6,7} = 30^\circ$
Figure 31. - Continued.

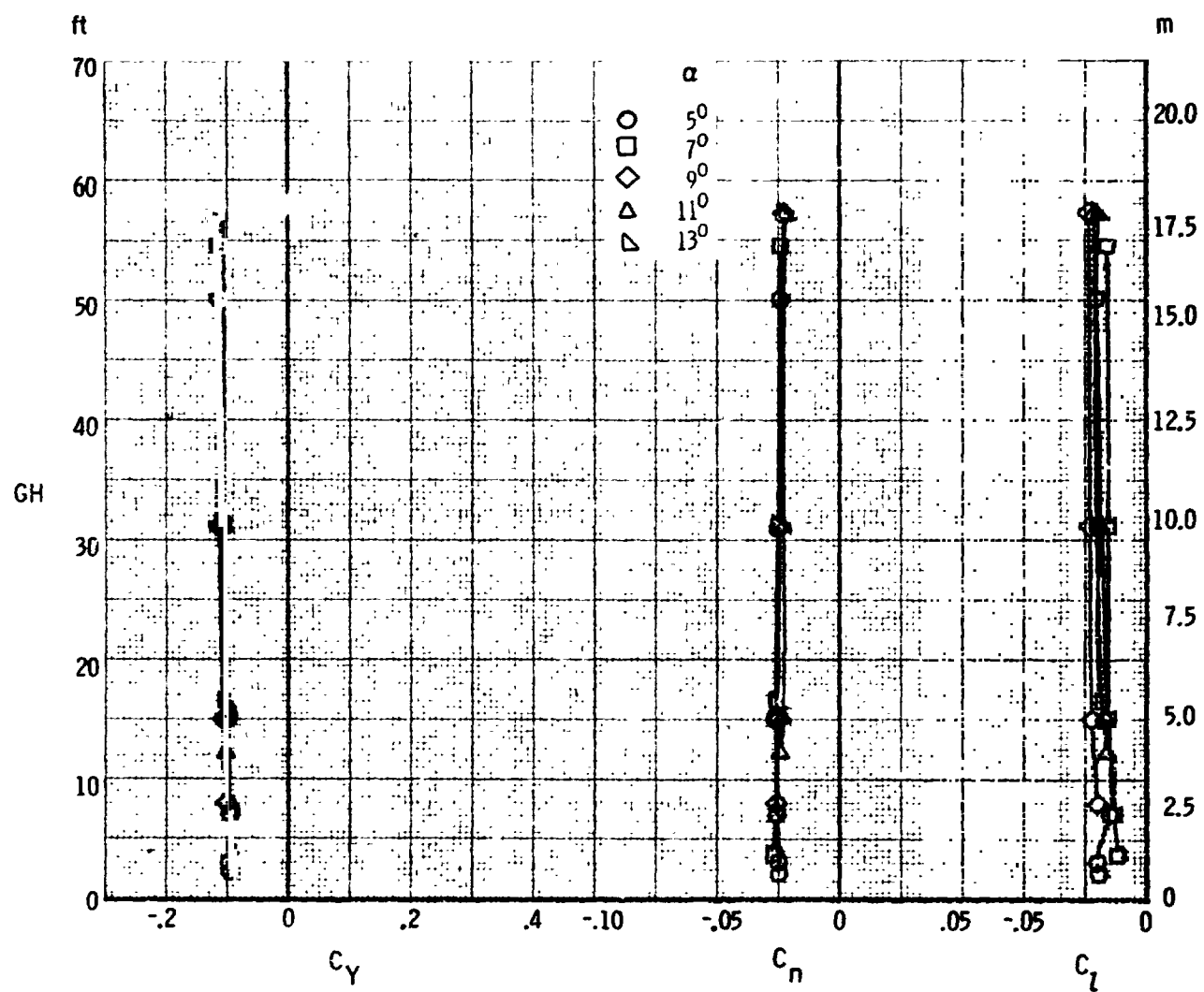


(h) $\delta_{sp2,3,6,7} = 40^\circ$
Figure 31. - Concluded.

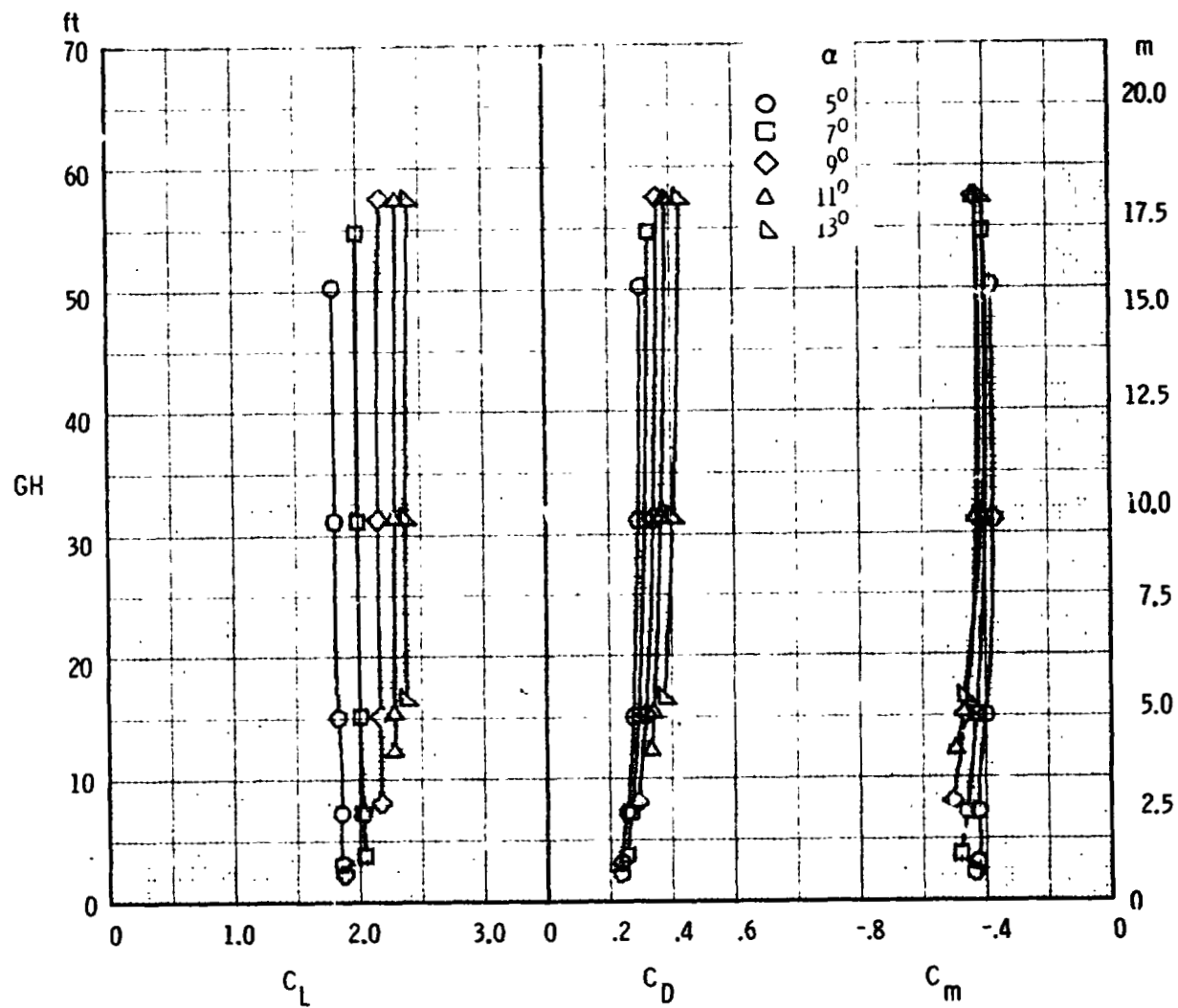


(a) Longitudinal characteristics, $\beta = 0^\circ$, $\delta_{sp2,3,6,7} = 6^\circ$

Figure 32. - Effect of ground height on the aerodynamic characteristics of the $F, W, F_{40}, N, G, H_T, V_T$ configuration at various sideslip angles with DLC spoiler deflections.

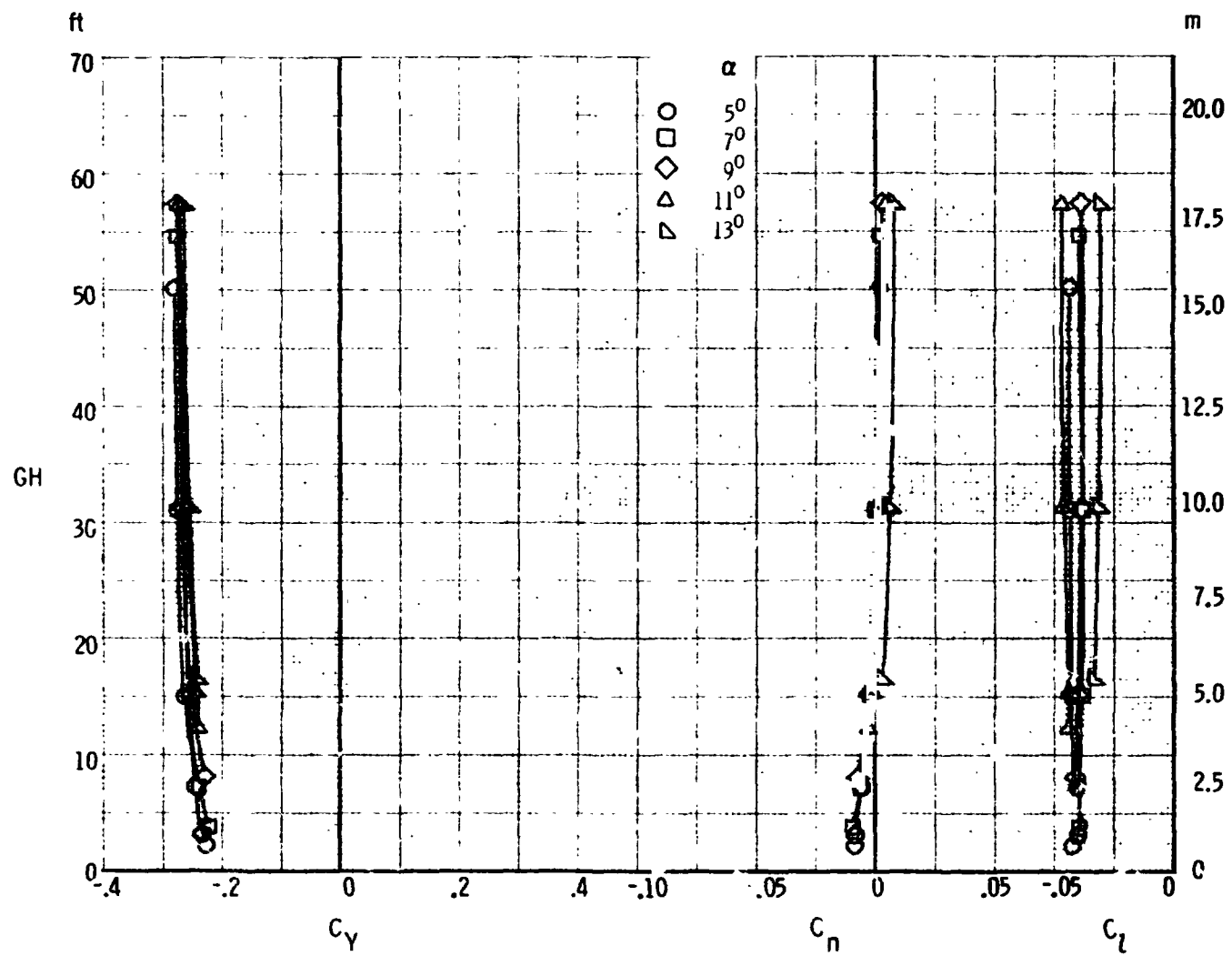


(b) Lateral-directional characteristics, $\beta = 0^\circ$, $\delta_{sp2,3,6,7} = 6^\circ$
 Figure 32. - Continued.



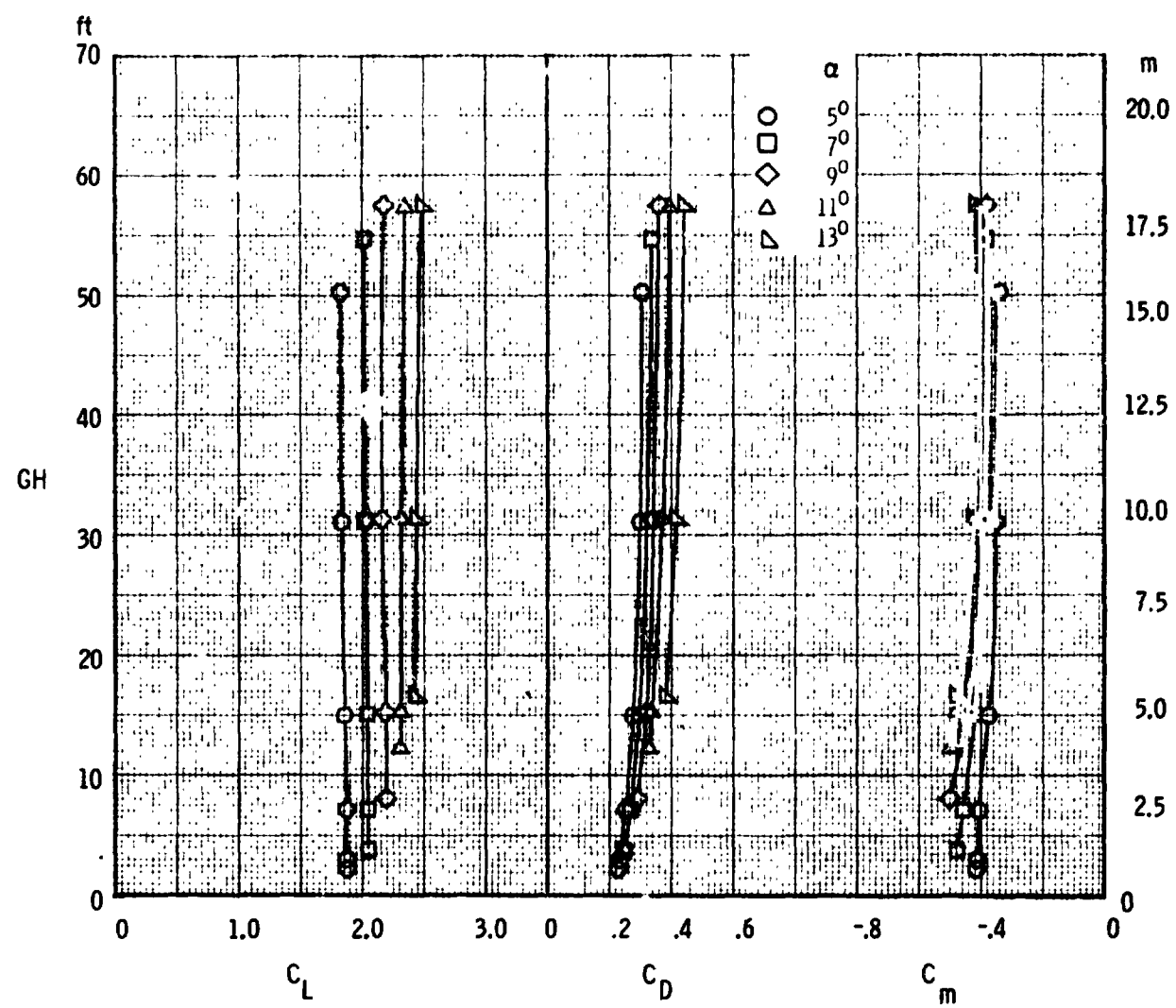
(c) Longitudinal characteristics, $\beta = 5^\circ$, $\delta_{sp2,3,6,7} = 6^\circ$

Figure 32. - Continued.



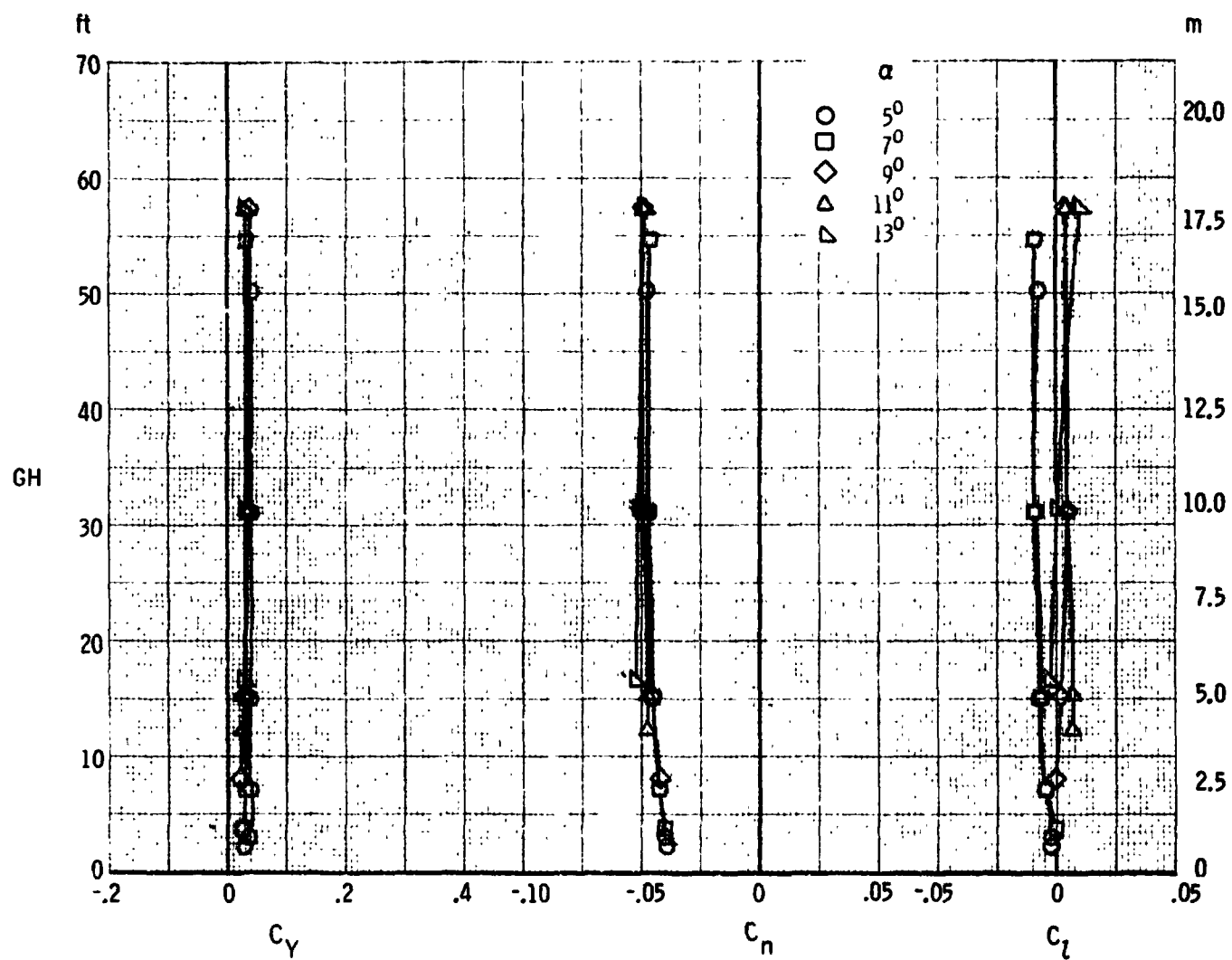
(d) Lateral-directional characteristics, $\beta = 5^\circ$, $\delta_{sp2,3,6,7} = 6^\circ$

Figure 32. - Continued.



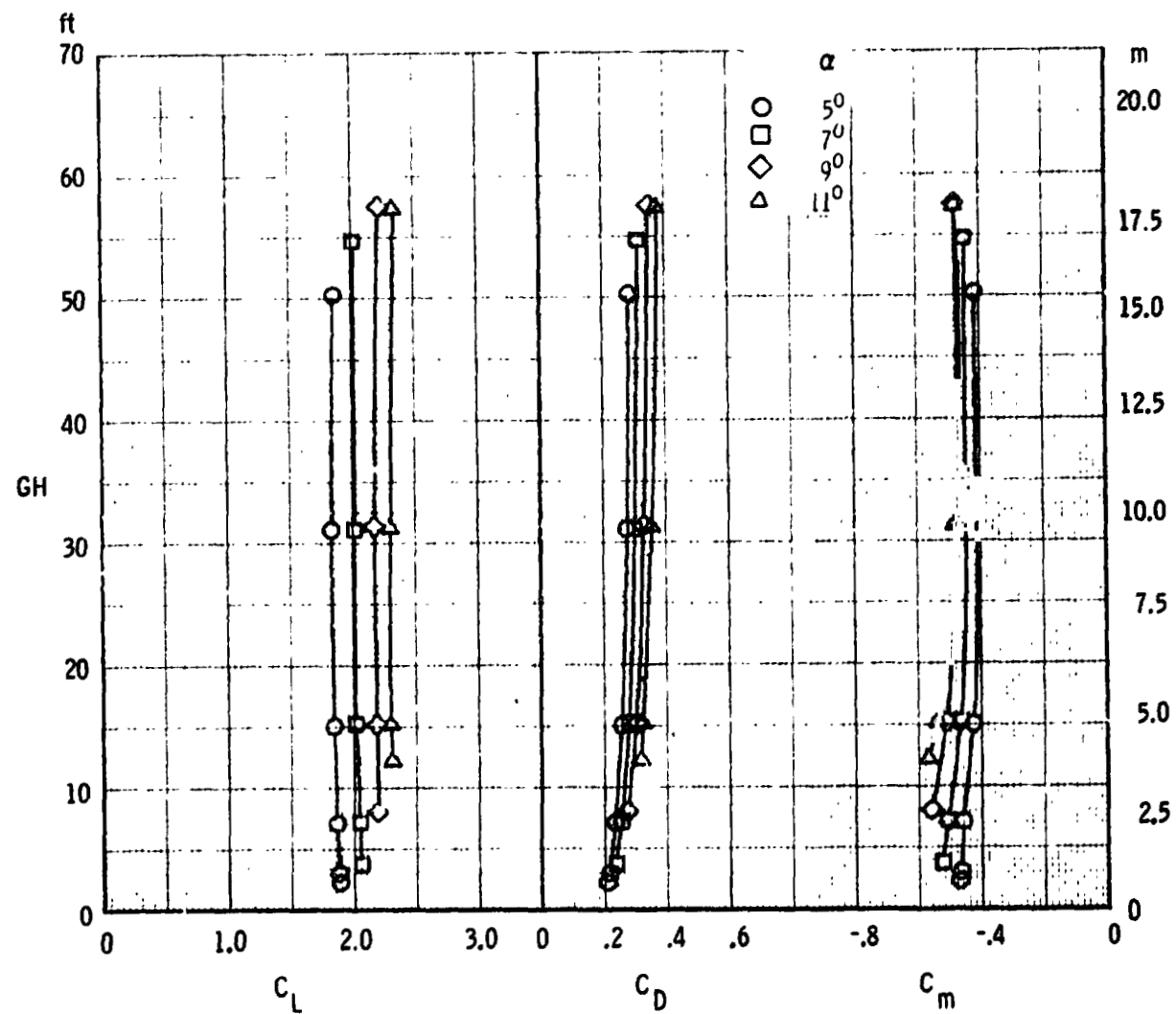
(e) Longitudinal characteristics, $\beta = -5^\circ$, $\delta_{sp2,3,6,7} = 6^\circ$

Figure 32. - Continued.



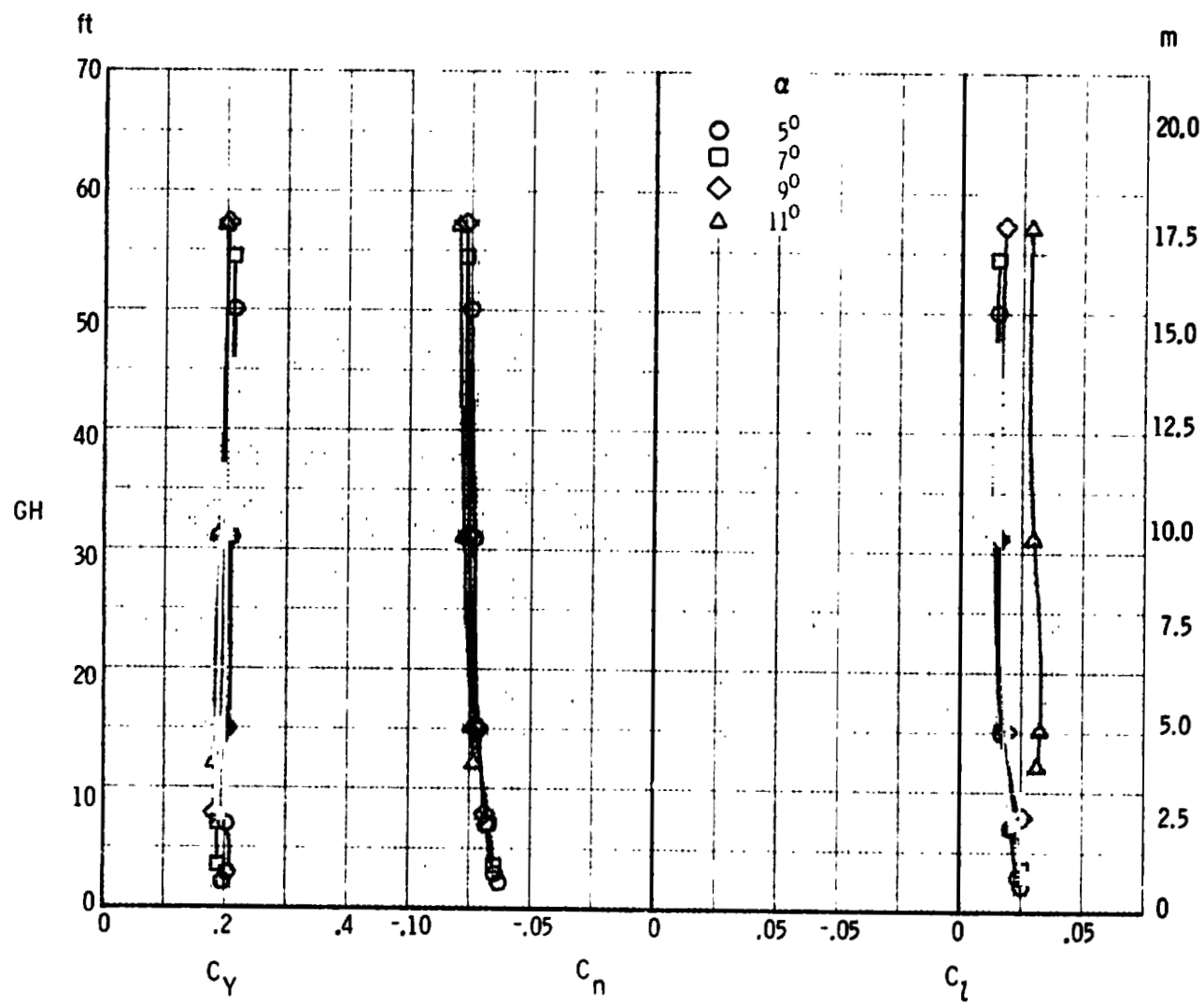
(f) Lateral-directional characteristics, $\beta = -5^\circ$, $\delta_{sp2,3,6,7} = 6^\circ$

Figure 32. - Continued.



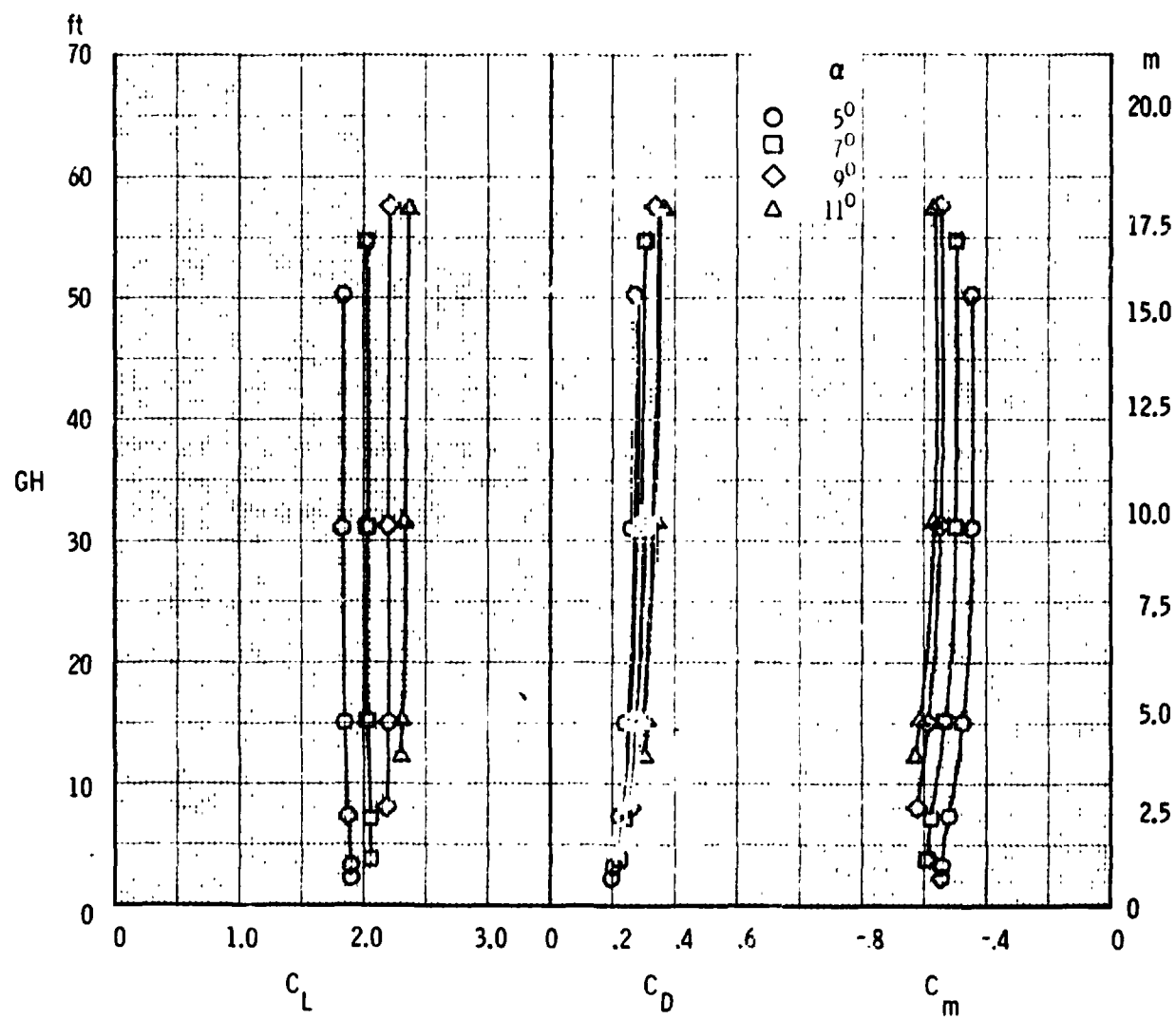
(g) Longitudinal characteristics, $\beta = -10^\circ$, $\delta_{sp2,3,6,7} = 6^\circ$

Figure 32. - Continued.

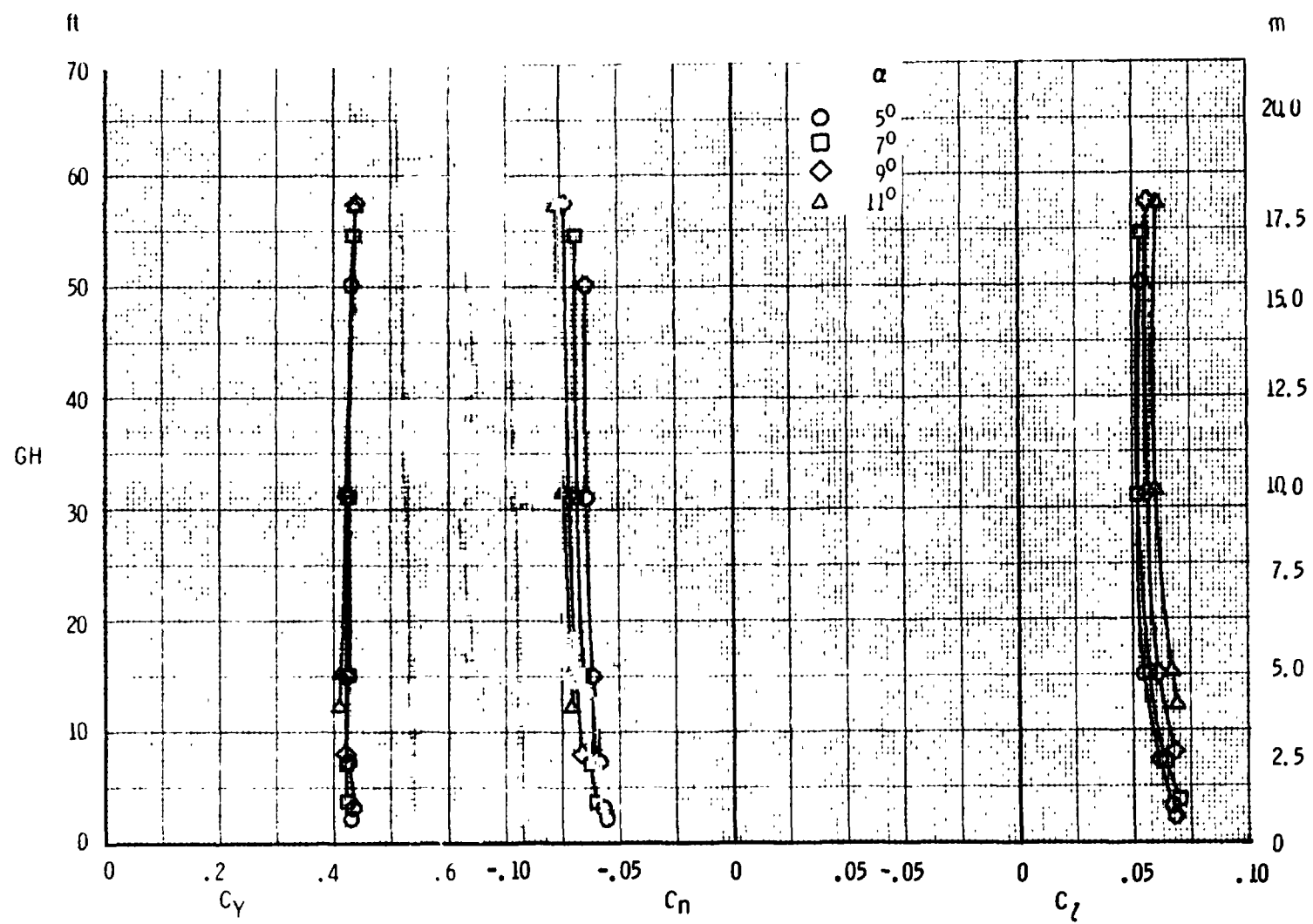


(h) Lateral-directional characteristics, $\beta = -10^\circ$, $\delta_{sp2,3,6,7} = 6^\circ$

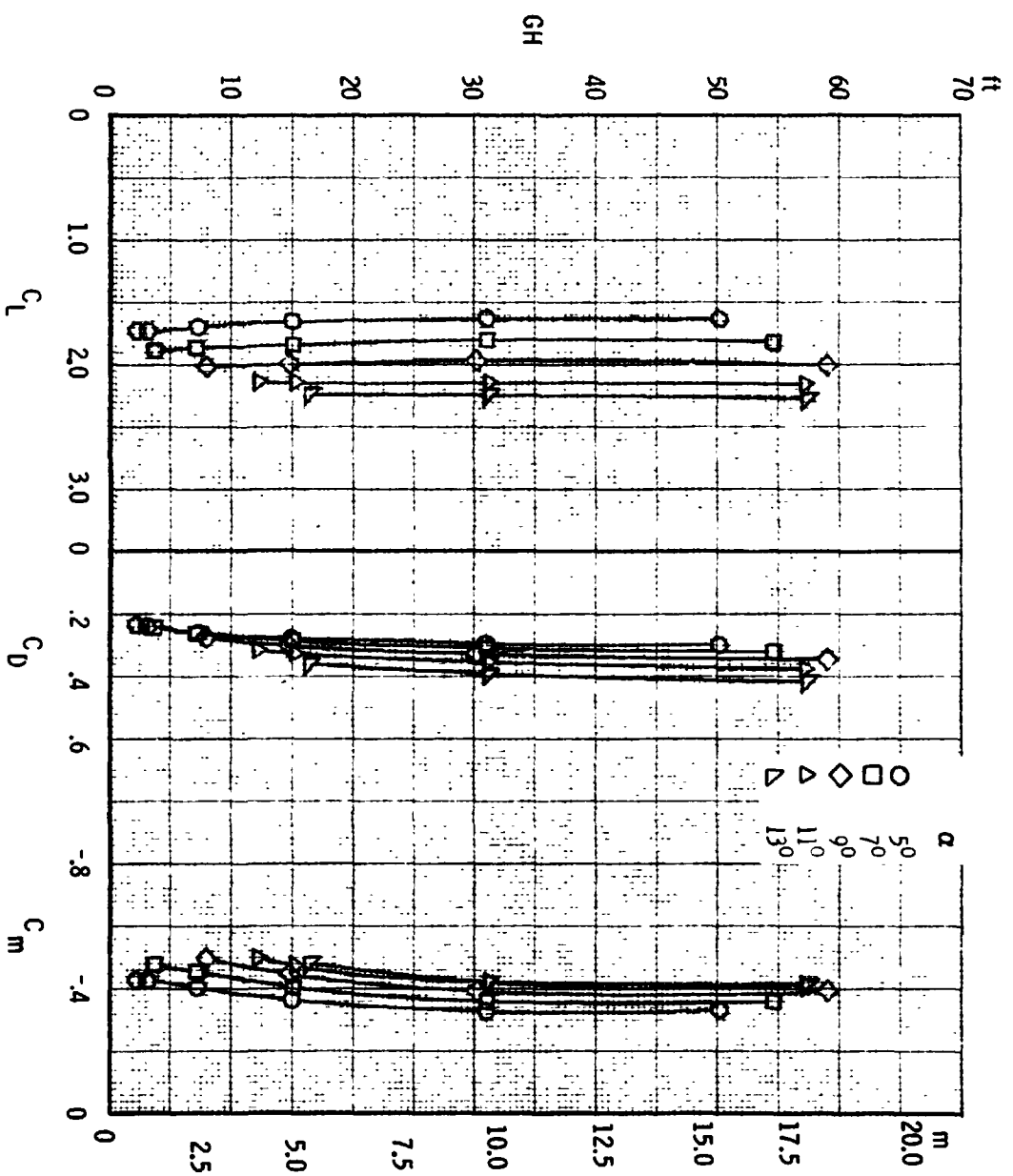
Figure 32. - Continued.



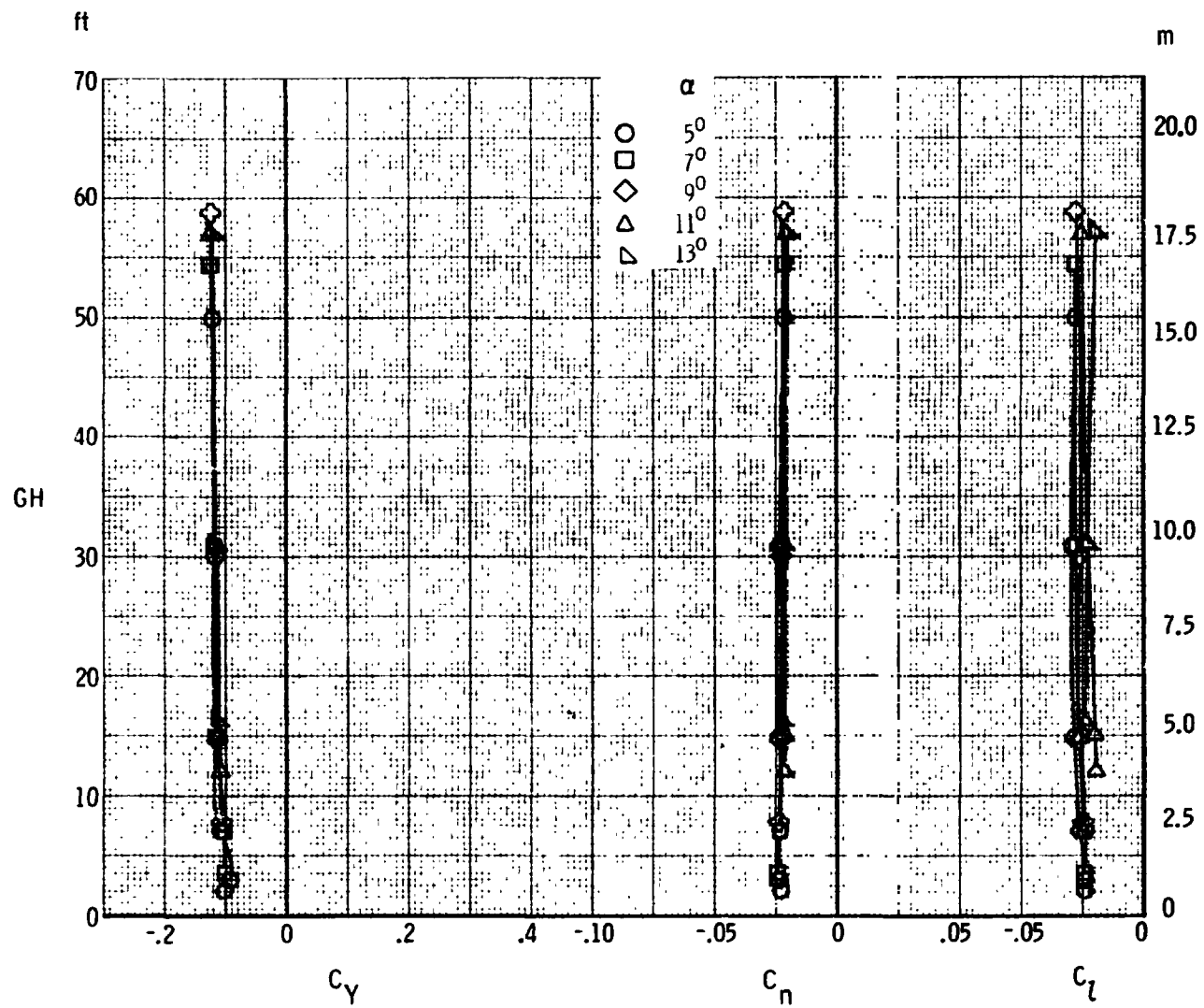
(i) Longitudinal characteristics, $\beta = -15^\circ$, $\delta_{sp2,3,6,7} = 6^\circ$
 Figure 32. - Continued.



(j) Lateral-directional characteristics, $\beta = -15^\circ$, $\delta_{sp2,3,6,7} = 6^\circ$
Figure 32. - Continued.

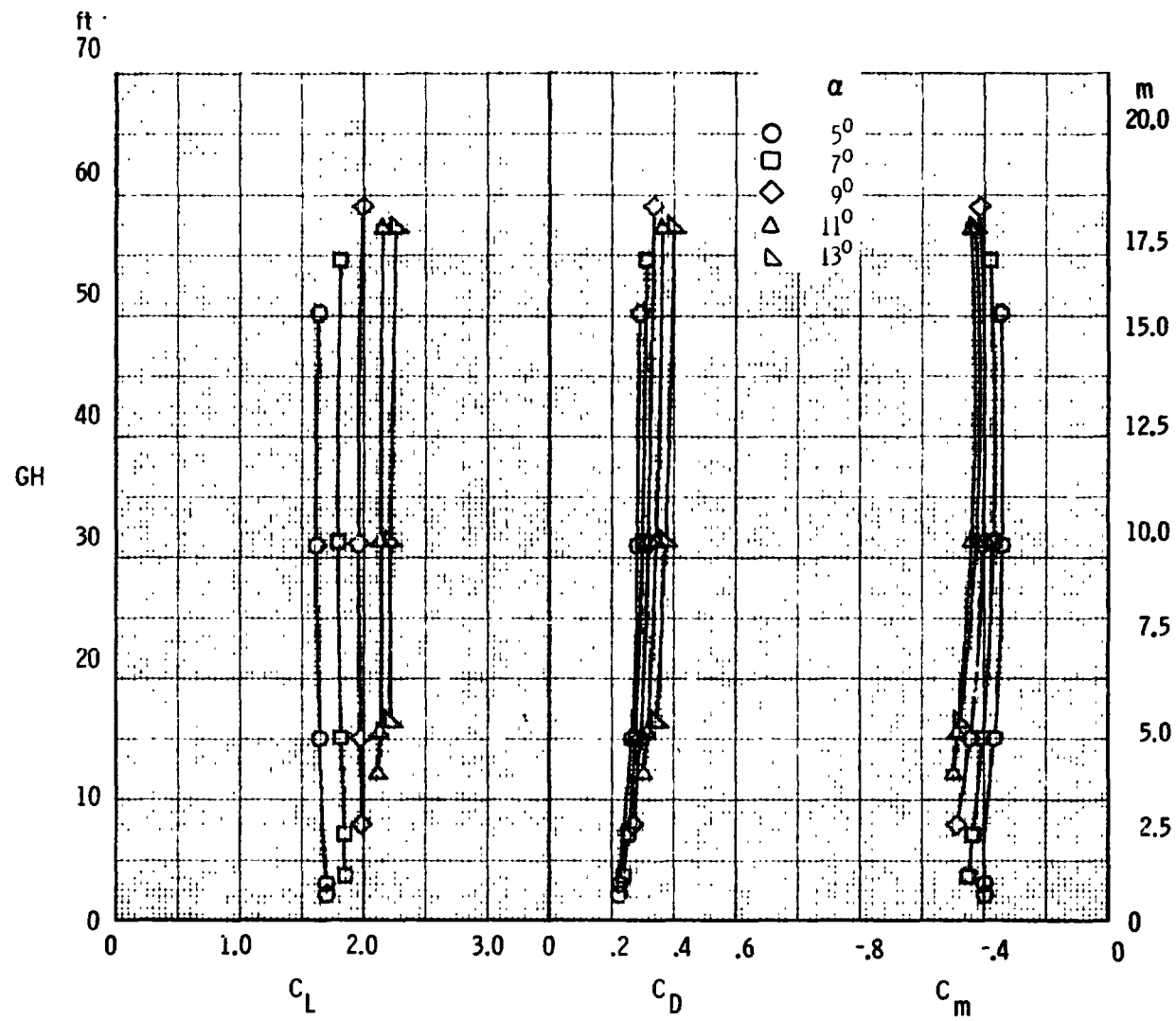


(k) Longitudinal characteristics, $\beta = 0^\circ$, $S_{p2,3,6,7} = 9^\circ$
 Figure 32. - Continued.



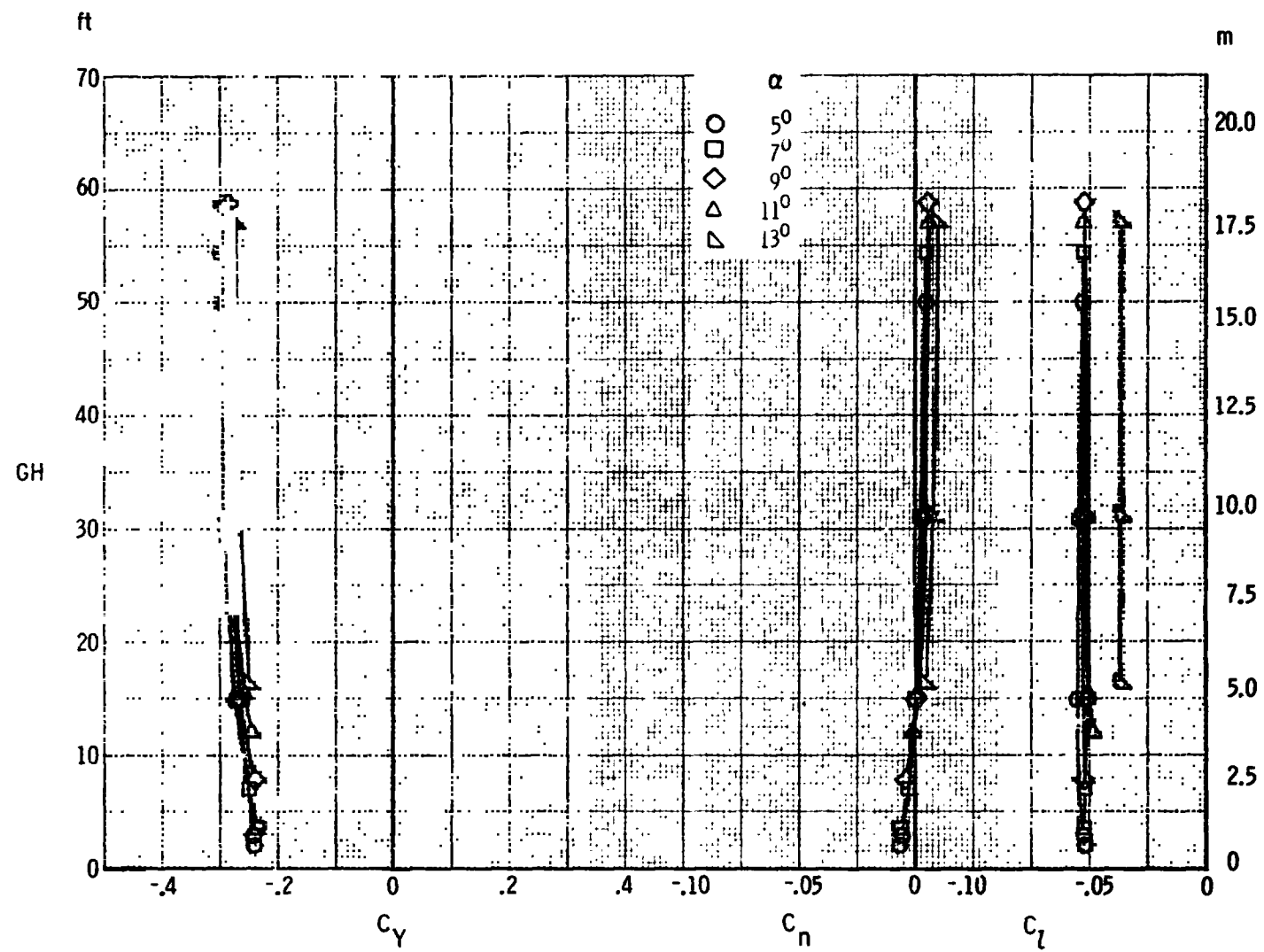
(I) Lateral-directional characteristics, $\beta = 0^\circ$, $\delta_{sp2,3,6,7} = 9^\circ$

Figure 32. - Continued.



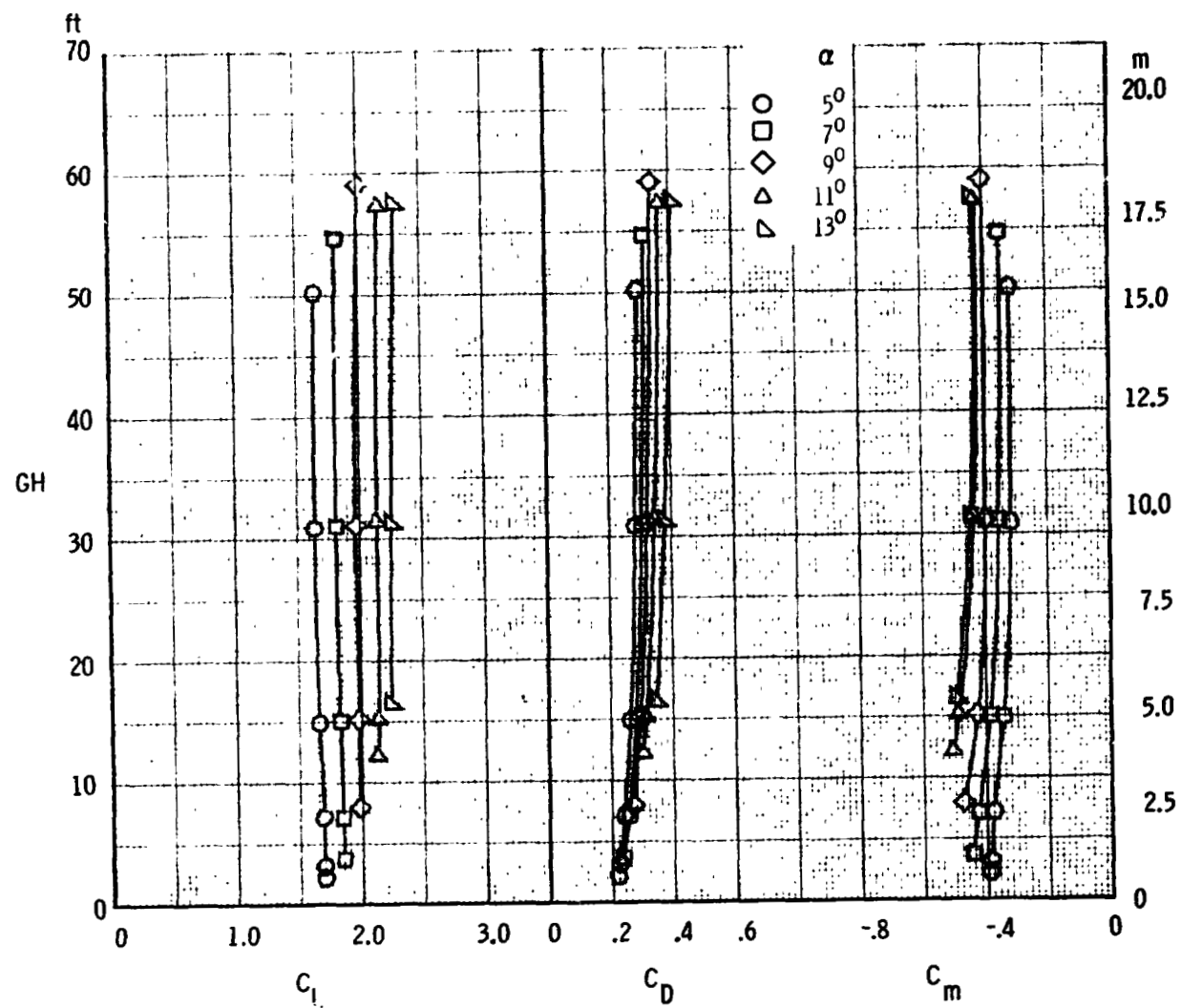
(m) Longitudinal characteristics, $\beta = 5^\circ$, $\delta_{sp2,3,6,7} = 9^\circ$

Figure 32. - Continued.



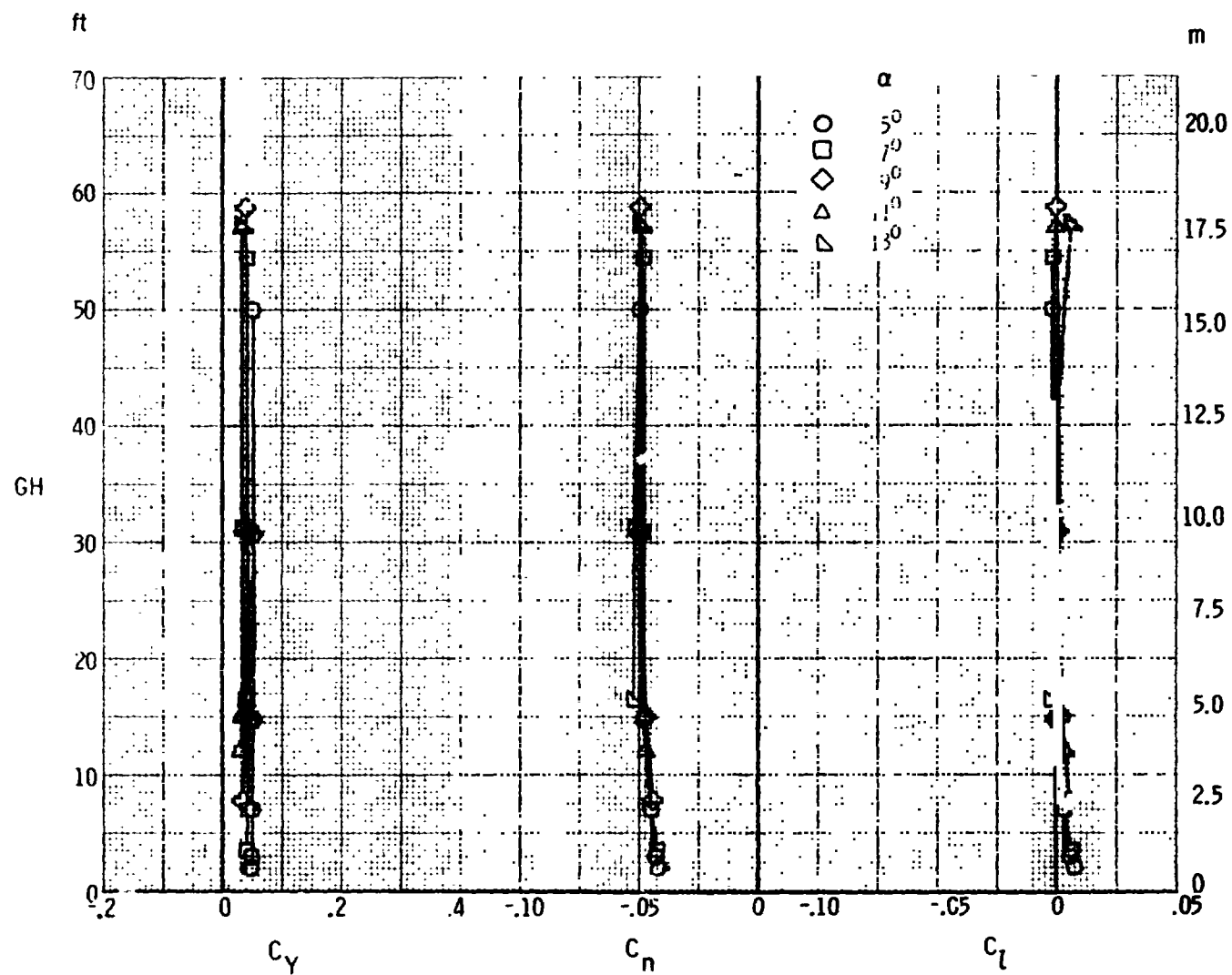
(n) Lateral-directional characteristics, $\beta = 5^\circ$, $\delta_{sp2,3,6,7} = 9^\circ$

Figure 32. - Continued.



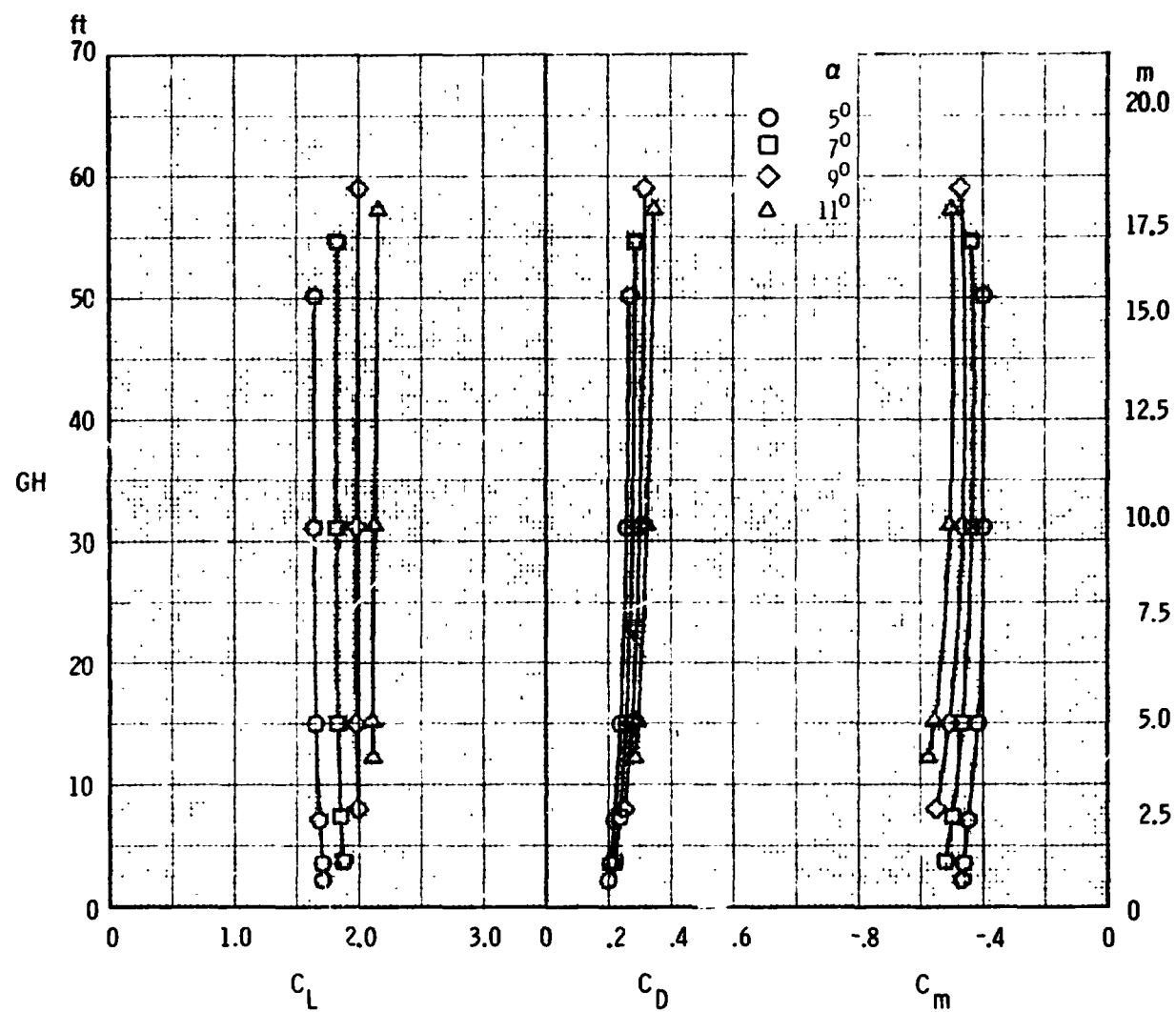
(a) Longitudinal characteristics, $\beta = -5^\circ$, $\delta_{sp2,3,6,7} = 9^\circ$

Figure 32. - Continued.



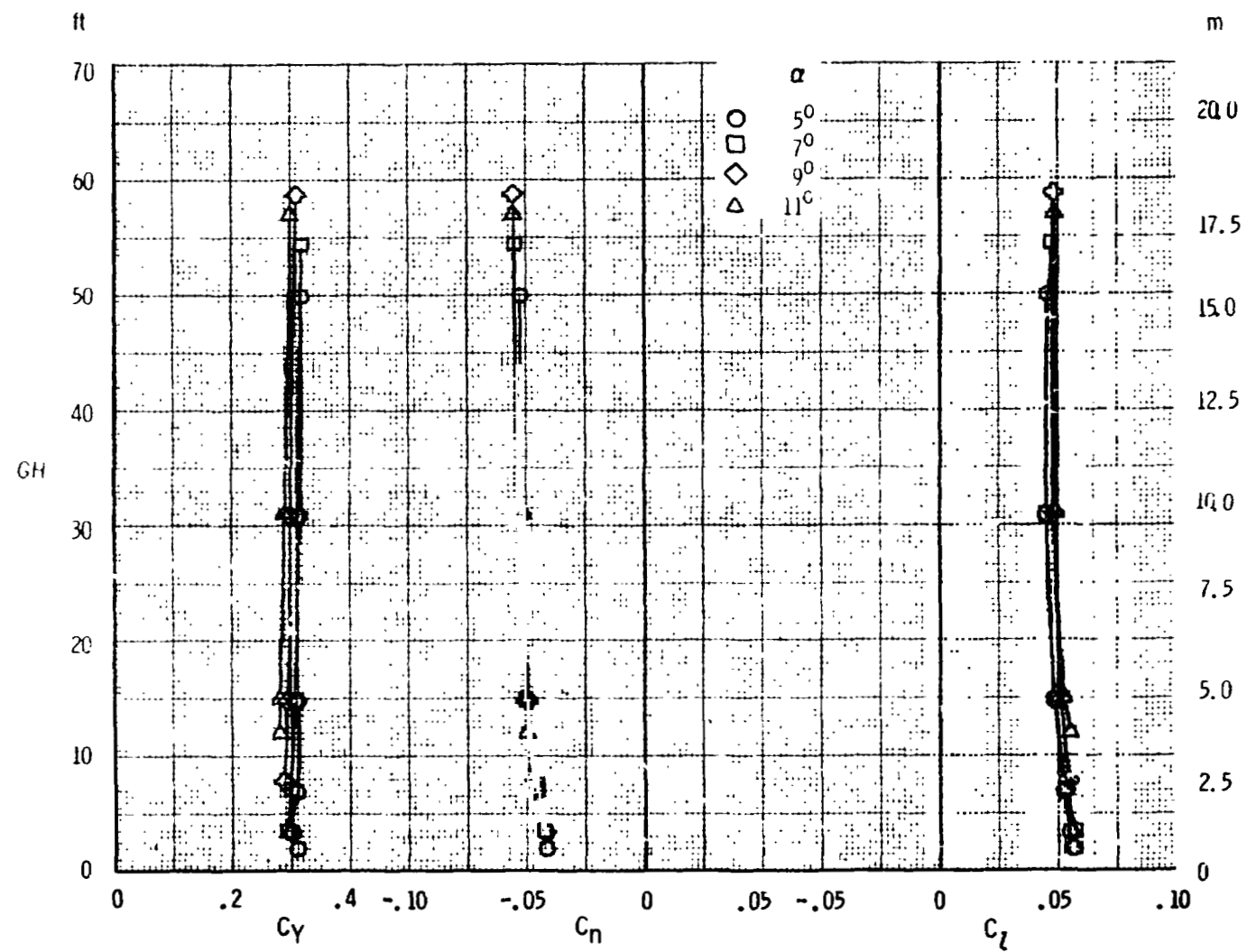
(p) Lateral-directional characteristics, $\beta = -5^\circ$, $\delta_{sp2,3,6,7} = 9^\circ$

Figure 32. - Continued.



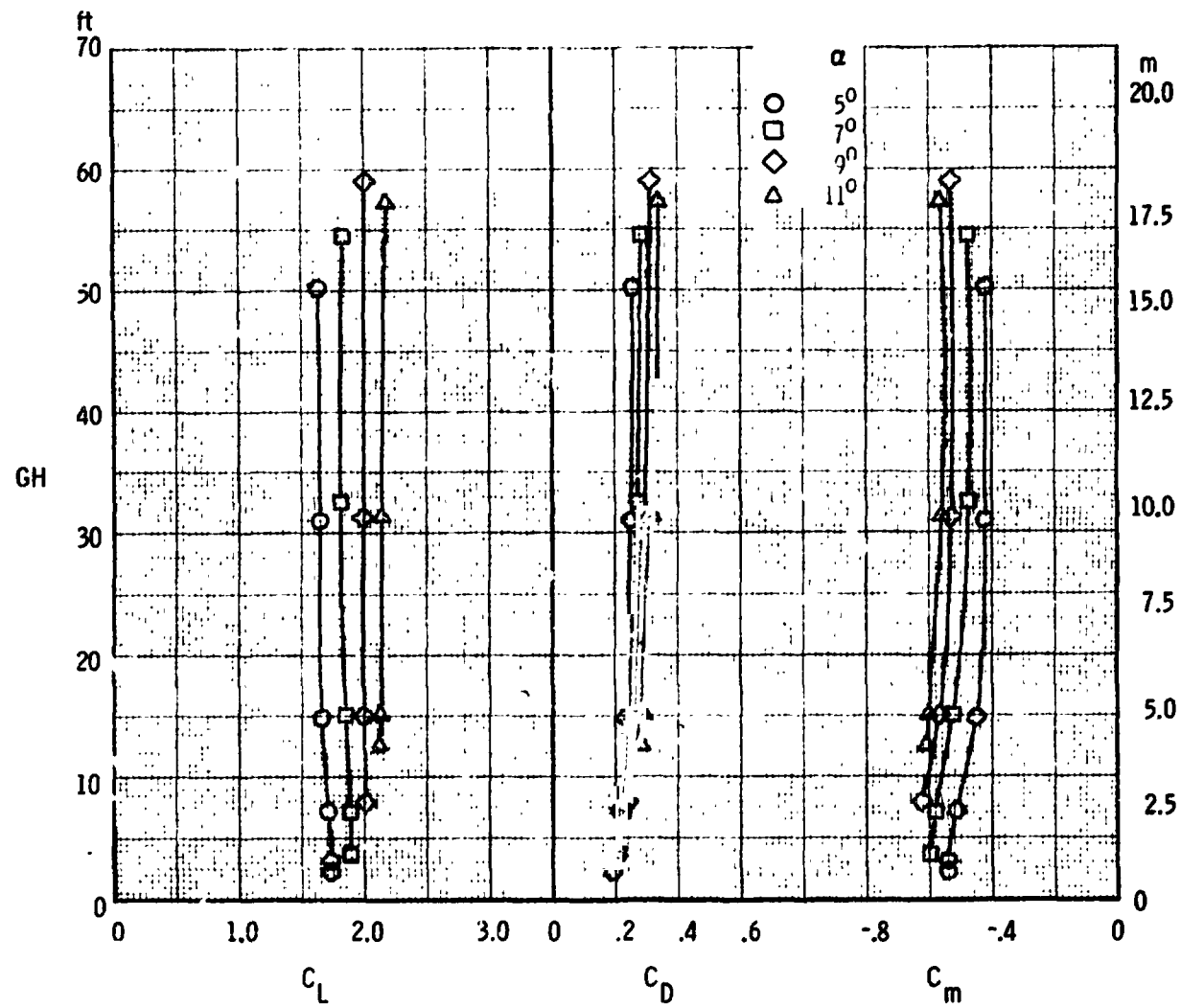
(q) Longitudinal characteristics, $\beta = -10^\circ$, $\delta_{sp2,3,6,7} = 9^\circ$

Figure 32. - Continued.



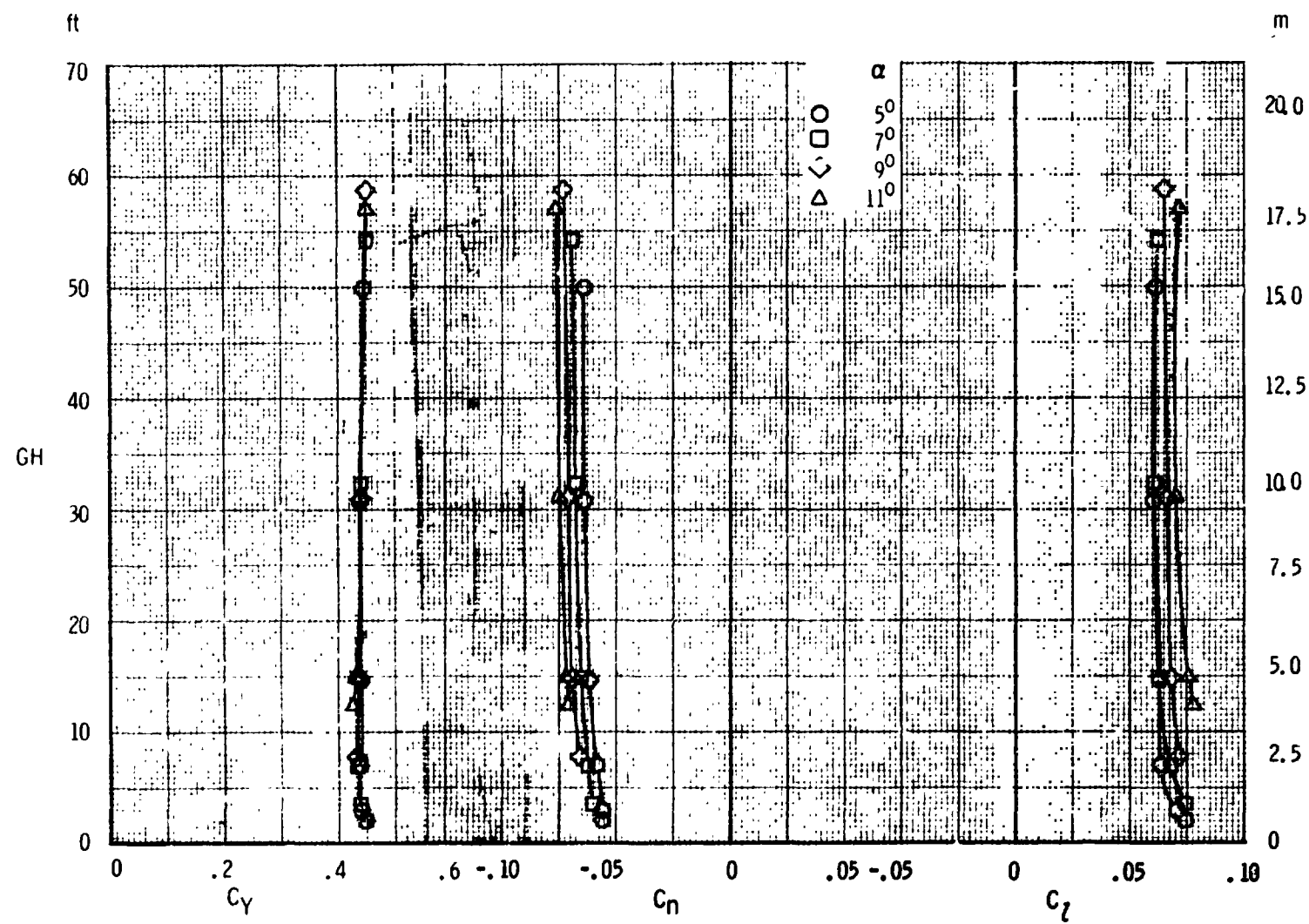
(r) Lateral-directional characteristics, $\beta = -10^\circ$, $\delta_{sp2,3,6,7} = 9^\circ$

Figure 32. - Continued.



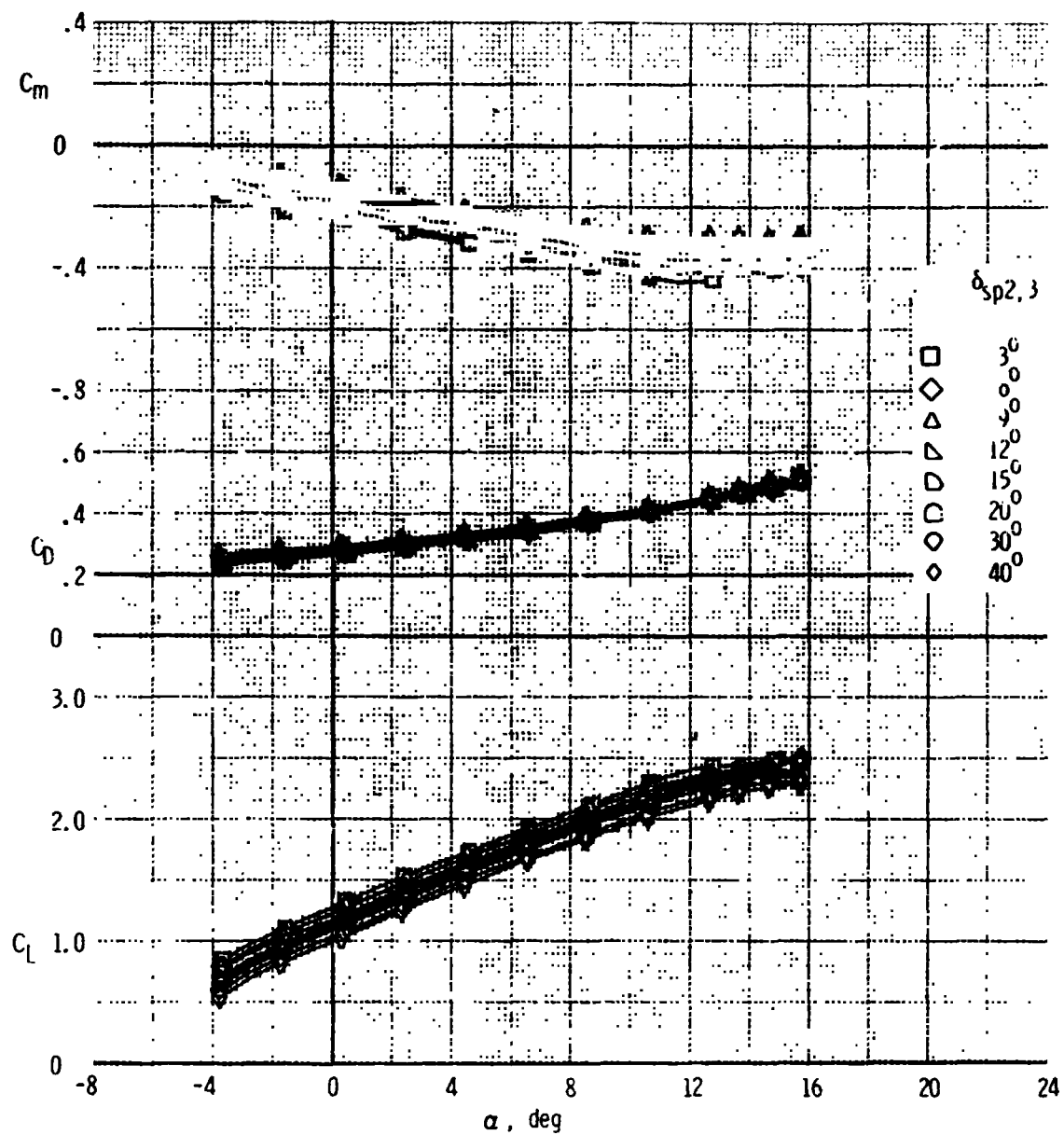
(s) Longitudinal characteristics, $\beta = -15^\circ$, $\alpha_{n2,3,6,7} = 9^\circ$

Figure 32. - Continued.



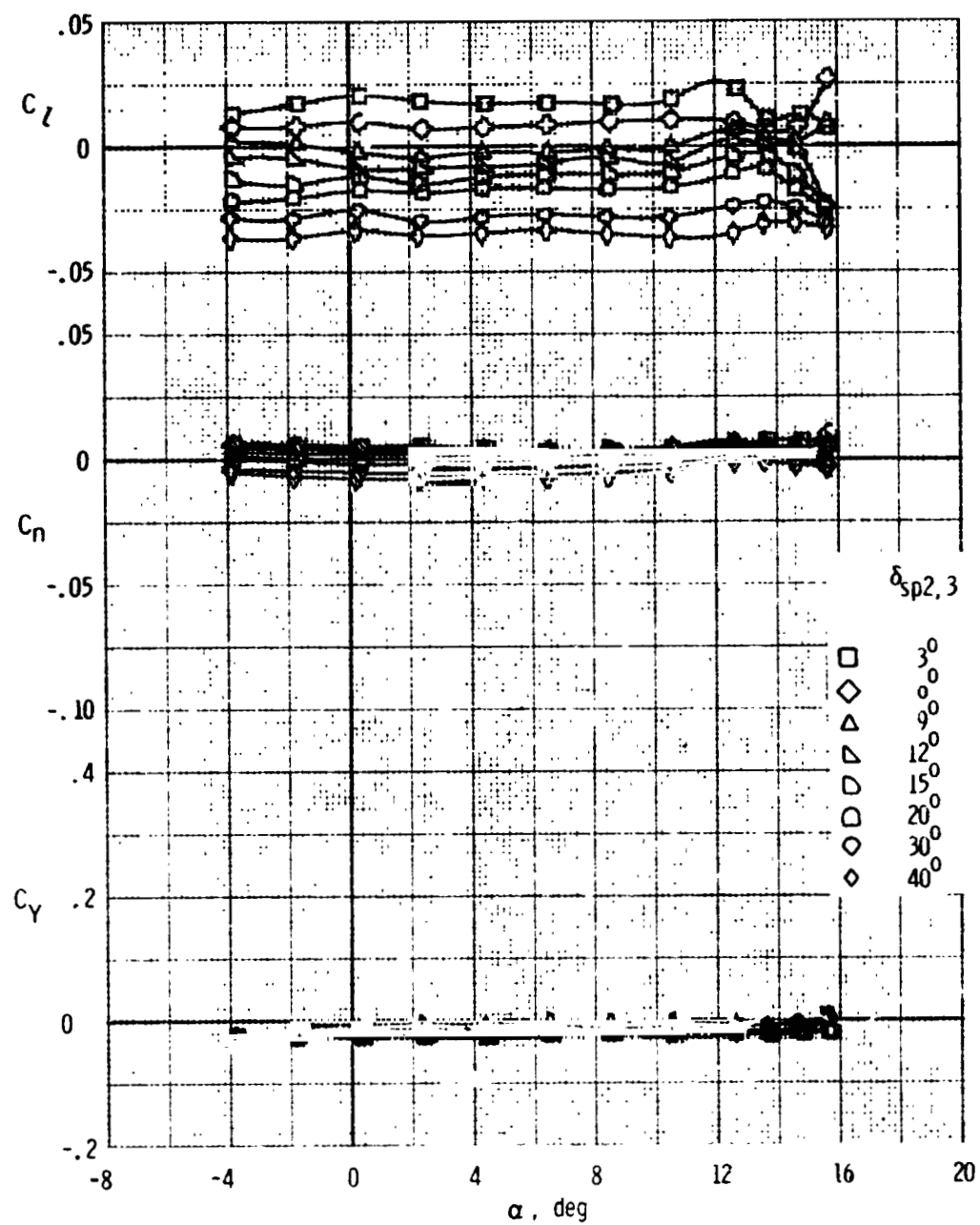
(t) Lateral-directional characteristics, $\beta = -15^\circ$, $\delta_{sp2,3,6,7} = 9^\circ$

Figure 32. - Concluded.

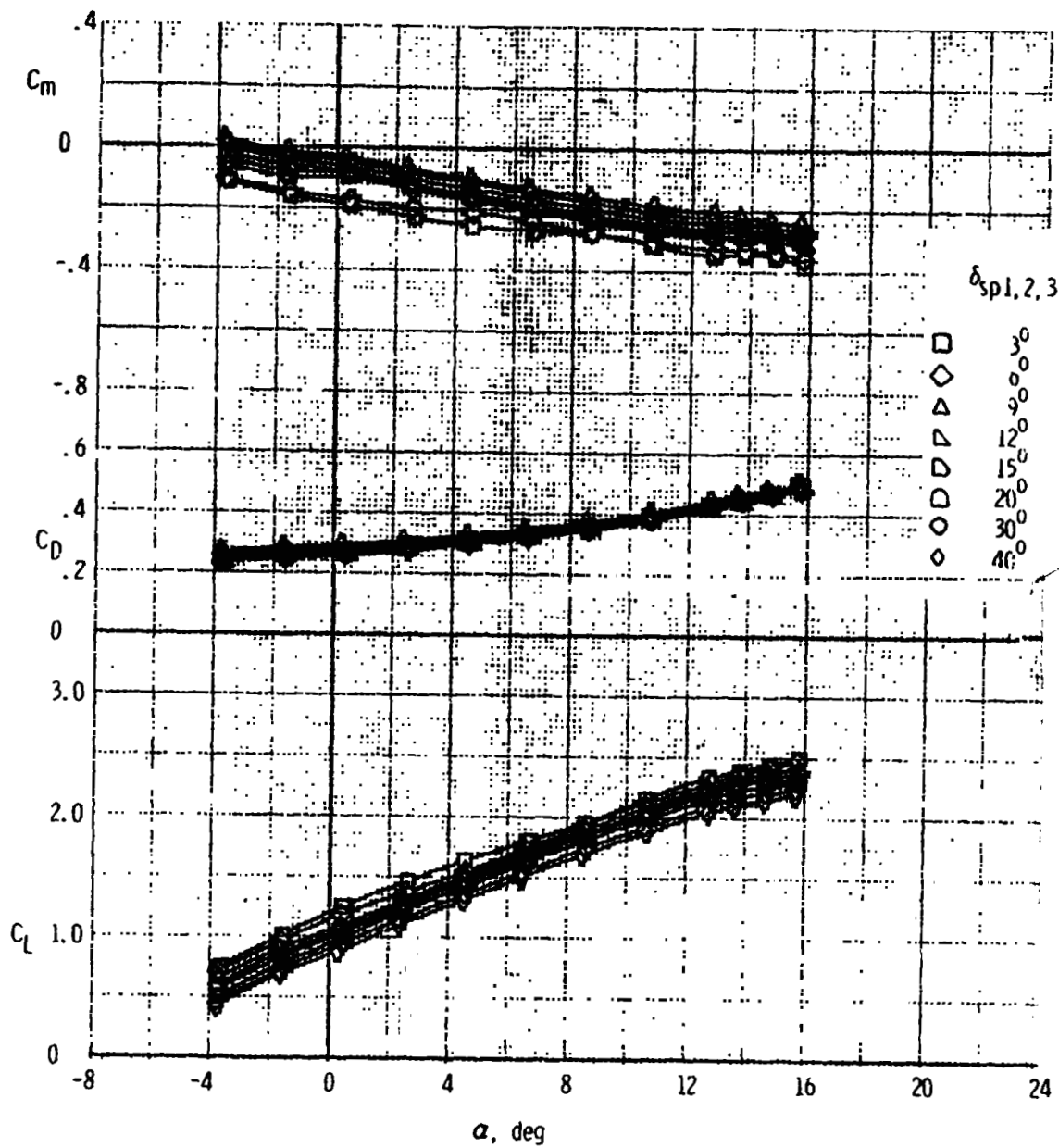


(a) Longitudinal characteristics, $\delta_{sp6,7} = 6^\circ$

Figure 33. - Effect of differential DLC spoiler deflection on the aerodynamic characteristics of the F, W, F₄₀, N, G, H_T, V_T configuration.



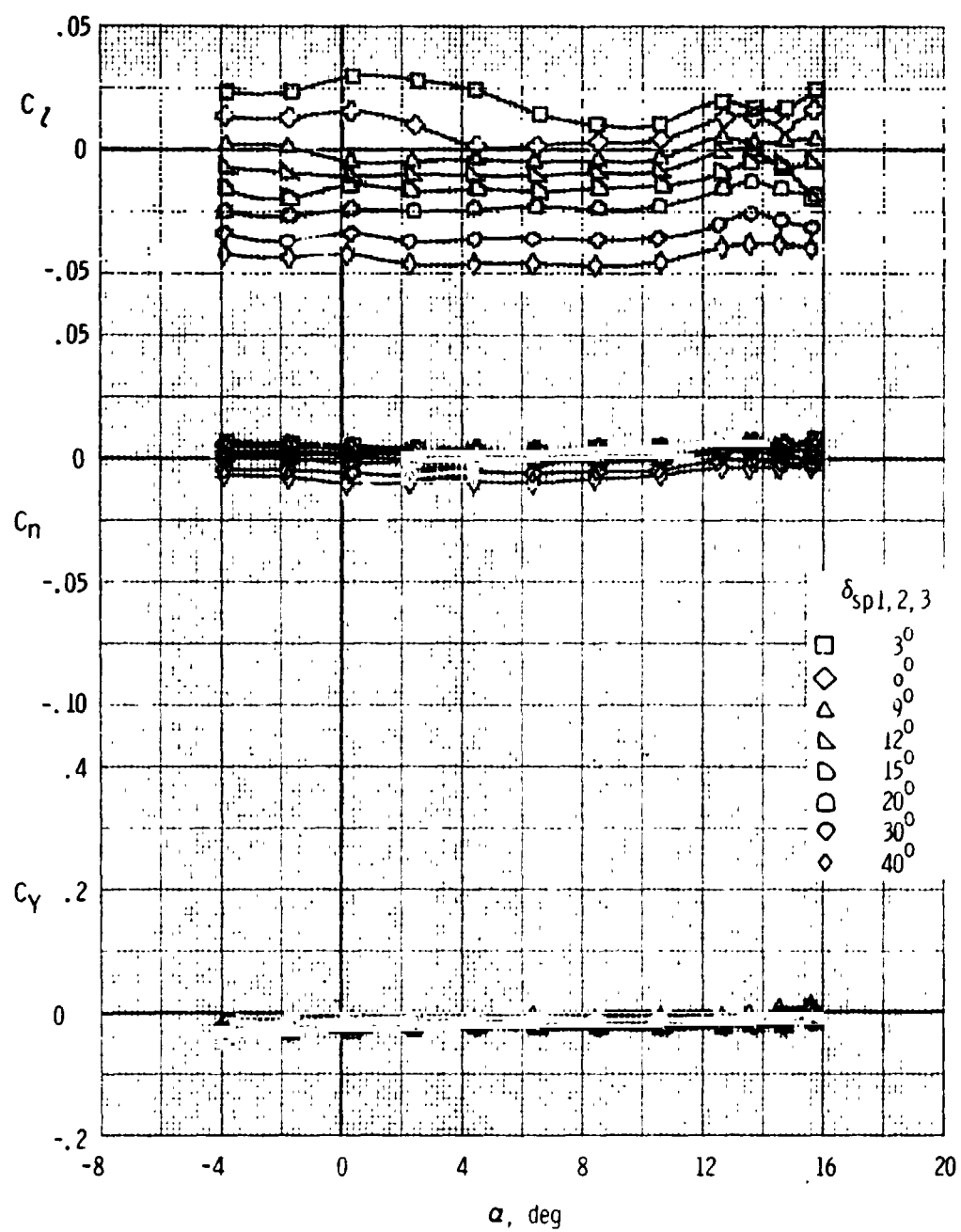
(b) Lateral-directional characteristics, $\delta_{sp6,7} = 6^\circ$
Figure 33. - Continued.



(c) Longitudinal characteristics, $\delta_{sp6,7,8} = 6^\circ$

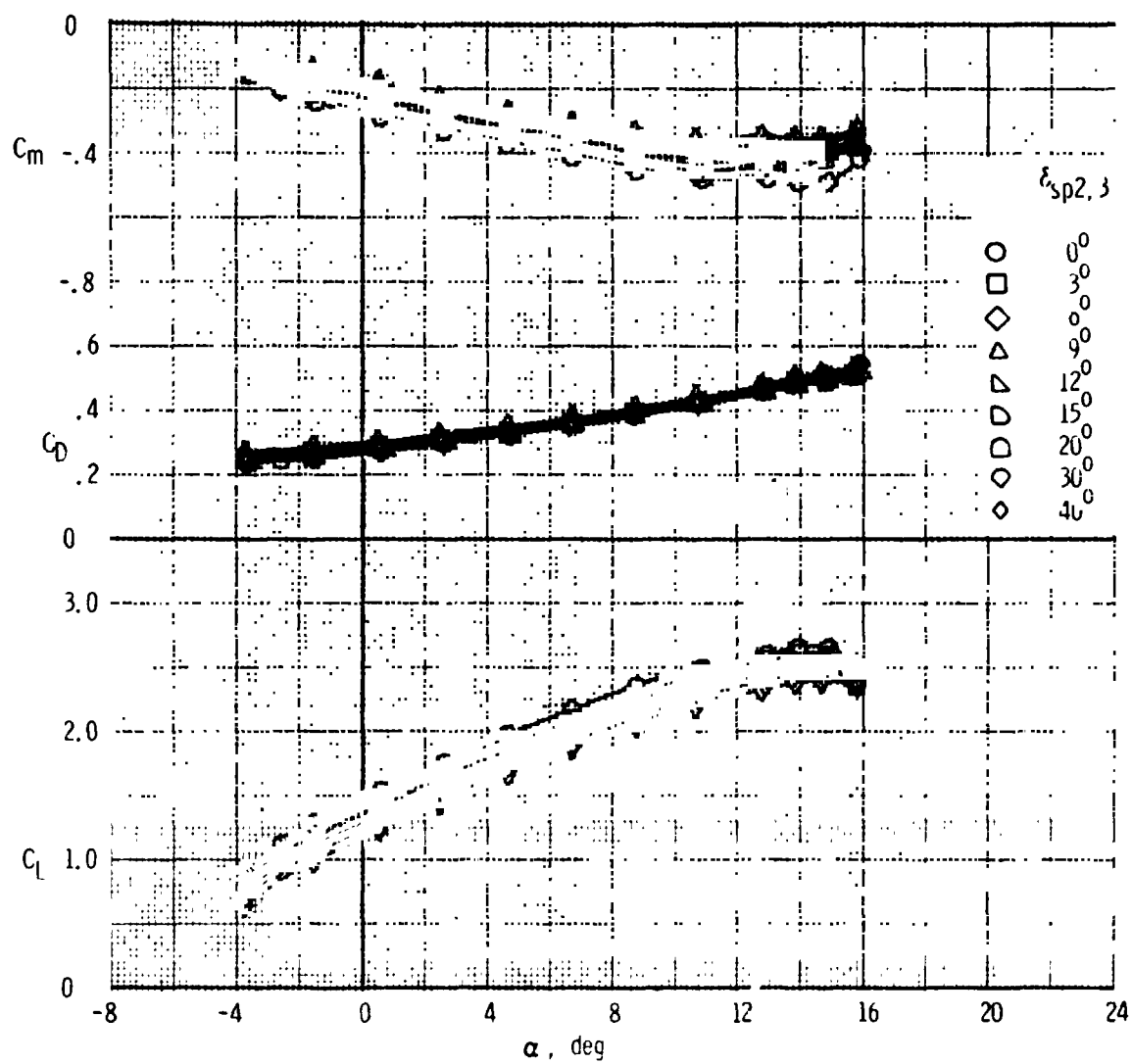
Figure 33. - Continued.

REPRODUCIBILITY OF THE
ORIGINAL PAGE IS POOR



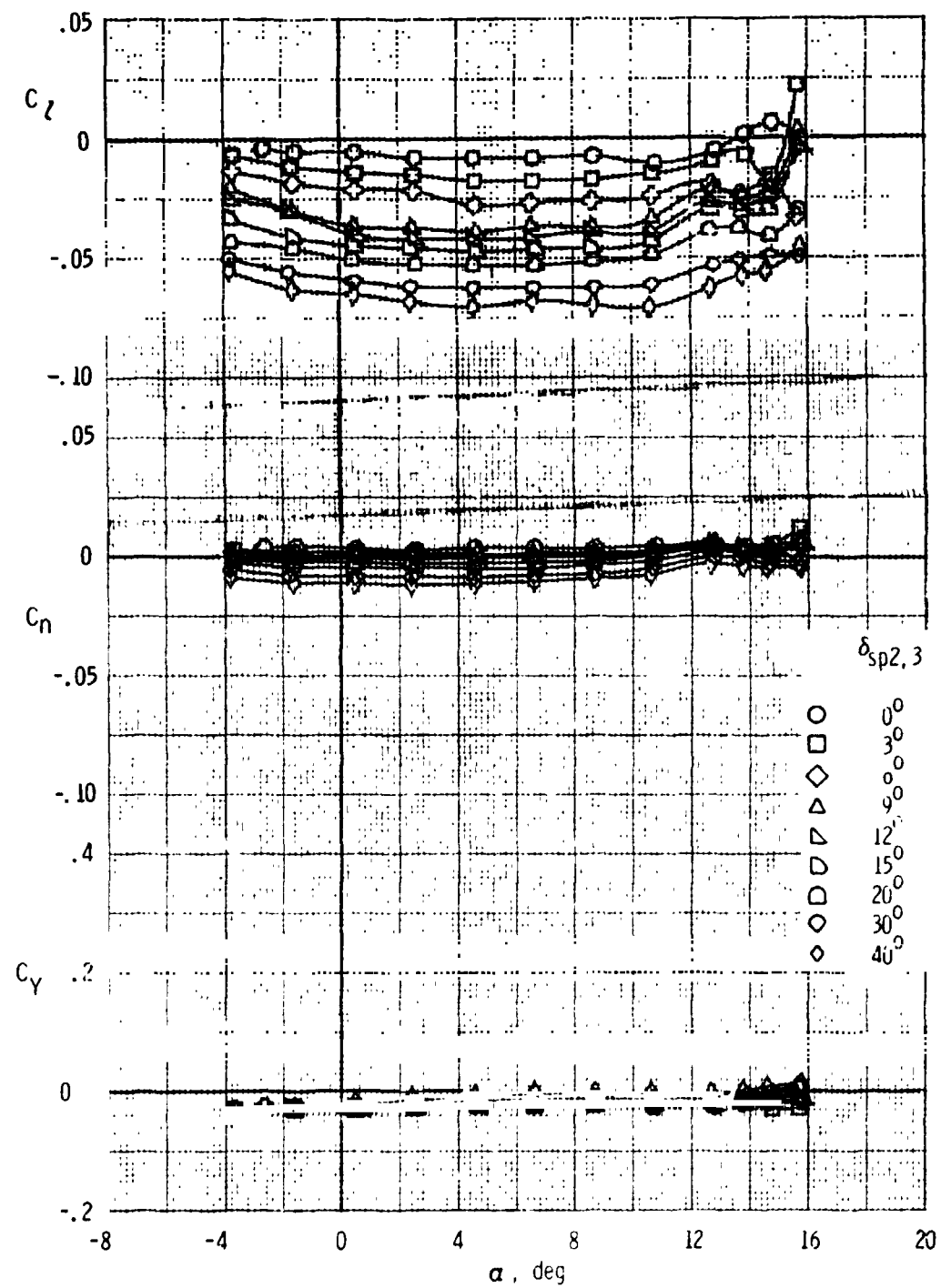
(d) Lateral directional characteristics, $\delta_{sp6,7,8} = 60^\circ$

Figure 33. - Concluded.



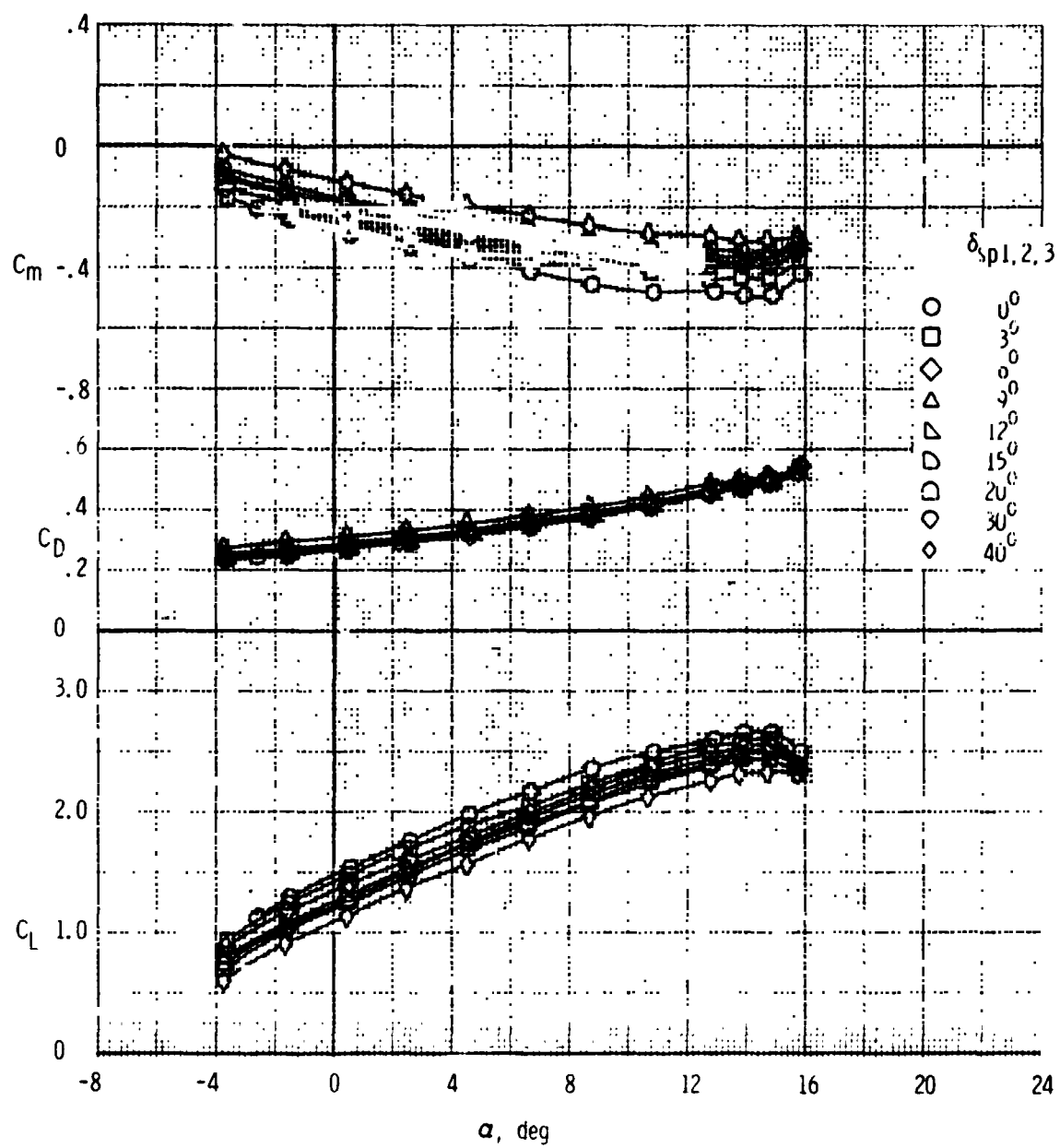
(a) Longitudinal characteristics, $\delta_{sp6,7} = 0^\circ$

Figure 34. - Effect of flight spoiler deflection on the aerodynamic characteristics of the $F, W, F_{40}, N, G, H_T, V_T$ configuration.

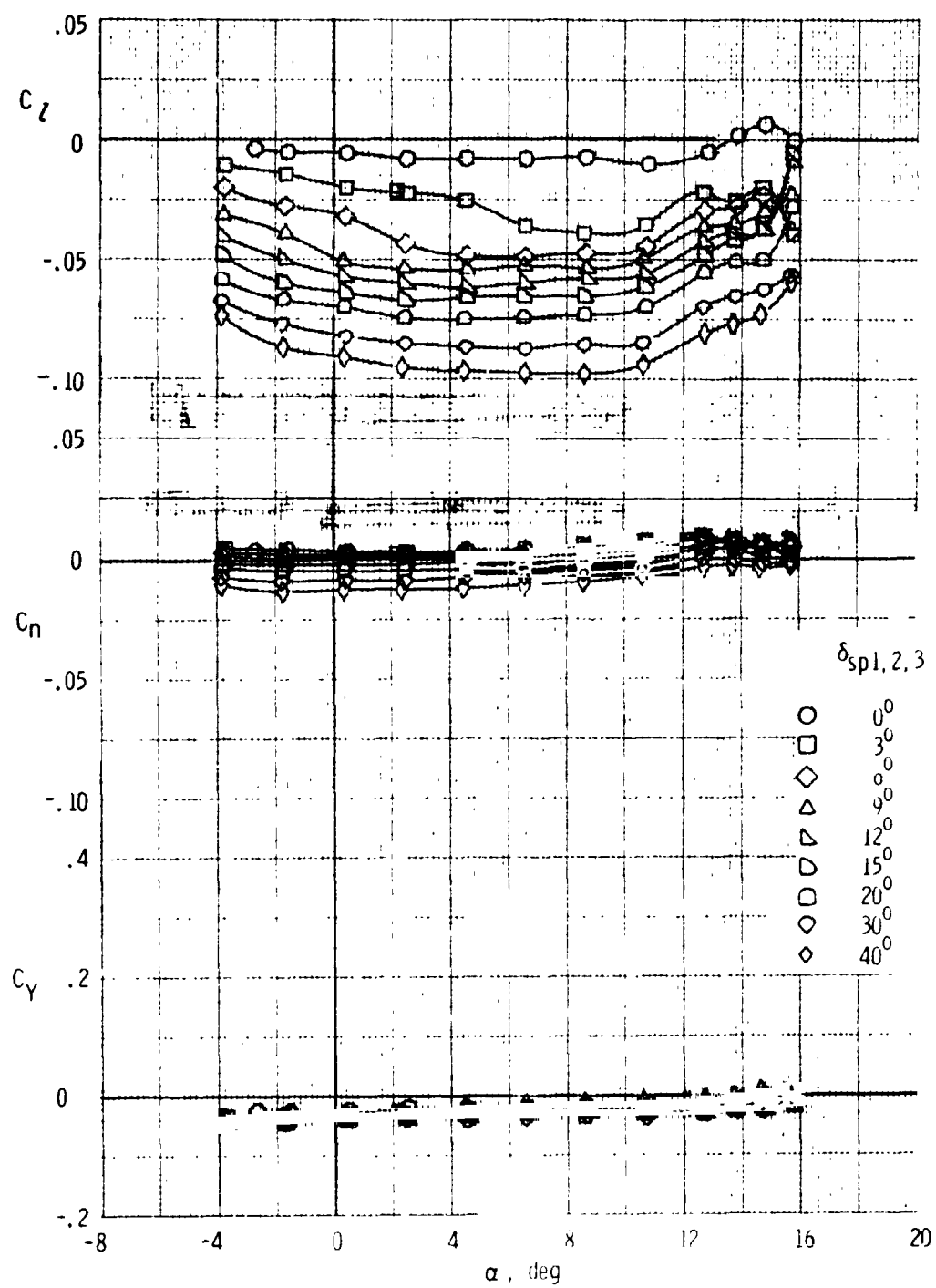


(b) Lateral-directional characteristics, $\delta_{sp6,7} = 0^\circ$

Figure 34. - Continued.

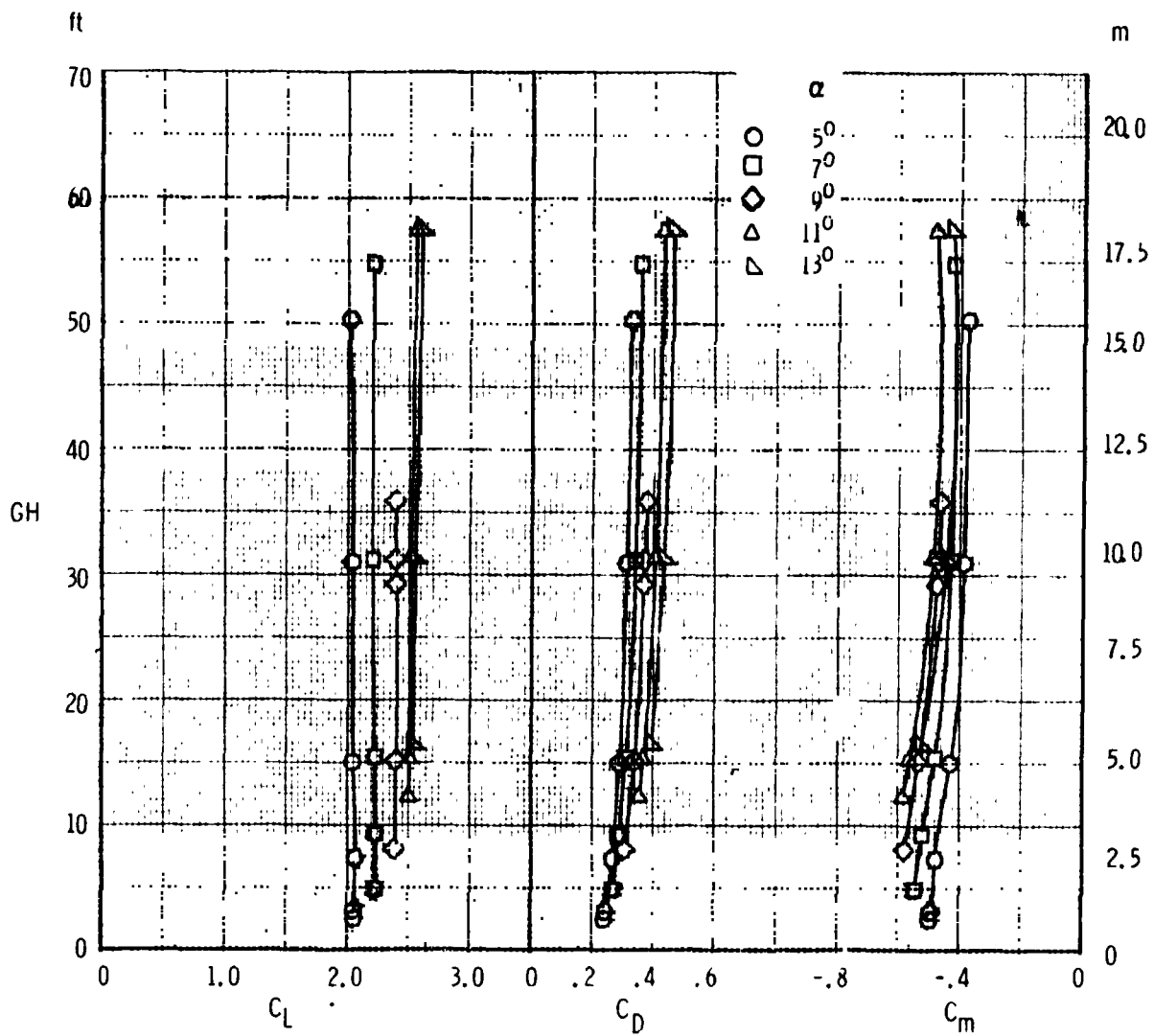


(c) Longitudinal characteristics, $\delta_{sp6,7,8} = 0^\circ$
Figure 34. - Continued.



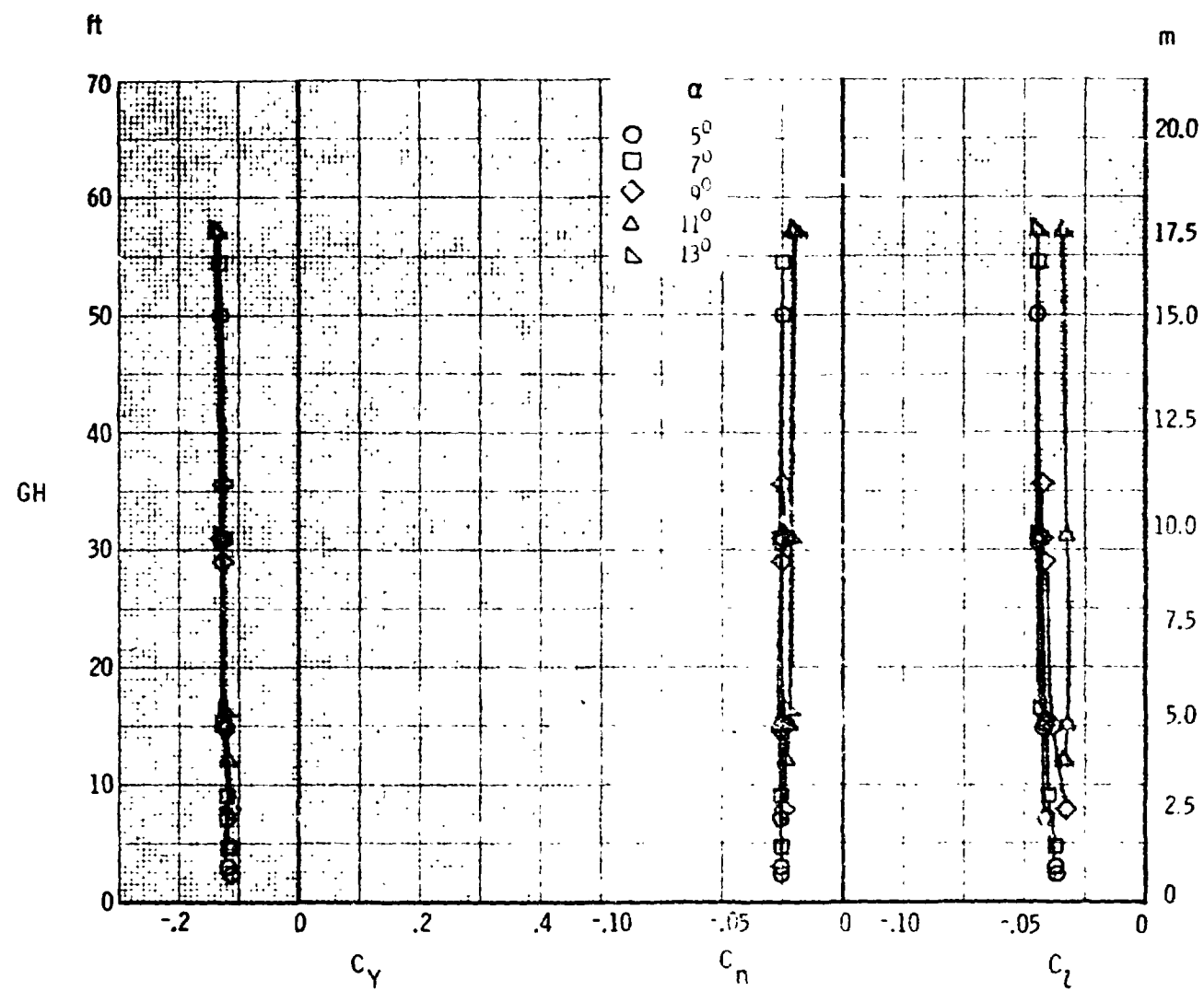
(d) Lateral-directional characteristics, $\delta_{sp6,7,8} = 0^\circ$

Figure 34. - Concluded.



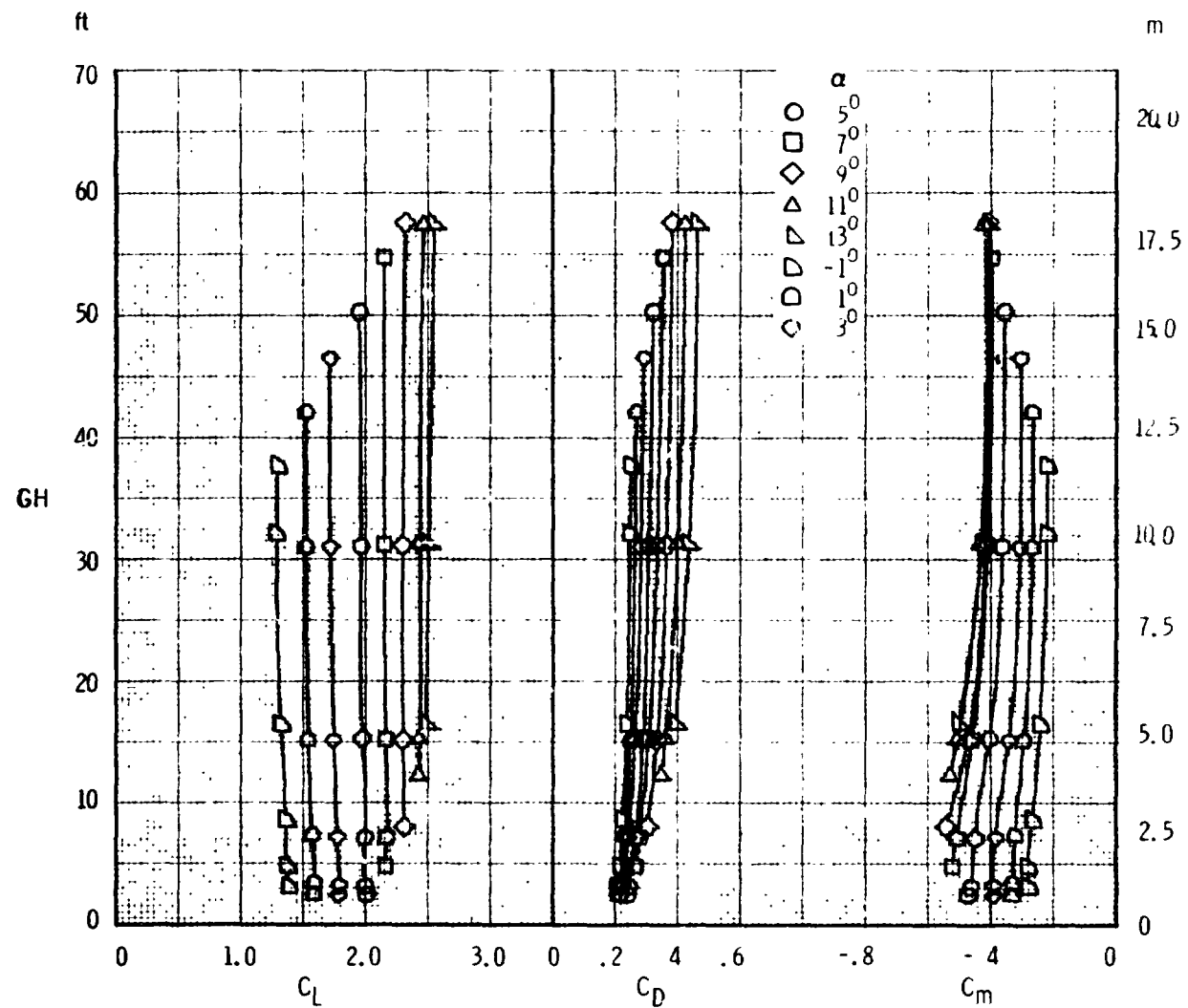
(a) Longitudinal characteristics, $\delta_{sp2,3} = 3^\circ$

Figure 35. - Effect of ground height on the aerodynamic characteristics of the $F, W, F_{40}, N, G, H_T, V_T$ configuration with flight spoilers deflected.



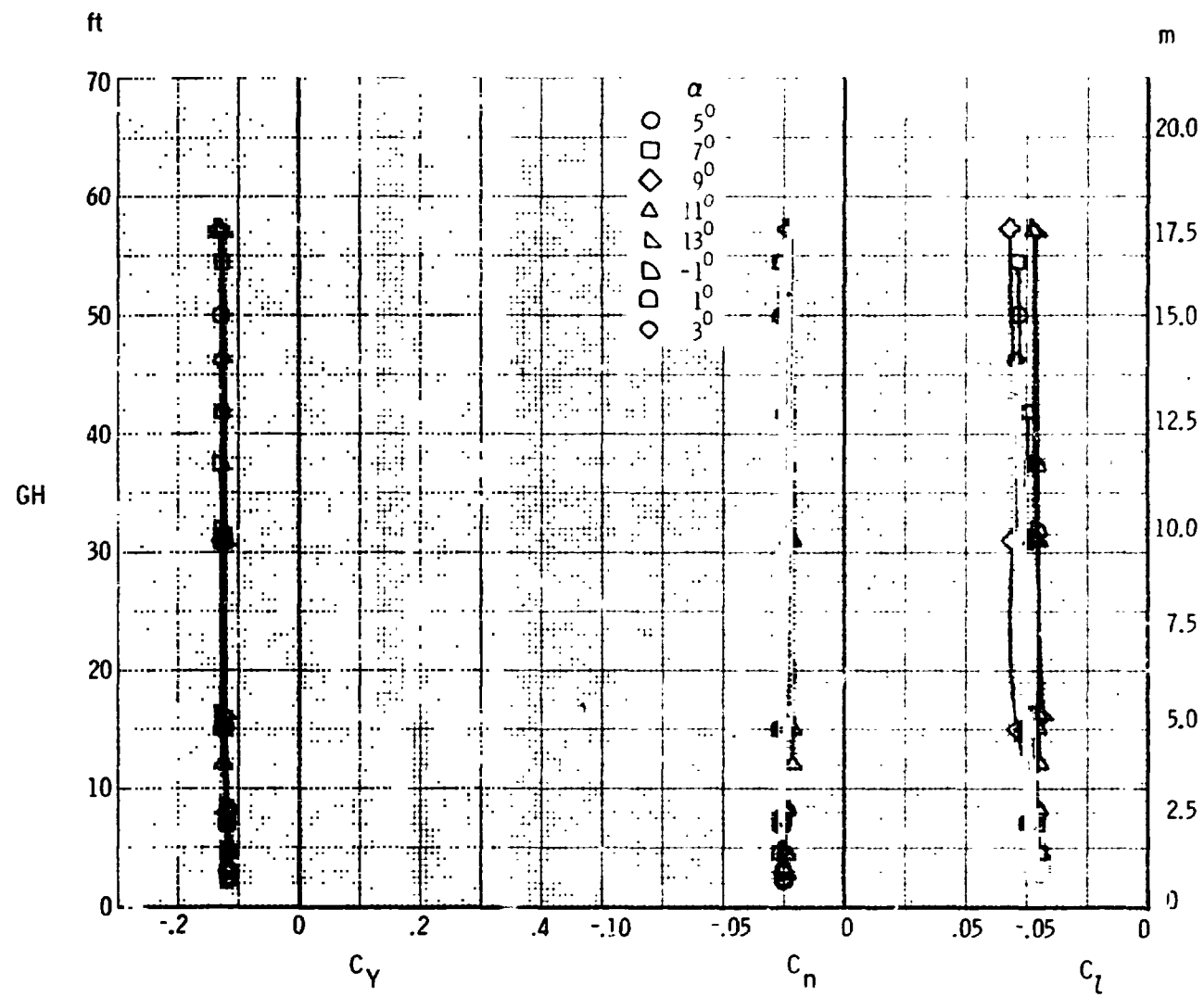
(b) Lateral-directional characteristics, $\delta_{sp2,3} = 3^\circ$

Figure 35. - Continued.



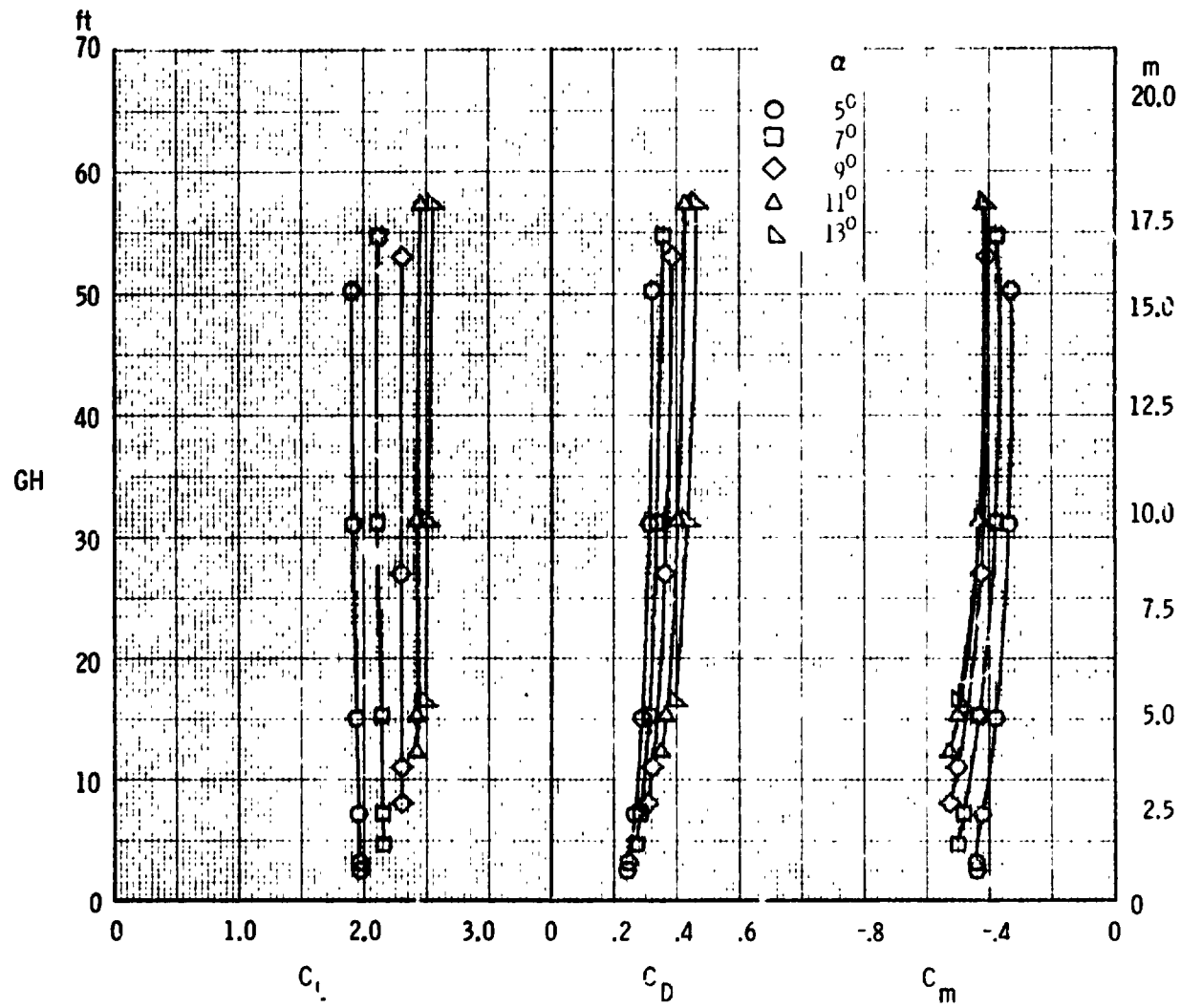
(c) Longitudinal characteristics, $\delta_{sp2,3} = 6^\circ$

Figure 35. - Continued.



(d) Lateral-directional characteristics, $\delta_{sp2,3} = 6^\circ$

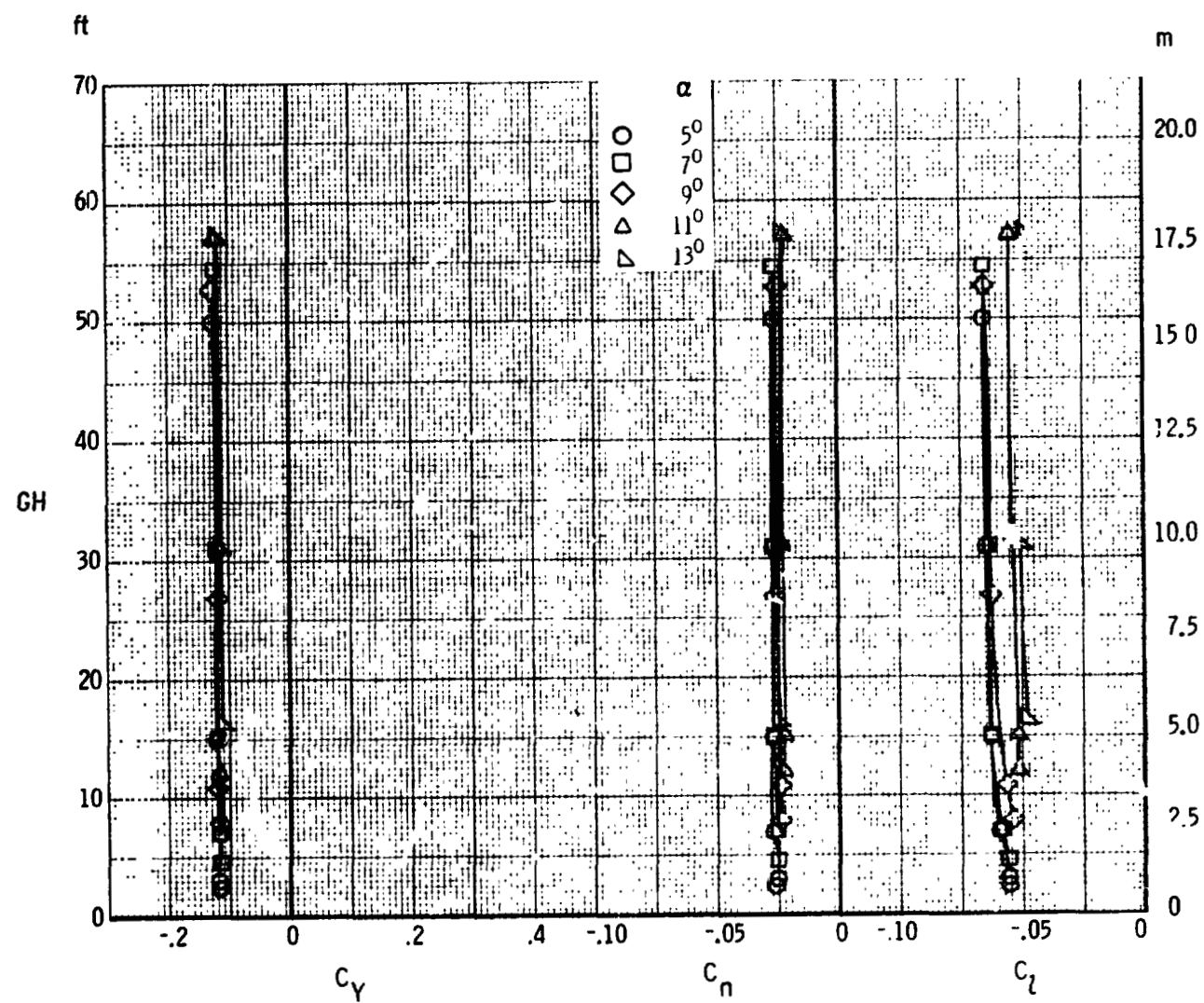
Figure 35. - Continued.



(e) Longitudinal characteristics, $\delta_{sp2,3} = 90^\circ$

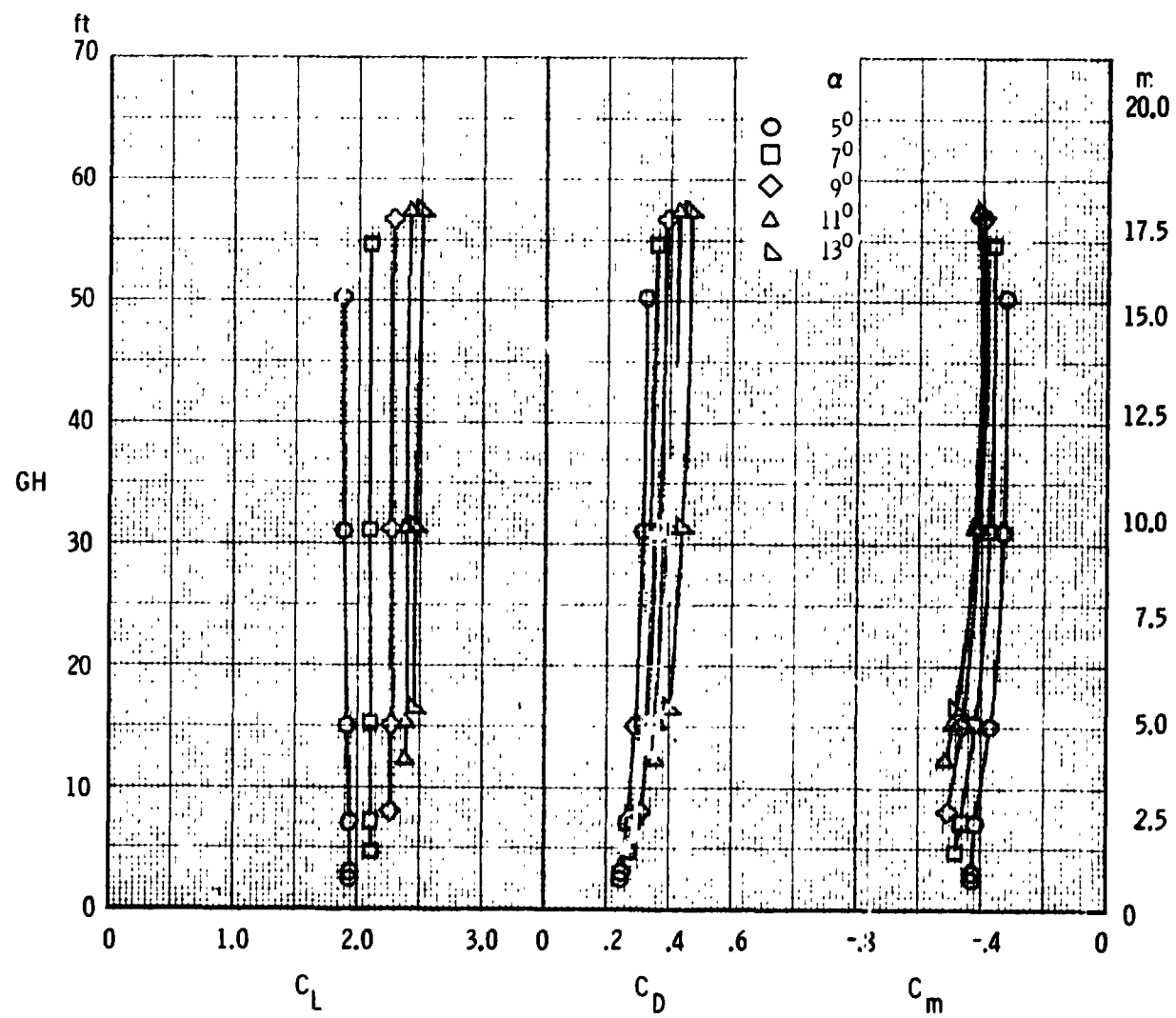
Figure 35. - Continued.

REPRODUCIBILITY OF THE
ORIGINAL PAGE IS POOR

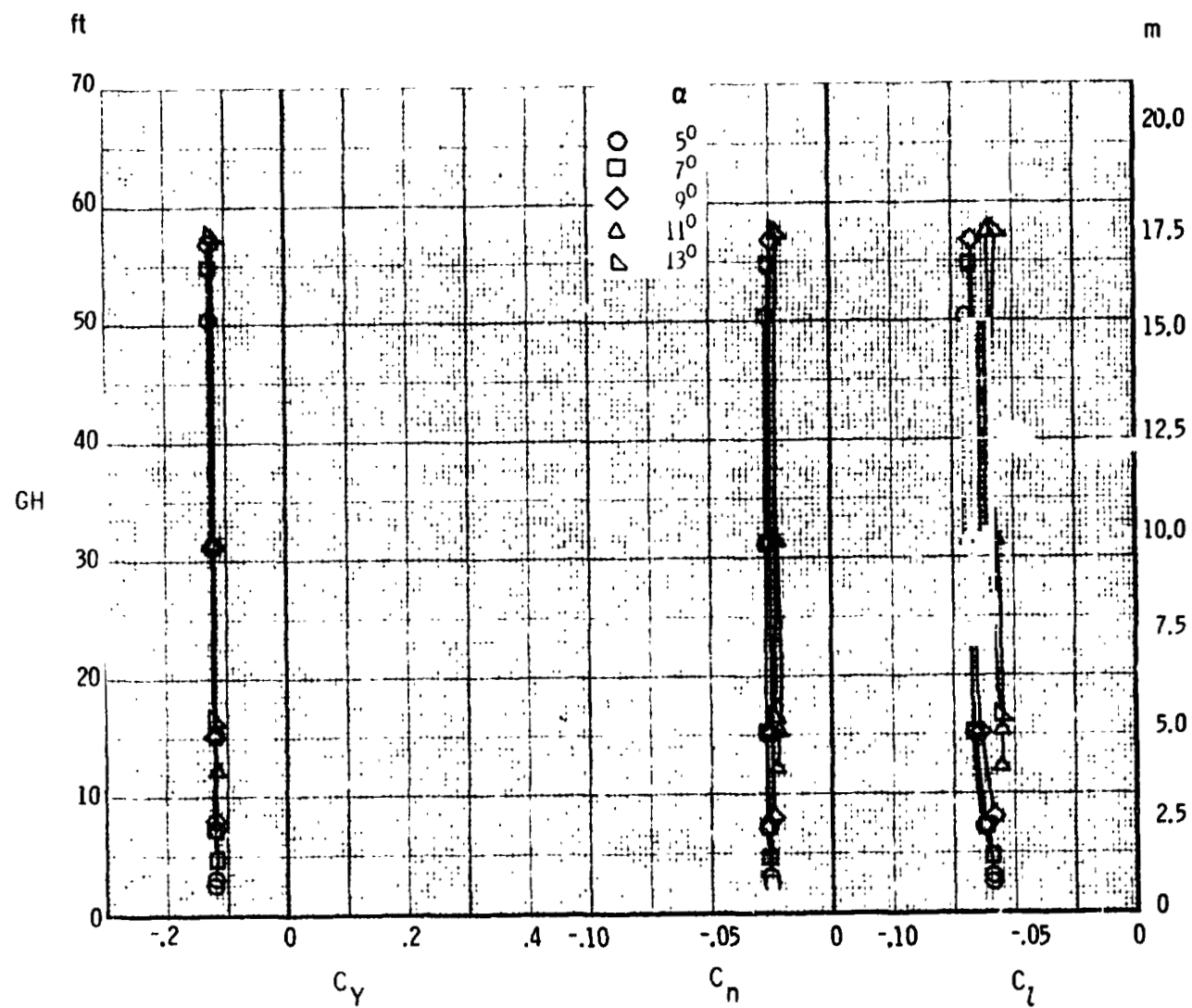


(f) Lateral-directional characteristics, $\delta_{sp2,3} = 9^\circ$

Figure 35. - Continued.

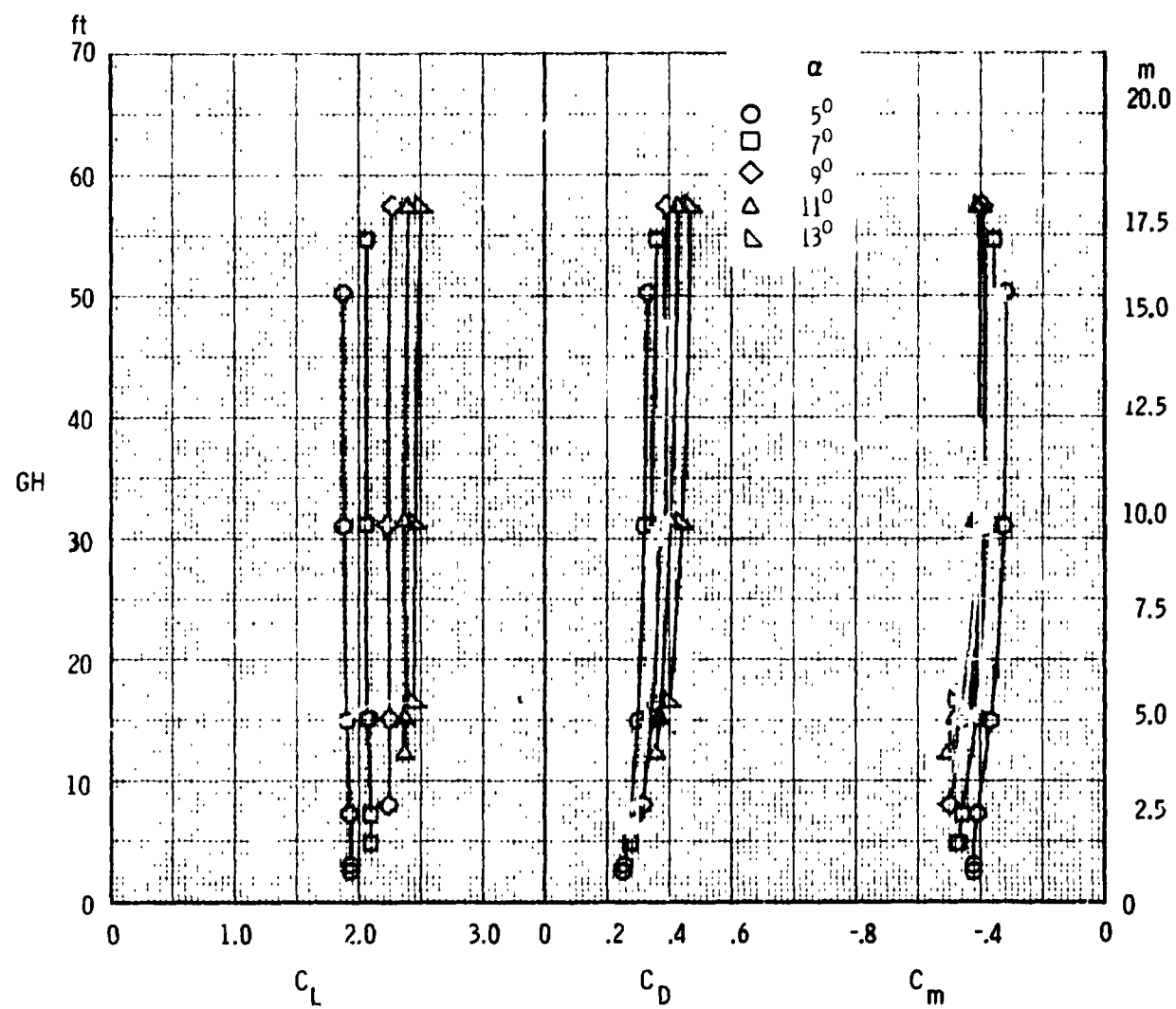


(g) Longitudinal characteristics, $\delta_{sp2,3} = 12^\circ$
Figure 35. - Continued.

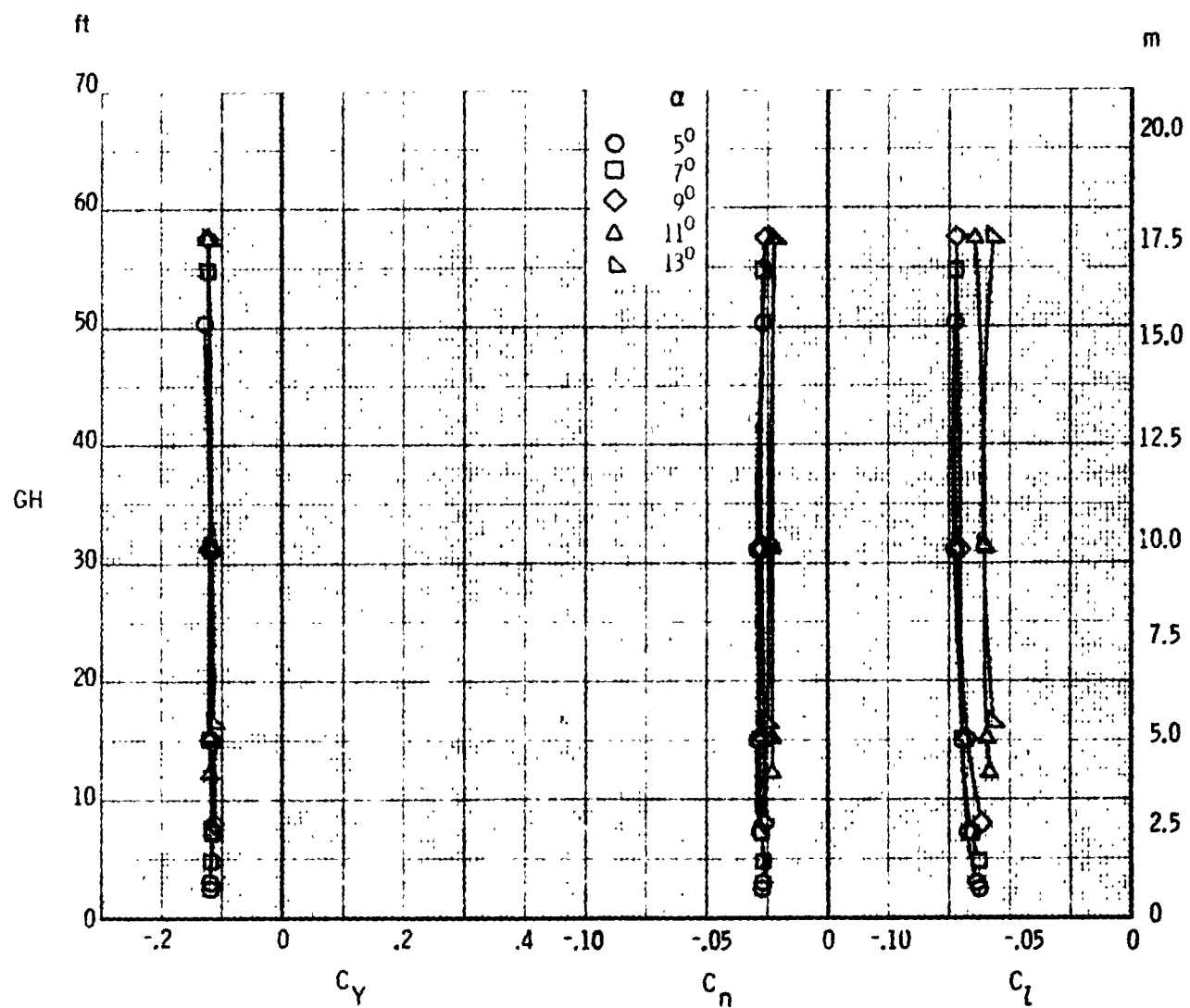


(h) Lateral-directional characteristics, $\delta_{sp2,3} = 12^\circ$

Figure 35. - Continued.

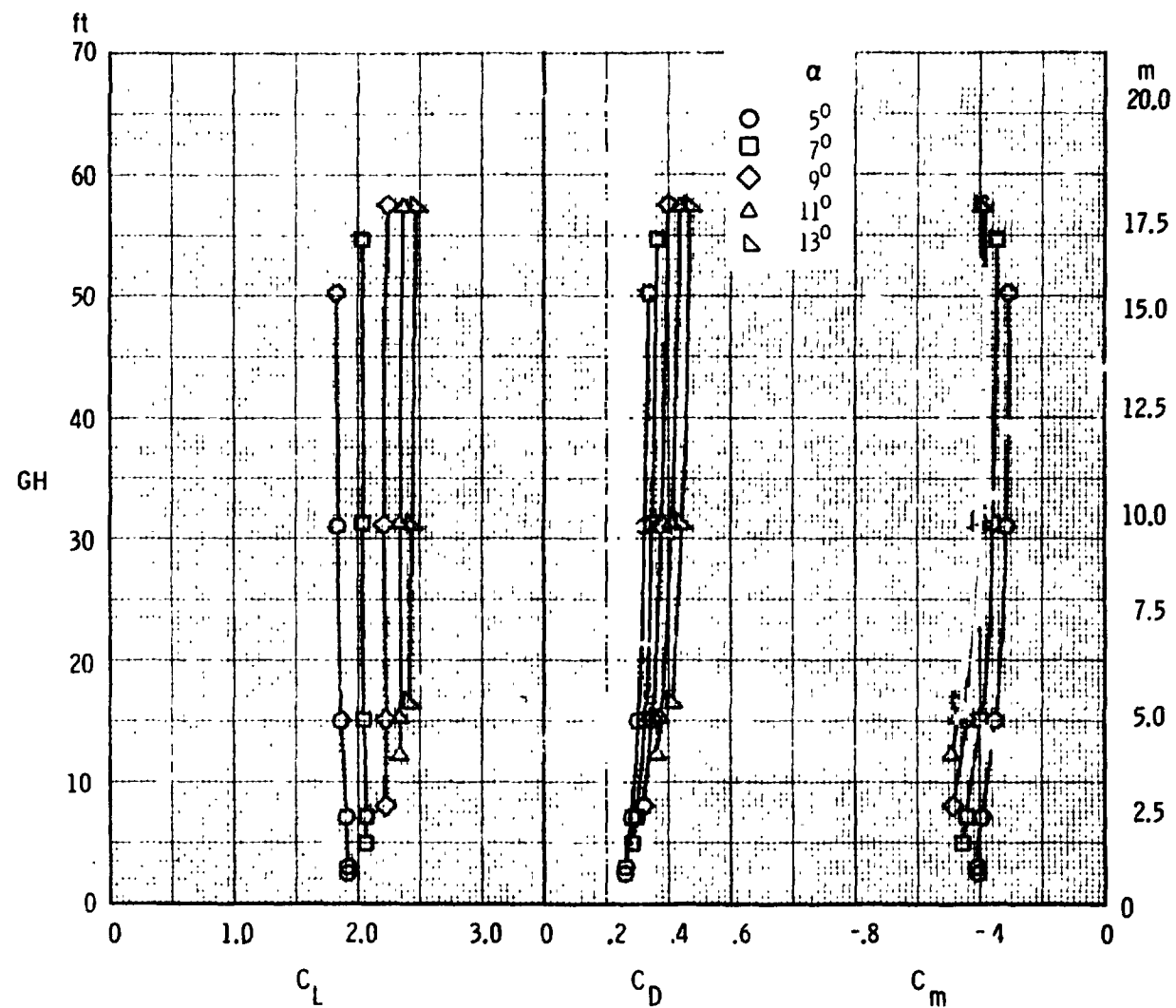


(i) Longitudinal characteristics, $\delta_{sp2,3} = 15^\circ$
 Figure 35. - Continued.



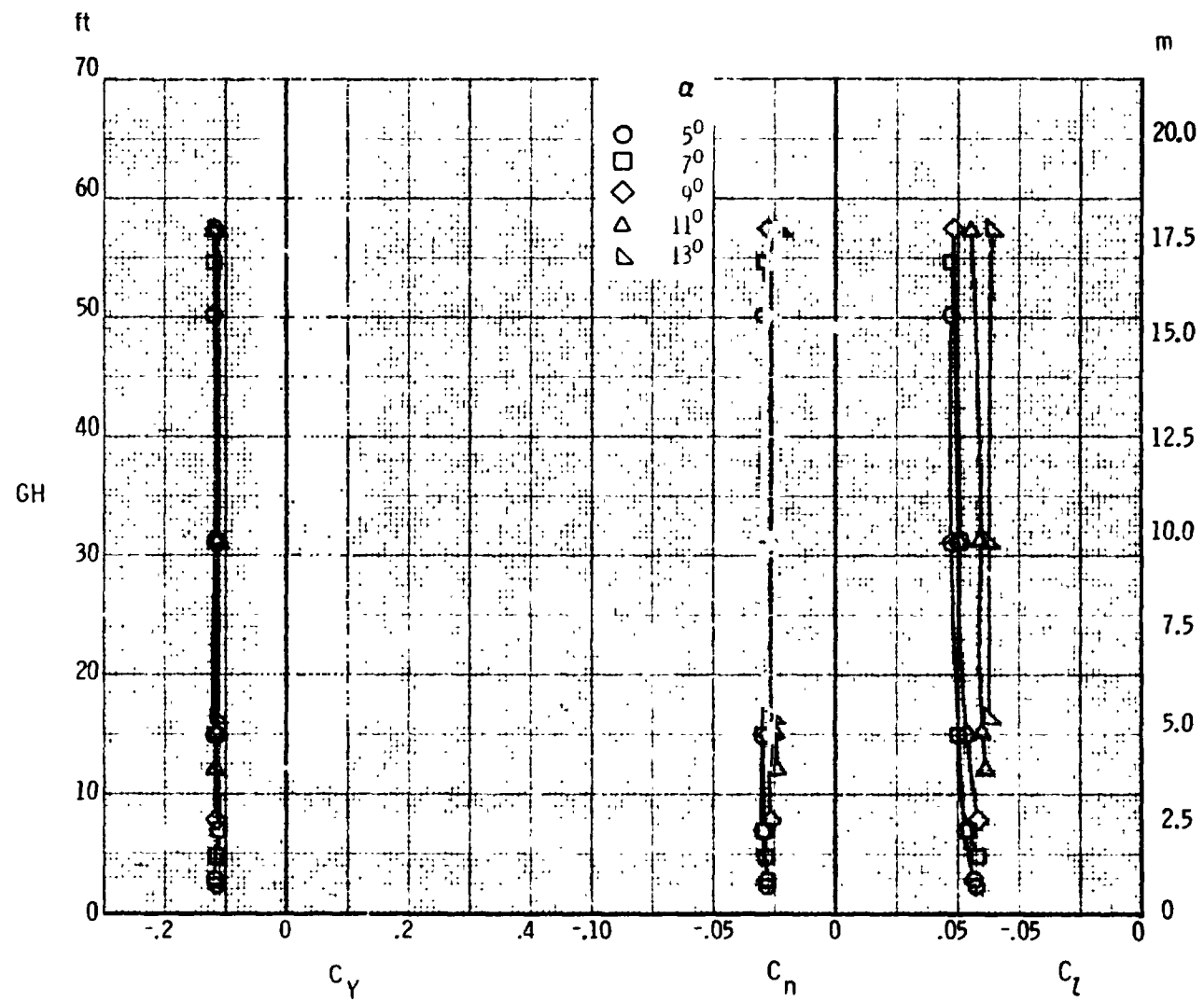
(j) Lateral-directional characteristics, $\delta_{sp2,3} = 15^\circ$

Figure 35. - Continued.



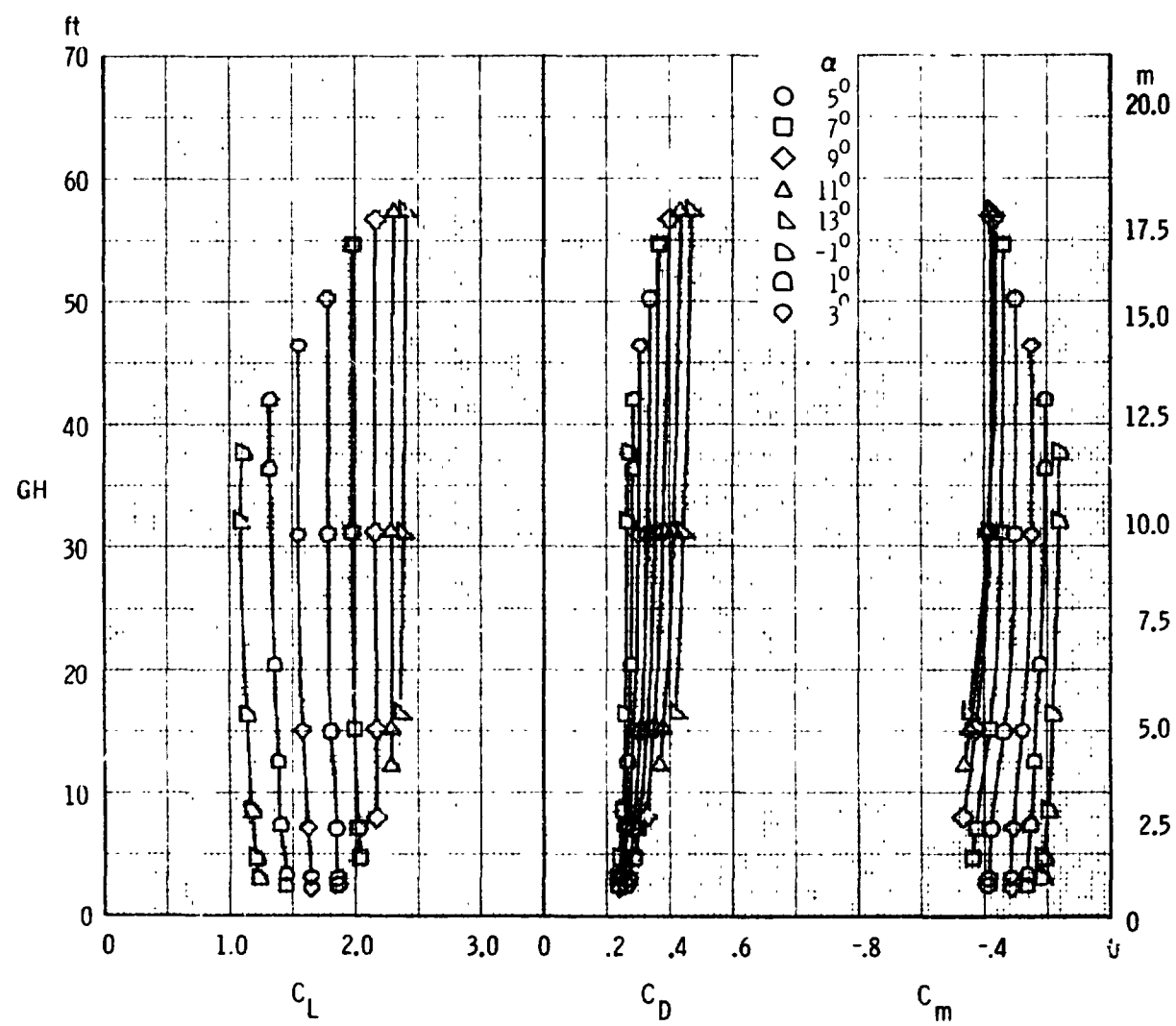
(k) Longitudinal characteristics, $\delta_{sp2,3} = 20^\circ$

Figure 35. - Continued.



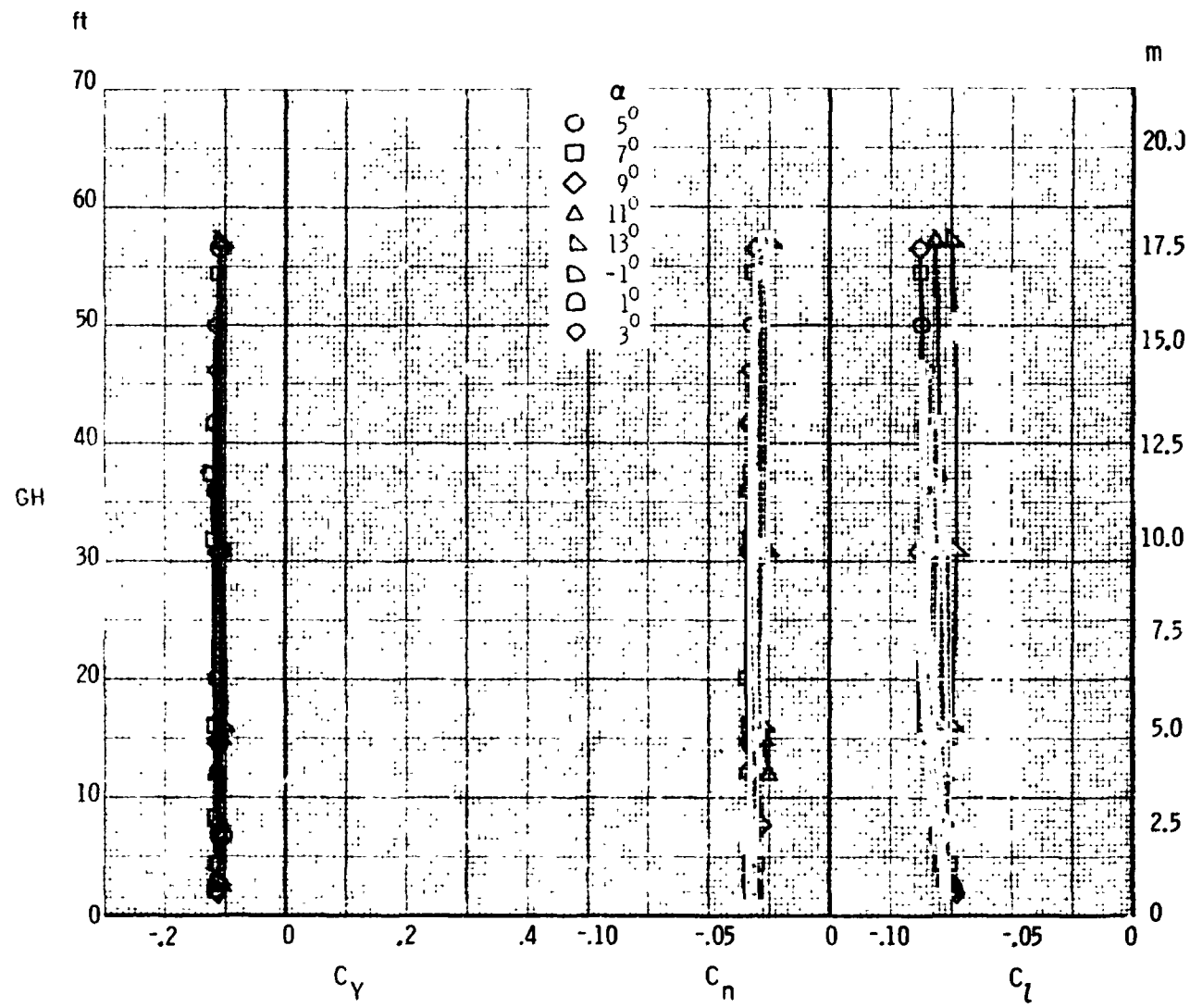
(I) Lateral-directional characteristics, $\delta_{sp2,3} = 20^\circ$

Figure 35. - Continued.



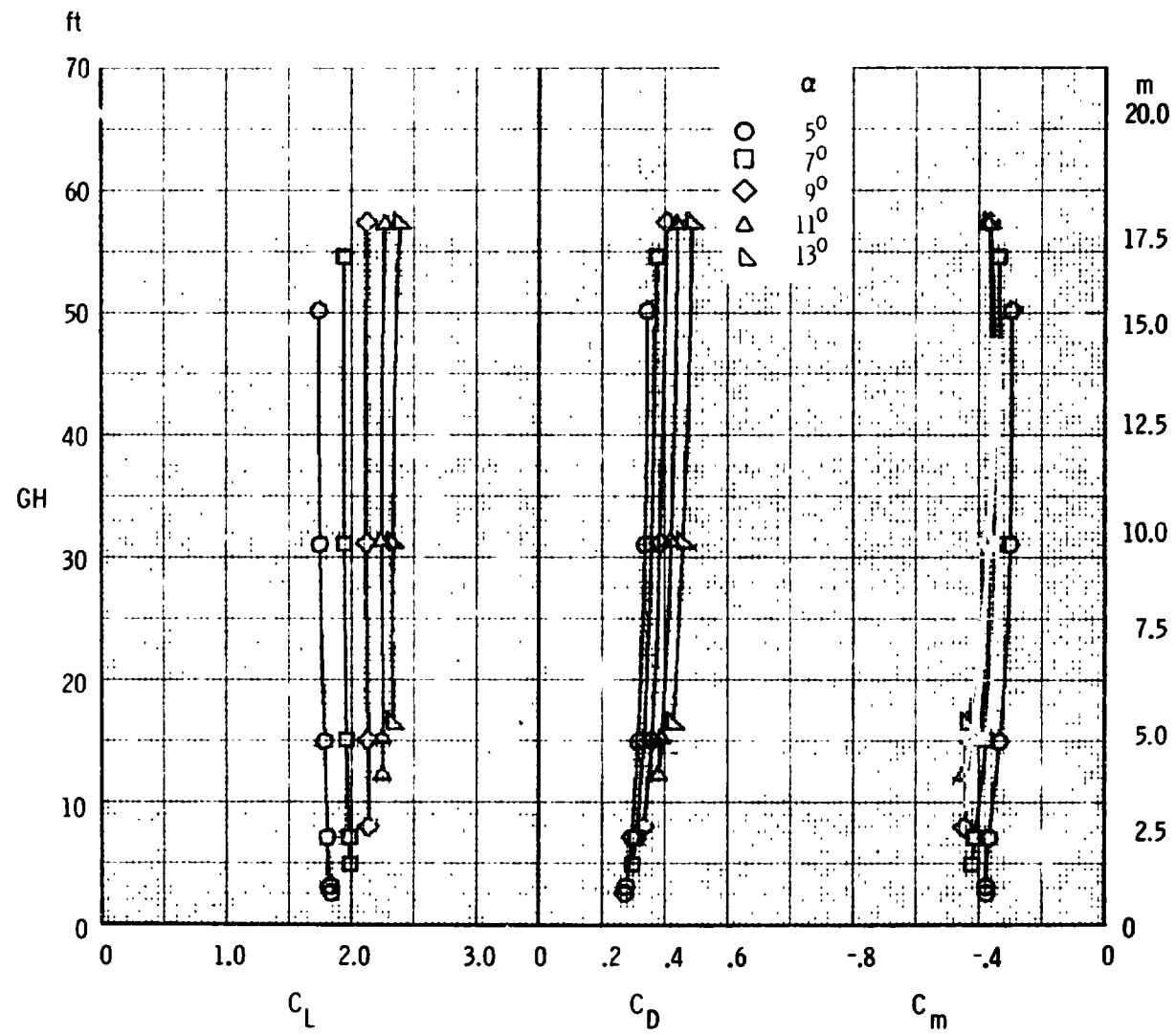
(m) Longitudinal characteristics, $\delta_{sp2,3} = 30^\circ$

Figure 35. - Continued.



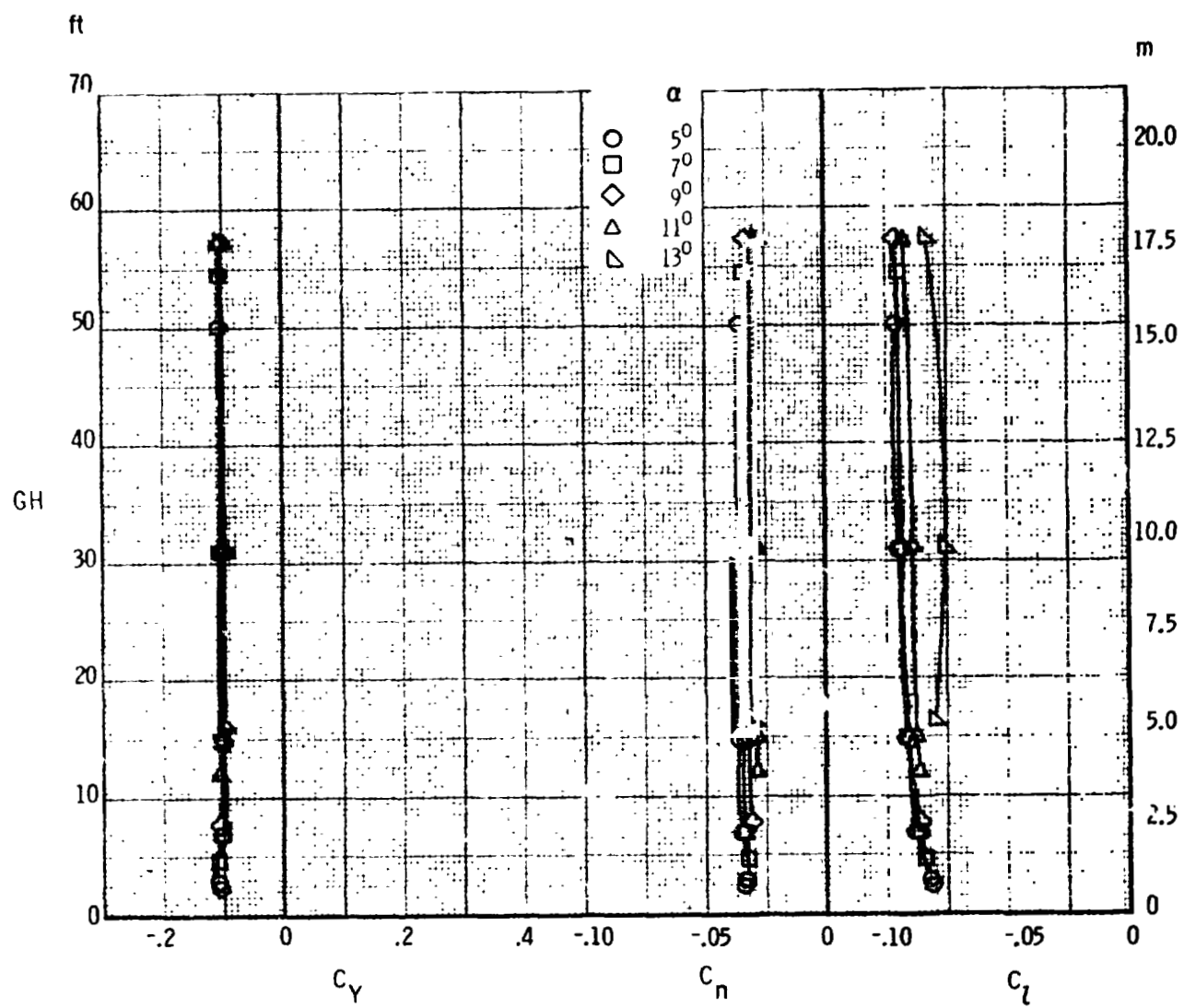
(n) Lateral-directional characteristics, $\delta_{sp2,3} = 30^\circ$

Figure 35. - Continued.



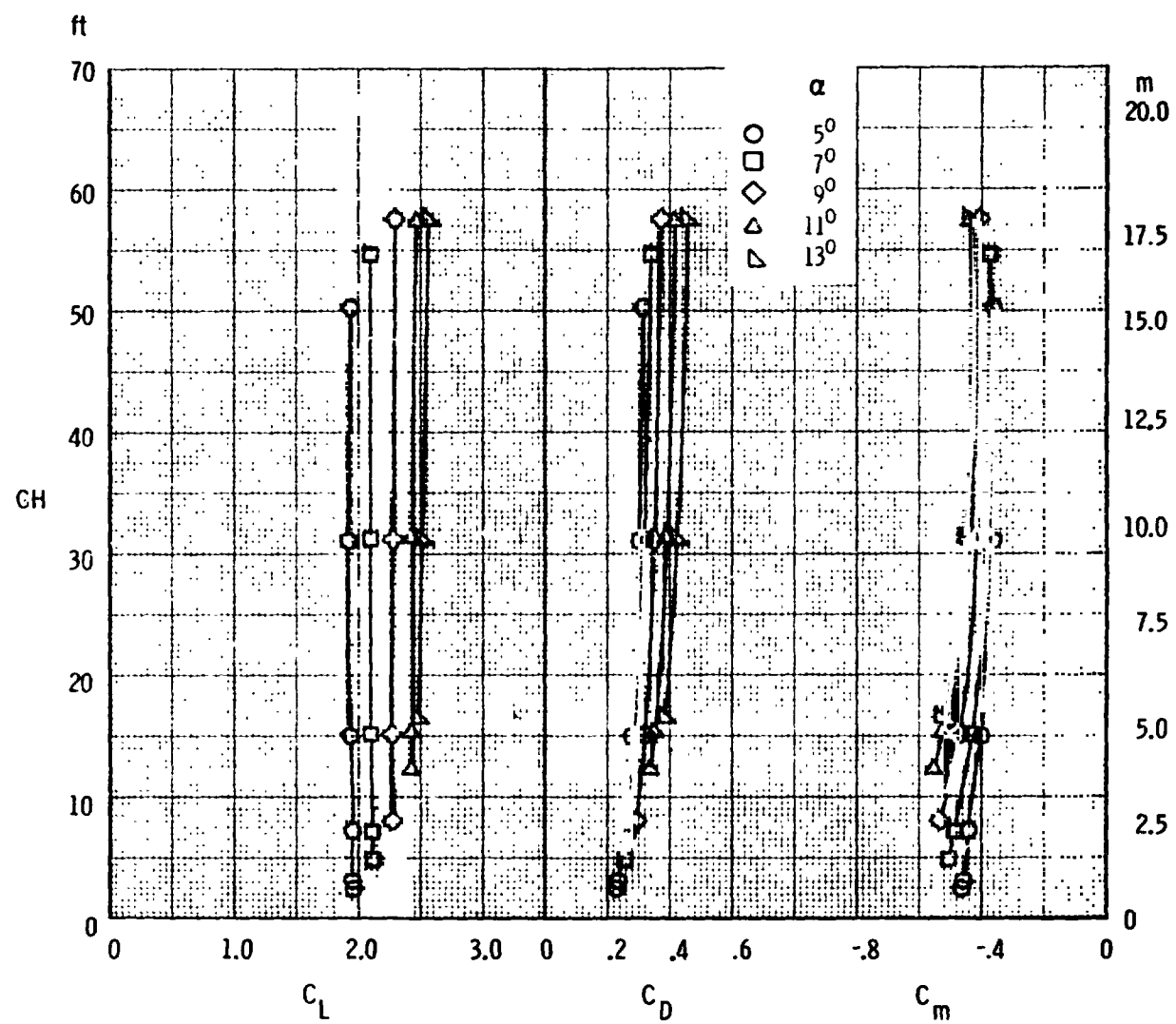
(c) Longitudinal characteristics, $\delta_{sp2,3} = 40^\circ$

Figure 35. - Continued.



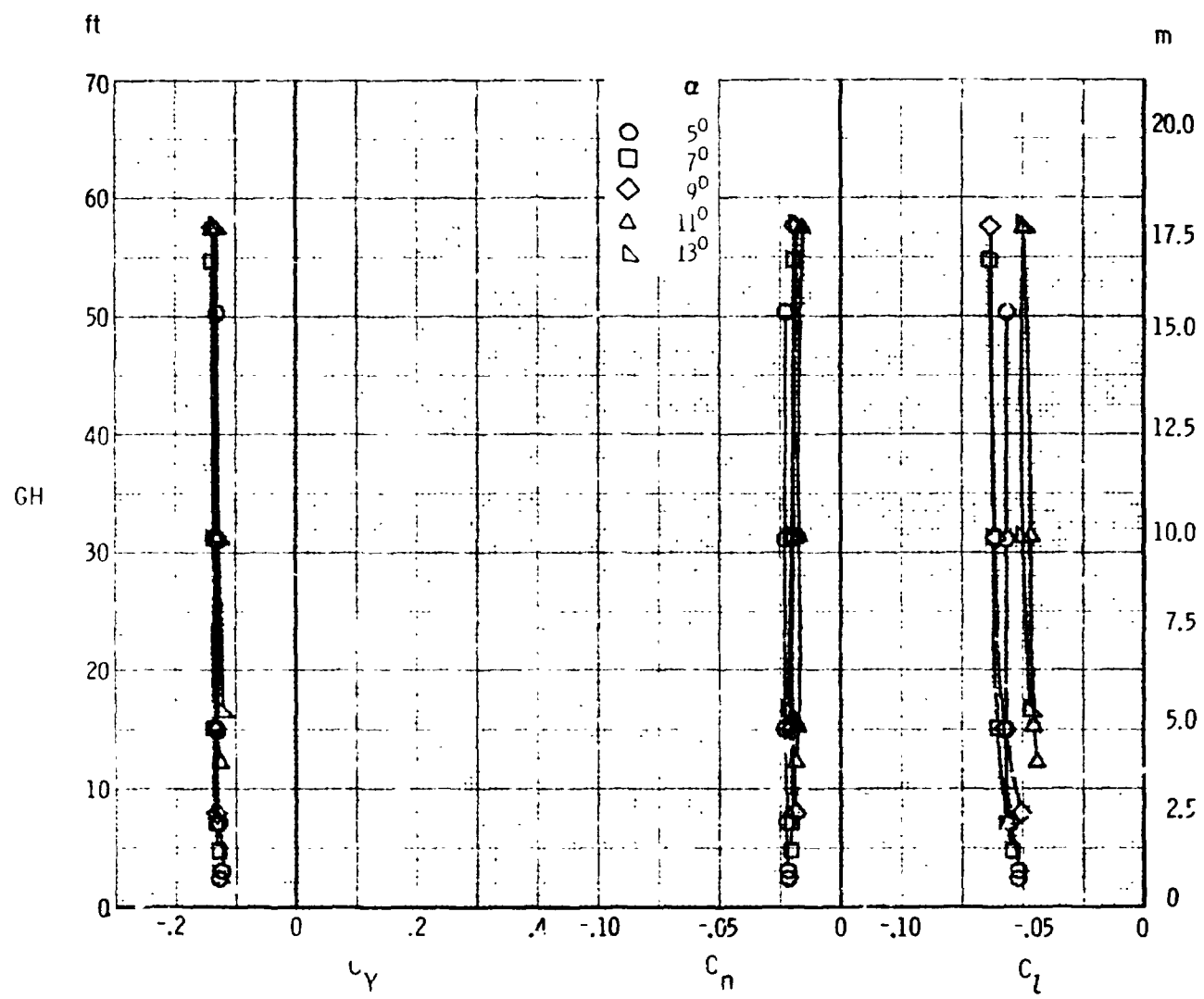
(p) Lateral-directional characteristics, $\delta_{sp2,3} = 40^\circ$

Figure 35. - Concluded.



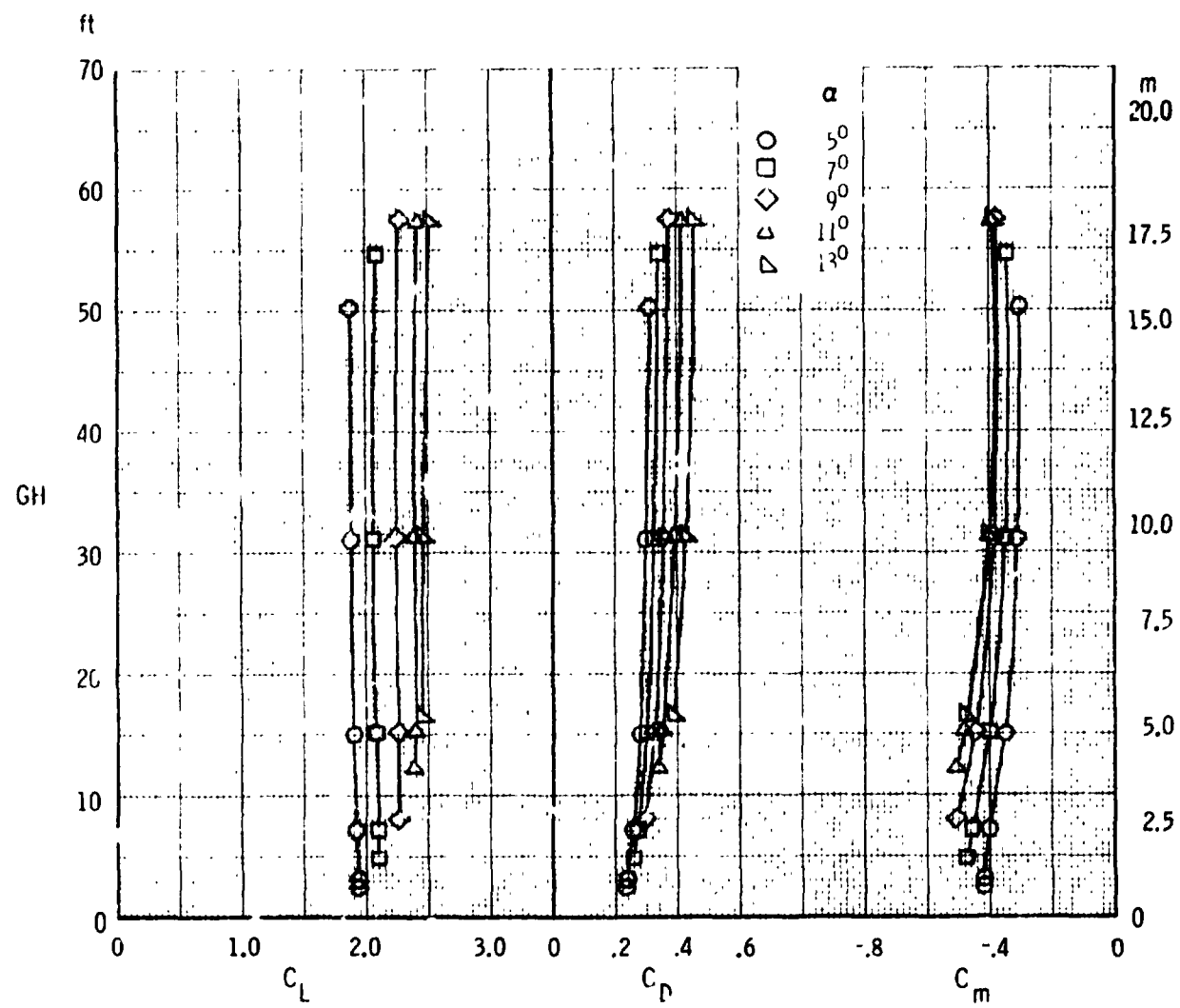
(q) Longitudinal characteristics, $\delta_{sp1,2,3} = 3^\circ$

Figure 35. - Continued.



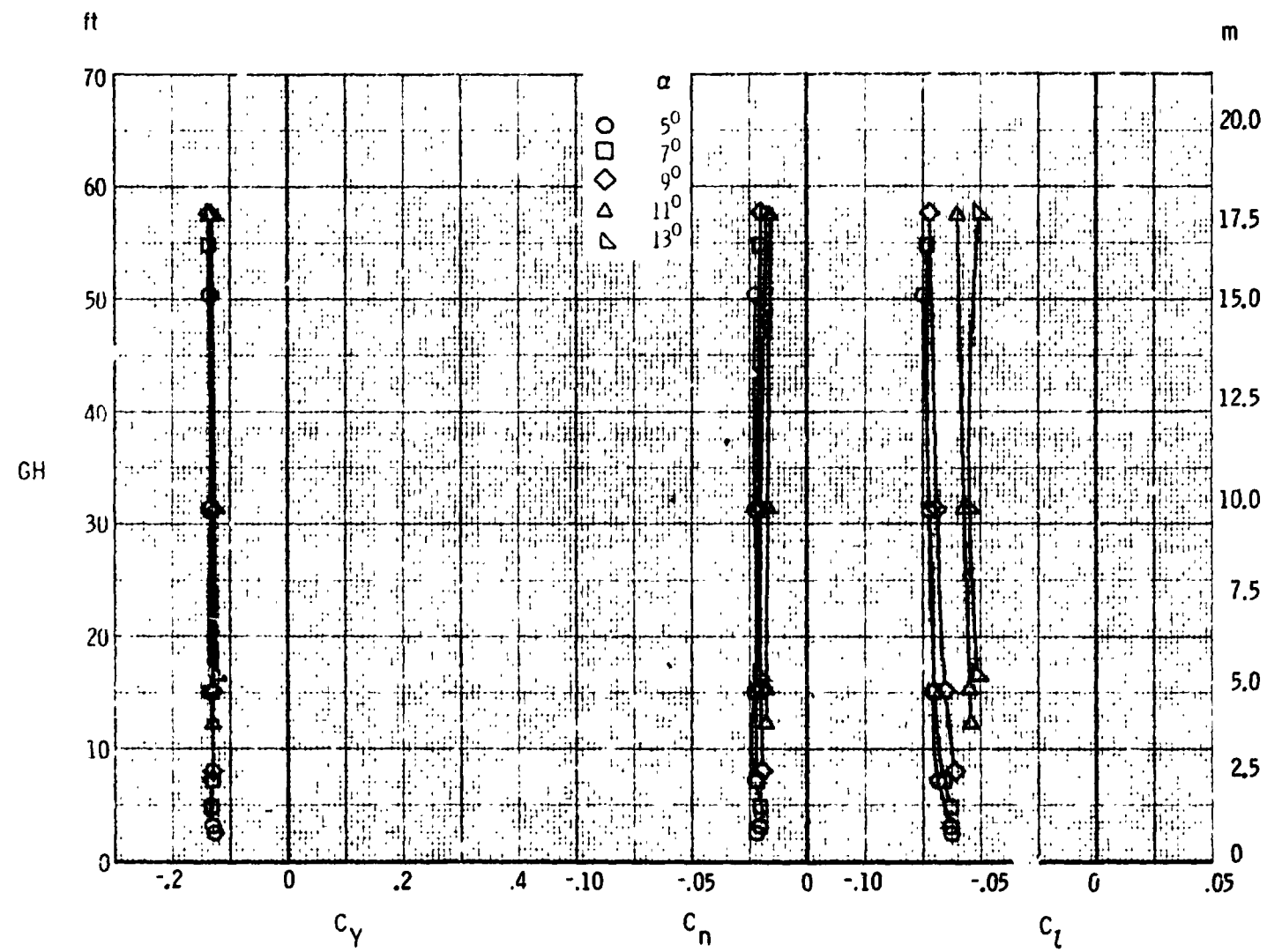
(r) Lateral-directional characteristics, $\delta_{sp1,2,3} = 3^\circ$

Figure 35. - Continued.



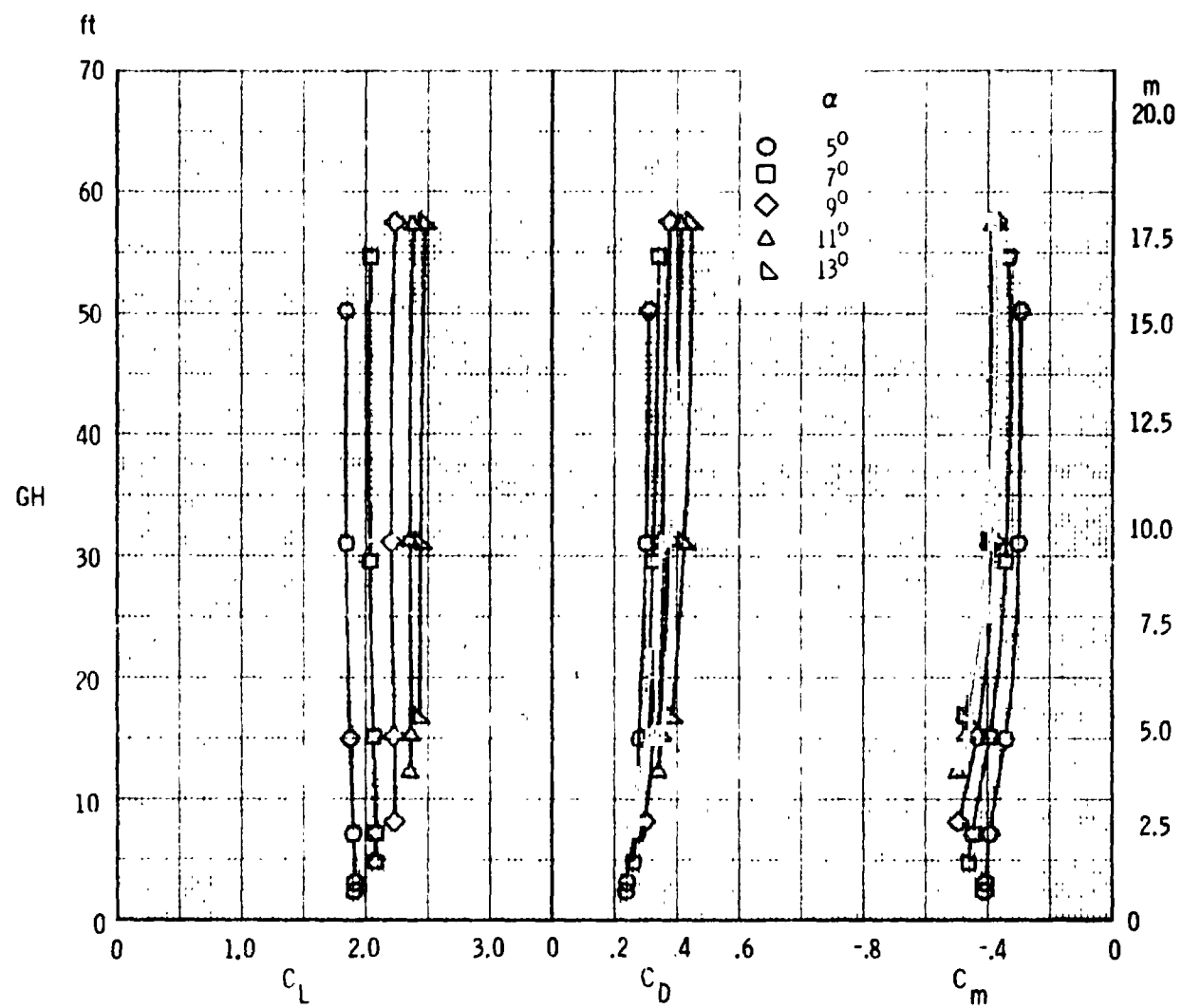
(s) Longitudinal characteristics, $\delta_{sp1,2,3} = 6^\circ$

Figure 35. - Continued.

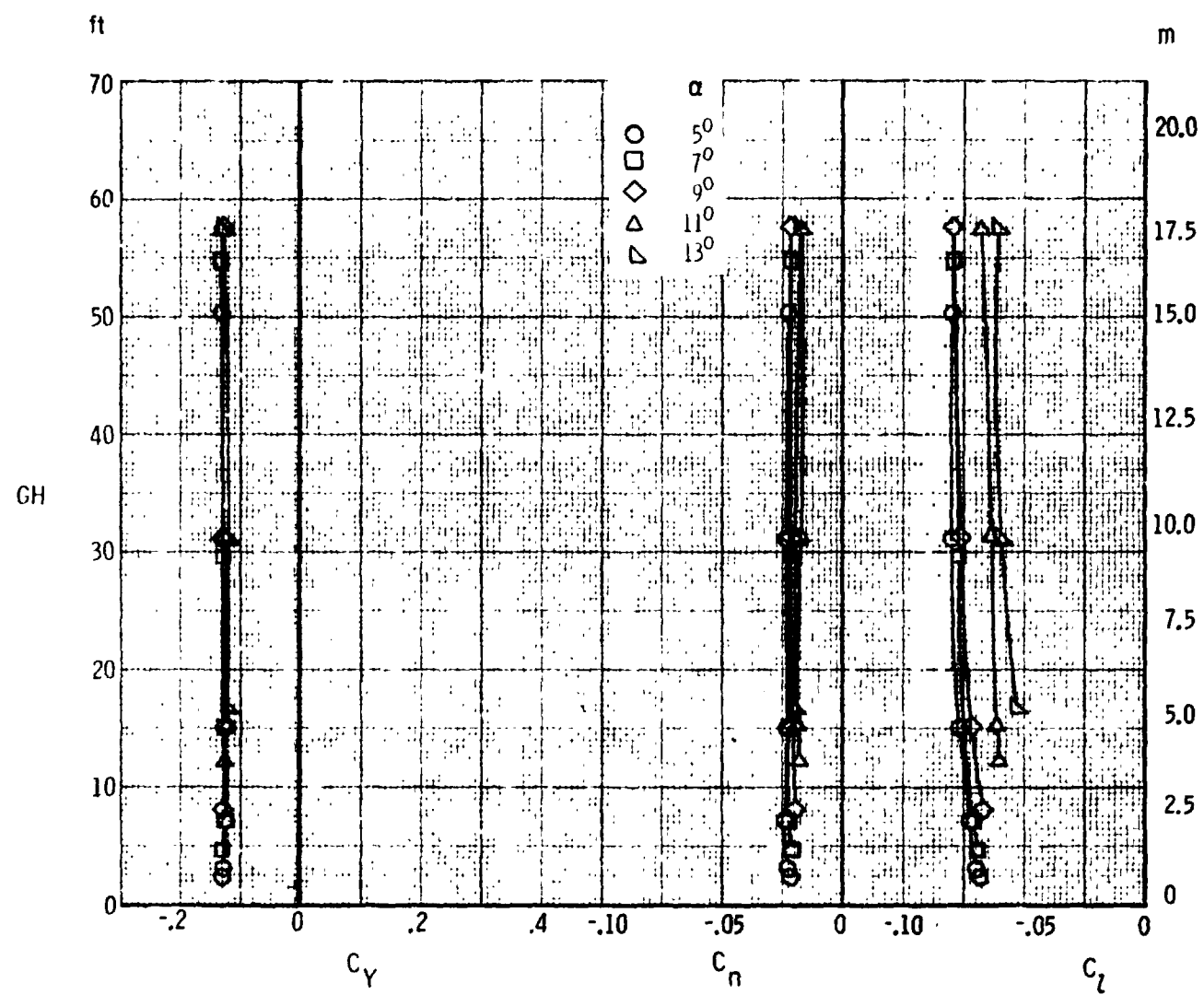


(f) Lateral-directional characteristics, $\delta_{sp1,2,3} = 6^\circ$

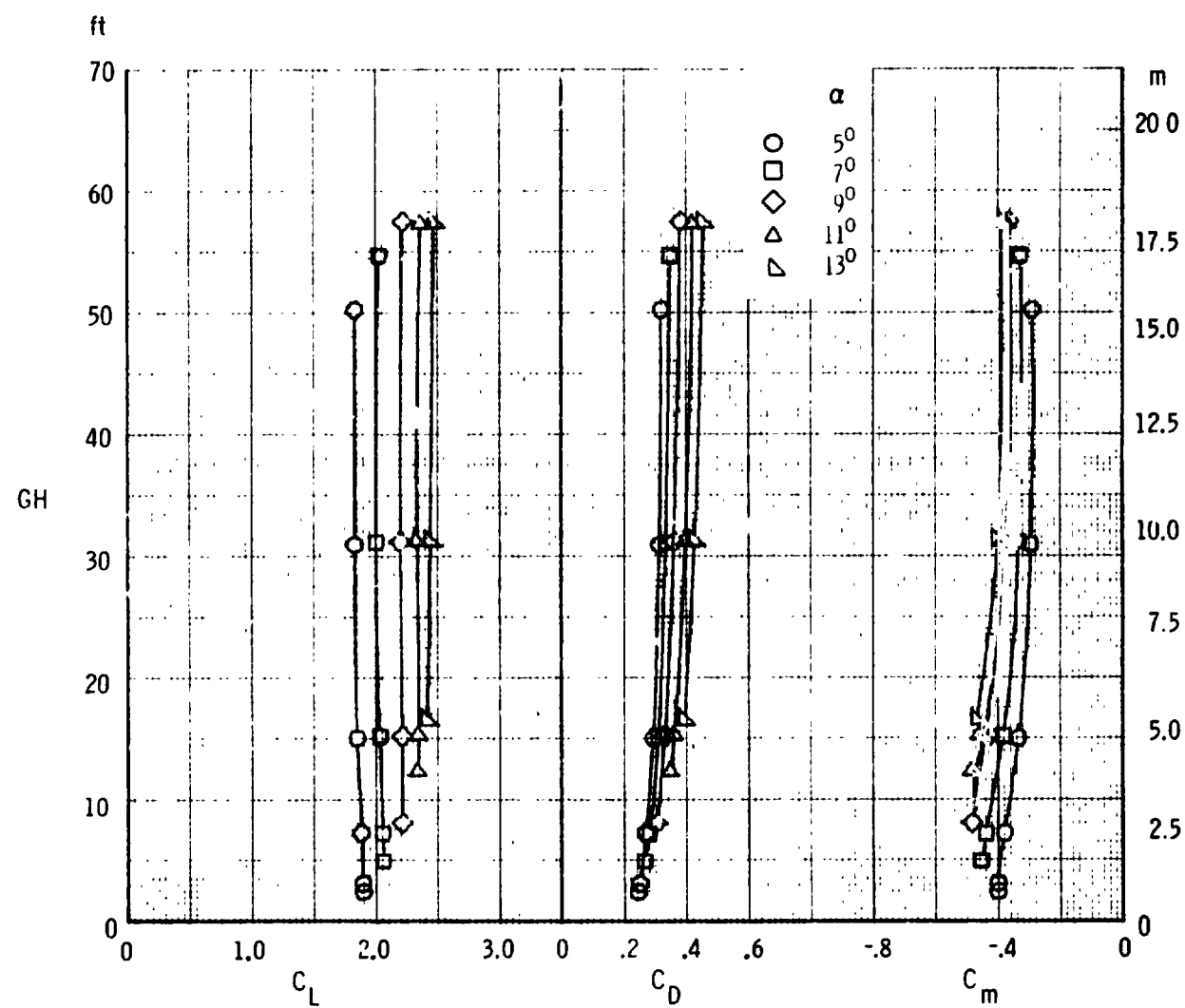
Figure 35. - Continued.



(u) Longitudinal characteristics, $\delta_{sp1,2,3} = 9^\circ$
 Figure 35. - Continued.

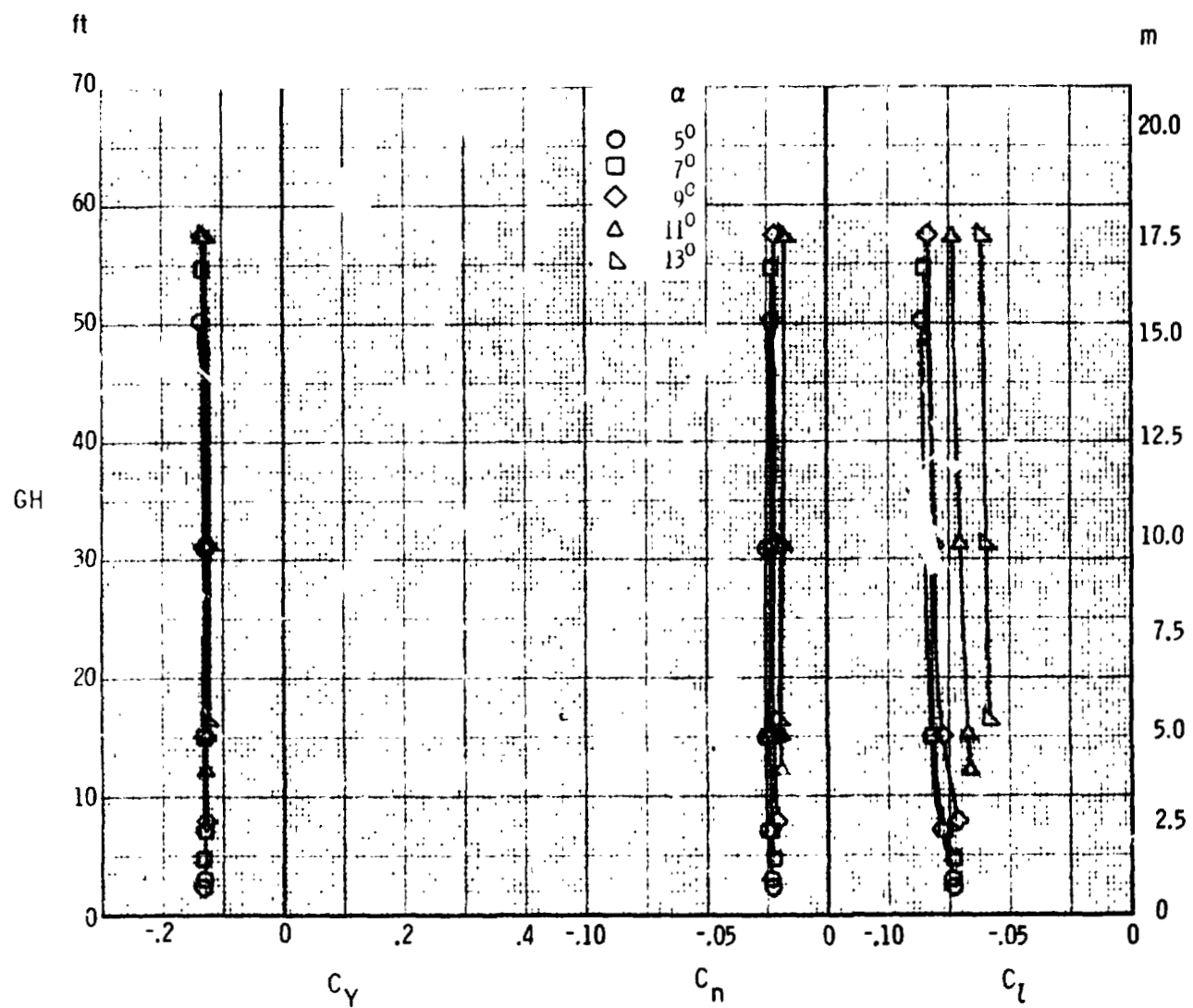


(v) Lateral-directional characteristics, $\delta_{sp1,2,3} = 90^\circ$
 Figure 3a. - Continued.



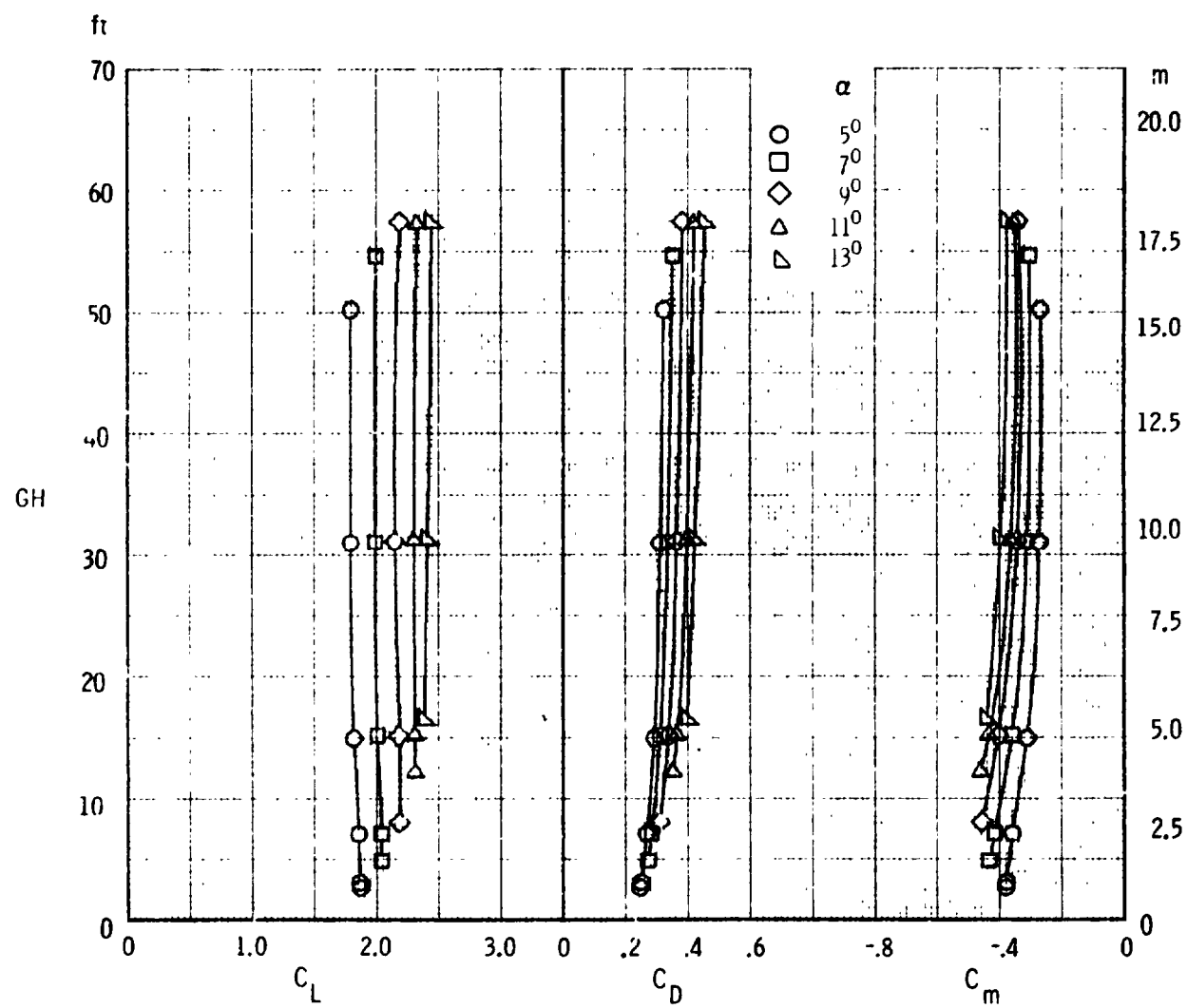
(v) Longitudinal characteristics, $\delta_{sp1,2,3} = 12^\circ$

Figure 35. - Continued.



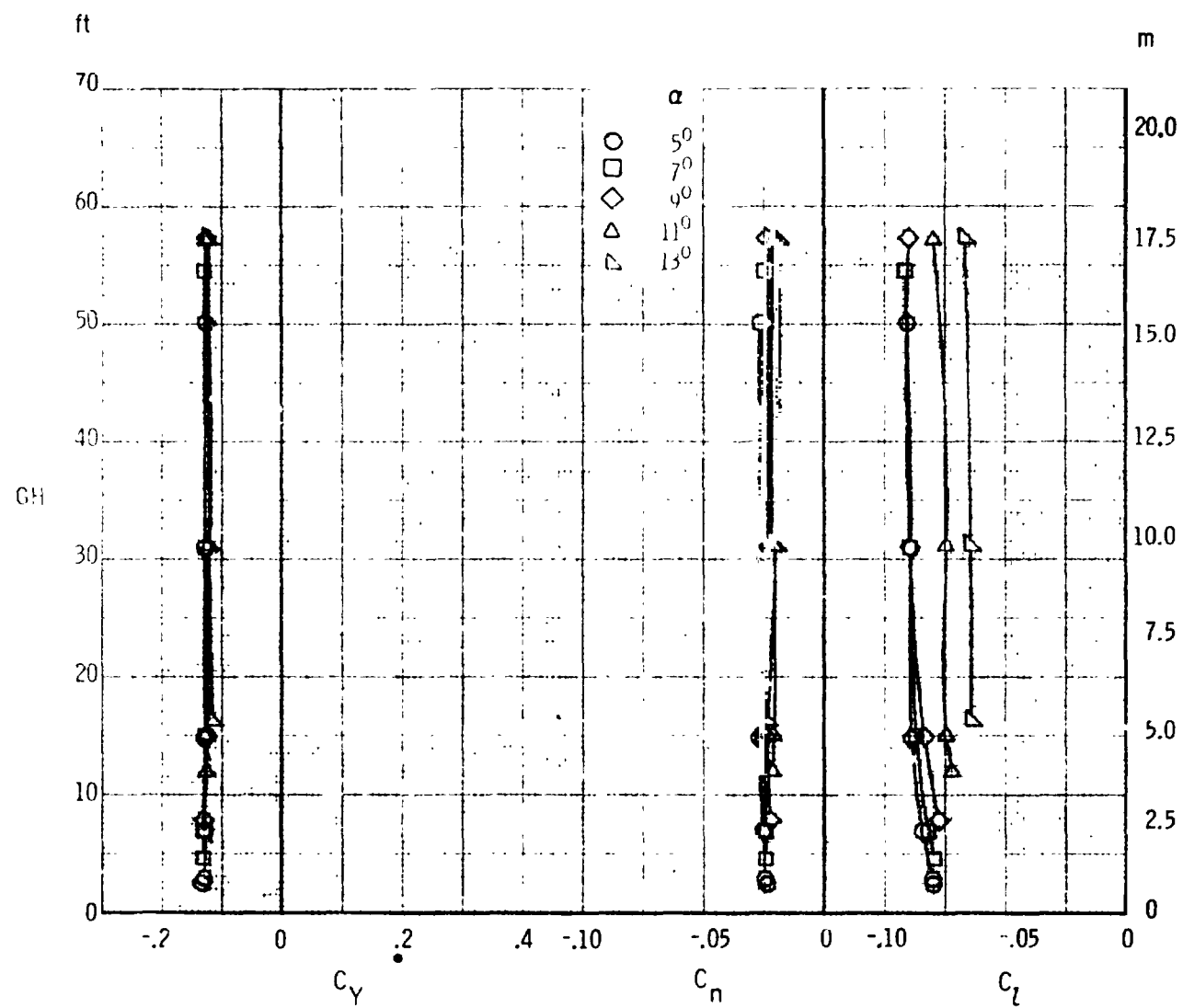
(x) Lateral-directional characteristics, $\delta_{sp1,2,3} = 12^\circ$

Figure 35. - Continued.



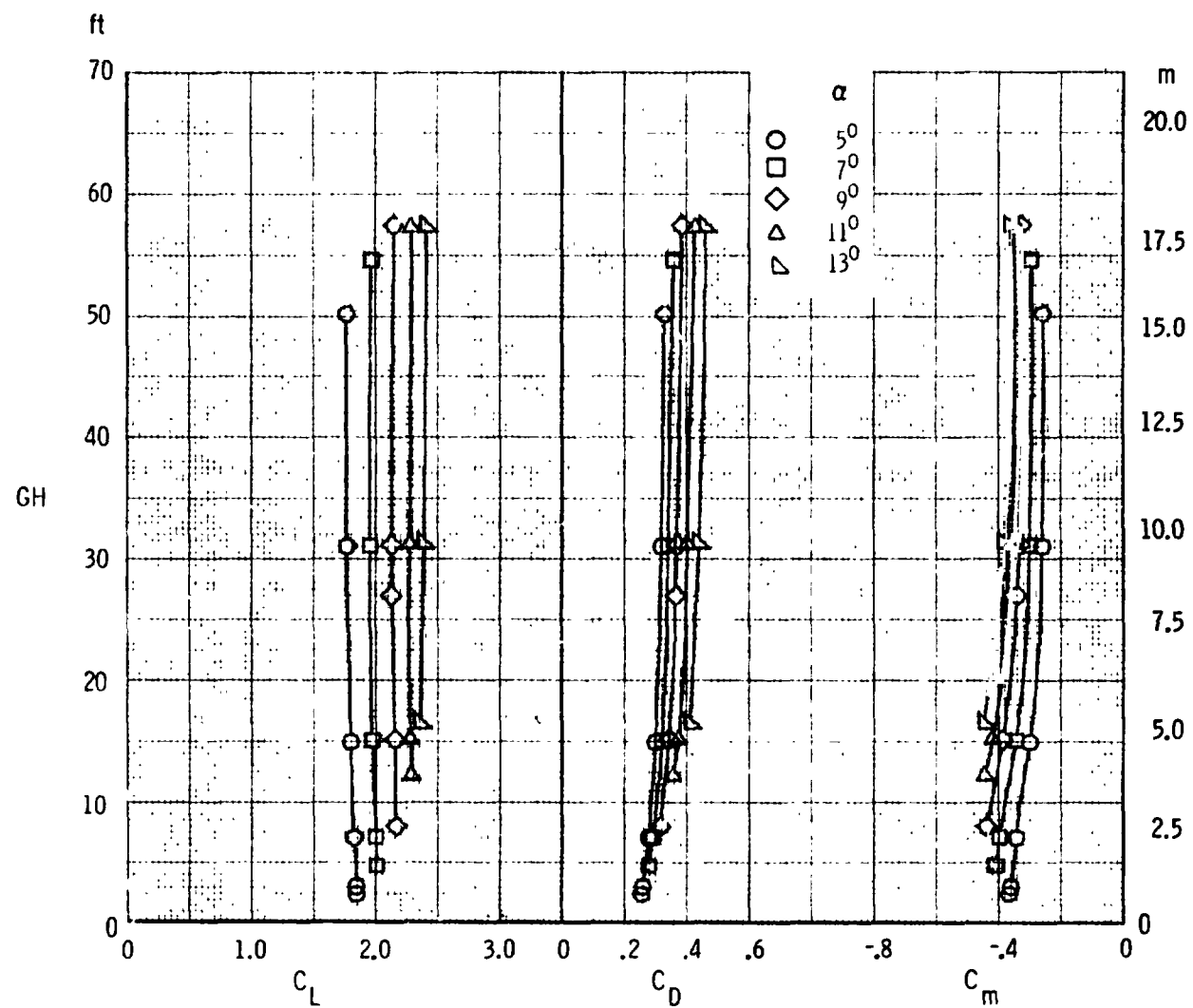
(y) Longitudinal characteristics, $\delta_{sp1,2,3} = 15^\circ$

Figure 35. - Continued.



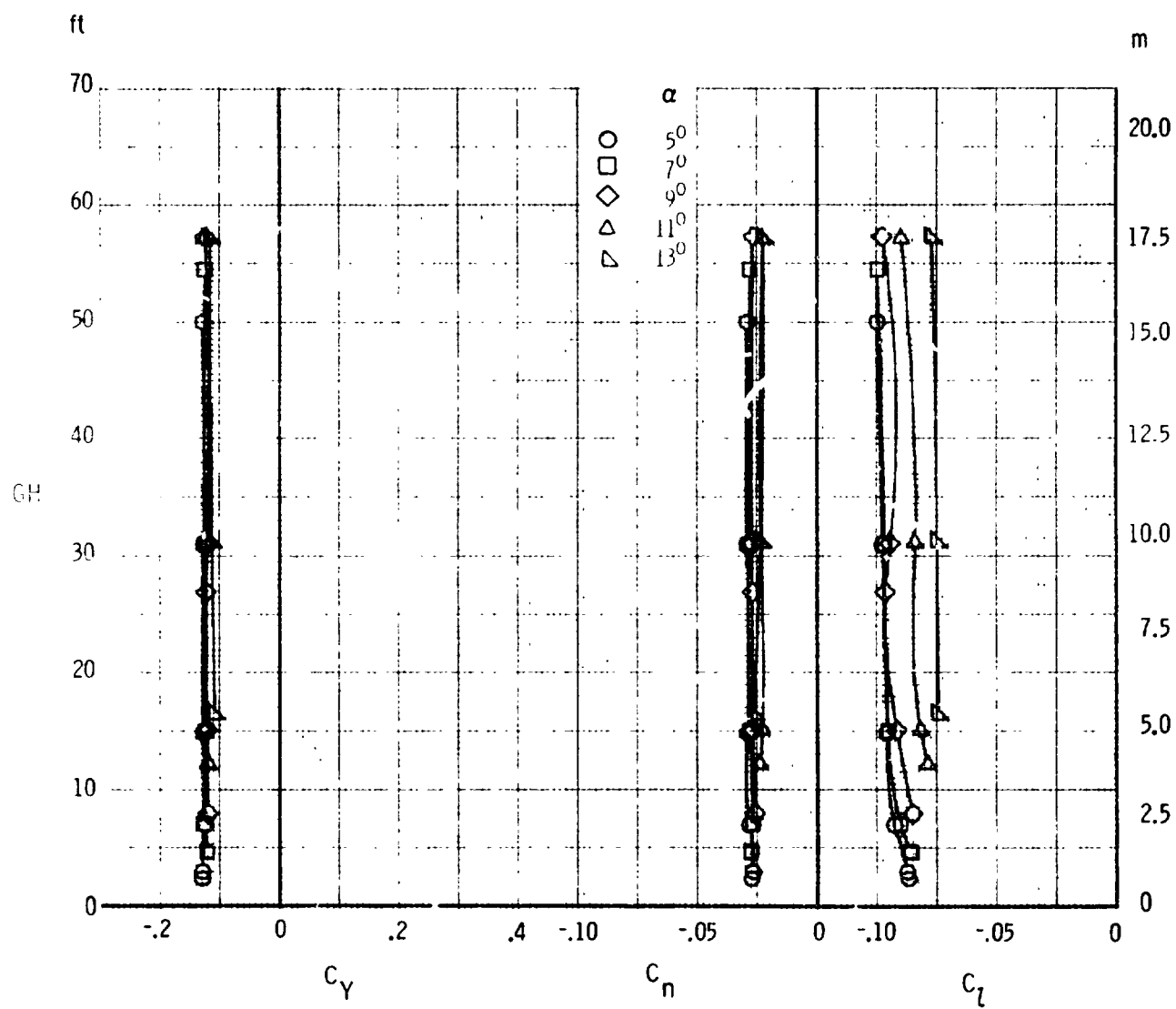
(z) Lateral-directional characteristics, $\delta_{sp1,2,3} = 15^\circ$

Figure 35. - Continued.



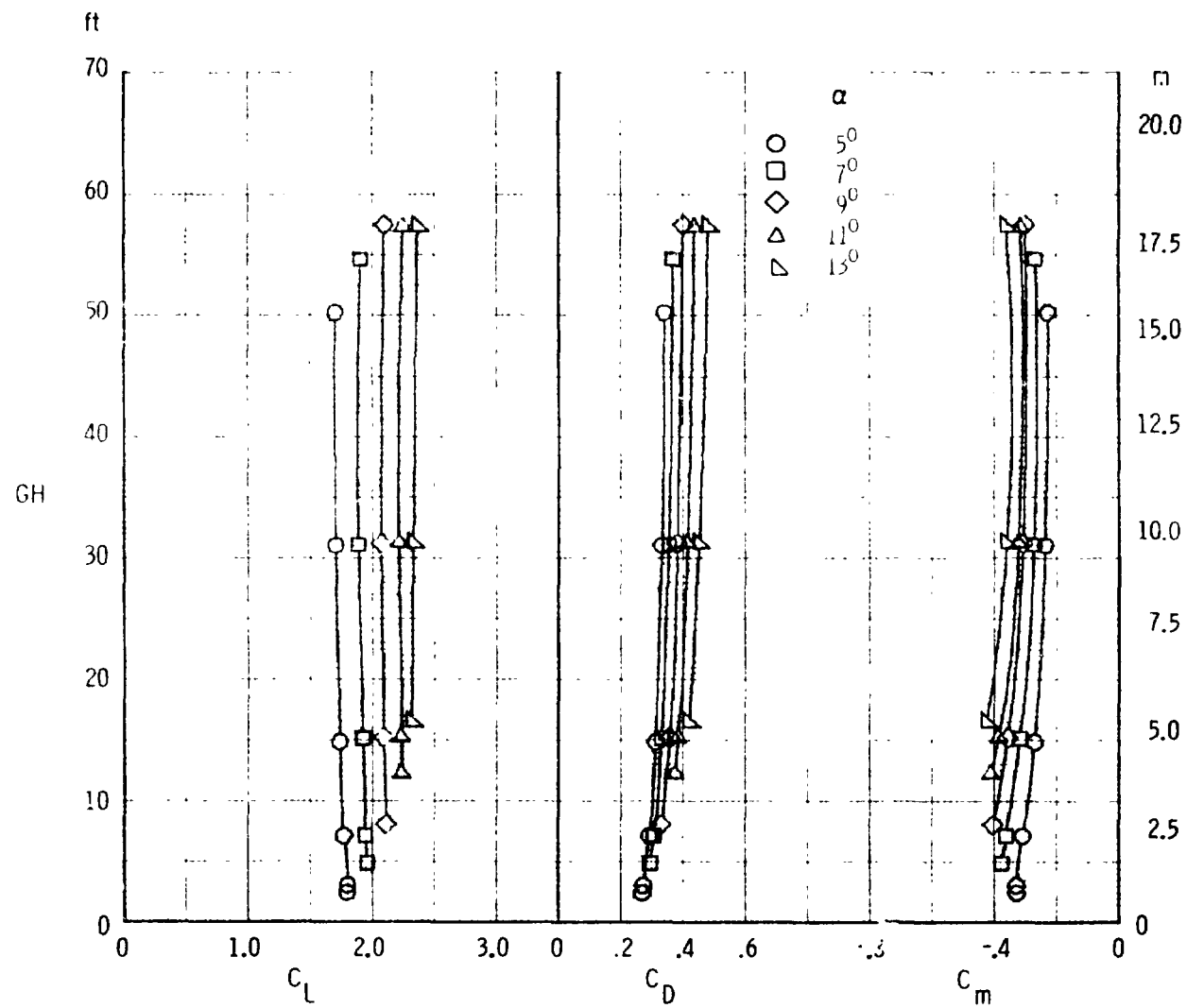
(aa) Longitudinal characteristics, $\delta_{sp1,2,3} = 20^\circ$

Figure 35. - Continued.



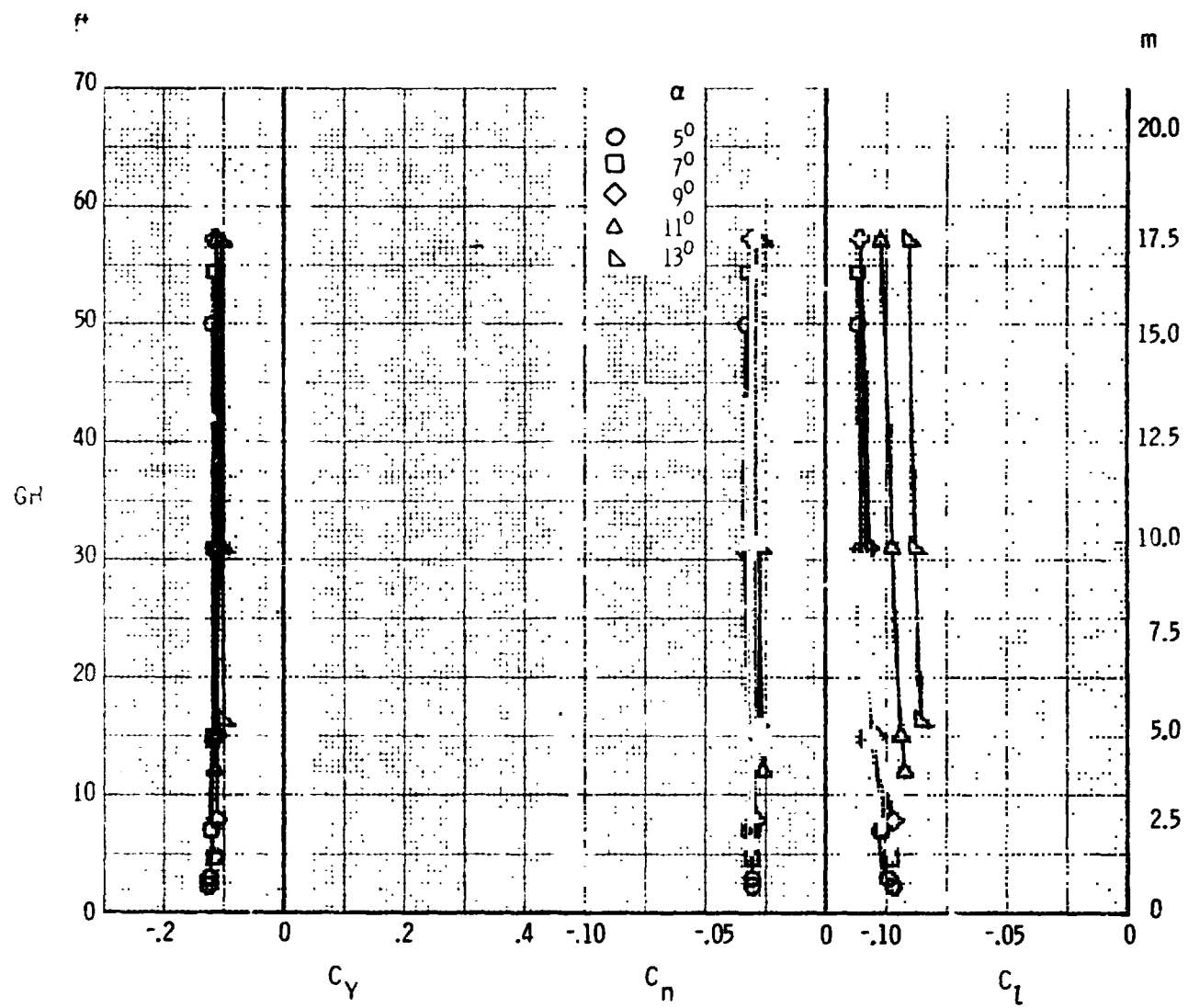
(bb) Lateral-directional characteristics, $\delta_{sp1,2,3} = 20^\circ$

Figure 35. - Continued.



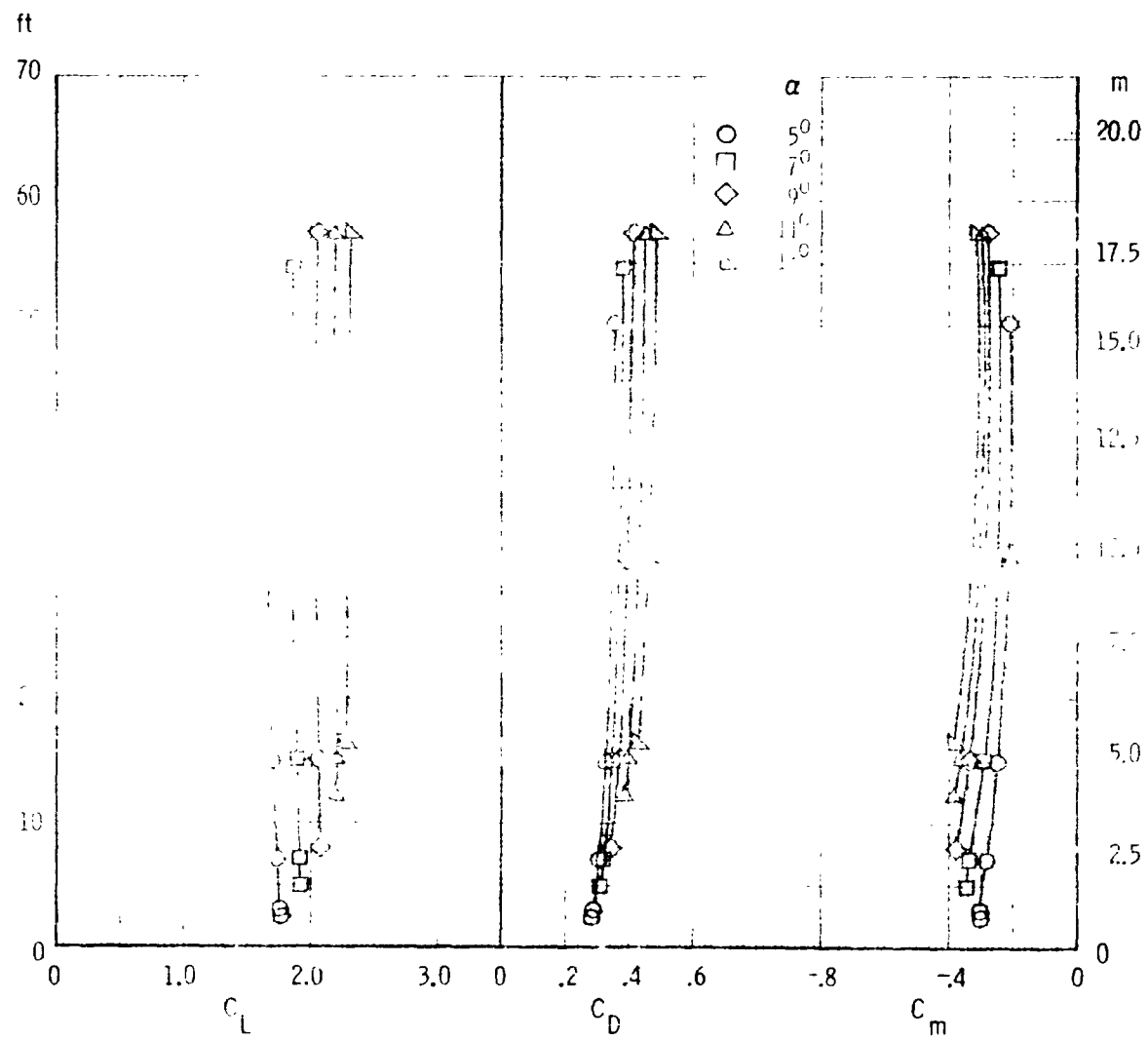
(cc) Longitudinal characteristics, $\delta_{sp1,2,3} = 30^\circ$

Figure 35. - Continued.



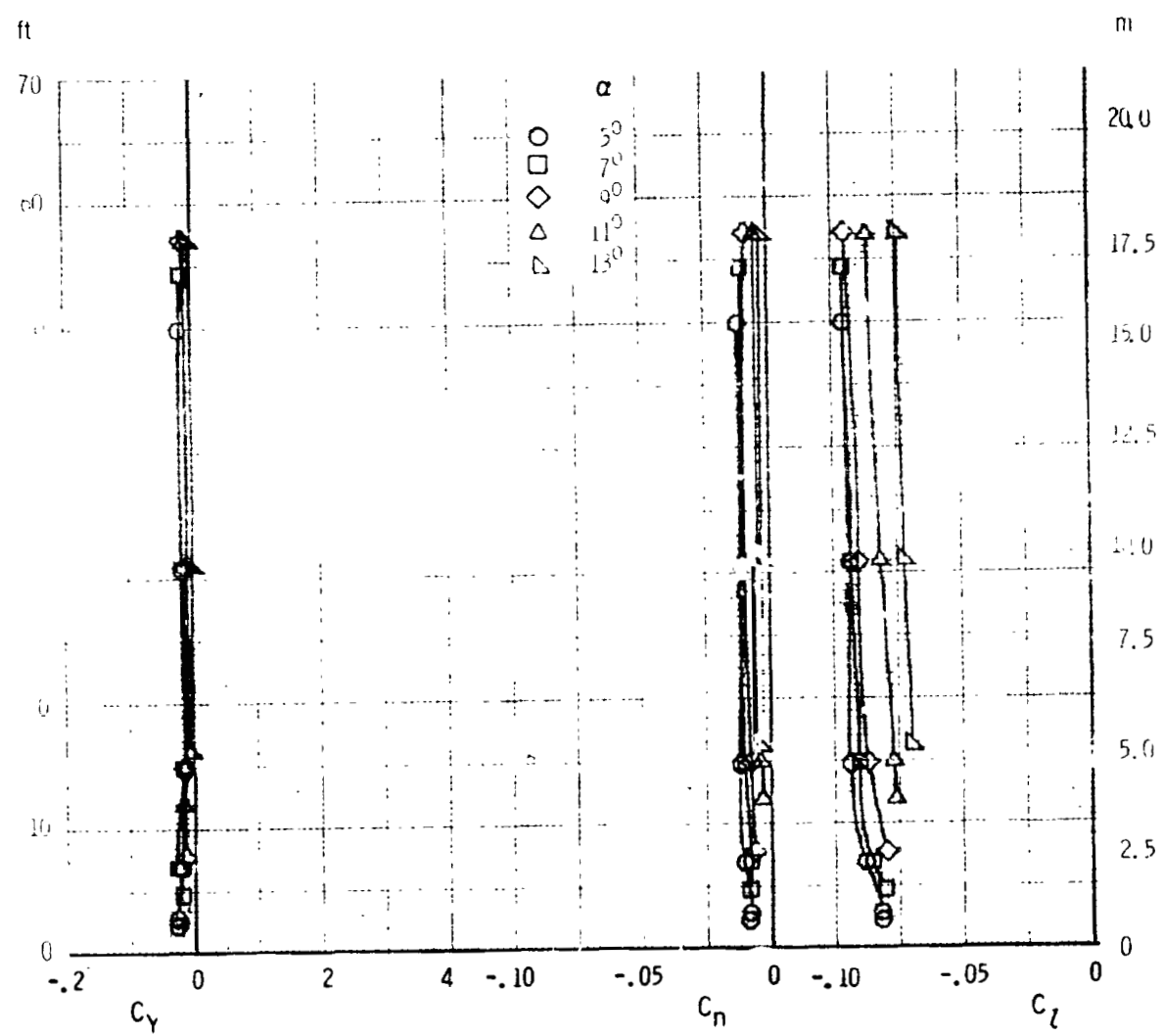
(dd) Lateral-directional characteristics, $\delta_{sp1,2,3} = 30^\circ$

Figure 35. - Continued.



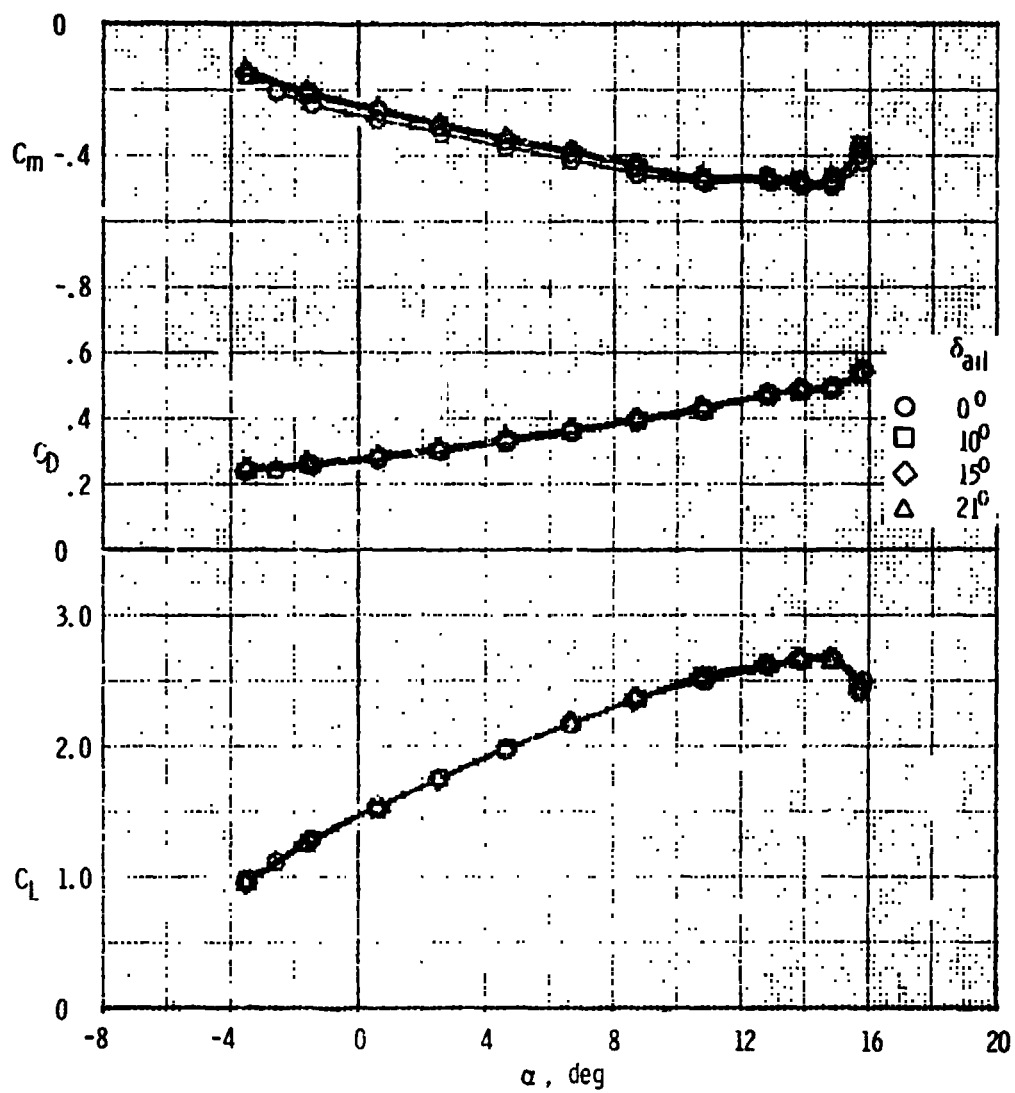
(ee) Longitudinal characteristics, $\delta_{p1,2,3} = 40^\circ$

Figure 35. - Continued.



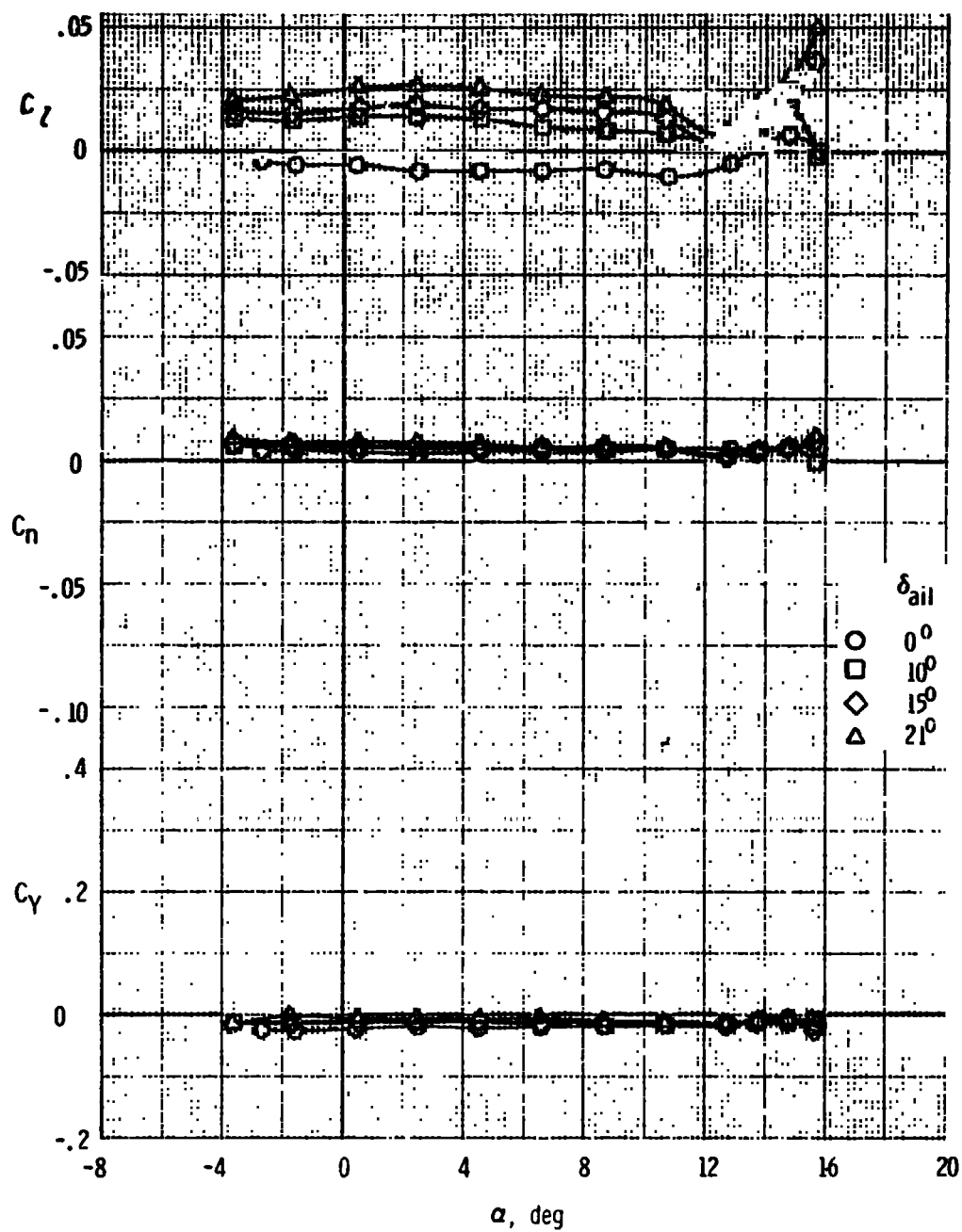
(ff) Lateral-directional characteristics, $\delta_{sp1,2,3} = 40^\circ$

Figure 35. - Concluded.



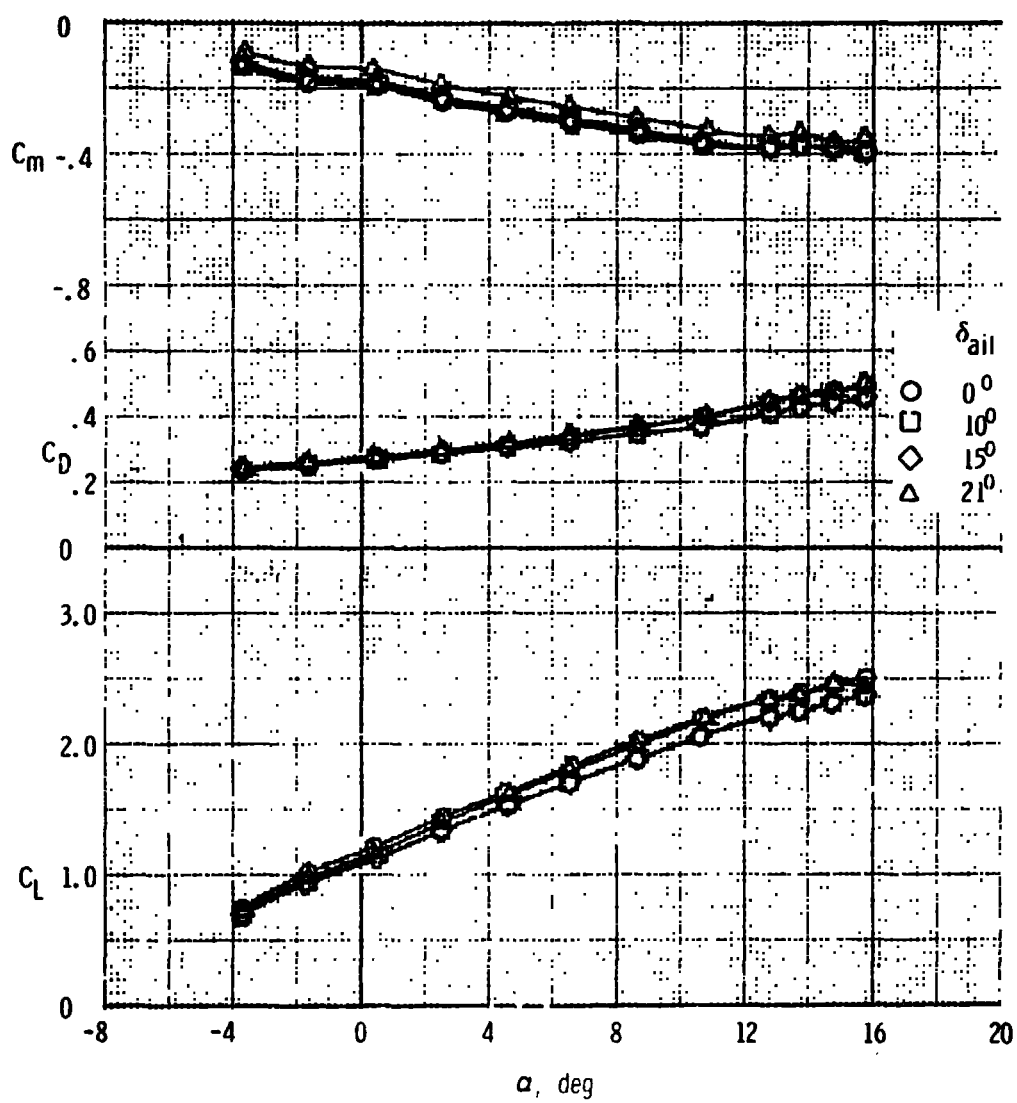
(a) Longitudinal characteristics, $\delta_{sp2,3,6,7} = 0^\circ$

Figure 36. - Effect of aileron deflection on the aerodynamic characteristics of the F, W, F₄₀, N, C, H_T, V_T configuration with and without DLC spoilers deflected.



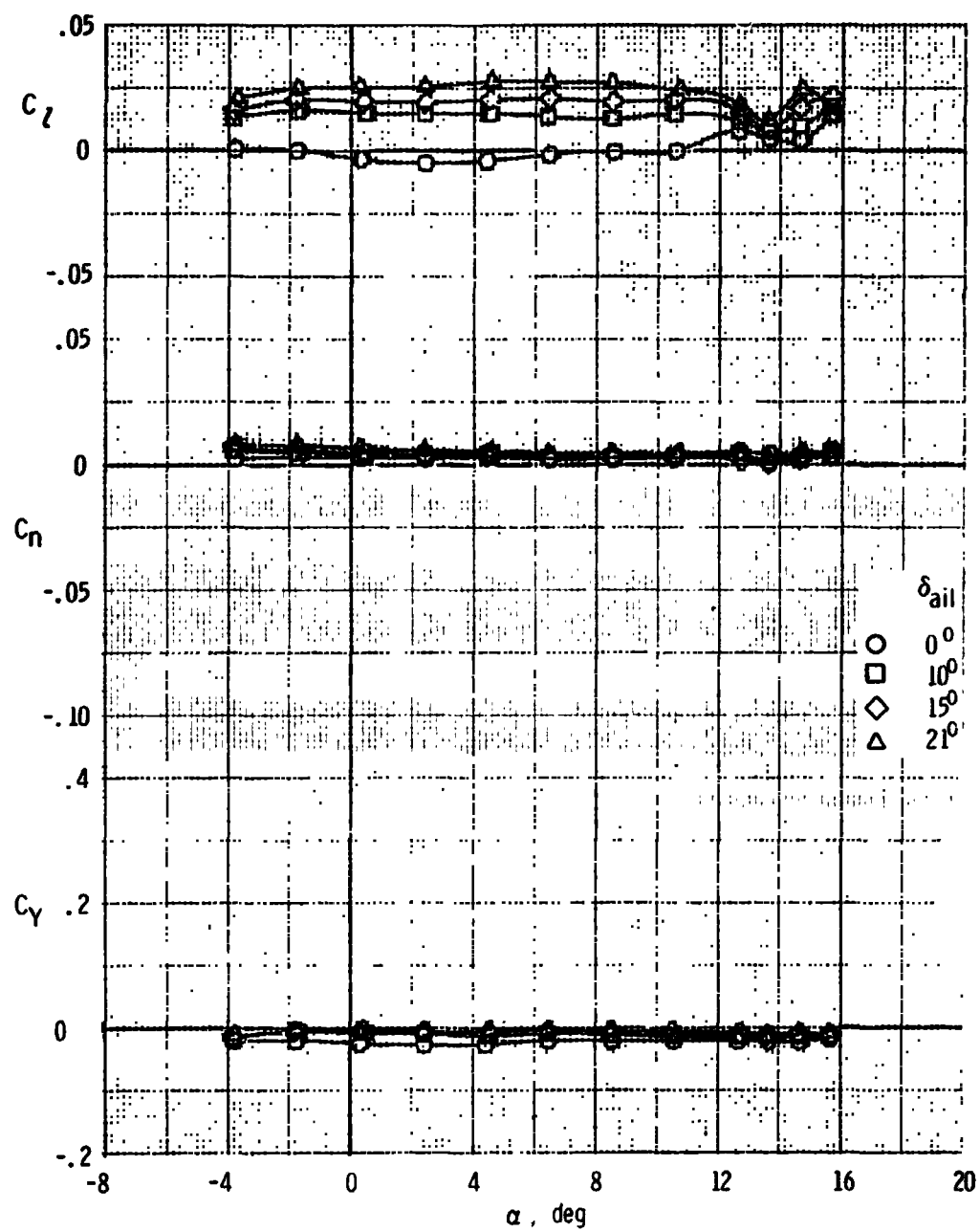
(b) Lateral-directional characteristics, $\delta_{sp2,3,6,7} = 0^\circ$

Figure 36. - Continued.



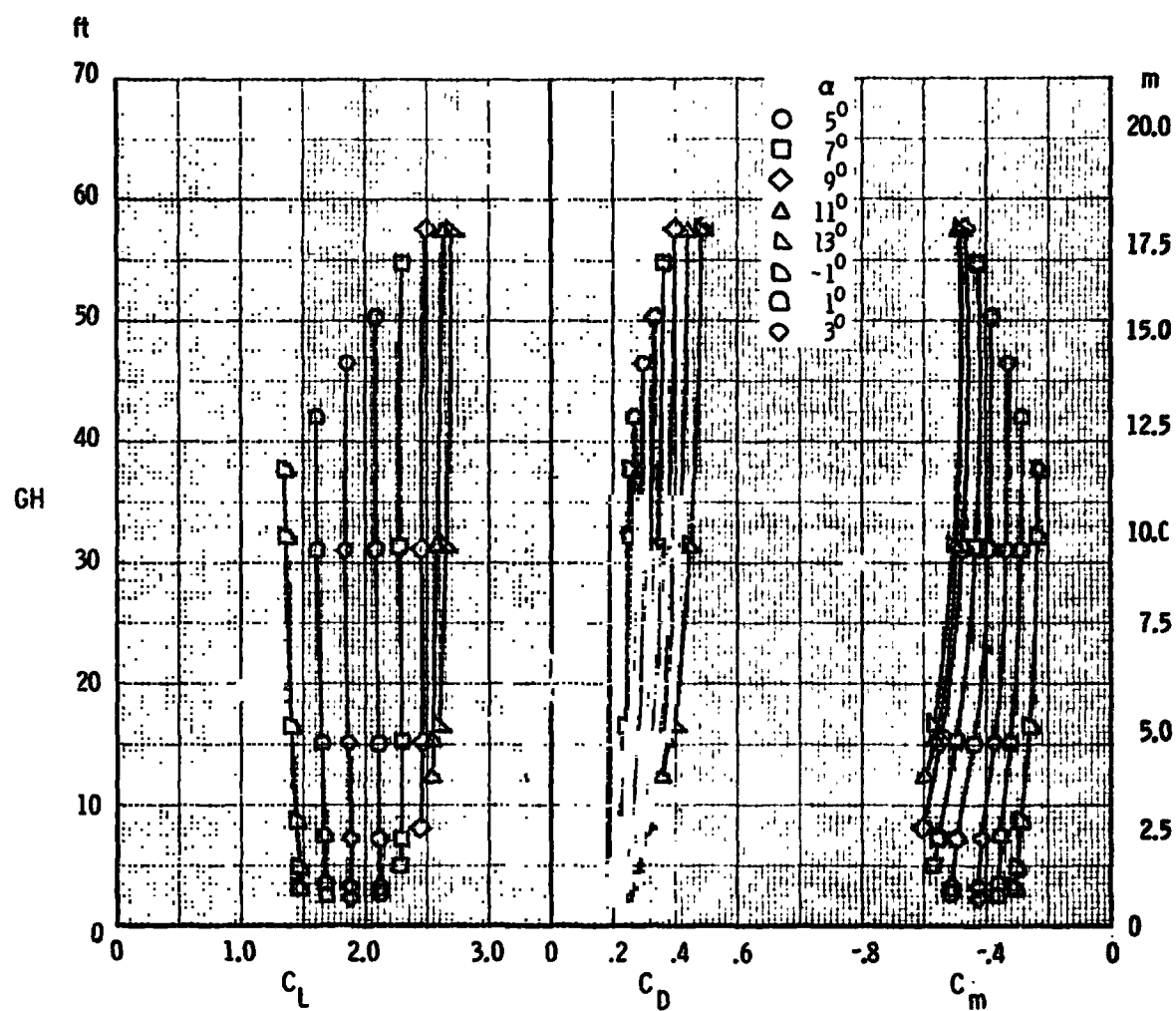
(c) Longitudinal characteristics, $\delta_{sp2,3,6,7} = 9^\circ$

Figure 36. - Continued.



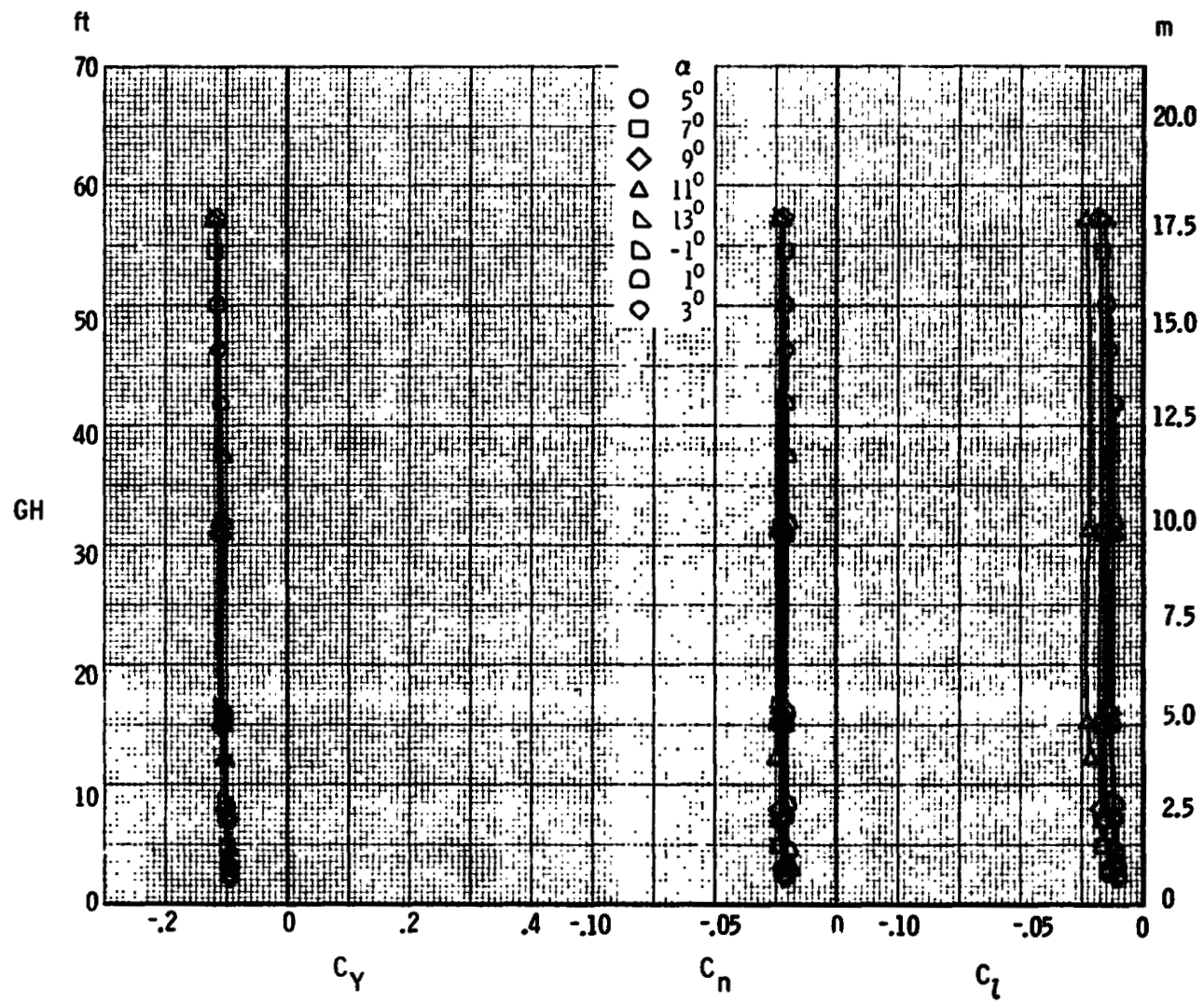
(d) Lateral-directional characteristics, $\delta_{sp2,3,6,7} = 9^\circ$

Figure 36. - Concluded.



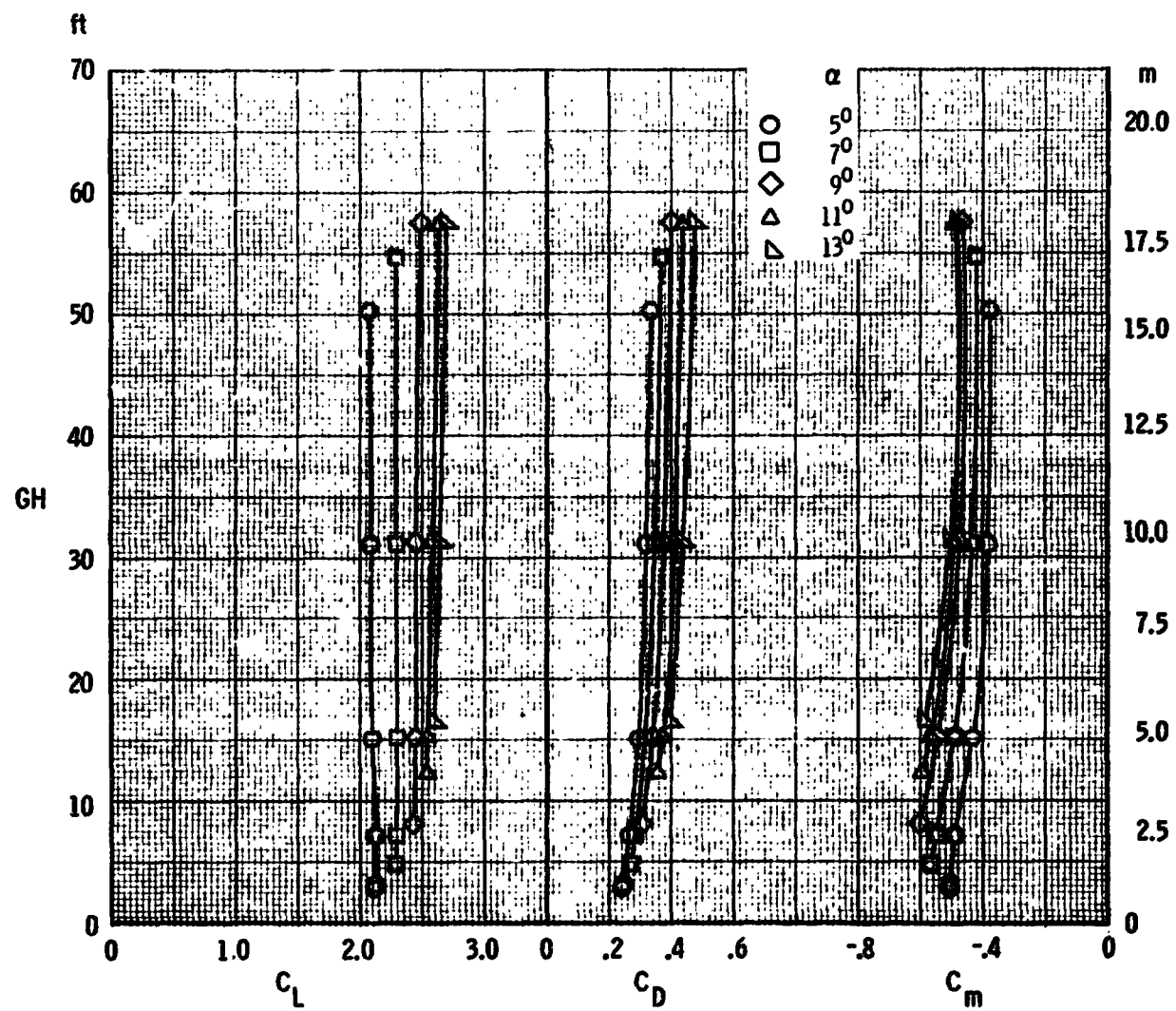
(a) Longitudinal characteristics, $\delta_{all} = \pm 10^\circ$, $\delta_{sp2,3,6,7} = 0^\circ$

Figure 37. - Effect of ground height on the aerodynamic characteristics of the F, W, F₄₀, N, G, H_T, V_T configuration with various alleron deflections with and without DLC spoilers deflected.



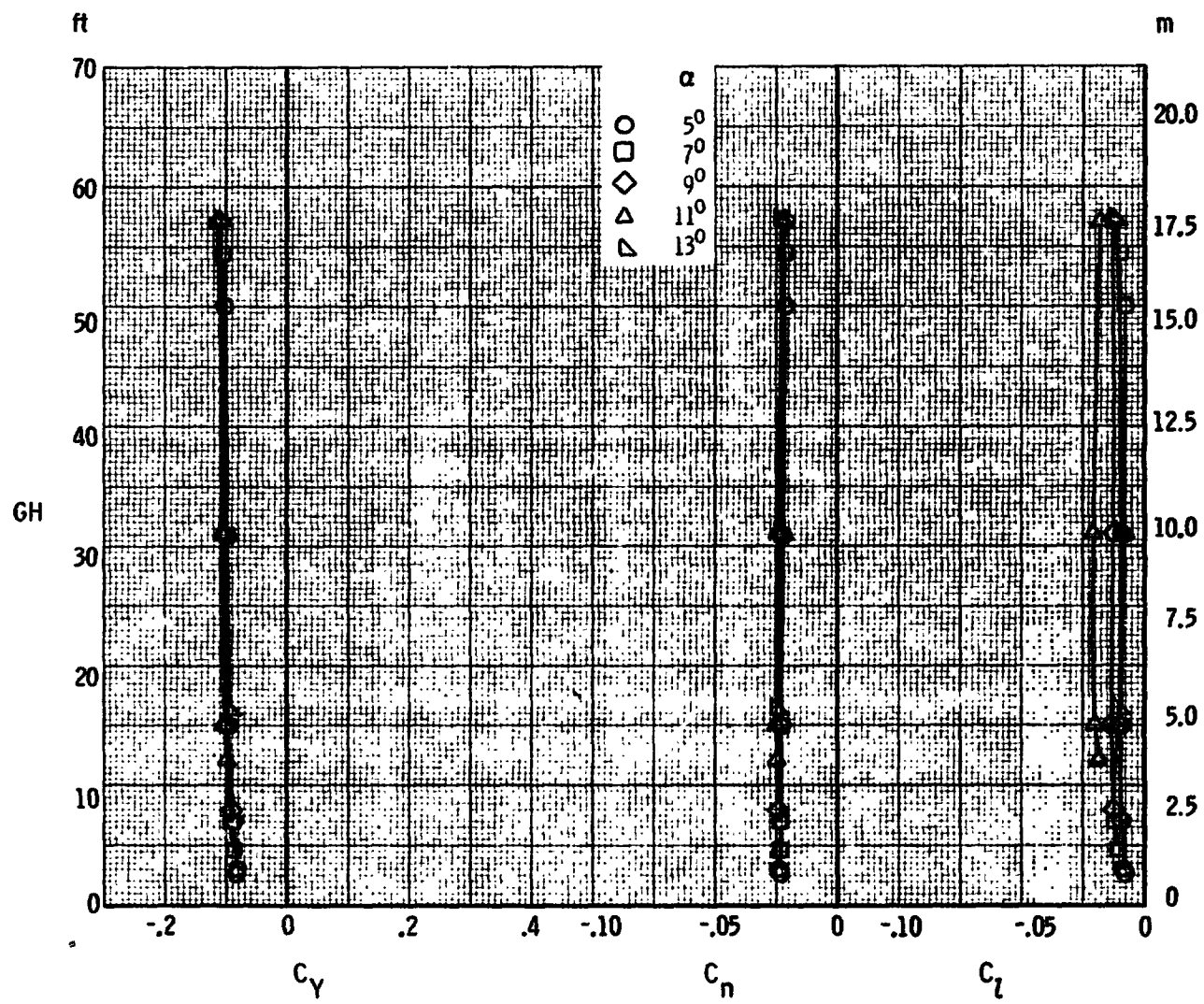
(b) Lateral-directional characteristics, $\delta_{ail} = \pm 10^\circ$, $\delta_{sp2,3,6,7} = 0^\circ$

Figure 37. - Continued.



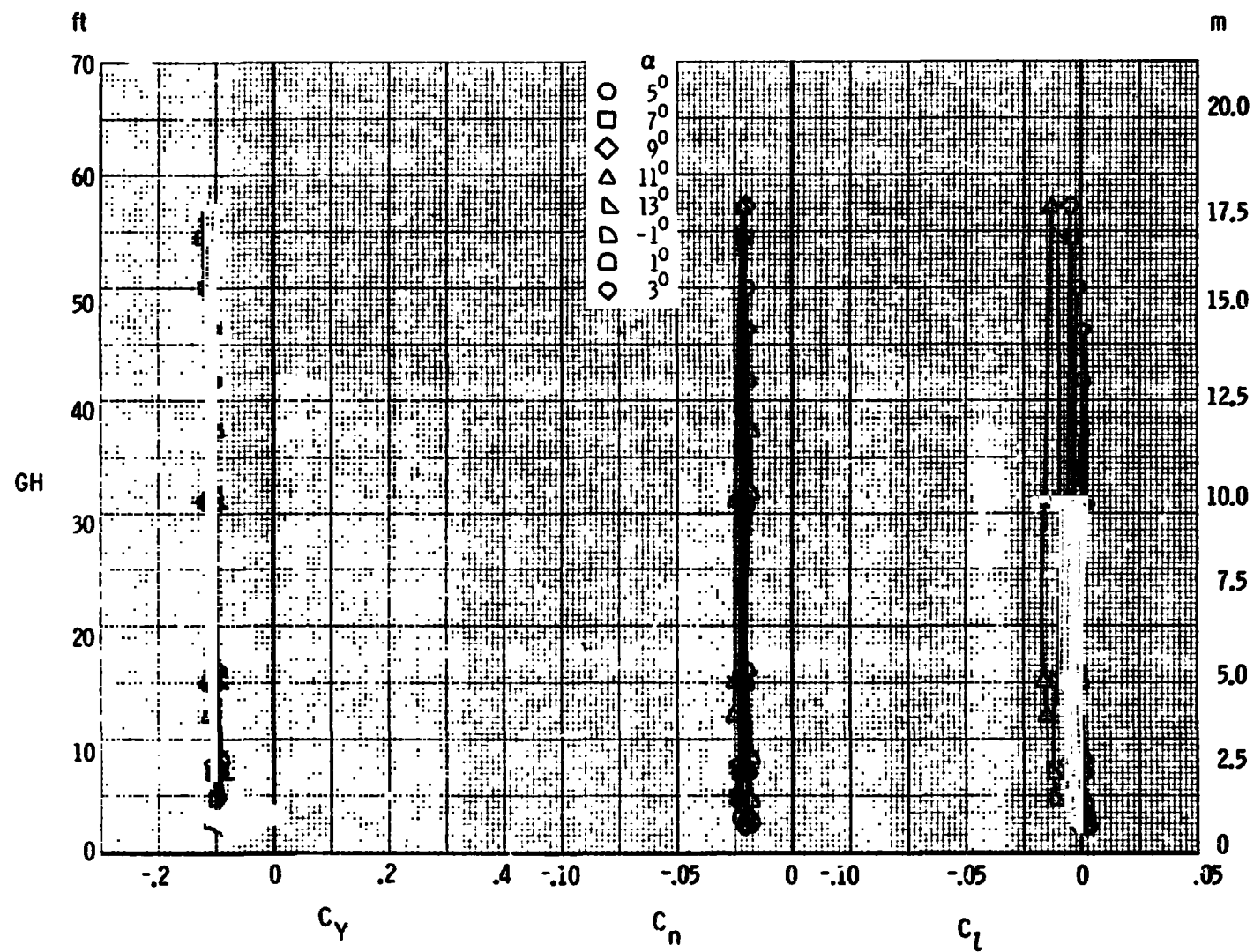
(c) Longitudinal characteristics, $\delta_{all} = \pm 15^\circ$, $\delta_{sp2,3,6,7} = 0^\circ$

Figure 37. - Continued.



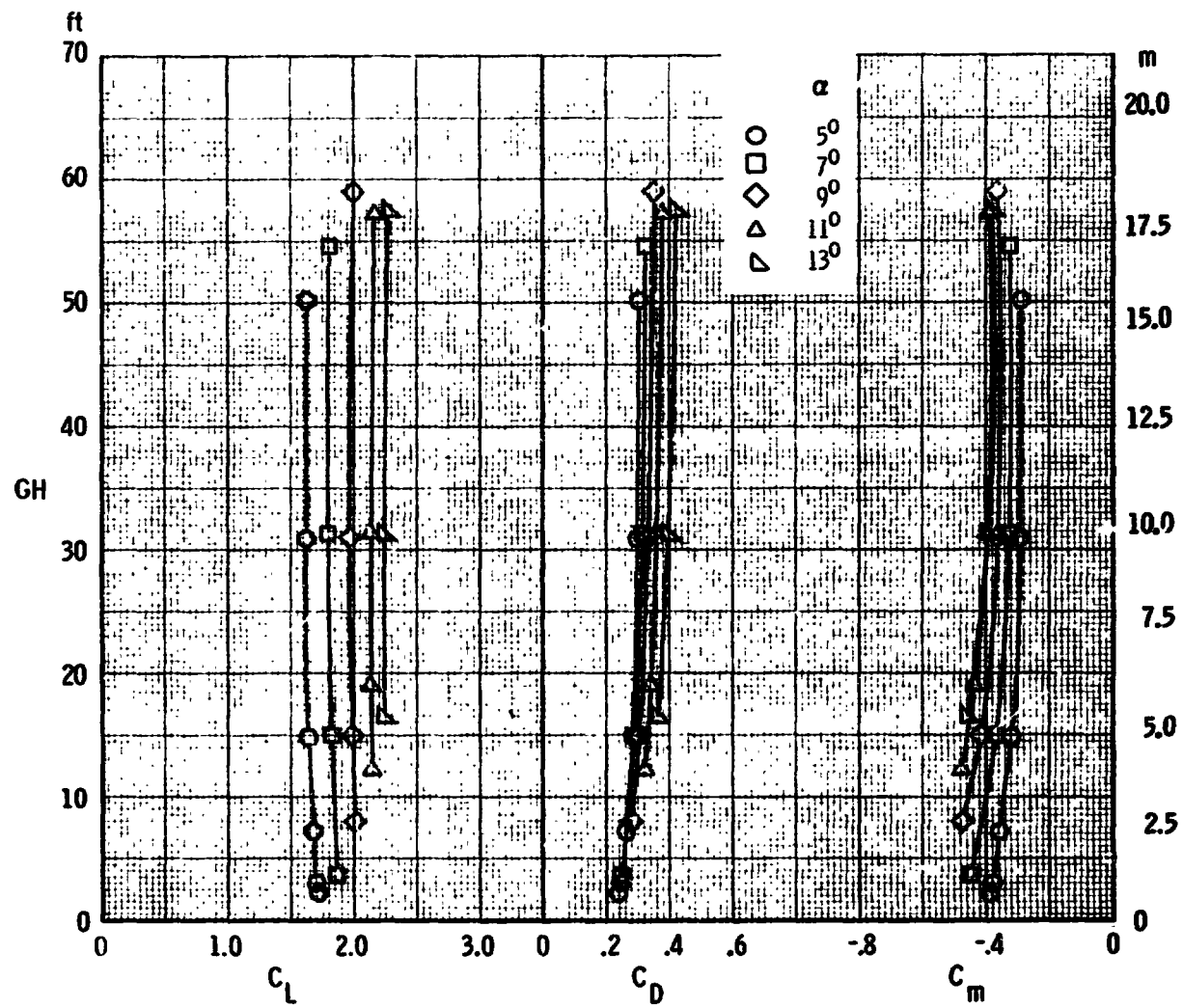
(d) Lateral-directional characteristics, $\delta_{all} = \pm 15^\circ$, $\delta_{sp2,3,6,7} = 0^\circ$

Figure 37. - Continued.



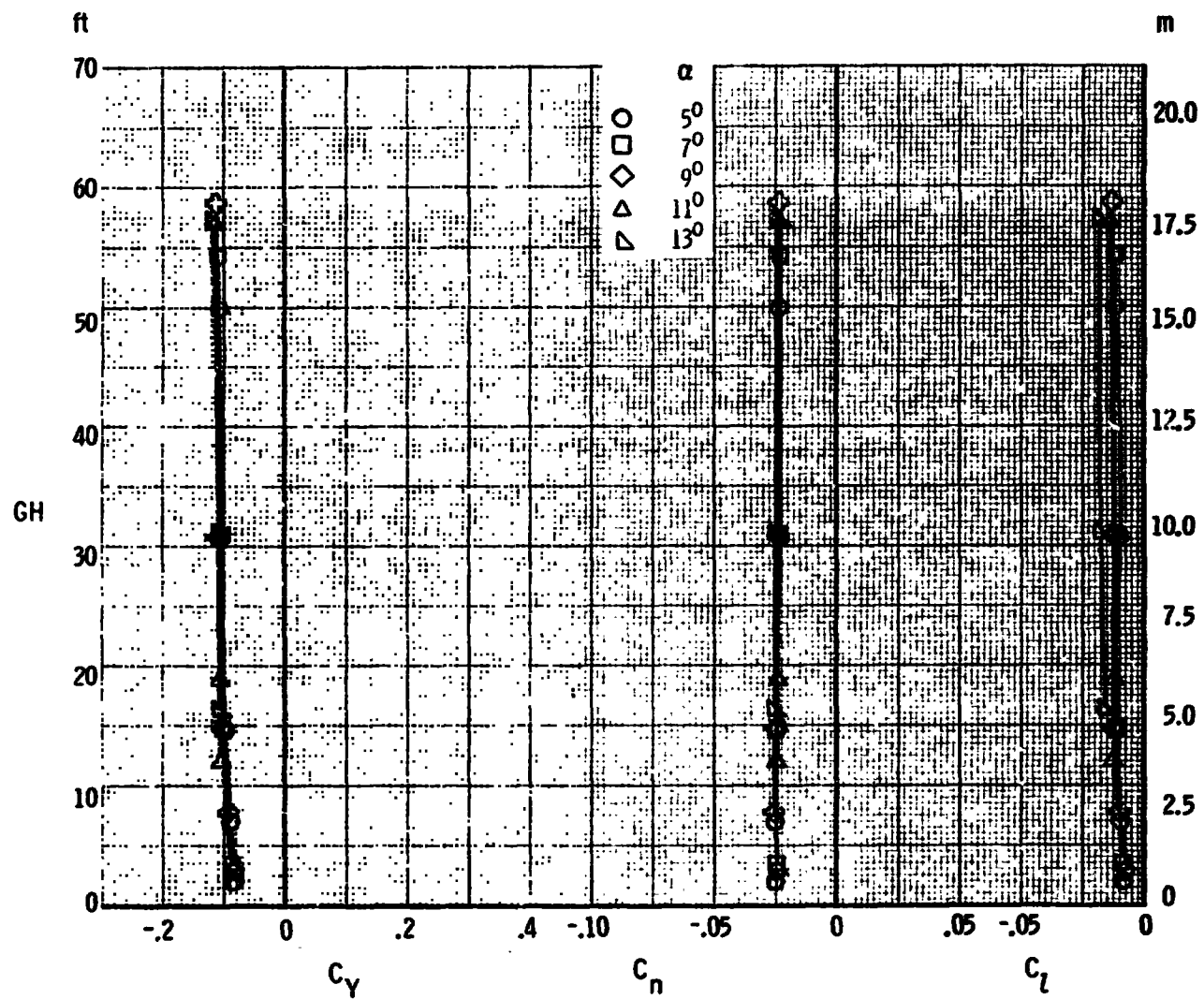
(f) Lateral-directional characteristics, $\delta_{all} = \pm 21^\circ$, $\delta_{sp2,3,6,7} = 0^\circ$

Figure 37. - Continued.



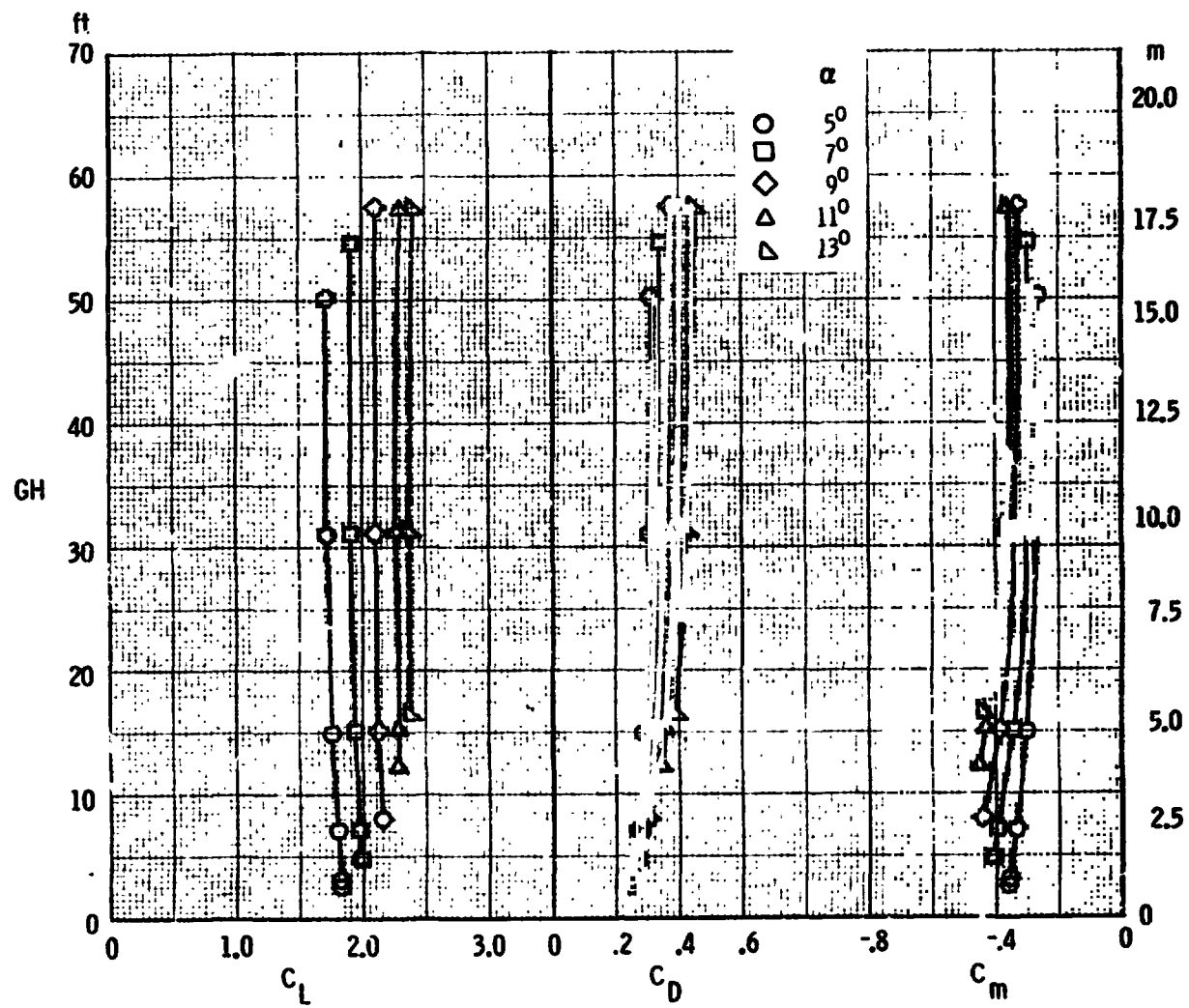
(g) Longitudinal characteristics, $\delta_{ail} = \pm 10^\circ$, $\delta_{sp2,3,6,7} = 9^\circ$

Figure 37. - Continued.



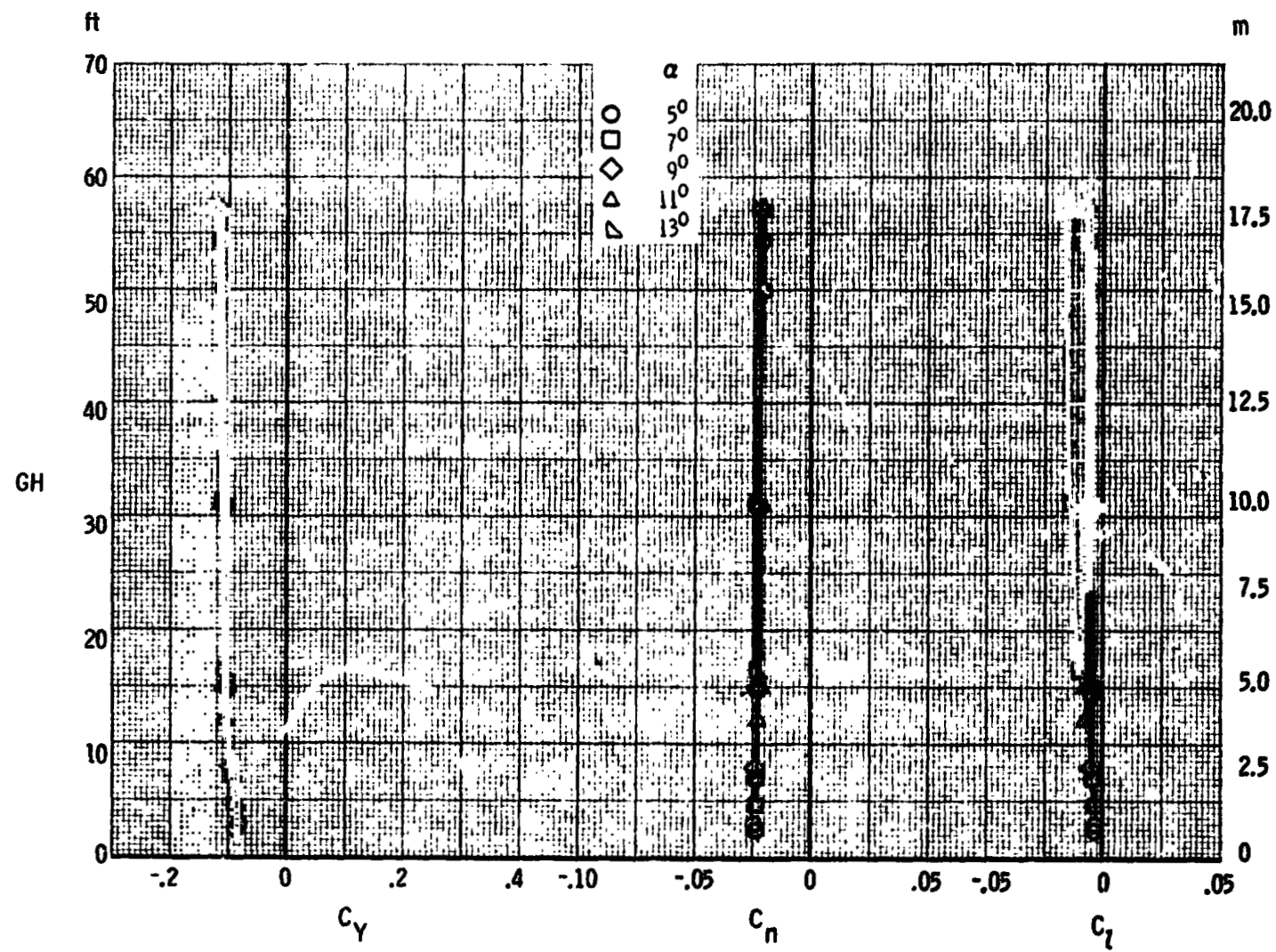
(h) Lateral-directional characteristics, $\delta_{all} = \pm 10^\circ$, $\delta_{sp2,3,6,7} = 9^\circ$

Figure 37. - Continued.

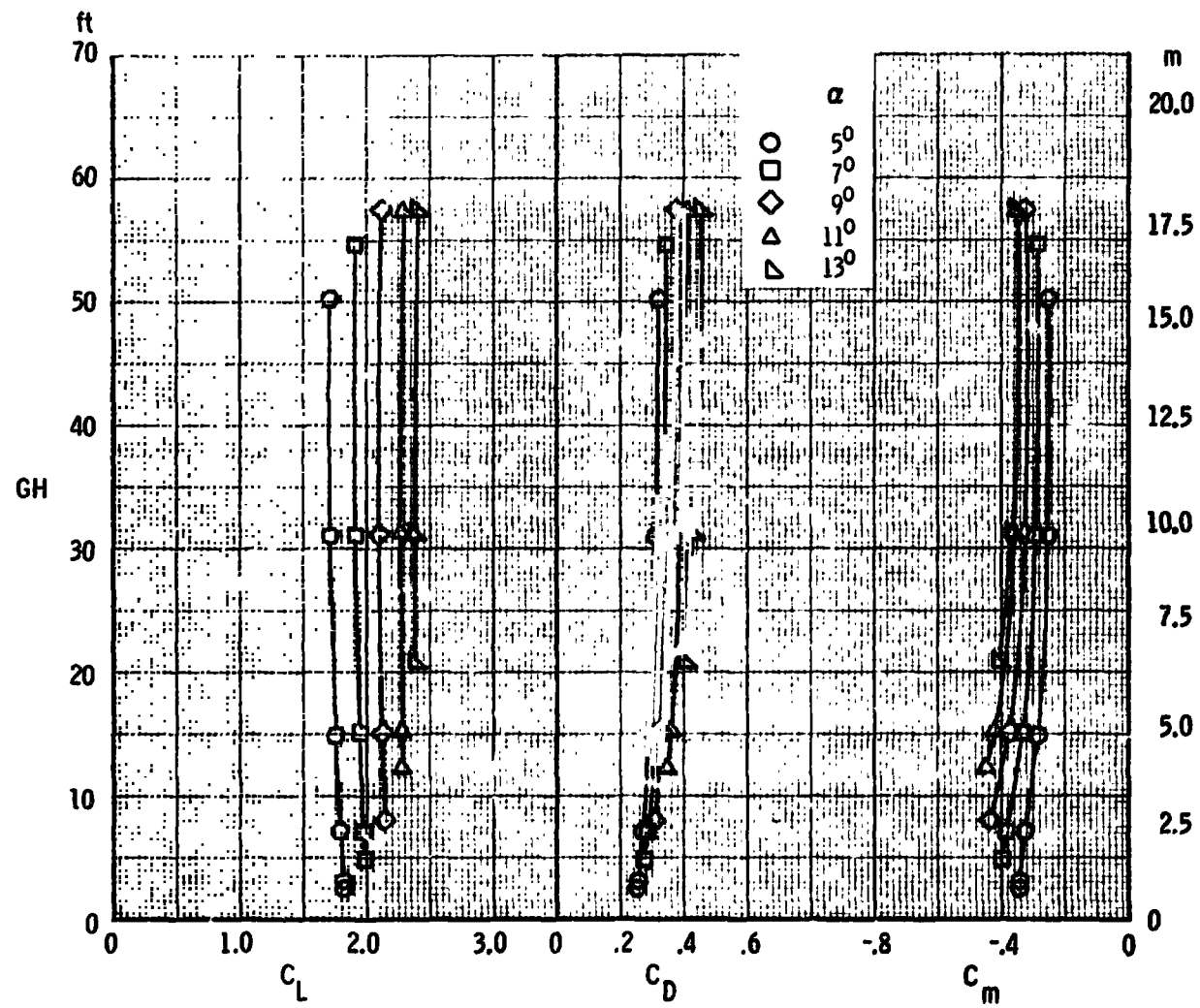


(I) Longitudinal characteristics, $\delta_{all} = \pm 15^\circ$, $\delta_{sp2,3,6,7} = 9^\circ$

Figure 37. - Continued.

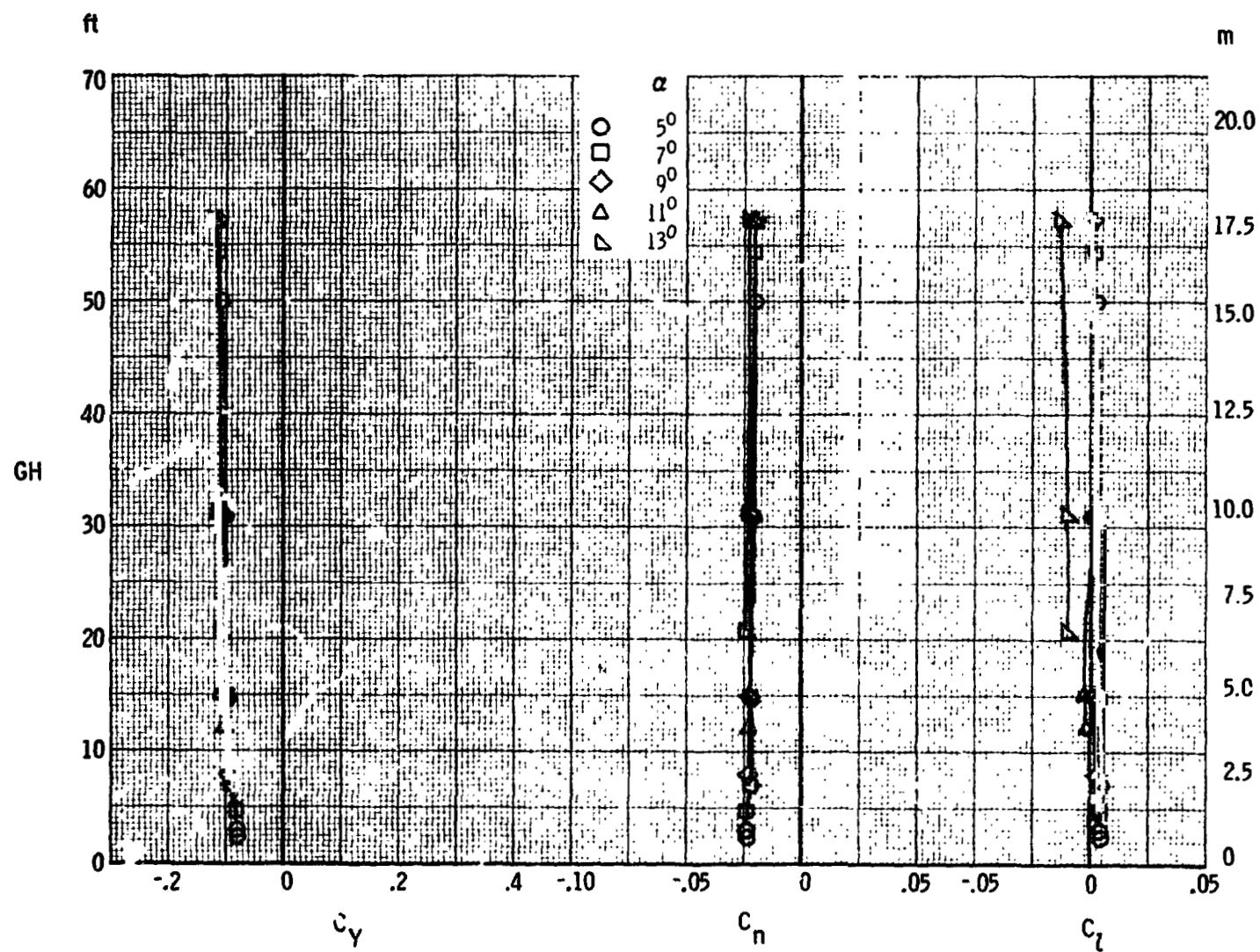


(j) Lateral-directional characteristics, $\delta_{all} = \pm 15^\circ$, $\delta_{sp2,3,6,7} = 90^\circ$
 Figure 37. - Continued.



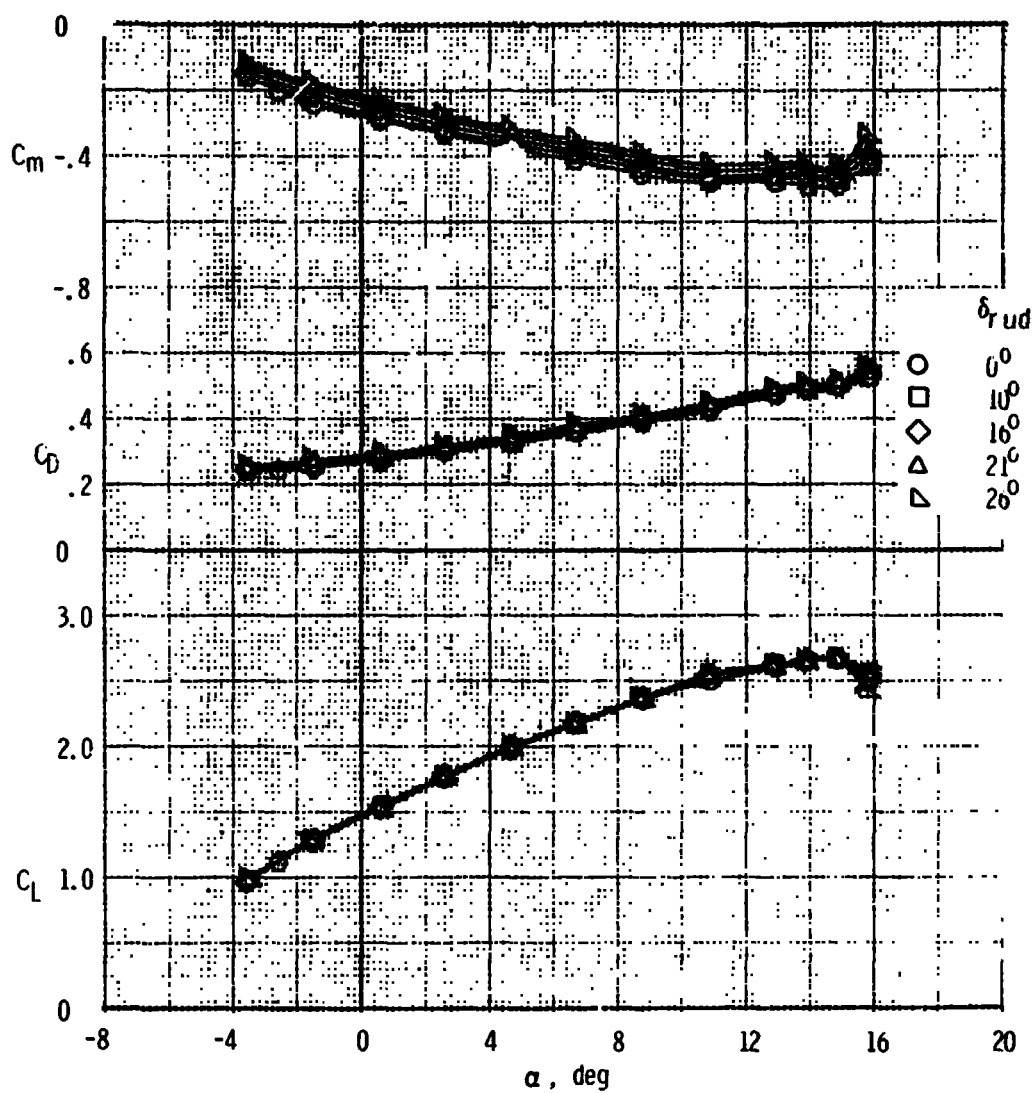
(k) Longitudinal characteristics, $\delta_{ail} = \pm 21^\circ$, $\delta_{sp2,3,6,7} = 90^\circ$

Figure 37. - Continued.



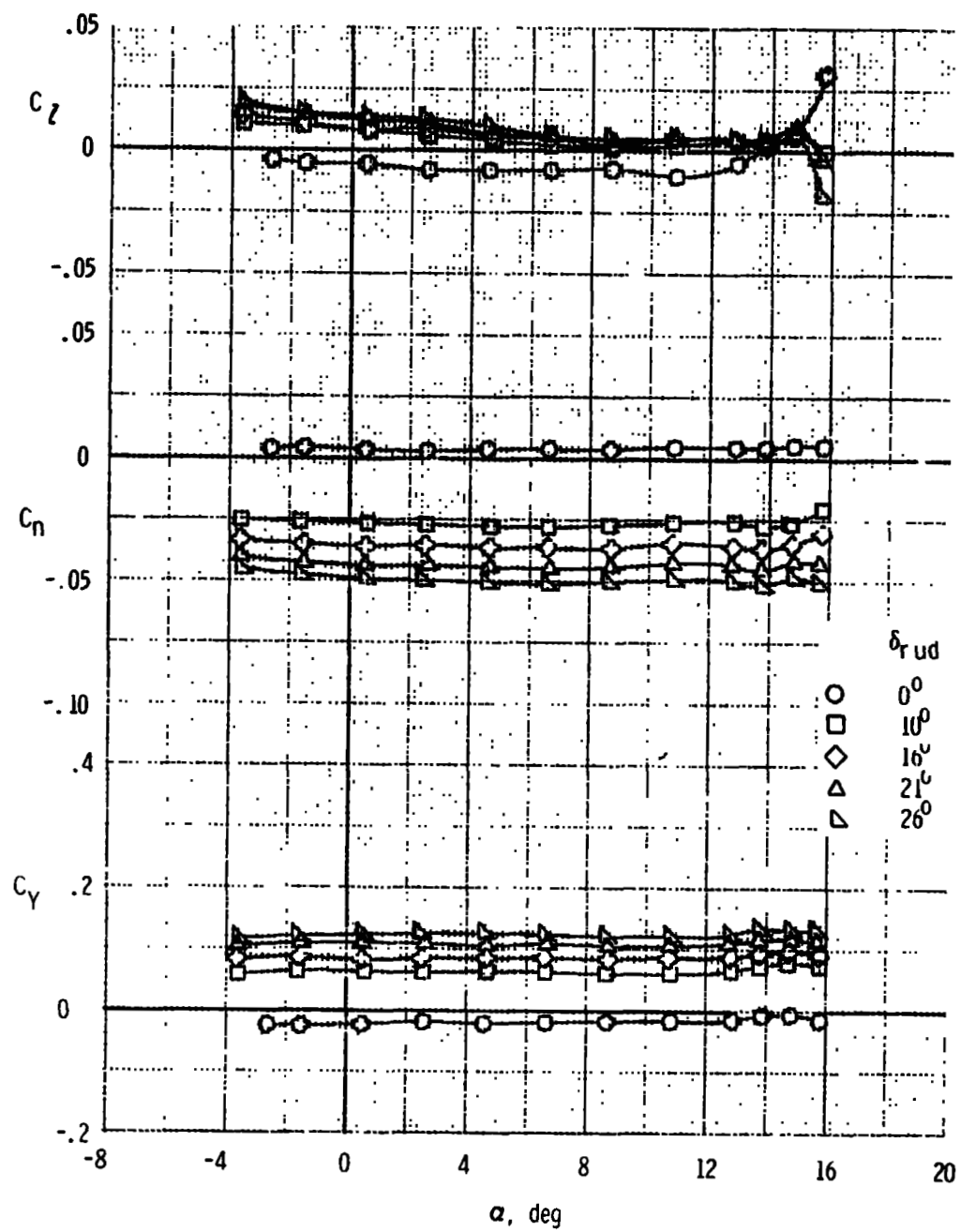
(I) Lateral-directional characteristics, $\delta_{all} = \pm 21^\circ$, $\delta_{sp2,3,6,7} = 9^\circ$

Figure 37. - Concluded.



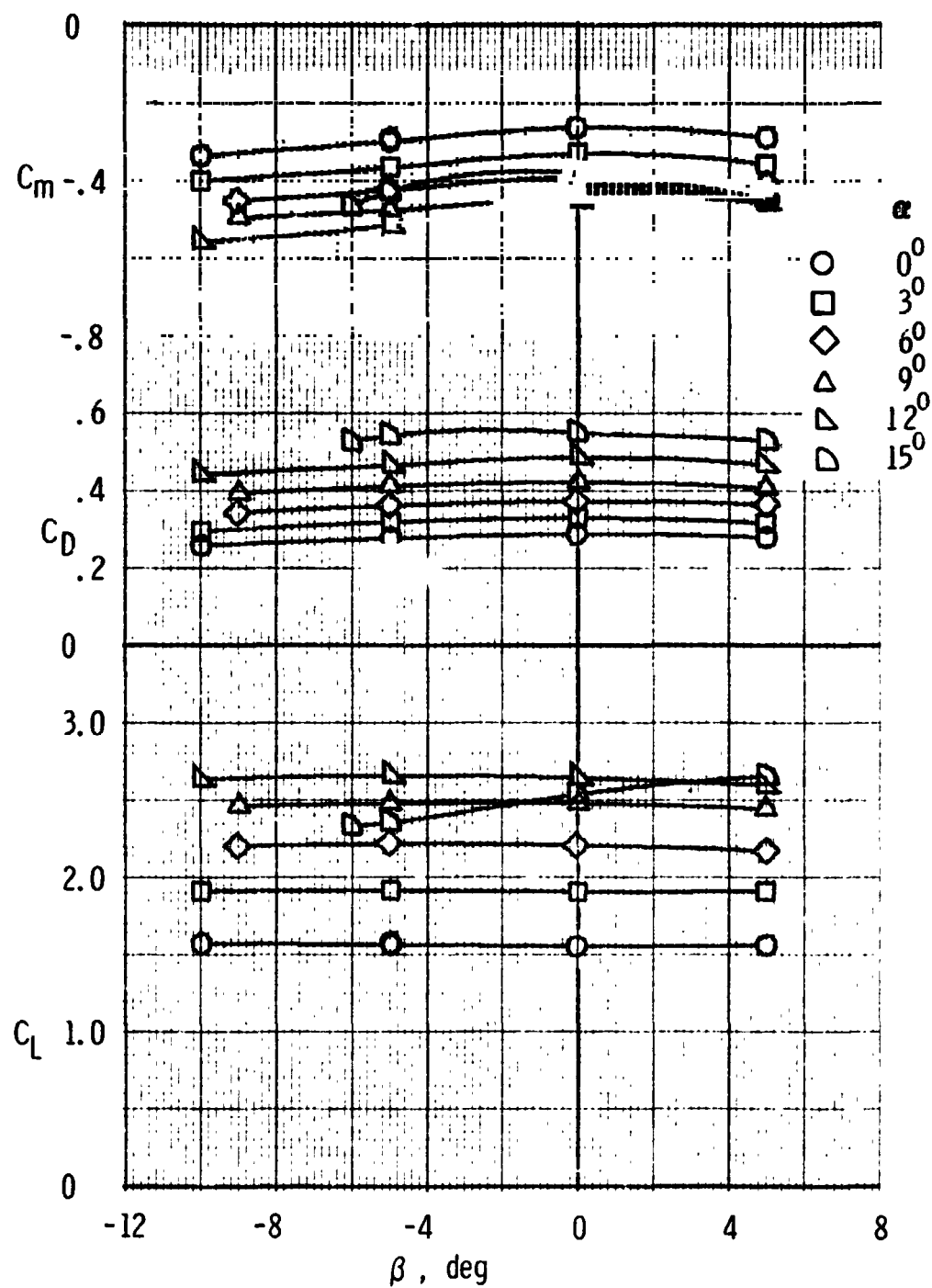
(a) Longitudinal characteristics

Figure 38. - Effect of rudder deflection on the aerodynamic characteristics of the F, W, F₄₀, N, G, H_T, V_T configuration.



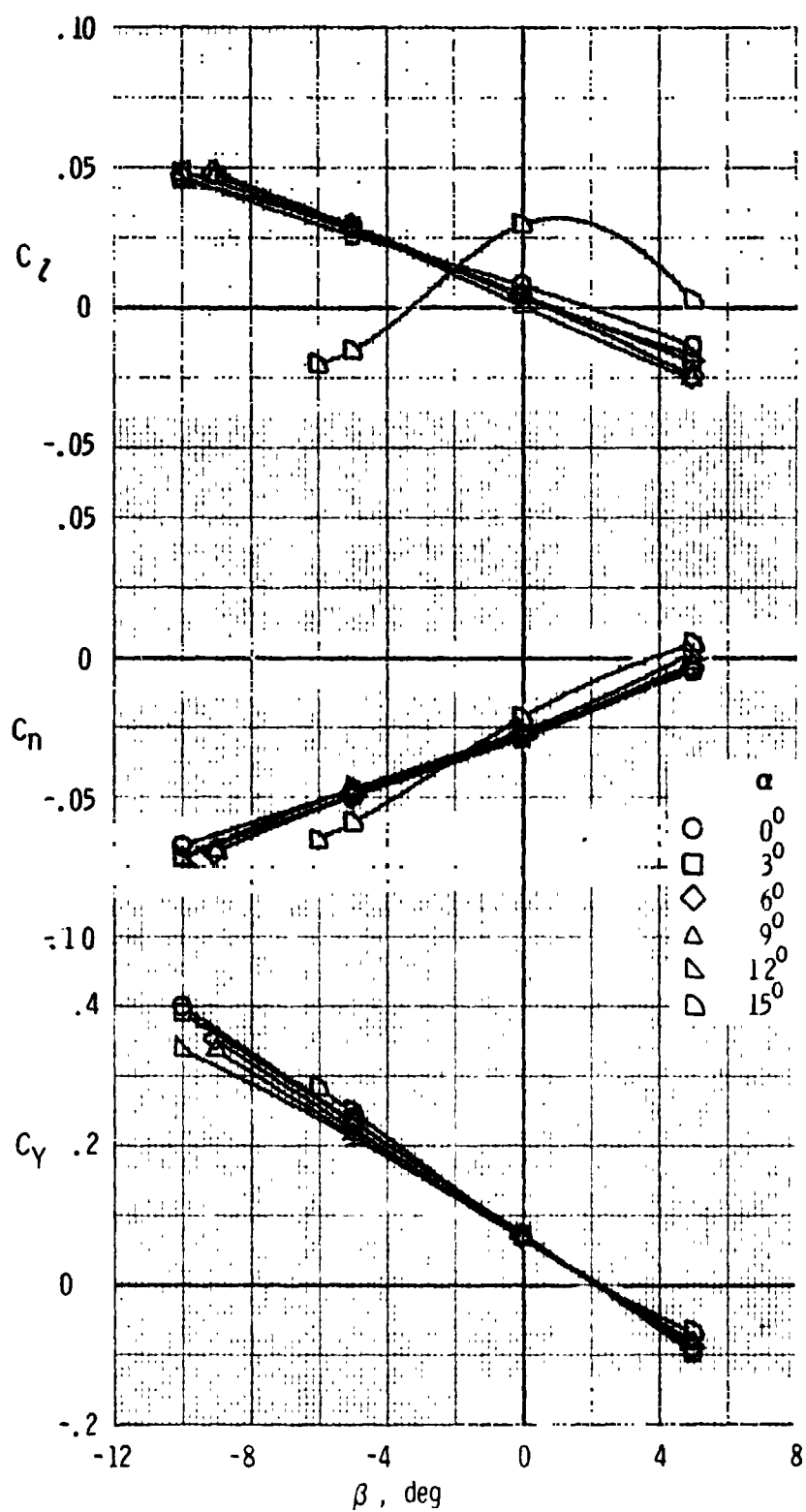
(b) Lateral-directional characteristics

Figure 38. - Concluded.



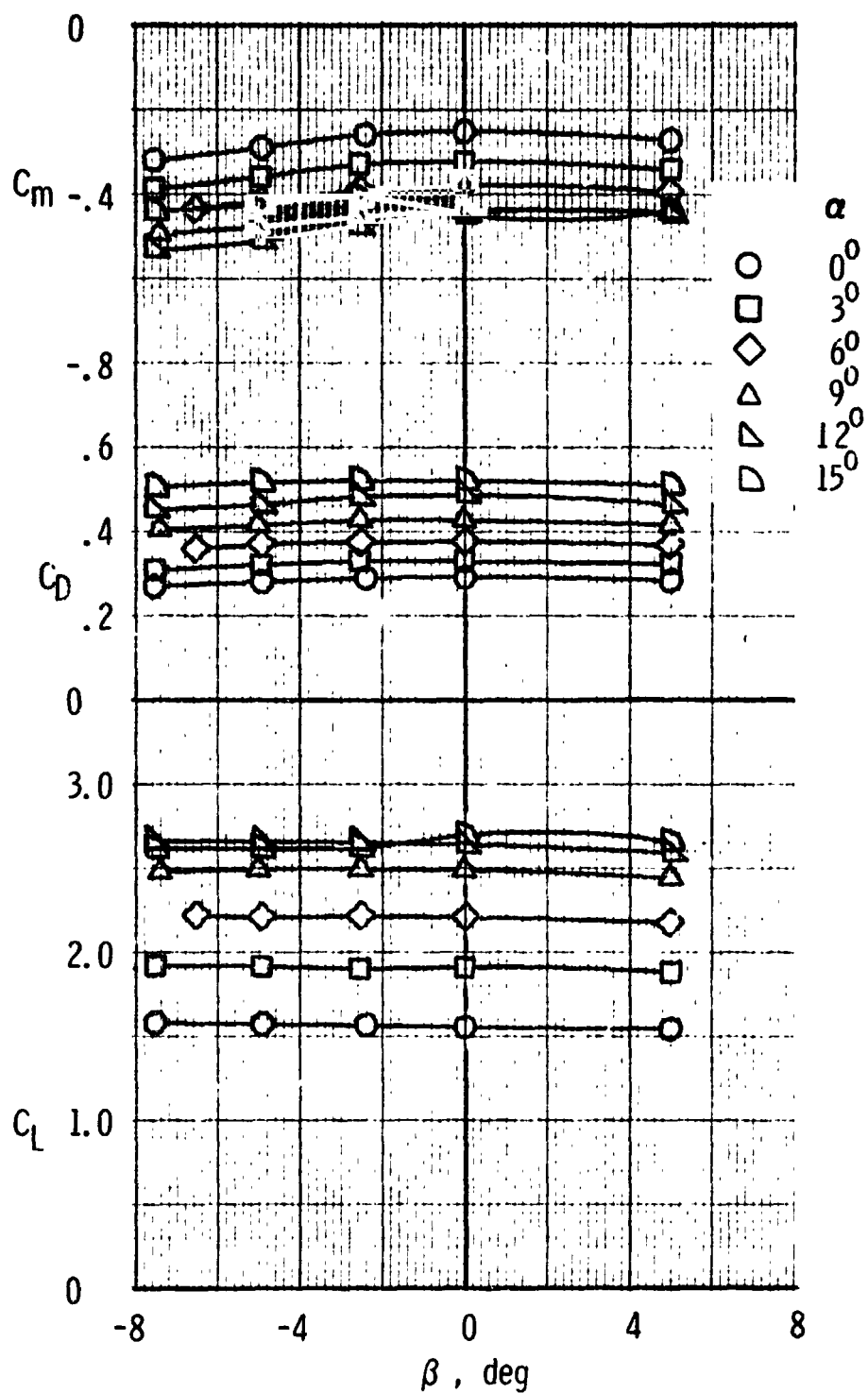
(a) Longitudinal characteristics, $\delta_r = 10^\circ$

Figure 39. - Effect of sideslip angle on the aerodynamic characteristics of the F, W, F₄₀, N, G, H_T, V_r configuration with various rudder deflections.



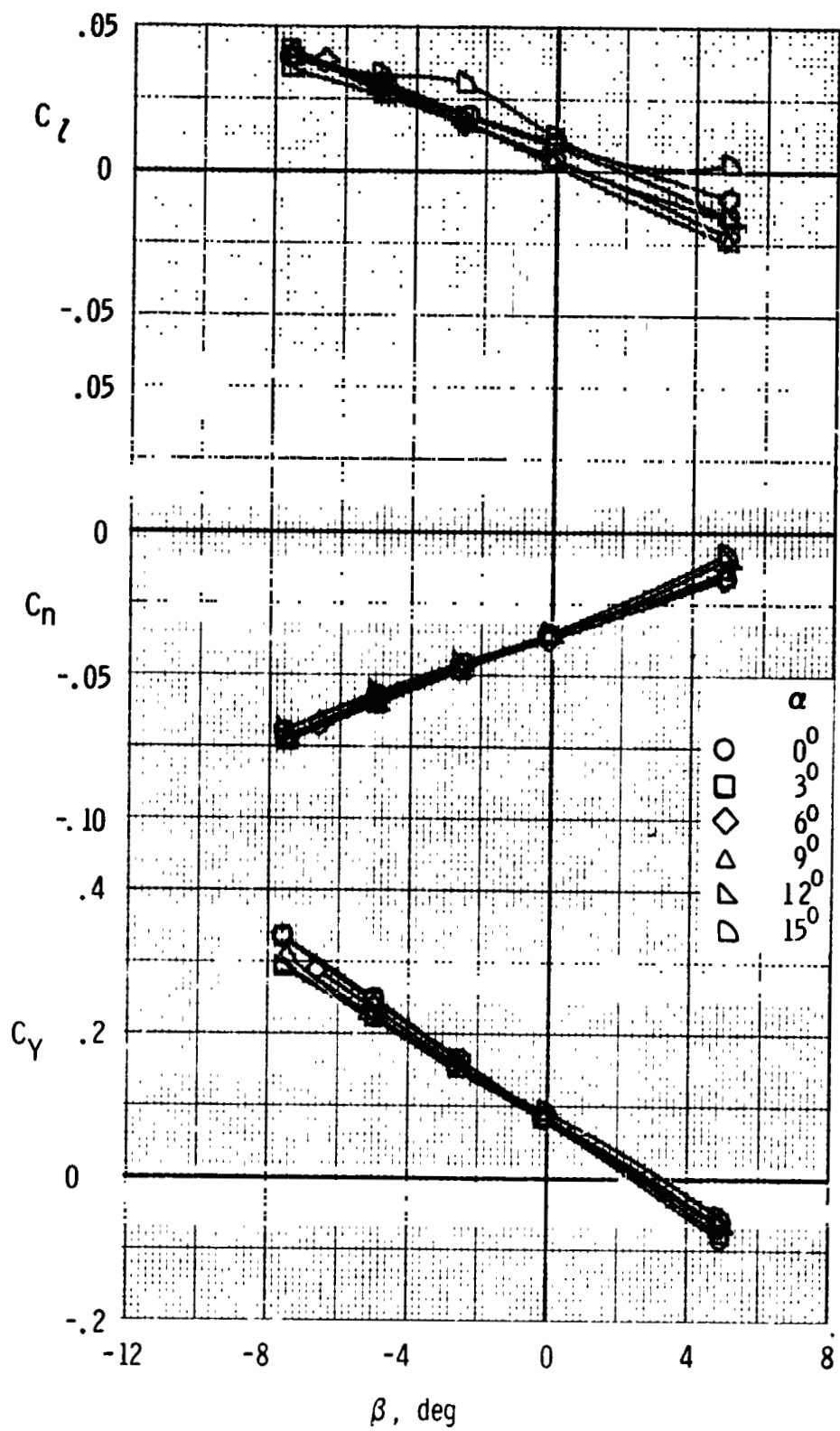
(b) Lateral-directional characteristics, $\delta_r = 10^\circ$

Figure 39. - Continued.



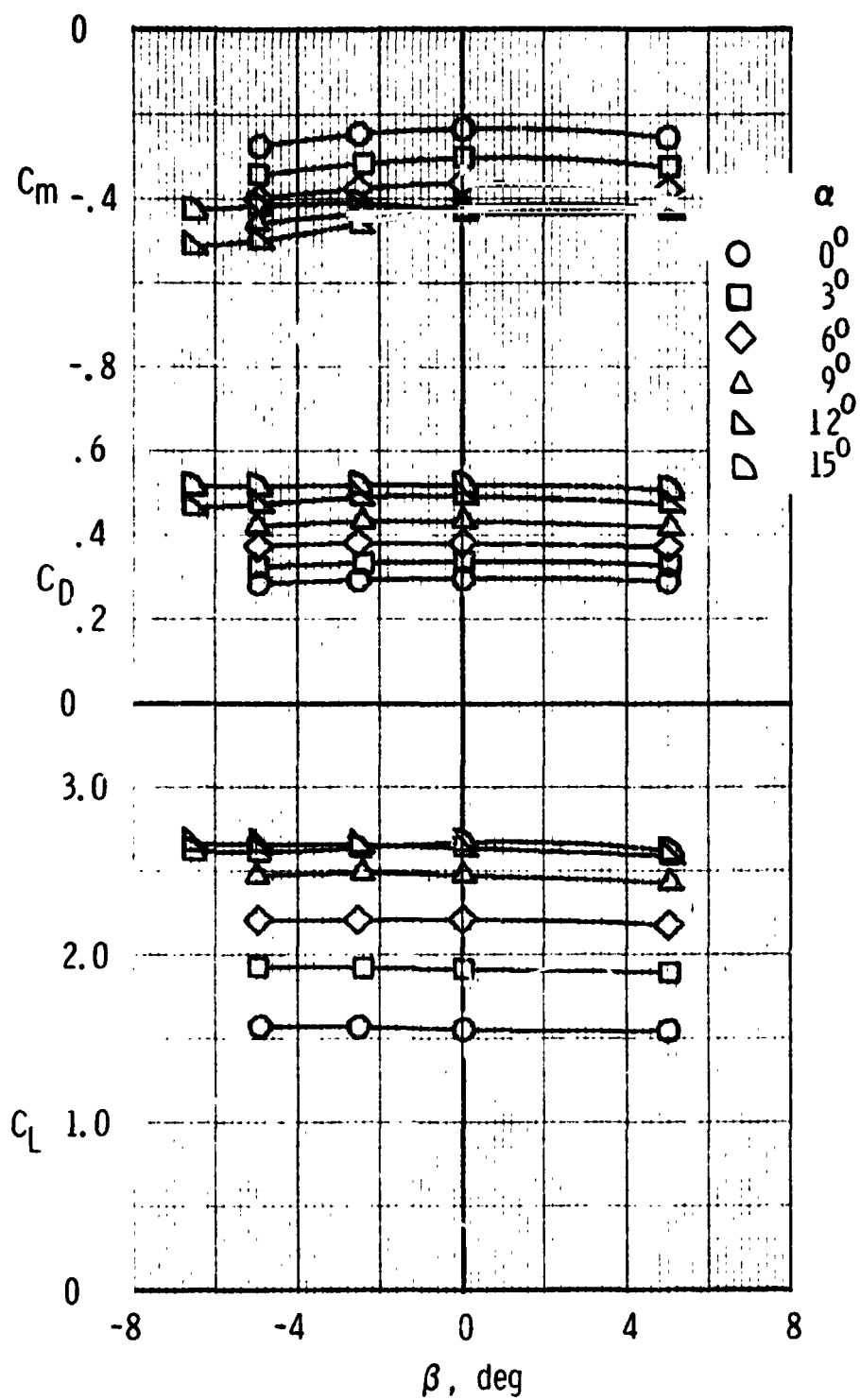
(c) Longitudinal characteristics, $\delta_f = 15^\circ$

Figure 39. - Continued.



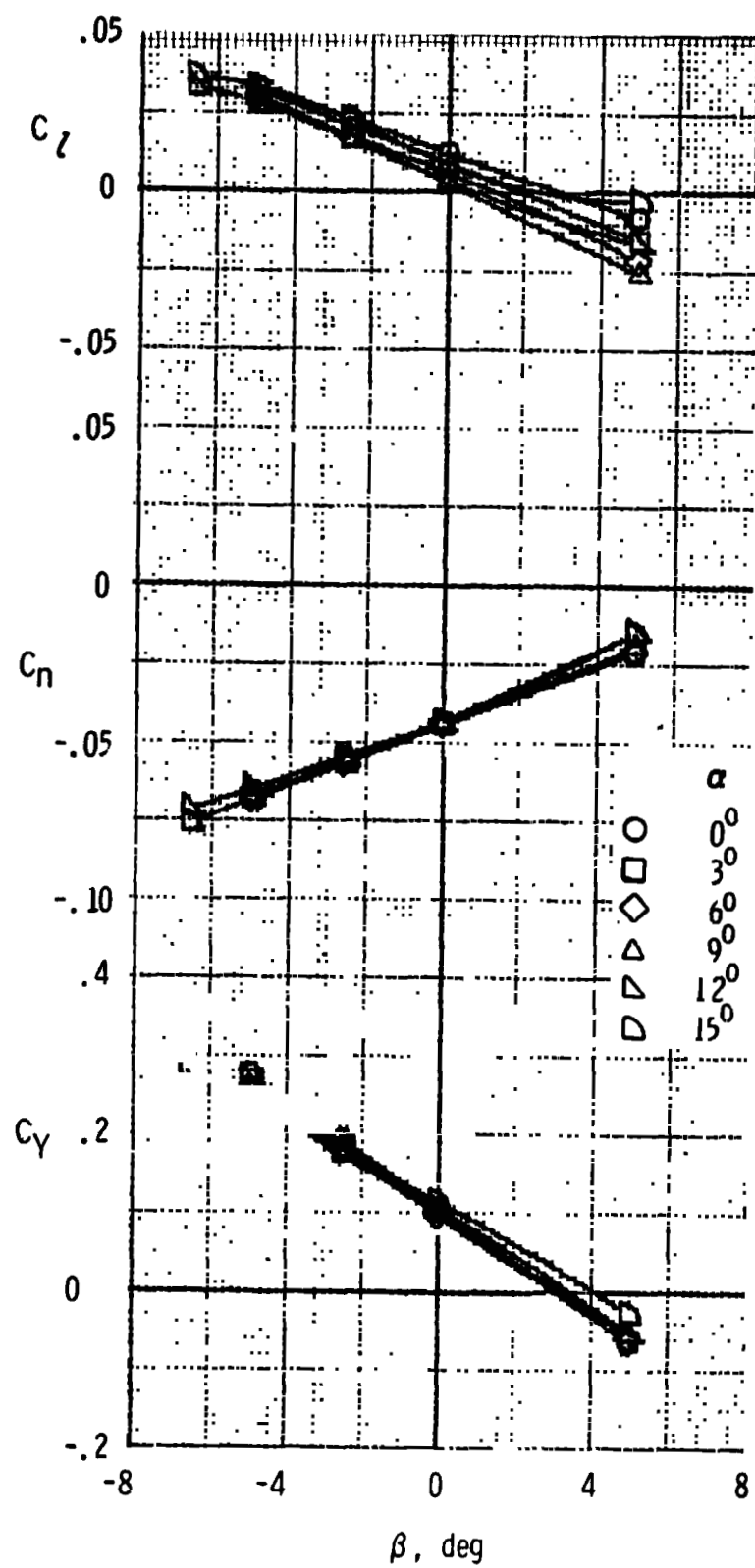
(d) Lateral-directional characteristics, $\xi_r = 15^\circ$

Figure 39, - Continued.



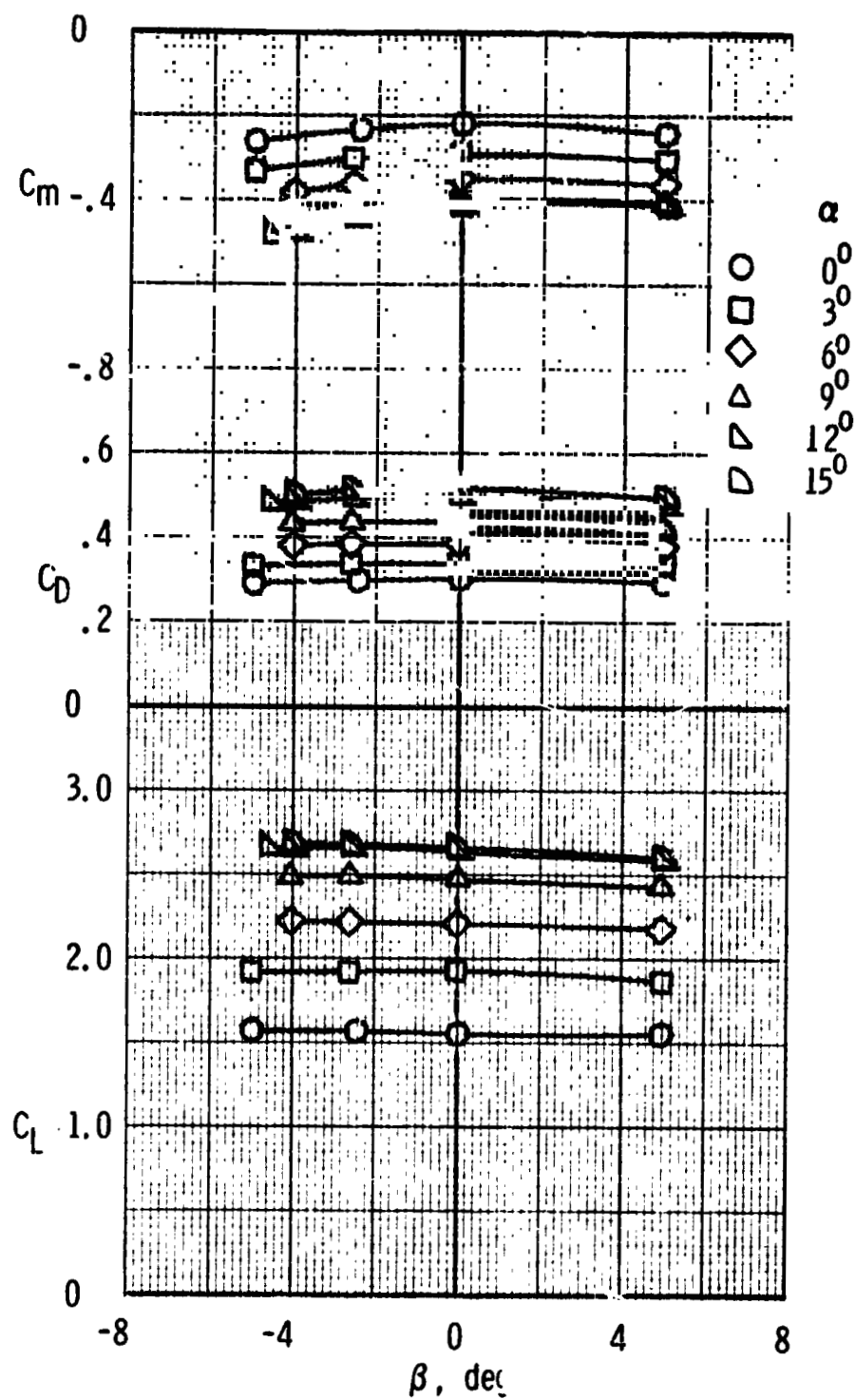
(e) Longitudinal characteristics, $\delta_r = 21^\circ$

Figure 39. - Continued.



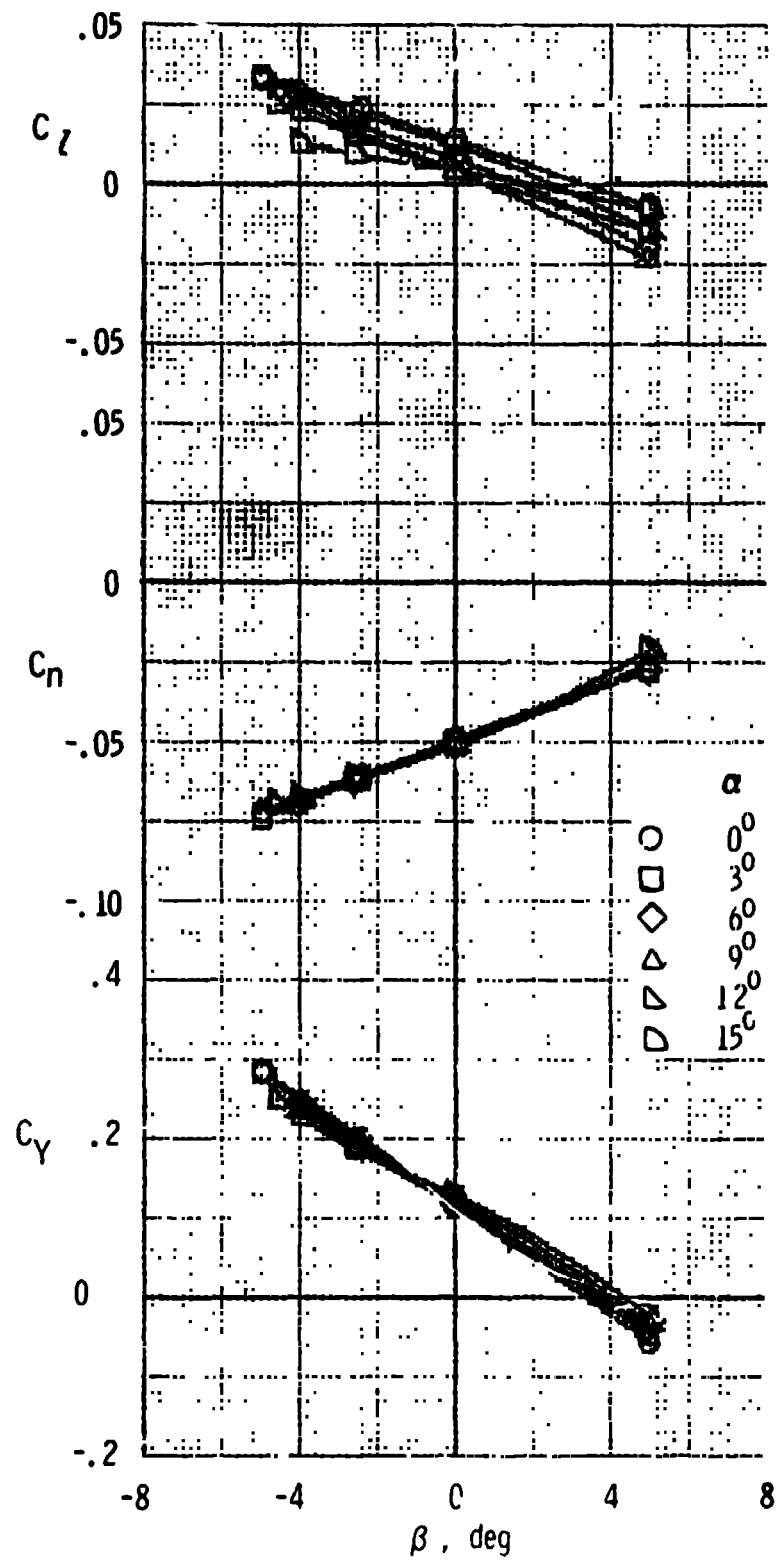
(f) Lateral-directional characteristics, $\delta_r = 21^\circ$

Figure 39. - Continued.



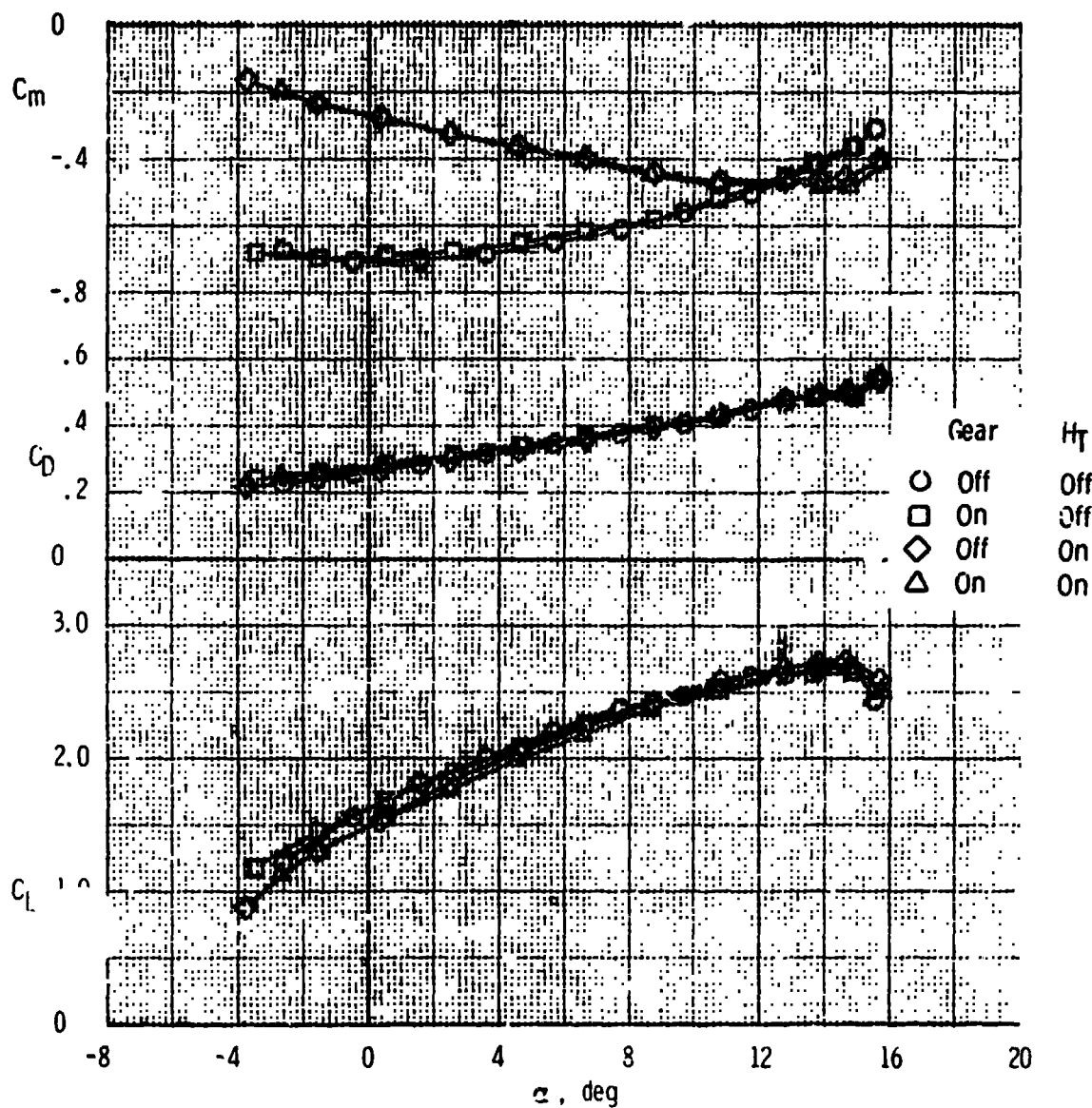
(g) Longitudinal characteristics, $\delta_r = 26^\circ$

Figure 39. - Continued.



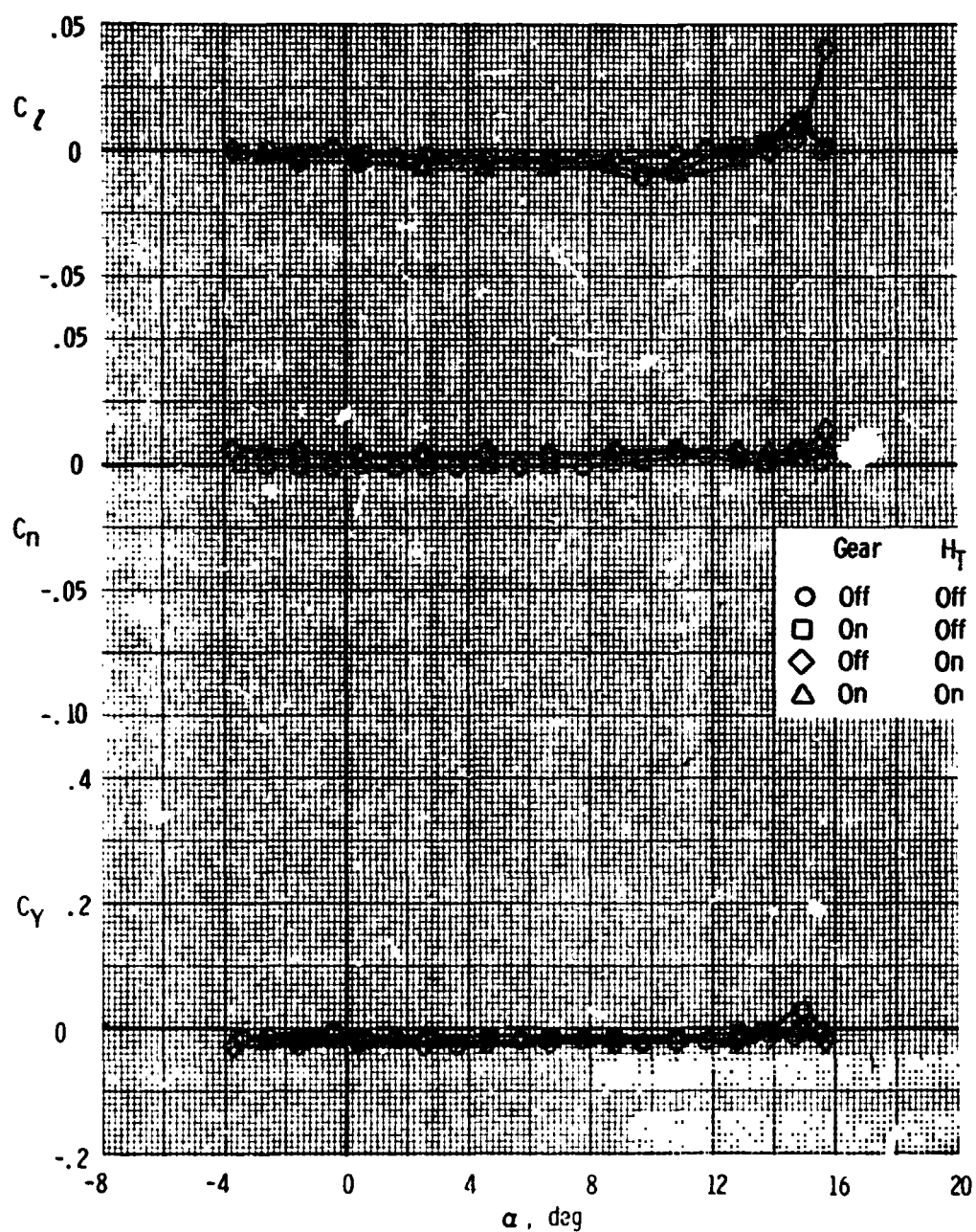
(n) Lateral-directional characteristics, $\delta_r = 26^\circ$

Figure 39. - Concluded.



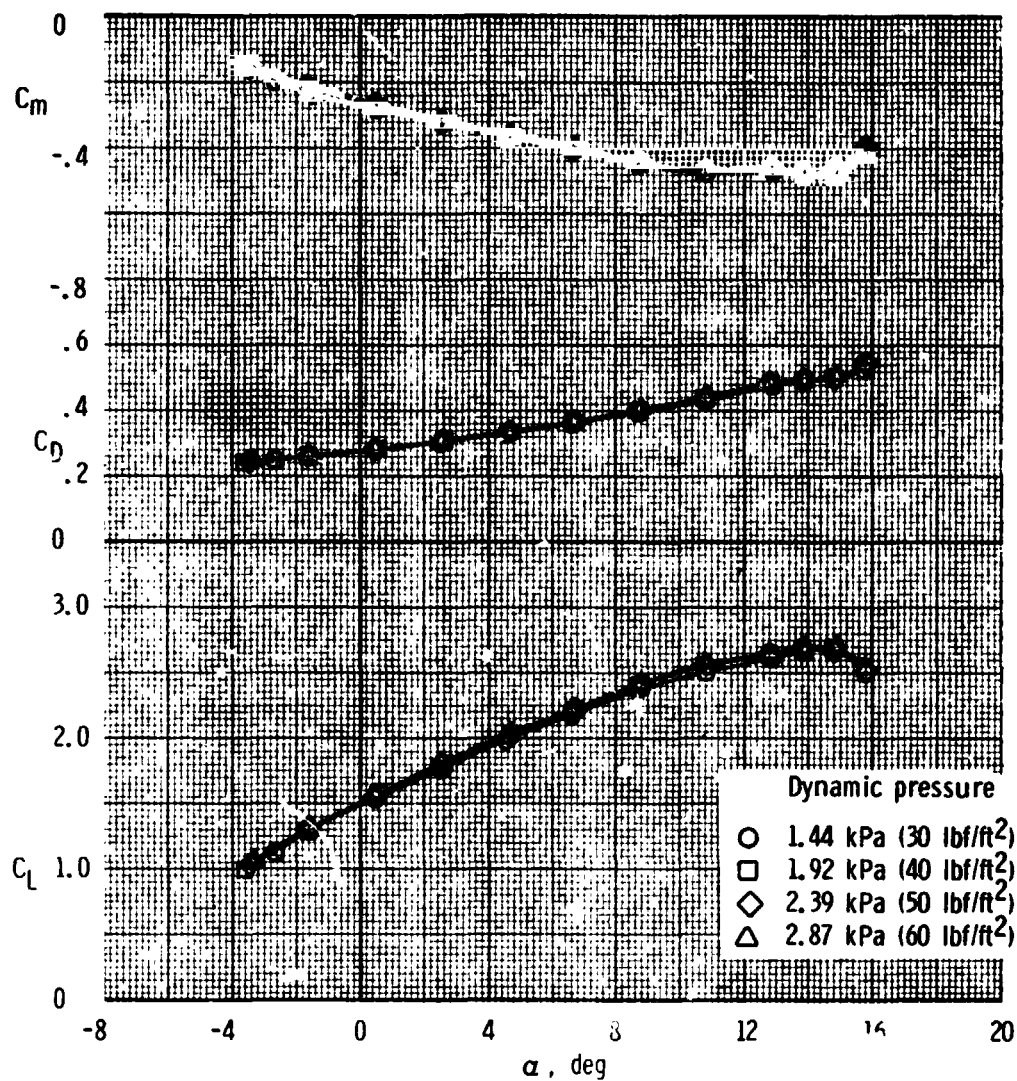
(a) Longitudinal characteristics

Figure 40. - Effect of landing gear on the aerodynamic characteristics of the F, W, F₄₀, N, H_T, V_T configuration.



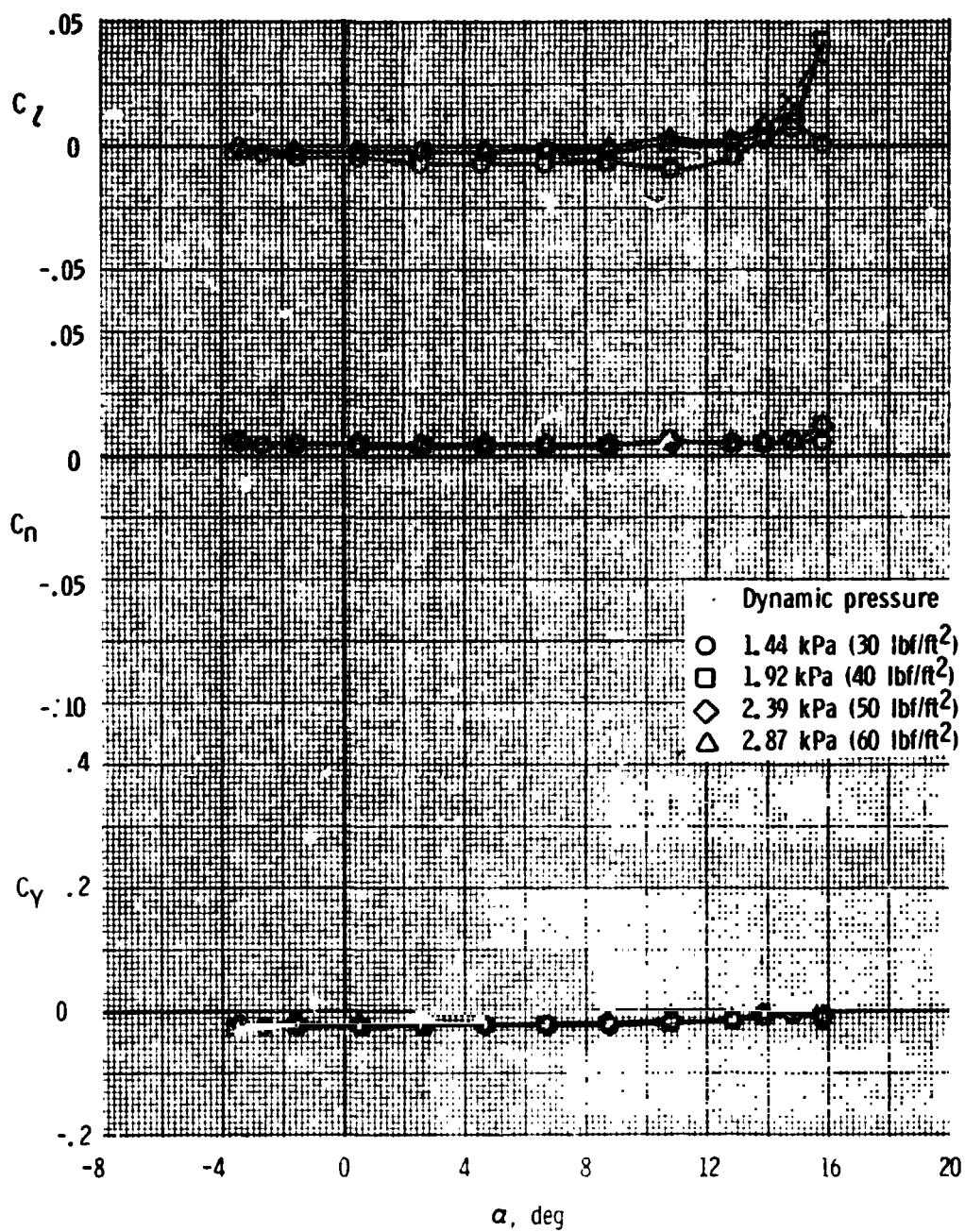
(b) Lateral-directional characteristics

Figure 40. - Concluded.



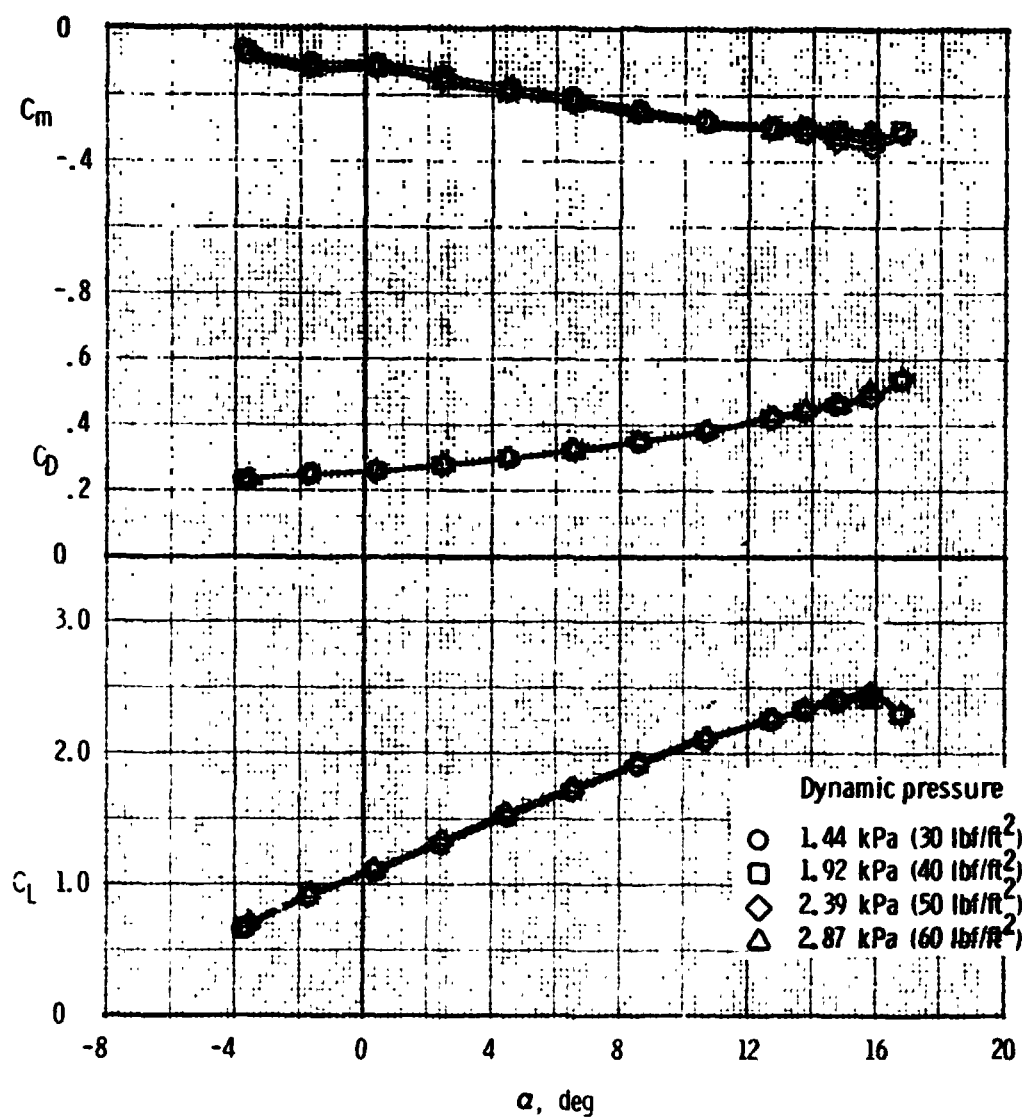
(a) Longitudinal characteristics, $\delta_{sp2,3,6,7} = 0^\circ$

Figure 41. - Effect of dynamic pressure on the aerodynamic characteristics of the F, W, F₄₀, N, G, H_T, V_T configuration.



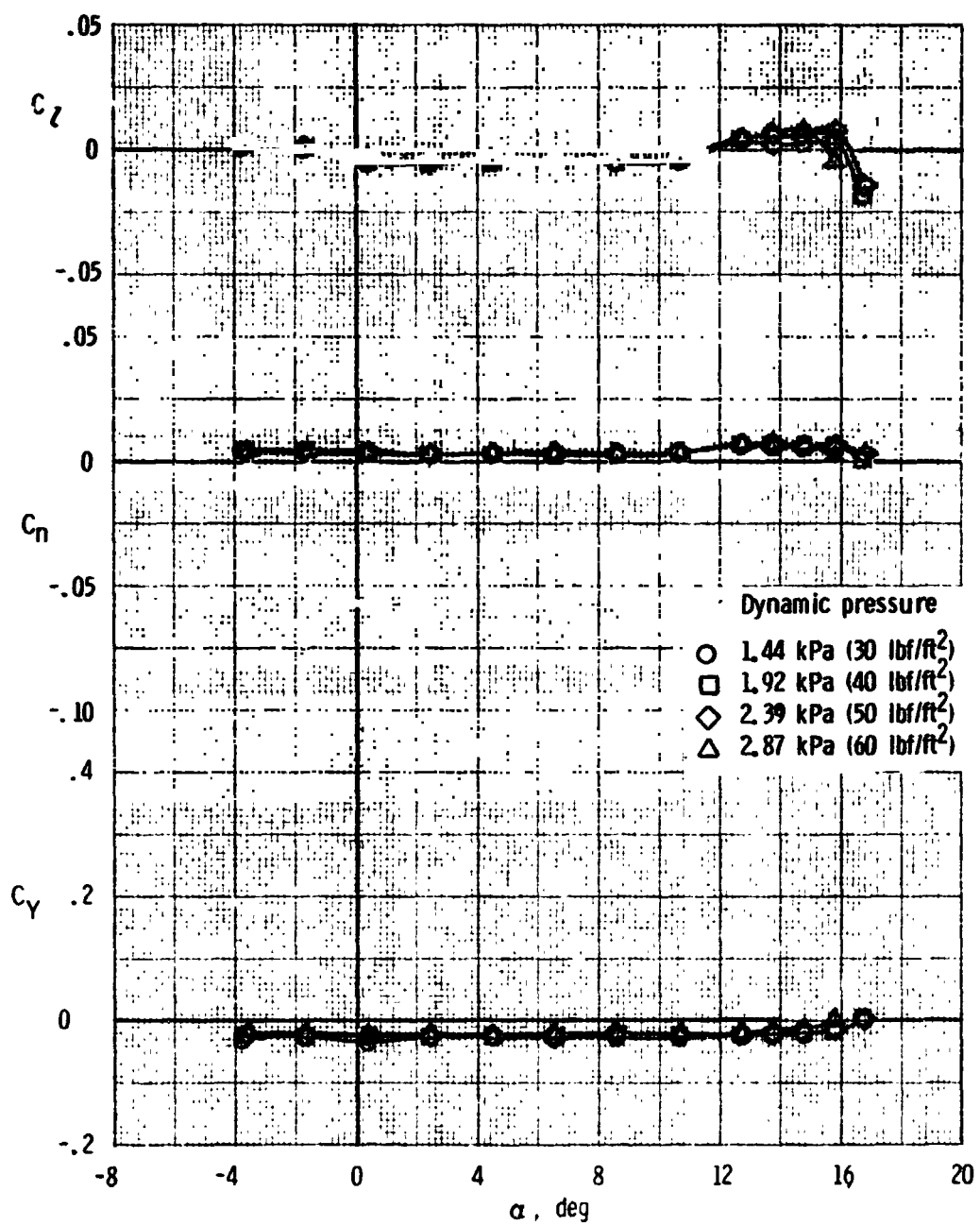
(b) Lateral-directional characteristics, $\delta_{sp2,3,6,7} = 0^\circ$

Figure 41. - Continued.



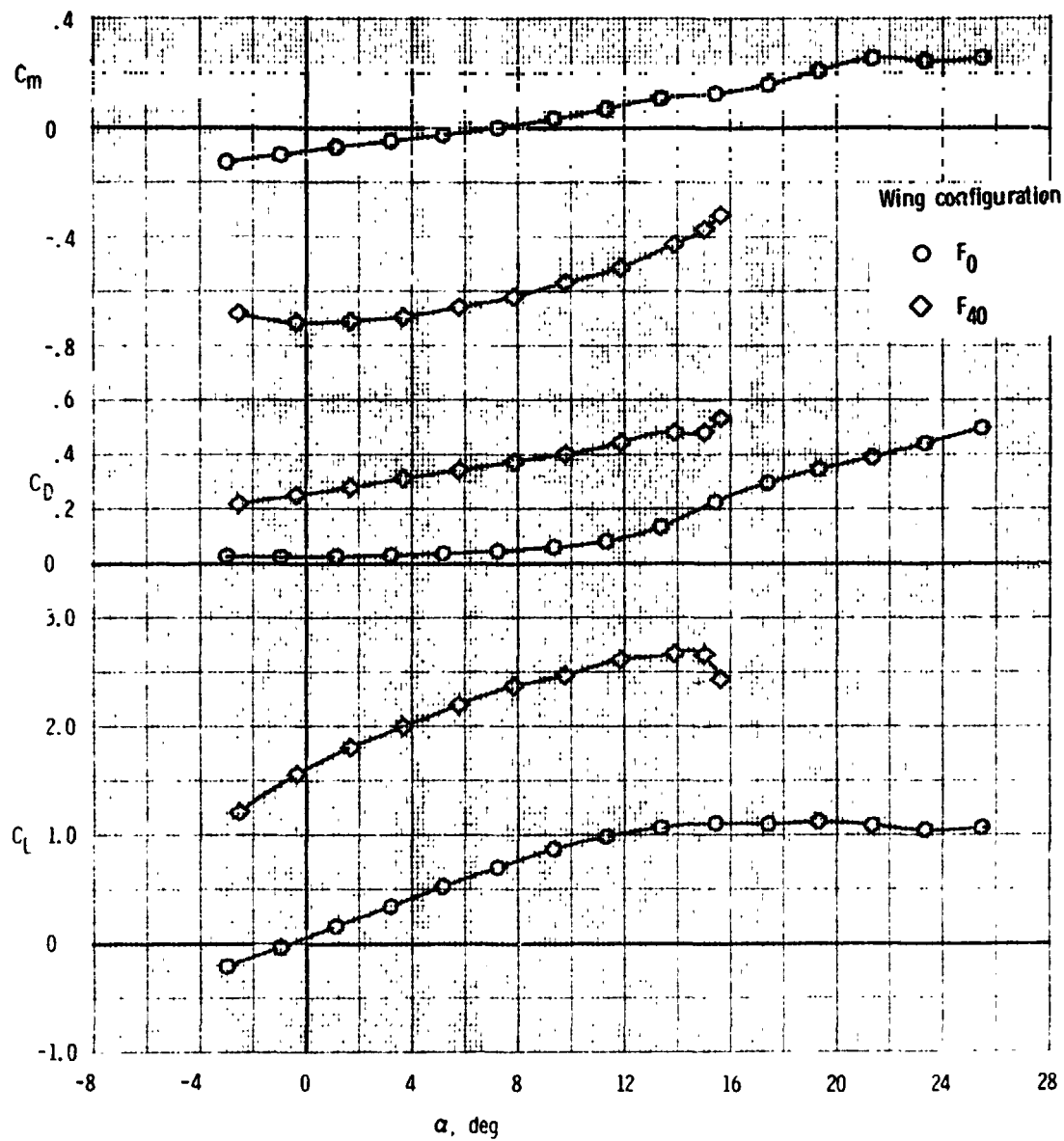
(c) Longitudinal characteristics, $\delta_{sp2,3,6,7} = 9^\circ$

Figure 4L - Continued.



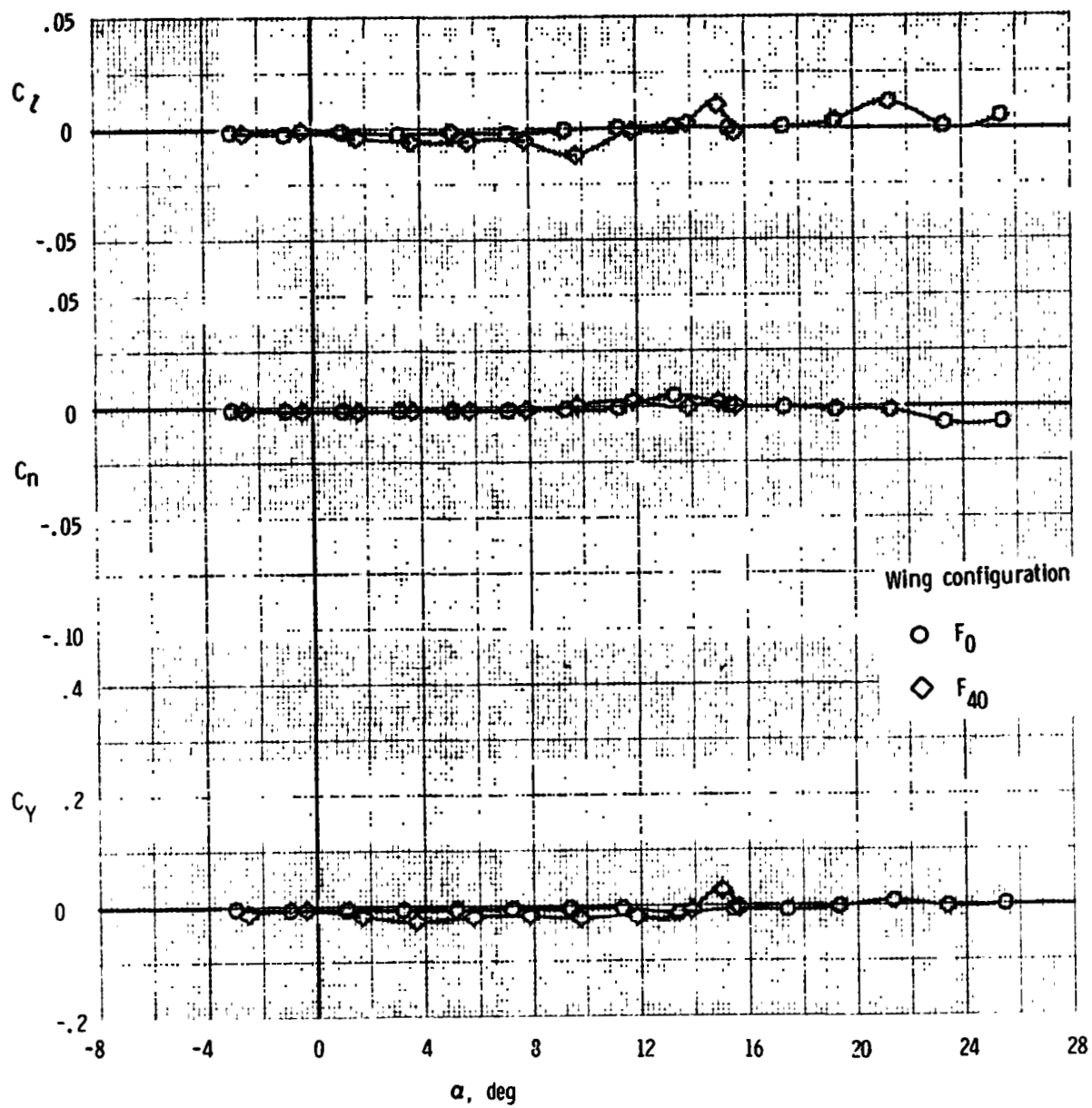
(d) Lateral-directional characteristics, $\delta_{sp2,3,6,7} = 9^\circ$

Figure 41. - Concluded.

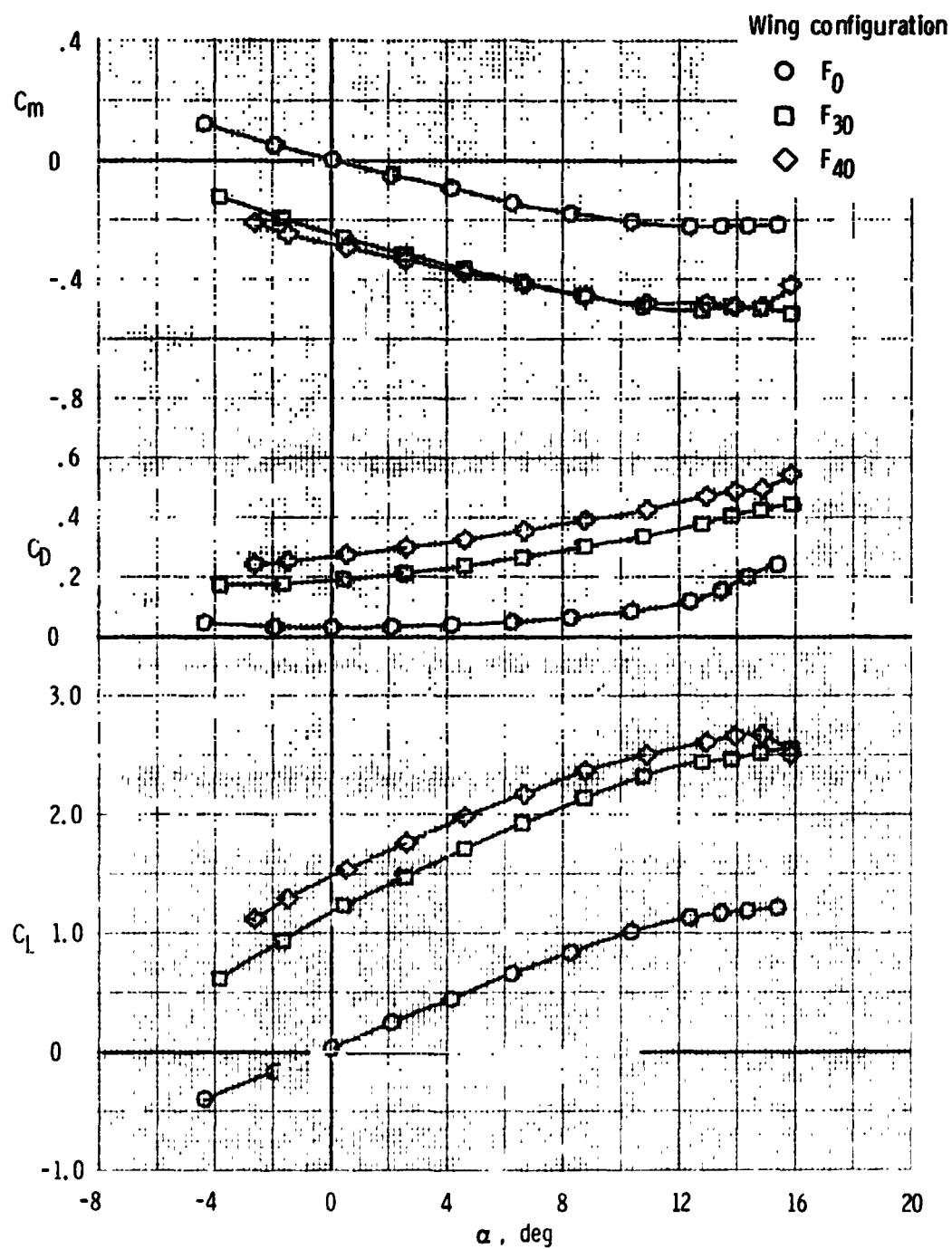


(a) Longitudinal characteristics, tail off

Figure 42. - Effect of flap deflections on the aerodynamic characteristics of the complete configuration with and without the horizontal tail.



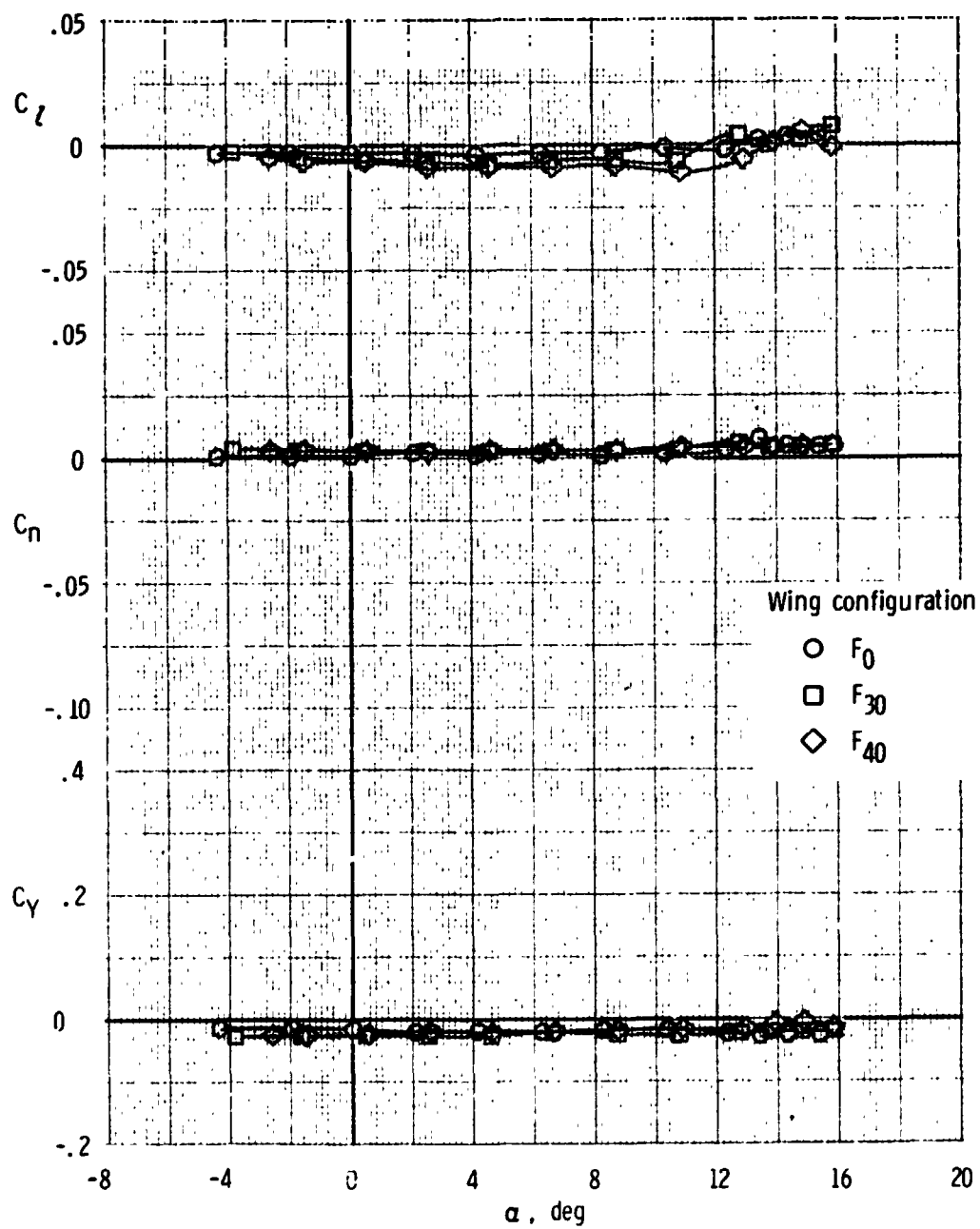
(b) Lateral-directional characteristics, tail off
Figure 42, - Continued.



(c) Longitudinal characteristics, tail on

Figure 42. - Continued.

REPRODUCIBILITY OF THE
ORIGINAL PAGE IS POOR



(d) Lateral-directional characteristics, tail on

Figure 42. - Concluded.